Volume 49 *January 1963* *Number 1*

Proceedings of the
National Academy of Sciences
of the United States of America

★ ★ ★ ★ ★

★ ★ ★ ★ ★

The Proceedings of the National Academy of Sciences

OFFICERS OF THE ACADEMY

FREDERICK SEITZ
President

J. A. STRATTON
Vice President

HARRISON S. BROWN
Foreign Secretary

HUGH L. DRYDEN
Home Secretary

L. V. BERKNER
Treasurer

EDITORIAL BOARD OF THE PROCEEDINGS

SAUNDERS MAC LANE
Chairman

HUGH L. DRYDEN, *Home Secretary*
L. V. BERKNER, *Treasurer*

HARRISON S. BROWN, *Foreign Secretary*
EDWIN B. WILSON, *Managing Editor*

S. CHANDRASEKHAR
THOMAS FRANCIS, JR.
DAVID R. GODDARD
G. EVELYN HUTCHINSON
ARTHUR KORNBERG
WILLARD F. LIBBY
J. R. PIERCE
S. S. STEVENS
FRANCIS J. TURNER

Subscription price is $17.50 for one year, $33.50 for two years, and $48.00 for three years. The price of a single issue beginning with volume 47 (1961), is $2.25; through volume 46 (1960), $1.50. Make all remittances payable to the National Academy of Sciences in U.S. currency or its equivalent.

Editorial correspondence should be addressed to the PROCEEDINGS OF THE NATIONAL ACADEMY OF SCIENCES, 2101 Constitution Avenue, Washington 25, D. C.

Business correspondence should be addressed to the Printing and Publishing Office, National Academy of Sciences, 2101 Constitution Ave., Washington 25, D. C.

Subscribers are requested to notify the Printing and Publishing Office of the Academy and their local postmaster immediately of change of address. Notices to the Academy should provide both the old and the new address.

Microfilms of complete volumes of this journal are available to regular subscribers only and may be obtained at the end of the volume year from University Microfilms, 313 N. First Street, Ann Arbor, Michigan.

Second-class postage paid at Easton, Pennsylvania.

PRINTED IN THE U. S. A.

THE PROCEEDINGS OF THE NATIONAL ACADEMY OF SCIENCES
is published monthly by
THE NATIONAL ACADEMY OF SCIENCES

Proceedings of the
NATIONAL ACADEMY OF SCIENCES

Volume 49 · Number 1 · January 15, 1963

*CRYSTAL STRUCTURE OF POTASSIUM OZONIDE**

By Leonid V. Azároff and Irene Corvin

METALLURGICAL ENGINEERING DEPARTMENT AND ARMOUR RESEARCH FOUNDATION, ILLINOIS INSTITUTE OF TECHNOLOGY

Communicated by M. J. Buerger, October 31, 1962

Although potassium ozonide can be synthesized at room temperature, it is extremely difficult to retain it in a pure form. Upon contact with water vapor, it tends to decompose partially to KOH and KO_2. This instability is the main reason why several attempts to grow single crystals have been unsuccessful so far, so that any investigation of the structure must be undertaken by the powder method of X-ray crystallography.

Prior to this analysis, the crystal structure of KO_3 had been investigated by Zhdanova and Zvonkova,[1] who compared it to the structure of KN_3 previously determined by Hendricks and Pauling.[2] Because of the similarity of the powder diagrams of KO_3 and KN_3, they assumed that both substances had the same space group, $I4/mcm$, and similar cell dimensions, $a = 6.094$ Å, $c = 7.056$ Å, and on this basis indexed seventeen out of twenty reported powder-photograph lines of KO_3. It should be noted, however, that Zhdanova and Zvonkova did not observe a single reflection having an odd l index so that the correct value of c in their analysis should have been one-half of the reported value.

Using the same atomic coordinates for potassium and oxygen in KO_3 that had been reported for potassium and nitrogen in KN_3,[2] Zhdanova and Zvonkova calculated the intensities for KO_3 and obtained a fair agreement with the observed ones. This led them to conclude that the two compounds were isotypic although Zhdanova and Zvonkova speculated in their paper that the absence of the 121 reflection ($d = 2.55$ Å) may be due to the fact that the O_3^- ion is not linear the way the N_3^- ion is. They also failed to index three reflections, having $d = 3.38$, 2.26, and 2.02 Å, and attributed them to unidentified impurities. In the present investigation, these three reflections, along with fifty-one others, were ascertained to belong to KO_3 while four more observed reflections were identified as belonging to KOH and KO_2.

Crystallographic Data.—Potassium ozonide is markedly dichroic with O = dark red and E = light yellow. Microscopic analysis of the KO_3 samples used in this analysis showed them to consist of cube- and needle-shaped crystallites. Repeated optical examinations of several samples indicated that the cubes and needles were merely two different habits of the same phase.

In the X-ray examination, fifty-four of the observed fifty-eight reflections could be indexed on the basis of a body-centered tetragonal unit cell, $a = 8.597 \pm 0.002$ Å and $c = 7.080 \pm 0.002$ Å. The relatively high accuracy claimed for the lattice constants is based on the remarkably close agreement between the observed and calculated values. The unit cell of KO_3 can be related to that of KN_3 by setting $a_{KO_3} = \sqrt{2}a_{KN_3}$ and $c_{KO_3} = c_{KN_3}$. It should be noted however that such a transformation of axes normally leads to a face-centered tetragonal cell instead of the body-centered cell indicated by the absence of all reflections for which $h + k + l = 2n + 1$. The similarity between the intensities of KO_3 reflections for which h, k, and l are all even and the corresponding reflection intensities of KN_3, already noted, suggests that the two structures are related.

Intensity Measurement.—In order to inhibit the decomposition of KO_3, X-ray diffraction intensities were measured at $-35°C$ by blowing precooled nitrogen over the powder samples. Several attempts to use a diffractometer for collecting intensity data failed to yield reproducible results, the most notable variations being observed among the relative intensities of the $00l$ reflections. This was attributed to the preferential packing of the needle-shaped crystallites, so that it became necessary to use film methods since they did not show evidence of shape orientation. KO_3 of about 97 per cent initial purity was encapsulated in glass capillaries in a dry box and several powder photographs were obtained using nickel-filtered Cu$K\alpha$ radiation. A scanning Leeds and Northrup photometer was used to determine the intensities of the lines. A comparison of several films showed that the intensities of the first twenty-four reflections were reproducible within 10–15 per cent, so that the present analysis is based on these reflections. The intensities of the remaining lines were also measured, but these values were deemed less reliable, particularly since the higher-order reflections may be superpositions of reflections. After correcting the observed intensities for absorption and Lorentz-polarization effects, the proper multiplicities were used to establish F_{OBS} by assuming equal contributions from all possible planes.

Crystal-Structure Analysis.—According to the above-established unit-cell content, it is necessary to distribute $8K^+$ and $8O_3$ ions among the equipoints of the appropriate space group. The tetragonal indexing and the observed systematic absences require the diffraction symbol $4/mmm\ I-/-c-$ which includes space groups $I4/mcm$, $I\ 4cm$, and $I\ \bar{4}c2$. The eight potassium ions have to be distributed among an appropriate combination of equipoints of rank two, four, or eight. An examination of such available equipoints in all three space groups discloses that the x and y coordinates of the equipoint sets of $I4/mcm$ include the relevant sets in the other two space groups. Accordingly, the location of the potassium ion positions can begin by an analysis of the projection along c.

Considering fourfold positions, $4a$ projects the same as $4c$ and $4b$ as $4d$. Combinations of $4a + 4c$ or $4b + 4d$ are not acceptable because the c axis is too short to accommodate four potassiums. Combinations such as $4a + 4b$ or $4c + 4d$ are sterically acceptable and project as the same pattern. Considering eightfold equipoints, $8f$ and $8g$ can be eliminated similarly because they require four atoms along c. Equipoint $8h$ is unacceptable because it requires two potassiums to be contained within half the cell diagonal. The remaining equipoint $8e$ projects the same as $4a + 4b$ except for a shift of origin by $\frac{1}{4}\ \frac{1}{4}$. Therefore, the only acceptable projected potassium ion positions have the same pattern as $4a + 4b$.

The structure factors of the $hk0$ reflections for which h and k are both even are dominated by the potassium-ion contributions. Of the twelve observed $hk0$ reflections only one has h and k both odd so that the signs of the remaining eleven reflections can be fixed as positive. The sign of the 770 reflection then serves to determine the origin of $\rho(xy)$. The electron density based on these signs and the observed F_{hk0}'s is shown in Figure 1 and not only shows the potassium ions at the

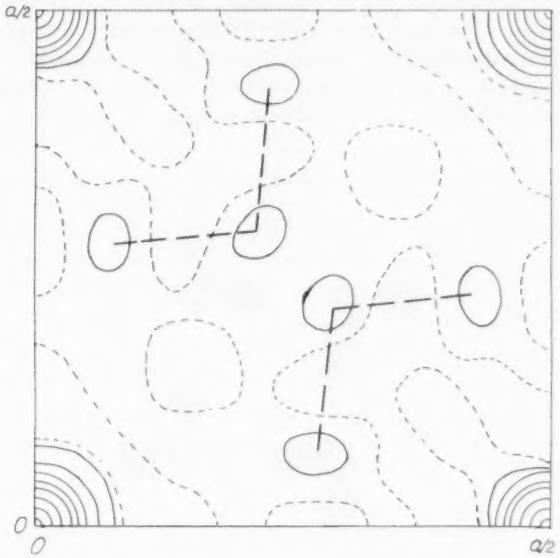

FIG. 1.—$\rho(xy)$ of KO_3 showing one quarter of the unit cell.

corners but also the ozonide groups. It can be seen that one of the oxygen atoms lies along the diagonal which corresponds to equipoint $8h$. It will be noted that this diagonal is a mirror plane so that the K^+ ion lying on the same mirror plane must be at either $0\frac{1}{2}$ or $\frac{1}{4}\ \frac{1}{4}$. If K^+ is placed at $\frac{1}{4}\ \frac{1}{4}$ ($8e$), the pair of oxygens in $8h$ near the center of Figure 1 must be coplanar to satisfy 4_2 symmetry. Since this places the centers of the two oxygens within 0.7 Å of each other, it is unreasonable. Conversely, if K^+ is placed at $0\frac{1}{2}$, the two oxygen atoms are no longer coplanar.

Similar arguments can be used for the preparation of the electron density $\rho(xz)$. It was established above that the only permissible equipoints remaining for the potassium ions are $4a + 4b$ or $4c + 4d$. It turns out that their projection along a also produces identical patterns. Since F_{h0l} is observable only when h and l are both even, the signs of all F_{h0l}'s can be taken as positive. The resulting electron density clearly shows that the ozonide groups lie along planes normal to c and halfway between the potassium ions. Since it was established that one of the oxygens was on a diagonal mirror, level $z = 0$, the potassium ions must be on level $z = \frac{1}{4}$ which permits $4a + 4b$ but eliminates the other equipoint sets.

The atomic distribution among the equipoints of $I4/mcm$ is:

K_I in $4a$ $00\frac{1}{4}$

K_{II} in $4b$ $0\frac{1}{2}\frac{1}{4}$

O_I in $8h$ $x,\frac{1}{2}+x,0$ $(x = 0.287)$

O_{II} in $16h$ $x,y,0$ $(x = 0.075), y = (0.275)$

The above coordinates were used to calculate the structure factors of the first twenty-four reflections (and the remaining $hk0$ and $h0l$ reflections). The residual factor was $R = 0.13$ for these twenty-four reflections only. An attempt to adjust the above atomic coordinates in the symmetry of the uneliminated space groups failed to decrease R. It was concluded therefore that these were the best attainable coordinates with the available intensity data.

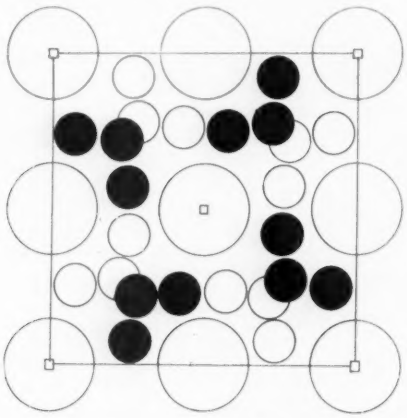

FIG. 2.—Structure of KO_3 projected along c. The small open and closed circles indicate O_3^- ions at $z = 0$ and $1/2$, respectively.

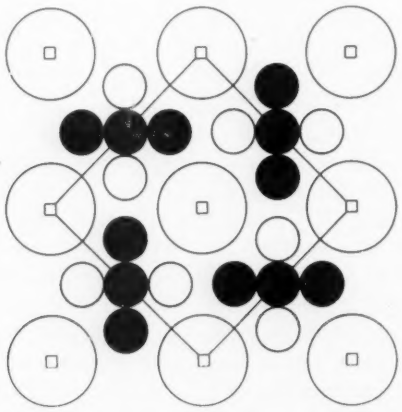

FIG. 3.—Structure of KN_3 projected along c. The small open and closed circles represent N_3^- ions at $z = 0$ and $1/2$, respectively.

Discussion.—The full unit-cell contents of KO_3 is shown in Figure 2 which can be compared to the KN_3 structure shown in Figure 3. Both are derivative structures[3] of the cesium chloride structure which can be seen by considering that either the N_3^- or O_3^- ion takes the position of Cl^- while K^+ replaces Cs^+. A linear array such as N_3^- in Figure 3 results in the tetragonal KN_3 structure in which each potassium ion is equally coordinated by eight atoms (nitrogen). If the linear array is bent as shown in Figure 2, then the unit cell is increased further (one set of translation equivalent fourfold axes is suppressed) and the eightfold coordination of the two kinds of potassium ions is no longer identical. The $K_I - O_{II}$ distance is 3.03 Å and $K_{II} - O_{II} = 2.70$ Å as compared to 2.73 Å for the sum of the ionic radii. In view of the limited reliability of the final atomic coordinates, however, it is not meaningful to speculate at this time about the nature of the bonding that is responsible for these differences.

Based on the above coordinates, the ozonide ion is bent, $< 000 = 100°$, and the distance separating the centers of adjacent oxygens is 1.19 Å. This can be compared to a theoretical prediction by Smith,[4] based on the structure of the O_3 molecule determined by Hughes[5] from microwave resonance spectra, that the O_3^- ion should have $< 000 = 110 \pm 5°$ and $0-0 = 1.34 \pm 0.05$ Å.

We wish to express our thanks to I. J. Solomon for synthesizing the KO_3 samples used in this investigation, to R. Pepinsky for making X-RAC available to check our hand calculations, and to M. J. Buerger for invaluable discussion.

*This investigation was supported by the U.S. Air Force Office of Scientific Research under a contract with the Armour Research Foundation.

[1] Zhdanova, G. S., and Z. V. Zvonkova, "The crystal structure of potassium ozonide" (in Russian), *Zhur. Fiz. Khim.*, **25,** 100 (1951).

[2] Hendricks, Sterling B., and Linus Pauling, "The crystal structures of sodium and potassium trinitrides and potassium cyanate and the nature of the trinitride group," *J. Amer. Chem. Soc.*, **47,** 2904 (1925).

[3] Buerger, M. J., "Derivative crystal structures," *J. Chem. Phys.*, **15,** 1 (1947).

[4] Smith, P., "Estimate of the size and shape of the O_3^- ion," *J. Phys. Chem.*, **60,** 1471 (1956).

[5] Hughes, Richard H., "Structure of ozone from the microwave spectrum between 9,000 and 45,000 mc./sec.," *J. Chem. Phys.*, **24,** 131 (1956).

---

*THE DETERMINATION OF THE ELECTROPHORETIC CONTRIBUTION TO CONDUCTANCE FROM THE CONCENTRATION DEPENDENCE OF TRANSFERENCE NUMBERS**

BY ROBERT L. KAY AND JAMES L. DYE

METCALF RESEARCH LABORATORY, BROWN UNIVERSITY, AND KEDZIE CHEMICAL LABORATORY, MICHIGAN STATE UNIVERSITY

Communicated by C. A. Kraus, November 1, 1962

Modern theories of electrolytes attribute the change in the equivalent conductance with concentration to ion association and to two long-range ion interactions known as the electrophoretic and the relaxation effects. Alteration of the solution viscosity due to the presence of the electrolyte will not be considered since we shall limit our discussion to dilute solutions of relatively small ions. The

electrophoretic effect takes into account the decrease in velocity of an ion due to the counterflow of solvent in the ion's atmosphere. The relaxation effect results from the perturbation of the applied field by the asymmetry of the ionic atmosphere. This asymmetry is produced by the movement of the central ion. The Onsager[1] conductance theory evaluates the influence of these two effects in terms of the physical properties of the solvent and the mobility and charge of the ions. The Fuoss-Onsager theory[2, 3] adds higher-order terms and also takes into account the finite size of the ions. This theory has been found to fit conductance data for aqueous solutions with great precision,[4] but, in some solvents of lower dielectric constant, deviations occur which have been attributed to ion association. While these deviations can be quantitatively accounted for by the introduction of an association constant, such an assumption tends to mask the contribution to conductance of the free ions. The reason for this is that both association and the higher-order terms involving ion size have the same concentration dependence in the first approximation and the separation of these two effects depends upon second-order terms in the association. In any case, it is hazardous to ascribe much physical significance to three parameters which are adjusted to give the best fit of the conductance data. If an independent measurement of the association constant were possible, the conductance data could be used to determine the conductance of free ions in solvents of low dielectric constant. Generally, such independent data are not available.

It is the purpose of this paper to show that, for symmetrical electrolytes, the concentration dependence of transference numbers can be used to calculate the electrophoretic contribution to conductance. This is possible even if some association is present, because transference numbers are relatively insensitive to association. The separation of the electrophoretic and relaxation terms is possible because, as was pointed out by Stokes,[5] the variation of transference numbers with concentration is independent of the relaxation effect.

Theory.—The steady-state velocity of an ion is proportional to the field felt by the ion, the proportionality factor being a measure of the frictional forces opposing its motion. At infinite dilution, the field felt by the ion is the external field, X, and the proportionality factor is the limiting ionic mobility u_j^0. At finite concentrations, the change in ionic velocity is due to a perturbation of the external field and a variation of the frictional forces due to the presence of other ions. This may be expressed by writing the velocity as

$$v_j = (u_j^0 + \Delta u_{e_j})(X + \Delta X_j). \tag{1}$$

Conversion to equivalent conductance units gives

$$\lambda_j = (\lambda_j^0 - \lambda_{e_j})(1 + \Delta X_j/X), \tag{2}$$

in which the sign has been changed for later convenience.

Using the hard-sphere, solvent-continuum model, we may identify λ_{e_j} with the electrophoretic effect and $\Delta X_j/X$ with the relaxation effect. Treatment of these effects, using the ionic atmosphere concept, results in $\Delta X_1 = \Delta X_2$ for an electrolyte which dissociates into only two kinds of ions, and $\lambda_{e_1} = \lambda_{e_2}$ for a symmetrical electrolyte.

Considering only symmetrical electrolytes, we can set $\Lambda_e = 2\lambda_e$ and write for the equivalent conductance

$$\Lambda = (\Lambda_0 - \Lambda_e)(1 + \Delta X/X) \tag{3}$$

and for the transference number

$$T_1 = (\lambda_1^0 - \lambda_e)/(\Lambda_0 - \Lambda_e) \tag{4}$$

since the relaxation terms cancel in the ratio. Rearrangement of equation (4) and introduction of the limiting transference number T_1^0 gives

$$\Lambda_e = \Lambda_0 \left[\frac{T_1^0 - T_1}{0.5 - T_1}\right]. \tag{5}$$

Thus, the electrophoretic correction to conductance can be calculated from precise transference data provided Λ_0 and T^0 are known. Both of these quantities are extrapolated values but, since Λ_0 enters as a factor in the product, its precision is not as critical as that of T^0 which enters in the difference. Extrapolation of conductance data is often uncertain because of the effects of association and transcendental terms in $\Delta X/X$. Transference numbers are independent of $\Delta X/X$ and are relatively insensitive to association. Fortunately, the extrapolation of transference numbers by any of several methods gives the same value. Of course, a precise value of Λ_e can be obtained from equation (5) only if the transference number differs substantially from 0.5.

It might be well to mention that equation (5) is valid even if association is present. The transference number of an ion in a symmetrical electrolyte can be expressed in many equivalent forms such as

$$T = \frac{\lambda}{\Lambda} = \frac{\lambda/\gamma}{\Lambda/\gamma} = \frac{\lambda_i}{\Lambda_i},$$

where λ_i and Λ_i are conductances based on the actual concentration of the free ions and γ is the ratio of the concentration of free ions to the total salt concentration. Transference numbers are affected by association only in that they refer to a solution of free ion concentration $C\gamma$ where C is the salt equivalent concentration.

In the absence of association, the combination of conductance and transference data can be used to calculate the relaxation term since combination of equations (3) and (5) gives

$$1 + \frac{\Delta X}{X} = \frac{\Lambda}{\Lambda_0}\left(\frac{1 - 2T}{1 - 2T^0}\right). \tag{6}$$

If association is present, equation (6) yields $(1 + \Delta X/X)\gamma$. Analysis of conductance data by a suitable theory evaluates both of these terms as well as Λ_e; consequently, the use of transference data in this way provides an independent check on the theory.

A general expression for T^0 can be obtained from equation (5).

$$T^0 = T + \frac{(0.5 - T)}{\Lambda_0}\Lambda_e. \tag{7}$$

Evaluation of Λ_e using theoretical expressions allows a test of the theory through the constancy of the T^0 obtained and provides a convenient method of extrapolation.

In the limiting Onsager theory,[1] the electrophoretic term is given by

$$\Lambda_e = \beta C^{1/2} \tag{8}$$

and in the Fuoss-Onsager theory[2, 3] by

$$\Lambda_e = \frac{\beta}{1 + \kappa a} C^{1/2}, \tag{9}$$

where the symbols have their usual significance.

Unsymmetrical electrolytes present difficulties in this type of analysis. Dye and Spedding[7] have shown that although the Onsager theory does not account for the change of transference numbers with concentration, the inclusion of higher terms in the electrophoretic effect gives a much improved fit. However, if the inclusion of such terms is valid, it is not possible to calculate Λ_e from transference data because there is no simple relationship between λ_{e_1} and λ_{e_2}. A further problem arises if association is present since more than two conducting species are involved.

TABLE 1

THE EXPERIMENTAL ELECTROPHORETIC CONTRIBUTION TO THE EQUIVALENT CONDUCTANCE, Λ_e, AND A COMPARISON WITH VARIOUS THEORETICAL EXPRESSIONS

10^4C	T^+	Λ_e	T_0^+ (equation 8)	T_0^+ (equation 9)
	LiCl in H_2O			$\mathring{a} = 3.29$ $\Lambda_0 = 115.05$
0.0	(0.3371)		(0.3369)	(0.3371)
98.4	0.3291	5.4(0.1)	0.3380	0.3371
111.0	0.3287	5.6(0.1)	0.3381	0.3372
185.2	0.3264	7.1(0.1)	0.3387	0.3372
325.5	0.3234	9.1(0.1)	0.3400	0.3373
499.4	0.3210	10.3(0.1)	0.3416	0.3378
	NaCl in H_2O			$\mathring{a} = 3.23$ $\Lambda_0 = 126.58$
0.0	(0.3964)		(0.3960)	(0.3964)
100	0.3919	5.3(0.2)	0.3967	0.3965
200	0.3900	7.4(0.2)	0.3974	0.3964
500	0.3878	9.7(0.2)	0.3997	0.3974
	NaCl in CH_3OH			$\mathring{a} = 3.73$ $\Lambda_0 = 97.53$
0.0	(0.4634)		(0.4634)	(0.4635)
30	0.4603	7.6(0.4)	0.4637	0.4634
50	0.4595	9.4(0.4)	0.4640	0.4635
70	0.4587	11.1(0.4)	0.4641	0.4634
100	0.4583	11.9(0.4)	0.4649	0.4638
	LiCl in C_2H_5OH			$\mathring{a} = 4.4$ $\Lambda_0 = 38.94$
0.0	(0.4392)		(0.4392)	(0.4392)
9	0.4343	2.9(0.2)	0.4388	0.4385
15	0.4326	3.8(0.2)	0.4385	0.4380
25	0.4302	5.0(0.2)	0.4380	0.4372
	NaCl in C_2H_5OH			$\mathring{a} = 4.0$ $\Lambda_0 = 42.17$
0.0	(0.4812)		(0.4812)	(0.4812)
10	0.4796	3.3(0.6)	0.4809	0.4809
15	0.4791	4.2(0.6)	0.4808	0.4806
20	0.4788	4.8(0.6)	0.4807	0.4806
25	0.4782	5.4(0.6)	0.4804	0.4802

Results and Discussion.—Calculations of the experimental values of Λ_e from equation (5) were carried out for all available transference data with the necessary precision and over concentration ranges low enough to make the results meaningful. These data are given in Table 1 along with the measured transference numbers. The numbers in parentheses give the uncertainty in Λ_e based on an estimate of the precision of the measured transference numbers. The data for 1:1 electrolytes with transference numbers close to 0.5 have not been included since the variation with concentration is so small that even an estimate of Λ_e could not be obtained and almost any theory would fit the transference data. The transference data[8] for NaCl in 50 per cent methanol-water mixtures were not analyzed because they were independent of concentration in the dilute range in contrast to the expectations of theory. Whether this is due to experimental error or results from a specific effect in solvent mixtures is not known at this time.

The results are given in Table 1 for NaCl and LiCl in water[9] and in ethanol[10] and for NaCl in methanol.[11] In the last two columns are the limiting cation transference numbers, T_0^+, calculated at each concentration using equation (7) and the indicated electrophoretic expressions. If a constant T_0^+ was not obtained, a plot of T_0^+ was extrapolated to infinite dilution to give the limiting values in parentheses.

In order to be consistent, the values of Λ_0 and $\mathring{a}$ used to calculate the electrophoretic term were those obtained from a fit of the conductance data by the corresponding theory. The fit of conductance data by the Fuoss-Onsager theory has been given by Kay.[4] For solutions in ethanol, it was necessary to assume association constants of 27 and 44 for LiCl and NaCl respectively. Consequently, this was taken into account in calculating ionic concentrations. The dielectric constants and viscosities used in these calculations were 78.54 and 0.8949 centipoise for water; 32.64 and 0.5445 centipoise for methanol; 24.3 and 1.084 centipoise for ethanol. These values were used in place of more recent determinations[6] in order to be consistent with the constants used in the analysis of the conductance data.

Table 1 shows that the electrophoretic effect calculated from the limiting law, equation (8), is too large in aqueous and methanol solutions, whereas the introduction of $(1 + \kappa a)$ in the denominator, equation (9), gives a value of T_0^+ which is constant within experimental error up to concentrations corresponding to $\kappa a = 0.2$. For water this limiting concentration is 0.035 N while for methanol it is 0.01 N. It can be seen that Λ_e can be determined from transference data within a few tenths of a conductance unit depending on the magnitude of the difference between T^+ and 0.5. Transference measurements are now being carried out for LiCl in methanol and should give Λ_e within a tenth of a conductance unit.

An inspection of the results given in Table 1 for ethanol solutions shows that T_0^+ calculated from equations (8) and (9) are concentration dependent in a concentration range well below 0.07 N which corresponds to $\kappa a = 0.2$. This is displayed in Figure 1, where the experimental Λ_e values are compared with theory for both salts. On this scale, one cannot distinguish between the results obtained from equation (9) with $\mathring{a} = 4.0$ and with $\mathring{a} = 4.4$. It is to be emphasized that the values calculated with equation (9) have been corrected for the presumed association. The values calculated from the limiting law and from equation (9) can be seen to lie below the experimental values of Λ_e and only negative values of $\mathring{a}$ would

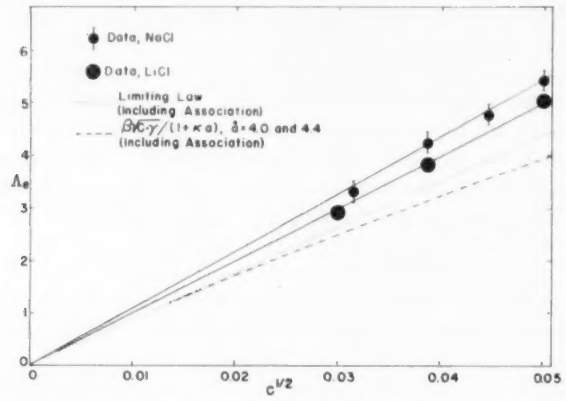

FIG. 1.—A comparison of the measured electrophoretic effect for NaCl and LiCl in ethanol solutions with that predicted by theory.

give agreement. As will be seen below this discrepancy in Λ_e can account for all the association required to fit the conductance data for these salts.

The experimental Λ_e values from transference numbers when combined with conductance data permit a calculation of the relaxation contribution to conductance provided association and other effects are absent. We define the quantity

$$\Delta\Lambda_r \equiv \Lambda - (\Lambda_0 - \Lambda_e)(1 - \alpha C^{1/2}) \tag{10}$$

so that $\Delta\Lambda_r$ contains the contribution to conductance from extended terms of the relaxation effect and from any association which may be present. In the absence of association, the extended Fuoss-Onsager equation predicts

$$\Delta\Lambda_r = EC \log C + J'(\mathring{a})C, \tag{11}$$

where

$$J'(\mathring{a}) = J(\mathring{a}) - \alpha\beta + \frac{\beta\kappa a}{C^{1/2}} \tag{12}$$

and the other symbols have their usual significance.[12] In the presence of association, equation (11) must be modified to

$$\Delta\Lambda_r = EC\gamma \log C\gamma + J'C\gamma - K_A C\gamma\Lambda f^2. \tag{13}$$

Equation (11) gives the correct values of $\Delta\Lambda_r$ for water and methanol solutions of the alkali halides investigated. This is to be expected since the Fuoss-Onsager theory agrees with the measured values of Λ and Λ_e. However, this theory uses equation (9) in an expanded form. Because of the large β for methanol and the dropping of significant higher-order terms in the expansion, an adjustment in the $\mathring{a}$ value of 0.2 must be made in order to bring the calculated and measured $\Delta\Lambda_r$ into agreement.

It is interesting to note, as indicated by Figure 2, that equation (11) also gives the correct values of $\Delta\Lambda_r$ for ethanol solutions indicating the absence of any significant association. The bottom curves, obtained from equation (13) using K_A and γ values from an analysis of the data by the Fuoss-Onsager equation[4] do not

agree with the experimental points. Thus, it appears that the treatment of conductance data by this method required the assumption of association because the value of the electrophoretic term obtained from equation (9) is smaller than the true value.

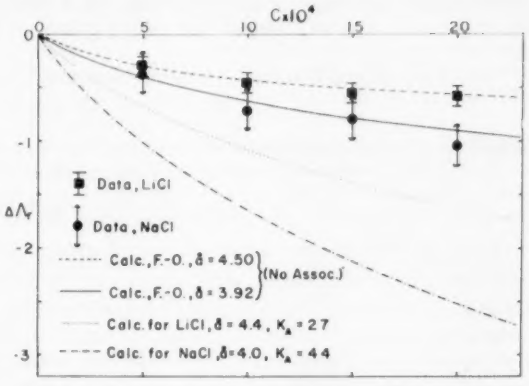

FIG. 2.—A comparison of the measured contribution to conductance from the extended terms of the relaxation effect for NaCl and LiCl in ethanol solutions with that obtained from equations (11) and (13).

The use of transference numbers outlined here affords an unambiguous method of separating the electrophoretic contribution to conductance from all other effects. Further studies of transference numbers should lead to a better evaluation of higher-order terms which in turn will enable association constants to be determined from conductance measurements with considerably more confidence. The results reported here for ethanol solutions suggest that other association constants evaluated from conductance data in the same range of dielectric constant are considerably in error. This treatment also emphasizes the necessity of measuring precise transference numbers as well as conductances in dilute nonaqueous solutions.

Since the electrophoretic effect can be obtained from transference numbers without requiring an adjustable parameter, it is possible to calculate salt diffusion coefficients at finite concentration from conductance, transference, and activity coefficient data. Possibly of more importance would be the determination of activity coefficients from diffusion measurements for solvents of very low dielectric constant for which reversible electrodes are not available. Methods are now available for the measurement of conductance, transference, and diffusion in such solvents.

*This work was supported by contract AT(30–1)2727 from the Atomic Energy Commission (R. L. K.) and by a grant from the National Science Foundation (J. L. D.).

[1] Onsager, L., *Physik Z.*, **28,** 277 (1927).

[2] Onsager, L., and R. M. Fuoss, *J. Phys. Chem.*, **36,** 2689 (1932).

[3] Fuoss, R. M., and L. Onsager, *J. Phys. Chem.*, **61,** 668 (1957); **62,** 1339 (1958).

[4] Kay, R. L., *J. Am. Chem. Soc.*, **82,** 2099 (1960).

[5] Stokes, R. H., *J. Am. Chem. Soc.*, **76,** 1988 (1954).

[6] Vidulich, G. A., and R. L. Kay, *J. Phys. Chem.*, **66,** 383 (1962).

[7] Dye, J. L., and F. H. Spedding, *J. Am. Chem. Soc.*, **76,** 888 (1954).

[8] Shemilt, L. W., J. A. Davies, and A. R. Gordon, *J. Chem. Phys.*, **16,** 340 (1948).

[9] Longsworth, L. G., *J. Am. Chem. Soc.*, **54,** 2741 (1932).

[10] Graham, J. R., and A. R. Gordon, *J. Am. Chem. Soc.*, **79,** 2350 (1957).

[11] Davies, J. A., R. L. Kay, and A. R. Gordon, *J. Chem. Phys.*, **19,** 749 (1951).

[12] Fuoss, R. M., and F. Accascina, *Electrolytic Conductance* (New York: Interscience Publishers Inc., 1959).

*THE BUOYANT BEHAVIOR OF VIRAL AND BACTERIAL DNA IN ALKALINE CsCl** †

By Jerome Vinograd, Janet Morris, Norman Davidson, and William F. Dove, Jr.

GATES AND CRELLIN LABORATORIES OF CHEMISTRY AND NORMAN W. CHURCH LABORATORY OF CHEMICAL BIOLOGY, CALIFORNIA INSTITUTE OF TECHNOLOGY

Communicated December 3, 1962

In equilibrium density gradient centrifugation, the banding polymer species is electrically neutral. The banding species for a negative polyelectrolyte with a polyanion P_n^{-zn} (where n is the degree of polymerization, and z the titration charge per monomer unit) in a CsCl salt gradient is $Cs_{zn}P_n$.[1] If the ion P_n^{-zn} is itself a weak acid, it may be titrated to the state $P_n^{-(zn+y)}$ by CsOH; the banding species is then $Cs_{(zn+y)}P_n$. Because of the large mass and high effective "density" of a Cs^+ ion, it is to be expected that the buoyant density in a CsCl gradient of a polymer acid will be increased by such a partial alkaline titration with CsOH. This expectation has been confirmed for polyglutamic acid (where $z = 0$ at low pH).[2] The guanine and thymine monomer units of DNA are weak acids. The present communication is concerned with the increase in buoyant density of DNA in alkaline CsCl solutions. It is well known that the guanine and thymine protons are more readily titrated in denatured DNA than in native DNA.[3] We find that the buoyant density of denatured DNA and of single strand φX-174 DNA gradually increases as the pH of the solution is increased beyond pH 9.8. The density of native DNA is not affected until a critical pH > 11 is reached, where the DNA abruptly denatures and increases in density. Similar increases in buoyant density have been observed independently by Baldwin and Shooter in their studies of 5$\overline{\text{BU}}$-substituted DNA's in alkaline solutions.[4]

Materials and Methods.—Materials: The *E. coli* DNA prepared by the method of Marmur[5] was a gift from Dr. P. O. P. Ts'o. The *M. lysodeikticus* DNA prepared by the method of Kirby[6] was a gift from Dr. T. W. Thompson. The T-4 DNA was prepared from T-4 $r+$ phage by the method of Mandel and Hershey.[7] Harshaw Chemical Company optical grade CsCl was used without further purification. Glass redistilled water was used.

Preparation of denatured DNA: The complementary DNA's were heat denatured by heating 40 γ/ml samples in 0.001 *M* tris buffer at pH 8 to 100°C for 10 min. The small containers were quickly chilled in ice and the contents poured onto solid CsCl. Samples of *E. coli* DNA were also alkali denatured at pH 12 at 100 γ/ml just prior to addition at 2γ/ml to buffered CsCl solution. The buoyant densities of alkali denatured material at pH 8 and pH 10.8 were the same as those found for the heat denatured material.

Buffer solutions: Solutions of 0.4 *M* reagent grade sodium carbonate or dibasic potassium phosphate were titrated with CO_2 gas or 50 per cent potassium hydroxide respectively to prepare carbonate buffers at pH 9.50 and 10.00 and phosphate buffers at pH 10.78, 11.18, 11.73, and 12.45. These solutions were stored in tightly closed polyethylene bottles and were checked frequently for pH.

Preparation of the alkaline DNA-cesium chloride solutions: The solutions for ultracentrifuge runs were prepared by volumetric additions of the following solutions to a 5 ml vial: CsCl, ρ = 1.900 gm/ml, 0.2 ml buffer, H_2O, and DNA solution to a final volume of 2.00 ml. The refractive index was checked, water or CsCl solution added if necessary, and 0.70 ml filled into the centrifuge cell. Without delay the remainder of the solution was poured into a 5 ml beaker and the pH measured with a small general purpose Beckman glass electrode, which had just been standardized against pH 10.0 buffer. For example, in the preparation of solutions for the φX-174 DNA buoyant

density study the following pH values were measured in the final solutions containing the above buffers at 0.04 *M*: 10.00, 10.50, 11.05, 11.50, 11.88, and 12.5. It is recognized that a potassium correction may be necessary for the more alkaline buffers. The pH values reported here are therefore regarded as reproducible instrument readings. It should be noted that the high concentration of CsCl is not likely to increase the junction potential because of the close similarity of the mobilities of the cesium and chloride ions.

Analytical ultracentrifuge: All runs were performed in Kel-F centerpieces in a Model E Spinco analytical ultracentrifuge at 25°. Two cells were run simultaneously and ultraviolet photographs of each cell were made with an alternating aperture mask. One cell of the pair was assembled with a lateral −1° bottom window. Both cells were assembled with longitudinal −1° windows. All runs were for at least 24 hr.

Measurement of buoyant density: The densities of the alkaline solutions were measured pycnometrically in 300 microliter pipets. Refractometry was avoided because of the complications caused by buffer addition. The buoyant density, i.e., the density of the solution in which the band forms at the root mean square position in a *ca.* 1.2 cm liquid column, was carefully determined for native T-4 DNA in alkaline solution between pH 8 and 10.8 and for denatured T-4 DNA between pH 11.5 and pH 12.5 by the procedure described by Vinograd and Hearst.[8] The T-4 DNA was used as a marker in the study of the other DNA's. In several twin-cell experiments the buoyant densities obtained in solutions buffered with cesium carbonate were compared with those in sodium or potassium carbonate solutions. The lighter cations caused a reduction of 0.006 gm/ml in the buoyant density. All of the measured buoyant densities in buffered alkaline solutions have been corrected by addition of 0.006 gm/ml.

Results.—The essential results are displayed in Figure 1. The buoyant densities of the native DNA's are substantially constant up to the pH at which denaturation occurs, and the density abruptly increases. The buoyant densities of denatured DNA's and of φX-174 DNA increase by about 0.045 units over about one unit of pH. This increase results from the titration of guanine and thymine residues.

Titration curves for single strand DNA's: The titration curve of a monomer acid has a width of two pH units between the 10 and 90 per cent titration points. The titration curve of a typical polyelectrolyte acid at moderate salt concentrations is usually several pH units broader than the titration curve of the monomer and the midpoint is displaced somewhat to higher pH, because of electrostatic repulsion effects.

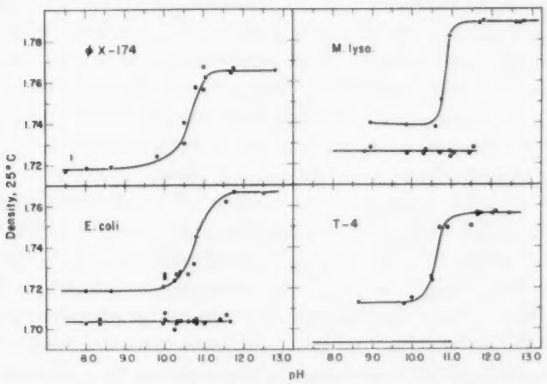

FIG. 1.—Buoyant densities of several DNA's as a function of pH at 25°. In each case the lower set of points is for the native material. The data for native T-4 DNA are not shown. Twenty-one concordant points were obtained with a standard deviation of ±0.0026.

The midpoints and 10–90 per cent widths of the density titration curves for φX-174 DNA and the heat denatured DNA's are: φX DNA, 10.6, 1.1; T-4 phage DNA, 10.6, 0.6; *M. lysodeikticus* DNA, 10.8, 0.4; *E. coli* DNA, 10.7, 1.1. The pK's of guanylic and thymidylic acids in dilute aqueous solution are reported as 9.7 and 10.0;[9] the pK of 5′ guanylic acid in 6.4 *M* CsCl is 9.9,[10] and we assume that CsCl has a similar small effect on thymidylic acid. The buoyant density change is probably approximately proportional to the degree of titration. Thus the titration curves for the denatured DNA's are displaced to higher pH by about one unit compared to the monomer but are narrower. The combination of displacement and sharpening shows that there are cooperative effects due to a substantial amount of base pairing in the denatured state before titration. Electrostatic shielding effects in the concentrated CsCl solution may also contribute to the lack of broadness in the titration curve.

The alkaline titration curves of denatured DNA at moderate ionic strengths (e.g., 0.10 *M*) also seem to be relatively narrow and displaced to high pH because of residual base pairing.[3] The optical properties of denatured DNA also indicate residual secondary structure.[11]

Density changes, secondary structure, and hydration: The buoyant densities are listed in Table 1. We observe the following relations for the complementary DNA's. The change in buoyant density in going from the native material to the fully titrated denatured form at alkaline pH is constant (*N*–*L* in Table 1). The

TABLE 1

BUOYANT DENSITIES OF NATIVE AND DENATURED DNA'S AS A FUNCTION OF pH

DNA	Mole fraction *GC*	Native pH 7–9 *L*	Denatured pH 7–9 *M*	Denatured alkaline *N*	Density shifts *M*–*L*	Density shifts *N*–*M*	Density shifts *N*–*L*
T-4	0.34	1.693	1.712_5	1.756	0.019_5	0.043_5	0.063
E. coli	0.50	1.704	1.719	1.766	0.015	0.047	0.062
M. lysodeikticus	0.72	1.726	1.739	1.788_5	0.013	0.049_5	0.062_5
φX-174	...	...	1.718	1.765	...	0.047	...

buoyant density change on denaturation at neutral pH (*M*–*L*) decreases with increasing GC content. Correspondingly, the density change on alkaline titration of the denatured DNA's (*N*–*M*) increases with increasing GC content. These trends indicate that the amount of secondary structure in the denatured DNA's at pH 7 increases with GC content. The fact that there is no dependence on base composition for the total density change from the neutral to the fully titrated material shows that the amount of residual secondary structure in the fully titrated DNA's is independent of base composition and is probably zero.

The average G + T content of the denatured DNA's derived from a complementary two-stranded DNA is 0.50 mole fraction, but the G + T content of φX DNA is 0.57.[12] From this factor alone, the density change for complete alkaline titration of φX DNA would be predicted to be 14 per cent greater than for a complementary DNA. The observed density change is about the same as for the complementary DNA's. The discrepancy may be due to a smaller amount of secondary structure in φX DNA, or it may be due to other structural effects, depending on base composition, which are not understood. (The optical data suggest that φX DNA is not deficient in secondary structure as compared to denatured DNA.[12])

The buoyant density change of a denatured DNA for complete alkaline titration

is less than expected for replacement of a covalently bound hydrogen atom by an anhydrous cesium ion. The following calculation indicates that the net hydration of the DNA increases upon alkaline titration. Consider T-4 DNA, for which the amount of secondary structure in the denatured form is the least of the three complementary DNA's studied. Take 2.12 as the buoyant density of anhydrous T-4 DNA;[13] and 944 as the formula weight of a Cs_2B_2 base pair (where B is a nucleotide monomer). Assume that the actual buoyant density of 1.712 in 7 *M* CsCl implies hydration by water with a density of 1.00. One then calculates that there are 14 molecules of water of hydration per base pair. The fully titrated alkaline DNA has a formula of Cs_3B_2; the formula weight per base pair is 1076. Assume a difference of molar volume for the anhydrous Cs^+ ion and displaced hydrogen atom of 32 cc.[13] The density of 1.756 in alkali corresponds to a hydration of 17 molecules of water per base pair. Such an increase in hydration of about 3 molecules of water per additional charge seems reasonable.

Band widths and the problem of complement separation: For a two-stranded Watson-Crick base-paired DNA, $X_A = X_T$ and $X_G = X_C$, so that $X_T + X_G$ is 0.50 mole fraction (where X_A is the mole fraction of adenine, etc.). There is no requirement however that $X_T + X_G$ in one strand should equal $X_T + X_G$ in the other. Thus, density gradient centrifugation in alkaline solution offers the possibility of separation of complementary strands. The fact is however that we observed no bimodal density distributions for the complementary DNA's in alkaline solution. In general, broader bands were observed for the fully titrated denatured materials at alkaline pH's than for the native DNA's at pH 7. This broadening might in part be due to the separation of complementary strands but it could also be due to a pronounced decrease in molecular weight and/or an increase in density heterogeneity resulting from single strand breaks present in the initial material. (We have ourselves obtained no evidence that the two strands of a complementary DNA do come apart on alkaline denaturation. However it has been reported that upon denaturation at pH 12 of heavy isotope hybrid *E. coli* DNA followed by density gradient centrifugation at pH 7, two bands are formed.[14] This shows that the two strands do come apart.) The possible separation of complementary strands from the DNA's of certain viruses by density gradient centrifugation of denatured materials at neutral pH has recently been reported.[15]

In order to minimize the amount of breakage during preparation, an experiment was done in which T-4 DNA was prepared by adding the bacteriophage directly to the centrifuge cell and then adding CsCl at pH 11.5. The optical density in the band indicated substantially complete lysis. The buoyant density was as expected, and the band profile corresponded now to an anhydrous molecular weight for Cs DNA of thirty million, approximately half the value obtained in comparable experiments at neutral pH with phenol extracted T-4 DNA. Thus again there is no clear evidence for complement separation.

Two experiments were performed with protoplasts from *E. coli* K12, which were lysed directly in the centrifuge cell by adding 0.010 ml of water at 5°C to 0.002 ml of a suspension containing 10^8 protoplasts. The addition of alkaline CsCl, pH 11.5, and subsequent centrifugation first at 10° and then at 25°, gave two native DNA bands at both temperatures, with densities close to 1.71 and differing by about 0.002. Each of these bands was approximately $^1/_5$ as wide as is normal for *E. coli* DNA

prepared by the variety of procedures discussed by Marmur.[5] In these experiments the alkaline hydrolysis of the sedimented RNA was signalized by the gradual invasion of the bottom fourth of the cell by optically absorbing material. It is apparent that the DNA in this organism under conditions in which deproteination is extensive is in a higher molecular weight form than has previously been observed in banding experiments. This result is consistent with the autoradiographic findings of very long DNA obtained by gentle lysis.[16] At the present time the significance of the duality of the *E. coli* DNA is not understood. These incomplete experiments are mentioned merely to suggest that alkaline CsCl may be a useful reagent for the extraction of DNA from viruses and bacteria with a minimum amount of degradation.

An important question for this study is the stability of DNA in alkaline solution. Some preliminary experiments bearing on this point have been made. A series of solutions containing 1 γ/ml of φX DNA were prepared in CsCl at varying pH and a final density of 1.70 gm/ml. These solutions were stored at 25°C for 48 hr and then assayed by the *E. coli* K-12 protoplast procedure of Guthrie and Sinsheimer.[17] The infectivities of the samples expressed as per cent survivors and normalized with the result obtained at pH 8.5 were 60, 67, 25, 44, and 25 at pH's 10.0, 10.5, 11.5, 12.0, and 12.5 respectively. These results indicate an average of about one lethal hit per φX-174 molecule in 48 hr at pH 11 (MW = 1.7×10^6). However it is clear from the sharpness of the T-4 bands in the fully titrated single strand material referred to above that there is not more than one or two physical breaks per molecule of 6×10^7 molecular weight in a typical 64-hr centrifuge experiment at alkaline pH. It has been reported that in 0.20 *M* NaOH–1% CH_2O at 25°, denatured T-4 DNA suffers one chain break per molecule per 40 hr.[18]

Denaturation and renaturation: Renaturation was observed with heat or alkali denatured T-4 DNA at pH's between 10.5 and 10.9. With amounts of DNA of the order of 40 μg/ml at band center, bands formed at the expected position for denatured DNA and then moved in the course of 20 hr and fused with the native band present as a marker. This renaturation was not observed when the concentration was reduced by a factor of 5 to 10. Thus, the renaturation is concentration dependent. At pH 7 at room temperature, quenched, denatured T-4 DNA was not observed to renature in the centrifuge. This is presumably due to the stability of the randomly formed hydrogen bonds. At pH 10.5 to 10.9, there is considerable dissociation of the short ordered regions and the conditions for reannealing are more favorable.

A few experiments were performed to observe the melting of native T-4 DNA at pH 10.8. After formation of the native band in the centrifuge at 25°, the temperature was gradually raised. In one experiment a melting point of 31° was found and the expected band shift of about 0.053 density units was seen. In a second experiment the melting point was apparently over 40°. These results show that melting studies can be performed at sedimentation equilibrium in a density gradient, but require very close pH control.

Summary.—Denatured DNA increases in buoyant density by about 0.045 density units in alkaline CsCl solution because of the titration of the N–H protons of the thymine and guanine residues. The pH at the midpoint and the narrow width of the titration curve indicate considerable residual hydrogen bonding in the denatured

state at neutral pH. The density of native DNA is not affected until a critical pH > 11 is reached, where the DNA abruptly denatures and increases in density. The change in buoyant density in going from the native material at neutral pH to the fully titrated denatured form at alkaline pH is constant and independent of the base composition. Density gradient centrifugation in alkaline CsCl has been demonstrated to be a useful method for the separation of native and denatured DNA. It may also be useful for the separation of complementary strands.

A neutral formaldehyde solution has been recommended as a medium for the study of single stranded DNA's obtained by denaturation without complications due to reannealing.[19] Alkaline solutions (without formaldehyde) are versatile in that at a pH somewhat below the critical pH for denaturation they are good reannealing media; at a higher pH, they are probably suitable for the study of independent separated strands.

We are indebted to Dr. G. D. Guthrie who performed the infectivity assays for φX-174 DNA.

* Supported by U.S.P.H.S. Grants No. HE-03394 and AM-03907.

† Contribution No. 2911 from the Gates, Crellin, and Church Laboratories.

[1] The buoyant density of DNA decreases when LiBr is added to a DNA solution in CsBr because of preferential binding of the Li^+ by the DNA (Hearst, J. E., and J. Vinograd, these PROCEEDINGS, **47,** 825 (1961)); in pure CsBr however, the buoyant species must be the CsDNA salt, irrespective of the amount of ion association between the polyanion and the Cs^+ ions.

[2] Vinograd, J., and J. Morris, private communication.

[3] See, for example, Jordan, D. O., *The Chemistry of Nucleic Acids* (Washington: Butterworth, 1960), pp. 169–173.

[4] Baldwin, R. L., and E. Shooter, private communication.

[5] Marmur, J., *J. Mol. Biol.*, **3,** 208 (1961).

[6] Kirby, K. S., *Biochem. J.*, **66,** 495 (1957).

[7] Mandel, J. D., and A. D. Hershey, *Anal. Biochem.*, **1,** 66 (1960).

[8] Vinograd, J., and J. E. Hearst, in *Progress in the Chemistry of Organic Natural Products* (Berlin: Springer-Verlag, 1962), Vol. 20, p. 395.

[9] Huist, R. O., A. M. Marko, and G. C. Butler, *J. Biol. Chem.*, **204,** 842 (1953).

[10] Jensen, R., private communication.

[11] Doty, P., H. Boedtker, J. R. Fresco, R. Haselkorn, and M. Litt, these PROCEEDINGS, **45,** 482 (1959).

[12] Sinsheimer, R., *J. Mol. Biol.*, **1,** 37 (1959).

[13] Hearst, J. E., *J. Mol. Biol.*, **4,** 415 (1962).

[14] Cox, R., J. Marmur, and P. Doty, unpublished, quoted by Schildkraut, C. L., J. Marmur, and P. Doty, *J. Mol. Biol.*, **3,** 595 (1961).

[15] Cordes, S., H. T. Epstein, and J. Marmur, *Nature*, **191,** 1097 (1961).

[16] Cairns, J., *J. Mol. Biol.*, **4,** 407 (1962).

[17] Guthrie, G. D., and R. L. Sinsheimer, *J. Mol. Biol.*, **2,** 297 (1960).

[18] Berns, K. I., and C. A. Thomas, *J. Mol. Biol.*, **3,** 289 (1961).

[19] Thomas, C. A., and K. I. Berns, *J. Mol. Biol.*, **4,** 308 (1962).

GENERALIZED RIEMANNIAN GEOMETRY, II

By Luther P. Eisenhart

DEPARTMENT OF MATHEMATICS, PRINCETON UNIVERSITY

Communicated November 19, 1962

What follows is an addition to my paper with the same title published in these Proceedings, **48,** 1529–1531 (1962).

The geometry is based upon the equations

$$g_{ij,k} = g_{ih}\Gamma^h_{jk} + g_{hj}\Gamma^h_{ik}, \tag{1}$$

where g_{ij} are the nonsymmetric components of the matrix tensor of the space of n dimensions and the Γ's are generalized Christoffel symbols of Riemannian geometry. This type of notation is used in what follows. When in a term there is the same upper and lower index, as h in equation (1), the term stands for the sum of terms as the index takes the values 1 to n. This notation is used in what follows.

Equation (1) is satisfied identically by

$$g_{ih}\,\Gamma^h_{jk} = {}^1/_2\, g_{ij,k} \tag{2}$$

$$g_{hj}\,\Gamma^h_{ik} = {}^1/_2\, g_{ij,k}. \tag{3}$$

In like manner, the equation

$$g_{ji,k} = g_{jh}\,\Gamma^h_{ik} + g_{hi}\,\Gamma^h_{jk} \tag{4}$$

is satisfied by

$$g_{jh}\,\Gamma^h_{ik} = {}^1/_2\, g_{ji,k} \tag{5}$$

$$g_{hi}\,\Gamma^h_{jk} = {}^1/_2\, g_{ji,k}. \tag{6}$$

Given the equations

$$g_{ih}g^{ih} = 1, \quad g_{jh}\,g^{jh} = 1, \tag{7}$$

where i and j are summed and h is not summed.

When equation (2) is multiplied by g^{ih} and summed for i, by (7) the result is

$$\Gamma^h_{jk} = {}^1/_2\, g^{ih}g_{ij,k} = {}^1/_2\, g^{mh}g_{mj,k}. \tag{8}$$

When equation (5) is multiplied by g^{jh} and summed for j, by (7) the result is

$$\Gamma^h_{ik} = {}^1/_2\, g^{jh}g_{ji,k} = {}^1/_2\, g^{mh}g_{mi,k}. \tag{9}$$

When k is replaced by j in this equation, the result is

$$\Gamma^h_{ij} = {}^1/_2\, g^{mh}g_{mi,j}. \tag{10}$$

The function Γ^h_{ijk} is defined by the equation

$$\Gamma^h_{ijk} = \Gamma^h_{ij,k} - \Gamma^h_{ik,j} + \Gamma^l_{ij}\,\Gamma^h_{lk} - \Gamma^l_{ik}\Gamma^h_{lj} \tag{11}$$

and is a generalization of the function R^h_{ijk} of Riemannian Geometry.[1]

For expressions of the type (10), equation (11) becomes

$$\Gamma^h_{ijk} = {}^1/_2\, g^{mh} g_{mi,jk} + {}^1/_2\, g^{mh}{}_{,k} g_{mi,j} - {}^1/_2\, g^{mh} g_{mi,kj} - {}^1/_2\, g^{mh}{}_{,j} g_{mi,k} + {}^1/_4\, g^{ml} g_{mi,j} g^{rh} g_{ri,k} - {}^1/_4\, g^{ml} g_{mi,k} g^{rh} g_{ri,j},$$

which reduces to

$$\Gamma^h_{ijk} = {}^1/_2 (g_{mi,j} g^{mh}{}_{,k} - g_{mi,k} g^{mh}{}_{,j}) + {}^1/_4\, g^{ml} g^{rh} (g_{mi,j} g_{ri,k} - g_{mi,k} g_{ri,j}).$$

The derivation of this equation is the purpose of this paper.

[1] Eisenhart, Luther P., *Riemannian Geometry* (Princeton University Press, 1949), equation (8.3), p. 19.

---

*RELATIVE HOMOLOGICAL ALGEBRA MADE ABSOLUTE**

BY PETER FREYD

DEPARTMENT OF MATHEMATICS, UNIVERSITY OF PENNSYLVANIA

Communicated by Saunders Mac Lane, November 14, 1962

Consider an abelian category $\mathfrak{A}$ together with a class of exact sequences E, satisfying the usual requirements needed for relative homology as described by Buchsbaum,[1] Heller,[3] Butler and Horrocks,[2] *et al.*

Let $(\mathfrak{A}^*, \mathfrak{S})$ be the category of all additive contravariant functors from $\mathfrak{A}$ into the category of abelian groups $\mathfrak{S}$, and define the functor $H: \mathfrak{A} \to (\mathfrak{A}^*, \mathfrak{S})$ to be that which assigns to each object $A \in \mathfrak{A}$ the group-valued functor $\mathrm{Hom}(-, A)$. Let $\mathfrak{L}_E(\mathfrak{A}^*)$ be the full subcategory of $(\mathfrak{A}^*, \mathfrak{S})$ consisting of all E-left-exact functors and define $H: \mathfrak{A} \to \mathfrak{L}_E(\mathfrak{A}^*)$ in the same way. Note that if E is the class of splitting sequences then $\mathfrak{L}_E(\mathfrak{A}^*) = (\mathfrak{A}^*, \mathfrak{S})$.

THEOREM 1. *$\mathfrak{L}_E(\mathfrak{A}^*)$ is an abelian category with enough injectives. The functor $H: \mathfrak{A} \to \mathfrak{L}_E(\mathfrak{A}^*)$ is left-exact, E-right-exact and carries* only *E-right-exact sequences into right-exact sequences.*

(The proof that $\mathfrak{L}_E(\mathfrak{A}^*)$ is abelian is not formal. One first constructs an adjoint of the inclusion functor $\mathfrak{L}_E(\mathfrak{A}^*) \to (\mathfrak{A}^*, \mathfrak{S})$. Such an adjoint, it may be noted, assigns to each group-valued functor its 0th-E-right-derived functor.)

THEOREM 2. *Let $\mathfrak{B}$ be any abelian category complete with respect to arbitrary direct sums, and let $F: \mathfrak{A} \to \mathfrak{B}$ be any additive functor. There exists (uniquely up to isomorphism) a right-exact and direct-sum-preserving functor $\bar{F}: (\mathfrak{A}^*, \mathfrak{S}) \to \mathfrak{B}$ such that*

$$\begin{array}{ccc} \mathfrak{A} & \to & (\mathfrak{A}^*, \mathfrak{S}) \\ & \searrow \swarrow & \\ & \mathfrak{B} & \end{array}$$

commutes. Moreover, given two functors $F_1, F_2: \mathfrak{A} \to \mathfrak{B}$ and a natural transformation $\eta: F_1 \to F_2$ there exists a unique extension $\bar{\eta}: \bar{F}_1 \to \bar{F}_2$ between any two extension functors as described above.

By restriction, we obtain a similar extension theorem for $\mathfrak{L}_E(\mathfrak{A}^*)$. A difficulty in its statement arises from the following: the inclusion functor $\mathfrak{L}_E(\mathfrak{A}^*) \to (\mathfrak{A}^*, \mathfrak{S})$ is left-exact but not right-exact and consequently the condition that the extension to $\mathfrak{L}_E(\mathfrak{A}^*)$ be right-exact will fail. We may, however, simply define the *canonical*

extension of $F_1\mathfrak{A} \to \mathfrak{B}$ to $\mathfrak{L}_E(\mathfrak{A}^*)$ to be that which arises (through restriction) by extending to a right-exact, direct-sum-preserving functor on $(\mathfrak{A}^*,\mathfrak{S})$.

THEOREM 3. *Given two functors $F_1,F_2:\mathfrak{A} \to \mathfrak{B}$ and an E-connecting homomorphism from F_1 to F_2, let $\bar{F}_1:\mathfrak{L}_E(\mathfrak{A}^*) \to \mathfrak{B}$ be the canonical extension of F_1 and $\bar{F}_2:\mathfrak{L}_E(\mathfrak{A}^*) \to \mathfrak{B}$ any extension of F_2. Then there is a unique* absolute *connecting homomorphism from $\bar{F}_1$ to $\bar{F}_2$ which when restricted to $\mathfrak{A}$ is the given E-connecting homomorphism.*

The E-satellites of a functor on $\mathfrak{A}$ may then be computed by first extending to $\mathfrak{L}_E(\mathfrak{A}^*)$, computing the absolute satellites of the extension, and finally restricting back to $\mathfrak{A}$. Even in the case that E is the class of all exact sequences, the result is useful; since $\mathfrak{L}_E(\mathfrak{A}^*)$ has enough injectives, all questions about the existence of satellites are answered.

Define $\mathfrak{A}_E$ to be the full subcategory of $\mathfrak{L}_E(\mathfrak{A}^*)$ of objects C such that there exist objects C_1 and C_2 in the image of $H:\mathfrak{A} \to \mathfrak{L}_E(\mathfrak{A}^*)$ and an exact sequence

$$C_1 \to C_2 \to C \to 0.$$

$\mathfrak{A}_E$ is an abelian category and the inclusion functor $\mathfrak{A}_E \to \mathfrak{L}_E(\mathfrak{A}^*)$ is exact. Again by restriction, Theorem 3 is true for $\mathfrak{A}_E$ in place of $\mathfrak{L}_E(\mathfrak{A}^*)$. Whereas we lose the existence of enough injectives, we gain the following.

THEOREM 4. *The functor $H:\mathfrak{A} \to \mathfrak{A}_E$ has an adjoint. The class E, therefore, arises from a pair of adjoint functors; that is, a short exact sequence is E-exact if and only if its image under the first functor in the pair is exact.*

From the beginning, the condition that $\mathfrak{A}$ be abelian was somewhat extraneous. It suffices to let $\mathfrak{A}$ be an additive category and to require that E be abelian in the sense of Heller.

* This work was partially supported by the National Science Foundation.

[1] Buchsbaum, D. A., *Ann. Math.*, **69**, 66–74 (1959).
[2] Butler, M., and G. Horrocks, *Phil. Trans. Roy. Soc.*, **A254**, 155–222 (1961).
[3] Heller, A., *Ann. Math.*, **68**, 484–525 (1958).

THE SAMPLING DISTRIBUTION OF PRIMES

BY D. D. KOSAMBI

P. O. DECCAN GYMKHANA, POONA 4, INDIA

Communicated by H. S. Vandiver, November 2, 1962

The real half-line $x \geq x_0 \geq 2$, upon which the integers are marked off unit distance apart, is mapped onto $y \geq 0$ by the transformation $y = \int_{x_0}^{x} dt/\log t = \mathrm{li}(x) - \mathrm{li}(x_0)$. Cover the whole of $y \geq 0$ by a sequence of intervals, each of length $u > 0$, fixed. The nth such interval will be $(n-1)u \leq y < nu$, and $\pi_n(u) = \pi(x_0, u; n)$ denotes the number of primes in its x-image. We show that the primes in an arbitrary connected stretch of the y-line have a Poisson distribution in the sense of probability theory, the sequences $\pi_n(u)$ constituting statistical *samples* thereof. Hereafter, take all positions of the initial point (on the y-line) as equally likely and x_0 neither restricted nor specified otherwise.

Textbook results in number theory and probability theory are taken for granted. In particular,

LEMMA 1. *The number of primes $p \leq x$ is $\sim li(x) \sim y$ (for any x_0, as $x \to \infty$). If $\vartheta(x) = \sum \log p$, $p \leq x$, then $\vartheta(x) \sim x$. If p_k be the kth prime in order, starting from $p_1 = 2$, then $p_k \sim k \log k$.*

The first of these is the prime-number theorem,[1] and the other two are equivalent, as is well known.

LEMMA 2. *For $p \leq x$, $\Pi(1 - 1/p) \sim e^{-\gamma}/\log x$; γ, Euler's constant.*

This is a classical theorem of Mertens.[2]

LEMMA 3. *If for any set Z of primes, $\Pi p = x$, $p \subset Z$, then $\Pi(1 - 1/p)^{-1}$ is less than $C \log_2 x$, $p \subset Z$, x large.*

Proof: The product of $(1 - 1/p)^{-1}$ will be greatest for any given number of primes if the primes are 2, 3, . . . in sequence and all distinct. Then $\log x = \log \Pi p = \sum \log p$ by hypothesis, $p \subset Z$. Lemma 1 says that, packing the primes at the beginning of the sequence, $\max p \sim \sum \log p$, and here $\sum \log p = \log x$. By Lemma 2 (the product being not greater than in this case) $\Pi(1 - 1/p)^{-1} < C \log_2 x$, $p \subset Z$. *Q.E.D.*

LEMMA 4. *The proportion of u-intervals for which $\pi(x_0,u,n) \geq 2$ is less than cu^2 for small u, regardless of x_0, if x is large.*

Proof: The sieve of Viggo Brun leads to the theorem:[3] *The number of primes $p \leq x$ for which $p + b$ is also a prime is $< (cx/\log^2 x)\Pi(1 - 1/p)^{-1}$, $p \mid b$.* The u-intervals containing two or more primes must contain one such pair $p, p + b$ for some $b \leq u \log x$ approximately. Not all b, however, are admissible, as no odd b will do for $p > 2$. The number of admissible b's within the same u-interval is easily seen to be not greater than the number of integers in (the x-image of) the covering interval prime to $N = 2.3 \ldots p$, provided $N \leq u \log x$. Clearly, $p + b$ not a prime to N cannot be a prime except in the interval that begins from $x_0 = 2$, which may be ignored; moreover, such numbers are arranged cyclically modulo N, which, being about the length of the interval on the x-axis, cannot be materially changed in the vicinity of any given x. By Lemmas 2 and 3, the admissible set will contain less than $c'u \log x/\log_3 x$ members, for large x. The bound for $\Pi(1 - 1/p)^{-1}$ for primes dividing any b in the interval cannot ultimately be greater than $c'' \log_3 x$. Finally, the total number of covering intervals in the range is $\sim x/u \log x$. The estimate therefore is not in excess of $(cx/\log^2 x)(c'u \log x/\log_3 x)(c'' \log_3 x)(u \log x/x) = \bar{c}u^2$. *Q.E.D.*

LEMMA 5. *If $f_0, f_1, f_2, \ldots$ be the relative frequencies, $\sum f_i = 1$, with which small u-intervals containing 0,1,2, . . . primes occur in a large range of x, then $f_1 = u + o(u)$.*

Proof: Corresponding to the theorem cited in the proof of Lemma 4 is an extension by P. Erdös:[4] *The number of primes $p \leq x$ for which all the numbers $p + b_1, p + b_2, \ldots p + b_r$, $0 < b_1 < b_2 < \ldots < b_r$ are also primes is less than*

$$(cx/\log^{r+1} x) \prod_{p \mid E} (1 - 1/p)^{-(r+1-\omega(p))}, \qquad E = \prod_{i=1}^{r} b_i \prod_{1 \leq i < k \leq r} (b_k - b_i) \quad (1)$$

where $\omega(p)$ is the number of solutions mod p of $m(m + b_1) \ldots (m + b_r) \equiv 0 (\mathrm{mod}\ p)$. From this point, the reasoning of the previous lemma holds, except that the number of choices for the set of r b's will not exceed the binomial coefficient ${}^nC_r$, with $n = c \log x/\log_3 x$ and $\Pi p, p \mid E$ cannot exceed $(u \log x)^m$, with $m = r^2(r - 1)/2$ (an overestimate which we shall not stop to refine). The upper bound, for small u, is therefore $cu^{r+1}/r!$ for each r, and the same c may be taken throughout, quite ob-

viously. For any u, the contribution of $f_2, f_3, \ldots$ to the expectation (mean value, average) of primes per covering interval may be assessed as not exceeding cu^2e^u. For, this mean value is $(0.f_0 + 1.f_1 + 2.f_2 + \ldots)$, so that f_0 contributes nothing. Any term from f_2 onwards, as assessed above, will contribute $0(u^2)$. The total contribution of those terms will be $0(u^2e^u)$, as may be seen from the upper bounds just given above. Now the mean value, by the prime number theorem, is exactly u, over the whole y-line, no matter what the x_0. It follows that for small u, $f_1 = u + 0(u^2)$. *Q.E.D.*

THEOREM. *With all x_0 equally likely, the probability that exactly r primes will lie in the x-image of $O \leq y < t$ is $e^{-t}t^r/r!$ (the Poisson distribution, with parameter t).*

Proof: Given x_0, there is no question of any probability; the entire sample is completely defined for the whole y-line. But under the present conditions, the irregularity of primes permits the use of the concept "probability" the "event" being 0, 1, 2, ... primes lying in the interval $0 \leq y < t$. These events are exhaustive and mutually exclusive. The conditions for a Poisson process are given by the following postulates:[5] The probability for one prime in $t \leq y < t + h$ for small h is $h + o(h)$; the probability for more than one prime in the small interval is $o(h)$; the probability for the small interval being totally void of primes is $1 - h + o(h)$. Lastly, none of these are affected if it is known that k primes have actually occurred in $0 \leq y < t, k = 0, 1, 2 \ldots$.

These postulates are obviously satisfied in view of our lemmas above. Lemma 4 says that the probability (approximated arbitrarily closely by the corresponding frequency) for more than one prime in the small interval is $o(h)$. Lemma 5 gives the probability for a single prime as $h + o(h)$. Since these two cases and that of the h-interval being void of primes are mutually exclusive and exhaustive, the third postulate is satisfied. Finally, the lemmas hold regardless of x_0 and t, over the whole of the y-line, $y > t$. Moreover, the number of primes known to have occurred in $0 \leq y < t$ does not in any way affect the frequencies or probabilities or permit x_0 to be determined even approximately. (It is possible to go much further in this direction, for not even the precise knowledge of the points $t_1, t_2, \ldots$ at which these primes may actually have occurred changes the situation. If it could then be said that there *must* exist a prime in $t \leq y < t + h$, no matter how small the h, it would follow that the $k + 1$st prime could be located from the positions on the y-line of the first k, for all large primes and some k. This implies a recurrence relation between the primes; no such relation is known and an algebraic one of any finite degree is demonstrably impossible. There is no finite upper bound for the gap between consecutive primes on the y-line[6] and no known positive lower bound. On the other hand, it is known that subsequences of primes (of positive density) exist[7] for which the y-distance between consecutive primes is dense over a certain positive range, whose precise termini are not known. This shows the impossibility of using any but probability methods.) *Q.E.D.*

The Poisson distribution of our theorem may be quickly derived as follows. For the argument, allow x to be any point (with equal likelihood) of a range $R(x) \approx x^\alpha$, $38/61 < \alpha < 1$. It is known (Ingham, A. E., *Quart. J. Math.*, **8**, 255–266 (1937)) that the prime-number theorem holds asymptotically over $R(x)$ as $x \to \infty$. Further, let $I(x)$ be a randomly selected interval within $R(x)$ of y-length t, hence containing $\sim t \log x$ integers regardless of position (since the variation in $\log x$ is

negligible over $R(x)$). No matter where $I(x)$ is located, alternate integers in it must be even, four out of every six (regularly arranged) divisible by 2 or 3, etc. This regularity of deletion by the sieve of Eratosthenes extends to all the smallest primes whose product $2.3.5 \ldots p = N \leq t \log x$. About $te^{-\gamma}\log x/\log_3 x = tg(x)$ integers in $I(x)$ will survive. Any p not a factor of N need not be the smallest prime factor of a surviving integer in $I(x)$ and a prime larger than $t \log x$ need not even have a multiple in $I(x)$, so that one of the "survivors" being deleted by any such prime is now a matter of chance with probability $1/p$. By the prime number theorem, the expectation of primes in $I(x)$ is exactly t (in the limit), hence the compound probability for primality of a "survivor" is asymptotic to $1/g(x)$. Moreover, if some k of these survivors be tested and found composite or prime (without revealing their numerical values), the knowledge does not modify the probability for primality for the rest. In all this, x is merely a background parameter, whose principal use is to furnish relative magnitudes of the various functions involved, as $x \to \infty$.

It follows that if P_r be the probability for precisely r primes in $I(x)$, then in the limit $P_0 = \lim(1 - 1/g)^{tg} = e^{-t}$. Using textbook definitions and procedures, the limit $P_1 = \lim(1 - 1/g)^{tg-1}(tg)(1/g) = te^{-t}$, and so on, with limit $P_r = e^{-t}t^r/r!$ But any limiting distribution over $R(x)$ as $x \to \infty$ will obviously be the distribution over the entire x-line, here the Poisson distribution with parameter t, as before.

[1] Prachar, K., *Primzahlverteilung* (Berlin, 1957), ch. 3.

[2] Hardy, G. H., and E. M. Wright, *An Introduction to the Theory of Numbers* (Oxford University Press, 1945), Theorem 430, pp. 349–354.

[3] Prachar, K., *op. cit.*, ch. 2, Theorem 4.4.

[4] *Ibid.*, Theorem 2.4.7.

[5] Feller, W., *An Introduction to Probability Theory and Its Applications* (New York: 1950), vol. 1, p. 366 *et passim*.

[6] For general known results on gaps in the sequence of primes, see Prachar, *op. cit.*, p. 154 ff.

[7] Ricci, G., "Sul pennello di quasi-asintoticità delle differenze di interi primi consecutivi," *Rend. Atti. Accad. Naz. Lincei*, **8**, 192–196 and 347–351 (1954–5).

DEPRESSION OF HOST-CONTROLLED RNA SYNTHESIS IN HUMAN CELLS DURING POLIOVIRUS INFECTION[*,†]

BY JOHN J. HOLLAND

DEPARTMENT OF MICROBIOLOGY, SCHOOL OF MEDICINE, UNIVERSITY OF WASHINGTON, SEATTLE

Communicated by Colin M. MacLeod, October 4, 1962

It was shown in a preliminary communication[1] that poliovirus infection of HeLa cells leads to synthesis of RNA with greatly altered base ratios. The rate of p-RNA (phenol-extractable RNA) synthesis was not greatly altered during this shift in base ratios during the first 6 hr of infection, although the rate of r-RNA (residual phenol-nonextractable RNA) synthesis showed a slight decline during infection.[2] Thus, it was suggested[1] that normal host RNA synthesis must be suppressed in order for the synthesis of predominantly virus-type RNA to proceed at about the normal rate, and the present study demonstrates that this does in fact occur. Salz-

man *et al.*[3] noted a continued incorporation of cytidine-2-C^{14} into RNA of poliovirus-infected HeLa cells despite the absence of net synthesis of RNA, and a gradual loss of cellular components into the medium beginning at about 6 hr post-infection. They suggested that an early effect of poliovirus infection is activation of a ribonuclease since the acid-soluble pool of infected cells increased starting 3 hr after infection. The work of other investigators[4] indicates that guanine from degraded host RNA may be used for virus synthesis.

The present study demonstrates that poliovirus infection depresses the synthesis of normal host-controlled RNA. This is shown by employing guanidine to inhibit virus-directed RNA synthesis. Guanidine·HCl at low concentrations has been shown[5] to inhibit poliovirus synthesis at concentrations which failed to alter normal cell growth detectably.[6] Guanidine acts to inhibit poliovirus synthesis at any stage of the infectious cycle and prevents virus-mediated abnormal accumulations of cytoplasmic RNA as detected with acridine orange.[6] It is shown here that guanidine strongly inhibits the synthesis of infectious RNA in poliovirus-infected HeLa cells without suppressing the rate of normal cell RNA synthesis. If guanidine was added to virus-infected cells 3.5 hr after infection to suppress virus-induced RNA synthesis, it was found that about 90 per cent of total p-RNA and r-RNA synthesis was subsequently arrested. It appears that virus infection strongly depresses host-controlled RNA synthesis while directing the synthesis of viral type RNA at near-normal rates. If, in turn, virus-directed RNA synthesis is suppressed with guanidine, the total synthesis of RNA drops to as little as 10 per cent of normal. This virus-induced inhibition of RNA synthesis seems analogous to phage DNA inhibition of host cell nucleic acid synthesis.

Materials and Methods.—Methods have been described in the preceding paper.[2] Guanidine·HCl was employed at a concentration of 10^{-3} *M* in cell culture medium with or without P^{32} as indicated. Infectious RNA was determined using only p-RNA from infected HeLa cells and plating on HeLa cell monolayers using 2 *M* $MgSO_4$ during exposure.[7] All base ratios presented in this paper are based on P^{32} in 2′3′ nucleotides of newly synthesized RNA.[2]

Results.—Preliminary experiments showed that guanidine at 10^{-3} *M* inhibits poliovirus production and the development of cytopathic changes in HeLa cells as it has been reported to do in monkey kidney cells.[5, 6] At this level of guanidine, uninfected HeLa cells continued to multiply in a normal manner over a period of 7 days or more. If HeLa cells were infected with a high multiplicity of Type 1 poliovirus and immediately placed into guanidine medium and incubated at 37°, no cytopathic effects were visible within the first 8 hr (by which time untreated cells have started to degenerate), but extensive cellular degeneration was evident 1 to 2 days later. Addition of Type 1 antiserum to the medium together with guanidine did not prevent this late degeneration; so it is not due to spread of guanidine-resistant mutants of virus. It appears then, that guanidine greatly delays but does not completely prevent virus-induced cell death.

Next, it was shown that 10^{-3} *M* guanidine arrests (or greatly retards) replication of infectious RNA just as it retards virus development.[5, 6] Table 1 shows that 10^{-3} *M* guanidine completely prevented infectious RNA accumulation up to 6 hr post-infection if added immediately after virus adsorption. Even when added 2 hr post-infection, 10^{-3} *M* guanidine arrested 97 per cent of infectious RNA synthesis.

TABLE 1

GUANIDINE INHIBITION OF INFECTIOUS RNA SYNTHESIS IN HELA CELLS INFECTED WITH TYPE 1 POLIOVIRUS

Treatment of cells	Total PFU infectious RNA 6 hours after infection*	Per cent infectious RNA formed‡
Control cells—RNA extracted after 6 hr incubation at 37° following virus absorption.	9×10^5	100
Control cells—RNA extracted 20 min after virus adsorption	2×10^3	0.2
Cells placed in guanidine medium† immediately following virus adsorption and incubated 6 hr at 37°	1×10^3	0.1
Cells incubated in normal medium for 2 hours following virus adsorption, then incubated in guanidine medium for 4 additional hours.	2×10^4	2.2

* 6×10^6 HeLa cells per bottle were infected with Type 1 poliovirus at an adsorption multiplicity >10. At the indicated intervals after infection, p-RNA was extracted with phenol and its infectivity determined on HeLa cell monolayers.
† Where indicated, guanidine·HCl was added to the medium at a final concentration of 10^{-3} *M*.
‡ Per cent plaque-forming units formed as compared to control cells.

The fact that 2.2 per cent of infectious RNA was produced, however, indicates that 10^{-3} *M* guanidine greatly retards, but does not completely prevent, virus RNA synthesis.

Table 2 shows the effect of 10^{-3} *M* guanidine on the synthesis of RNA in uninfected HeLa cells and in cells infected with Type 1 poliovirus. It can be seen that guanidine had little or no effect on the rate of RNA synthesis in uninfected cells. Nor did it greatly affect the rate of RNA synthesis when added to infected cells immediately after virus adsorption, although a small decrease in rate of synthesis was always observed.

It can also be seen that 10^{-3} *M* guanidine caused alteration in base composition of p-RNA but no significant changes in r-RNA. It is pointed out in reference 2 that other treatments of normal HeLa cells often lead to abnormal incorporation of pyrimidines into p-RNA. These changes vary in magnitude from experiment to experiment and were not usually found if the cells were allowed to adapt to 10^{-3} *M* guanidine for several days before testing. It can be seen that poliovirus infection

TABLE 2

EFFECT OF 10^{-3} *M* GUANIDINE ON p-RNA AND r-RNA SYNTHESIS IN NORMAL AND IN POLIOVIRUS INFECTED HELA CELLS

Treatment of cells before RNA extraction*	Moles per 100 moles P^{32} in each nucleotide of RNA				Per cent P^{32} incorporated into RNA
	U	G	A	C	
	p-RNA				
Untreated, uninfected cells	24.7	31.5	16.5	27.3	100 (control)
Uninfected cells incubated 6 hr in guanidine medium	29.3	29.3	15.6	25.8	87
Cells infected with Type 1 poliovirus and incubated for 6 hr in guanidine medium	35.0	25.0	17.0	23.0	67
	r-RNA				
Untreated, uninfected cells	29.5	24.1	24.2	22.2	100 (control)
Uninfected cells incubated 6 hr in guanidine medium	28.6	23.0	25.0	23.4	109
Cells infected with Type 1 poliovirus and incubated for 6 hr in guanidine medium	27.0	23.0	25.2	24.8	65

* P^{32} was added 3.5 hr prior to RNA extraction in each case. Where indicated, guanidine was added to Eagles medium (without and with P^{32}) to a final concentration of 10^{-3} *M*.

TABLE 3

REPRESSION OF HELA CELL RNA SYNTHESIS WHEN GUANIDINE IS ADDED SEVERAL HOURS FOLLOWING INITIATION OF TYPE I POLIOVIRUS INFECTION

Hours after infection before guanidine addition*	Hours incubation after addition of guanidine until RNA extraction	Moles per 100 moles P^{32} in each nucleotide of RNA				Per cent P^{32} incorporation into RNA
		U	G	A	C	
		p-RNA				
0 (control)†	0 (control)†	24.2	30.8	16.5	28.5	100
1.5	4	35.3	24.7	16.0	24.0	80
2.0	4.5	28.6	28.5	16.7	26.2	35
2.3	2.5	42.8	24.1	14.1	19.0	43
3.5	3.5	45.7	21.2	14.6	18.5	23
3.5	5	48.5	22.2	12.3	17.0	14
3.5	8.5	41.6	25.7	13.9	18.8	9
		r-RNA				
0 (control)†	0 (control)†	29.7	23.8	22.9	23.6	100
1.5	4	28.0	23.2	23.8	25.0	70
2.0	4.5	30.3	23.1	22.3	24.3	25
2.3	2.5	29.0	23.0	24.0	24.0	45
3.5	3.5	28.9	22.0	25.1	24.0	13
3.5	5	27.5	23.3	24.9	24.3	14
3.5	8.5	28.5	23.8	24.2	23.5	11

* In each case P^{32} was added 3.5 hr prior to extraction of RNA. Guanidine was added to a final concentration of 10^{-3} *M* at indicated times post-infection.
† Controls are uninfected, untreated, normal HeLa cell.

for 6 hr in the presence of guanidine caused little alteration in base ratios of r-RNA and slight alteration in p-RNA as compared with uninfected cells in guanidine.

Next, guanidine was added to cells in which poliovirus infection had been allowed to proceed normally for various intervals after virus adsorption. It can be seen in Table 3 that when poliovirus infection had been allowed to proceed for 3.5 hours before introduction of guanidine, the subsequent addition of the drug led to the suppression of up to 90 per cent of p-RNA and r-RNA synthesis. After shorter periods of normal virus infection, less inhibition of RNA synthesis was obtained upon guanidine treatment. Addition of the drug after 1.5 hr of infection effected no greater suppression of RNA synthesis than did addition immediately after infection (see Table 2). Table 3 shows (as did Table 2) that treatment of either infected or uninfected HeLa cells with guanidine usually caused distorted base ratios (heavy uridylate label) in p-RNA but not in r-RNA. Guanidine addition after virus infection prevented the usual virus-induced base ratio shifts in r-RNA. Even when guanidine was added at 3.5 hr post-infection (within 30 min of the time at which large shifts in base ratio are normally apparent during poliovirus infection[1]), there were no changes in base ratio, and the r-RNA, produced at a greatly reduced rate, resembled normal cell r-RNA in base composition. Thus, it appears that poliovirus infection causes a progressive repression of host-controlled RNA synthesis. Under usual conditions of infection, virus-controlled RNA synthesis replaces host-controlled RNA synthesis, but when a specific inhibitor of viral RNA synthesis is added, all RNA synthesis is depressed.

Cells that were treated with guanidine beginning 3.5 hr post-infection exhibited cytopathic effects and degenerated at about the same time as did untreated, poliovirus-infected HeLa cells, despite the fact that poliovirus-induced RNA synthesis was strongly inhibited. It is possible that the major cause of the rapid cytopathic effects of poliovirus infection is inhibition of vital host-directed RNA synthesis. It has been observed (unpublished observations) that 90 per cent depression of

HeLa cell RNA synthesis with actinomycin D leads to cell degeneration within 5 to 10 hr.

Discussion.—It might be argued that the effect described here is not actually poliovirus-induced repression of host RNA synthesis but some synergistic effect between guanidine action and virus action. This seems unlikely, however, since the two together did not significantly inhibit RNA synthesis unless the virus infection had proceeded in a normal manner for several hours.

The mechanism of repression can only be speculated upon at present. The apparent inhibition of synthesis could possibly be due to rapid breakdown of cell RNA synthesized at the normal rate. Such an explanation seems unlikely for several reasons. First, if there were a nuclease capable of selectively degrading host RNA so rapidly that only 10 per cent remained within an hour of synthesis, there should be very little host RNA present 5 or 6 hr after infection. This is not the case, since so much original host RNA remains during infection that P^{32} labeling must be employed to detect virus-induced RNA synthesis.[1] Second, rapid degradation of newly formed RNA would probably (depending on the nuclease) leave resistant acid-insoluble oligonucleotides that might greatly alter the base ratios of newly formed RNA. This was not observed (Table 3). Although the virus repression of RNA synthesis described here probably does not depend upon nuclease activity, there are good indications that poliovirus may activate nucleases capable of slow degradation of host RNA.[3, 4]

Other mechanisms which might be suggested are: (1) attachment of poliovirus RNA to critical DNA template sites, (2) activity of an interferon-like material. Poliovirus RNA base ratios are not incompatible with its being complementary to sequences along one or both strands of host DNA. Studies are in progress in an attempt to relate this phenomenon to interference, which might be viewed as another case of repression of heterologous nucleic acid synthesis. Preliminary results suggest that certain very concentrated interferon preparations from chick allantoic fluid may slightly suppress RNA synthesis in chick fibroblast cultures, but it is questionable whether this is a direct effect or merely a nonspecific result of cell damage. Work to be presented elsewhere will show that repression of RNA synthesis is not due to loss of capacity of DNA in infected cells to act as a template for RNA synthesis, although DNA-primed RNA polymerase activity is depressed in extracts from infected cells.[8]

The specific ability of guanidine to prevent poliovirus-infectious RNA synthesis and to prevent virus-induced synthesis of RNA with altered base ratios without inhibiting normal host-controlled RNA synthesis suggests that it may have considerable potential for elucidation of mechanisms involved in viral RNA replication.

Summary.—Guanidine at 10^{-3} *M* inhibits poliovirus-infectious RNA synthesis and virus-induced RNA base ratio alterations but does not greatly inhibit normal cell RNA synthesis. When guanidine was added to HeLa cells several hours after poliovirus infection in order to inhibit virus-directed RNA synthesis, host cell-directed RNA synthesis was found to be drastically inhibited. It is suggested that this inhibition of host RNA synthesis may be the chief reason for the rapid cell destruction caused by poliovirus infection.

* This investigation was supported by a grant from the National Science Foundation.

† Presented at the Atlantic City meeting of the Federation of American Societies for Experimental Biology, April, 1962.

[1] Holland, J. J., *Biochem. Biophys. Res. Comm.*, **6**, 196 (1961).

[2] Holland, J. J., these PROCEEDINGS, **48**, 2044 (1962).

[3] Salzman, N. P., R. Z. Lockart, Jr., and E. D. Sebring, *Virology*, **9**, 244 (1959).

[4] Diamond, L., and M. E. Balis, *Virology*, **15**, 210 (1961).

[5] Loddo, B., *Boll. Soc. It. Biol. Sper.*, **37**, 395 (1961); Rightsel, W. A., J. R. Dice, R. J. McAlpine, E. A. Timm, J. W. McLean, Jr., G. J. Dixon, and F. M. Schable, Jr., *Science*, **134**, 558 (1961).

[6] Crowther, D., and J. L. Melnick, *Virology*, **15**, 65 (1961).

[7] Holland, J. J., B. H. Hoyer, L. C. McLaren, and J. T. Syverton, *J. Exp. Med.*, **112**, 831 (1960).

[8] Holland, J. J., *Biochem. Biophys. Res. Comm.* (in press).

Note added in proof: Baltimore, D., and Franklin, R. M., these PROCEEDINGS, **48**, 1383 (1962) have recently reported inhibition of host-controlled RNA synthesis in cells infected with mengovirus, another small RNA animal virus.

---

*TRANSFORMATION INDUCED BY SIMIAN VIRUS 40 IN NEWBORN SYRIAN HAMSTER RENAL CELL CULTURES**

BY HARVEY M. SHEIN, JOHN F. ENDERS, JEANA D. LEVINTHAL, AND ANNE E. BURKET

RESEARCH DIVISION OF INFECTIOUS DISEASES, CHILDREN'S HOSPITAL MEDICAL CENTER, BOSTON; CHILDREN'S CANCER RESEARCH FOUNDATION, BOSTON; AND DEPARTMENT OF BACTERIOLOGY AND IMMUNOLOGY, HARVARD MEDICAL SCHOOL, BOSTON

Communicated November 8, 1962

In recent reports,[1-3] we have described transformation of human renal cells *in vitro* by simian virus 40 (SV40). Similar results were communicated shortly thereafter by Koprowski *et al.* using a different cell type.[4] This agent also has been found to induce sarcomas on subcutaneous inoculation into newborn (NB) Syrian hamsters.[5, 6] It became of interest, therefore, to determine whether SV40 would induce transformation in newborn hamster cells *in vitro*. Results of an experiment of this sort will be described.

Materials and Methods.—Virus: SV40 strain, VA 45–54 GMK 6/9/61, was originally obtained from M. R. Hilleman and passaged twice in human fetal renal cell cultures. Infectivity titer in grivet monkey kidney cultures was $10^{6.5}$ TID_{50}/0.1 ml.

Cultures: Newborn Syrian hamster renal cell cultures were obtained as confluent monolayers in screw-capped tubes from Microbiological Associates, Inc. Screw caps were replaced with rubber stoppers and cultures were thereafter treated as previously described[2] for maintenance of human renal cell cultures employed in experiments on transformation.

Viral inoculation and subcultivation of cells: Procedures were the same as previously described.[2]

Immunofluorescence techniques: Monolayers in Leighton tubes were fixed and stained by the indirect Coon's technique as previously described.[3]

Experimental.—Morphology and reproducibility of transformation: Ninety-four

cultures were inoculated with 0.1 ml of undiluted stock SV40; 50 uninoculated cultures were retained as controls. Inoculated cultures at no time exhibited cytolytic CPE nor were intranuclear inclusions observed, in contrast to the changes induced by SV40 in human and simian renal cell cultures.[1, 7, 8] Beginning 5–7 days after SV40 inoculation, small syncytia were visible in a small proportion of inoculated cultures. These contained usually 6 to about 15 nuclei, usually closely applied to one another in the center of the cell. After 21–28 days, "plaques" visible to the naked eye as small circularly elevated whitish areas and microscopically as aggregates of rapidly growing cells appeared in the cell monolayer of two of these cultures. These cellular aggregates were similar in appearance to those previously described in cultures of human renal cells infected with SV40.[2] Subsequently, additional cultures exhibited these plaques until by 80–90 days after inoculation they were present in all. None were seen in the uninoculated control cultures. Microscopically, such "plaques" consisted of closely packed "squat" fibroblasts and epithelioid cells, interspersed with syncytia (Figs. 1*a*, 1*b*). Although nuclear

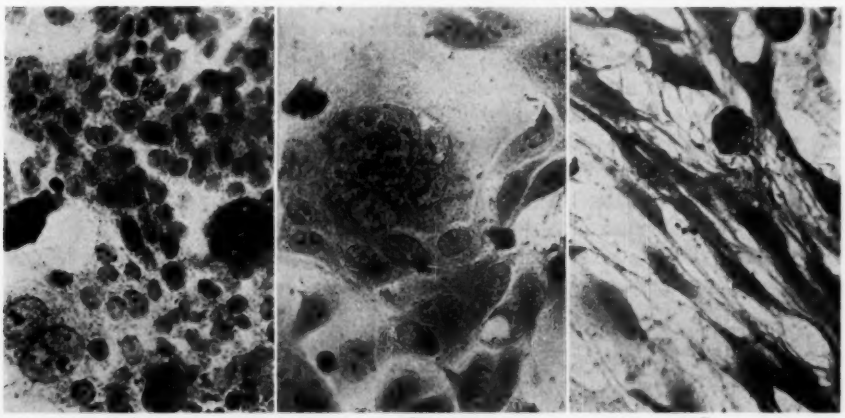

A. *B.* *C.*

FIG. 1.—(*A*) Epithelioid cells in primary culture 78 days after SV40 inoculation, stained with hematoxylin and eosin. Magnification 195 times. Random cellular pattern, multilayering, and several giant nuclei are evident.

(*B*) Another area from same SV40 inoculated primary NB hamster renal culture shown in Figure 1*a*. Magnification 305 times. H. & E. stain. Note a large syncytium with centrally aggregated nuclei surrounded by epithelioid cells.

(*C*) Control: primary uninoculated NB hamster renal cells 78 days. Magnification 305 times. H. & E. stain. Note sparse, elongated degenerating fibroblast-like forms with ballooned necrotic cells.

pleomorphism was seen in all, it was particularly marked in the epithelioid cells in which a wide range of nuclear size, clumping of chromatin, wide variations in nucleolar number, and bizarre mitotic figures were noted. The epithelioid cells characteristically exhibited a small cytoplasmic zone. Fibroblastoid elements were more uniform in morphology. All of the cells in plaque areas formed random patterns; in many places, multilayering was seen, and the whole area contrasted strongly with the adjacent unaffected cells of the monolayer and with those in control cultures where the population consisted predominantly of uncrowded elongated fibroblasts regularly oriented (Fig. 1*c*). Mitotic figures within both cell types of

plaques were strikingly more numerous than in adjacent areas or in control cultures. By 80–90 days after SV40 inoculation, plaques had become confluent in most cultures, largely replacing the sparse native fibroblast population by a thick white opaque mass of altered cells.

Subcultivation of cell types: In three experiments, a total of 22 SV40 inoculated cultures containing plaques were separately subcultured by the trypsinization technique. All subcultures grew rapidly, becoming confluent within 2–4 days. When a total of 20 control cultures were similarly subcultured, growth was sparse, the cells did not become confluent, and attempts at further subcultures were unsuccessful. Eight of the SV40 inoculated cultures were subcultured beyond the second passage and have now been passaged more than 15 times with no evidence of decreased growth potential. Even after 15 subcultures, all three types of cell (fibroblastoid, epithelioid, syncytial) were present in all cultures, although in different proportions. The syncytia were consistently seen in association with epithelioid cells and only very rarely with the fibroblastoid cells, suggesting that the syncytia were primarily derivatives of the epithelioid cells.

When inocula consisting of 1–10 transformed cells were explanted in plastic dishes and incubated in an atmosphere of 2% CO_2, macroscopically visible colonies were evident within 10 days in many of the preparations. Morphological differences corresponding to those described above in the mixed cell preparations were reflected in isolated cell colonies presumably developing from a single cell. Thus, colonies consisting only of fibroblastic-like elements or only of epithelioid forms or a mixture of the latter with syncytia were observed. Experiments are now underway to clone both cell types.

Immunofluorescence studies: Leighton tube cultures of primary NB hamster

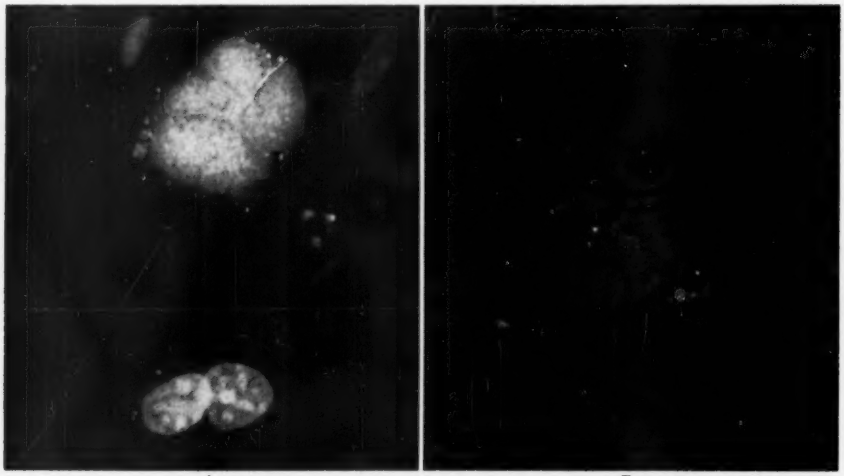

A. *B.*

FIG. 2.—(*A*) Immunofluorescence in primary culture five days after SV40 inoculation. Composite photograph, magnification 365 times. Lower portion, swollen fluorescing nuclei with concentration of antigen around areas resembling altered nucleoli. Upper portion, syncytium of four swollen fluorescent nuclei in midst of a group of smaller fluorescing nuclei.

(*B*) Syncytium from subcultured transformed NB hamster cells overexposed to show absence of SV40 specific fluorescence observed in primary cultures. Magnification 365 times.

renal cells were fixed and stained by the indirect Coon's technique at 5 and 10 days after SV40 inoculation. Approximately 1 per cent of cells in inoculated cultures exhibited SV40-specific nuclear fluorescence (Fig. 2*a*, 2*b*). This was characteristically most intense in areas surrounding structures resembling nucleoli. Certain fluorescent cells also exhibited nonstaining areas resembling "vacuoles" as with SV40 in human renal cultures.[3] Many of the cells exhibiting such fluorescence were swollen as compared with surrounding cells. Fluorescing cells tended to occur in loosely aggregated groups of 2–6 as with SV40 in primary cultures of human and monkey cells,[3, 9] but fluorescence appeared to be less intense at 10 days than in these other systems at a comparable time. All nuclei in syncytia in primary inoculated cultures exhibited immunofluorescence. When subcultured, none of the apparently transformed cells exhibited fluorescence that could be confidently accepted as specific. However, all cells in each of eight lines studied exhibited faint fluorescence about areas morphologically resembling nucleoli, which was not observed in primary control cultures. Specificity of this circumnucleolar fluorescence remains in doubt because cells in transformed cultures lacked the associated nuclear swelling and nonfluorescing "vacuoles" which helped to distinguish affected nuclei in primary cultures. Moreover (see below), infective virus was not demonstrated in such cultures.

Presence of infective virus in cell cultures: Immunofluorescence observed in primary cultures soon after inoculation was shown to be specific by appropriate control tests.[3] This suggests strongly that infective virus was present at that time. However, no tests for presence of infective virus were done with materials from primary cultures. Undiluted supernatant fluid from the 10th passage of each of eight independently transformed cell lines was inoculated in 0.1 ml aliquots into grivet monkey kidney cell cultures in duplicate. After more than eight weeks of observation, no cytopathic changes have been observed in these cultures.

Hamster cheek pouch: To test whether the apparently transformed cell types were neoplastic for the Syrian hamster, in collaboration with A. H. Handler and G. E. Foley of the Children's Cancer Research Foundation, trypsinized cells consisting of predominantly fibroblastoid cells with fewer epithelioid cells from one line subcultured seven times were inoculated by the method described by Foley *et al.*[10] in ten-fold decreasing increments into the cheek pouch of Syrian hamsters. These experiments are still in progress but no growth has occurred after an observation period of three weeks after implantation.† In a similar experiment, with apparently transformed human renal cells,[2] in collaboration with Foley and Handler, no growth has occurred after an observation period of more than four months after implantation in the hamster cheek pouch even when the inoculum consisted of 1,000,000 cells.

Discussion.—Relation of in vitro hamster transformation to induction of malignancies in vivo: Eddy *et al.*[5] found that SV40 induced sarcomas in NB hamsters not only at the subcutaneous site of viral inoculation but also, less often, at a distance, i.e., in the lungs and kidneys. Cytologically, the tumors were composed of closely packed cells with little cytoplasm, pleomorphic nuclei often with clumped or marginated nuclear chromatin, and large numbers of interspersed syncytia whose nuclei resembled those in surrounding tumor cells. In at least two of these tumors, they were able to demonstrate the persistence of SV40. In the present studies,

there were noted as occurring *in vitro* two basic "transformed" cell types, epithelioid and fibroblastoid, both closely packed but only the epithelioid type appearing to be consistently associated with syncytia. This association appeared to persist on passage. Accordingly, the epithelioid cells with the least cytoplasm and the most marked nuclear pleomorphism may represent the cell type which corresponds with the sarcoma cells of Eddy *et al.* Experiments are under way to explore this hypothesis. Thus, clones of transformed cells of both morphologies will be inoculated into the Syrian hamster cheek pouch to determine their relative potential for neoplastic growth. As noted above, experiments employing cell suspensions consisting of mixtures of both cell types are in progress.

Mechanism of transformation: Various possible mechanisms of transformation by SV40 in human cells have been discussed previously[3] and appear to be equally relevant to the phenomena here described. The results of the fluorescent antibody studies of the transformed hamster cells are, however, of additional interest in this regard. About 1 per cent of the nuclei in primary NB hamster cultures exhibited SV40 specific fluorescence. In contrast, no clearly specific fluorescence was seen in the transformed cell lines, but 100 per cent of the nuclei in the latter exhibited a faint, apparently circumnucleolar fluorescence not seen in uninoculated primary cultures and of uncertain significance for reasons noted earlier. When media from eight independently derived transformed cell lines was assayed for SV40 infectivity in grivet monkey kidney cultures, none was demonstrated. It is therefore likely that this faint fluorescence in transformed cell nuclei may be unrelated to the presence of viral antigen, but the possibility that it represents an SV40-specific antigen not associated with infective virus remains to be explored.

Comparison of in vitro transformations induced by SV40 and polyoma: In hamster renal cell cultures, the mammalian tumor virus SE polyoma induces transformation from which infective virus has not been recovered, and it achieves this without inducing associated marked cytolytic changes in the system.[11, 12] Thus far, our results with SV40 virus in this system are comparable in both these respects. If further investigation fails to reveal SV40 virus associated with these transformed cells, this would indicate that as with polyoma in hamster cells the continued maintenance of the transformed state does not require the presence of infective virus. This result may be relevant to the problem of the mechanism by which SV40 induces *in vitro* transformation in human renal cells, for it would appear unlikely that this agent induces transformation in one cell system (NB hamster renal) which apparently does not require continued associated infective virus and yet induces transformation in another cell system (human renal) in which continuance of the cell-virus relationship is essential.[3]

Significance of these findings: From at least three points of view, these findings appear to be of interest. First, transformation with SV40 in hamster tissue culture provides a means of comparing cells derived from malignancies induced by SV40 *in vivo* with transformation induced *in vitro* in cells of the same species. The problem of neoplastic capability of cells transformed *in vitro* can be investigated by explantation of the cells into the species of derivation without introducing complicating factors like interspecies histoincompatibility such as arise when SV40 transformed human renal cells are inoculated into hamsters. Furthermore, the process of SV40 transformation in hamster materials may now be compared to

those induced in the same systems by the morphologically related murine tumor-inducing virus SE polyoma.[12]

Second, if the SV40-transformed hamster cells prove malignant or neoplastic on explantation in hamsters, this will suggest that failure of SV40-transformed human cells to grow in the hamster cheek pouch under the experimental conditions so far employed may have been due to histoincompatibility or destruction of the cells by excessive replication of SV40 *in vivo* rather than to lack of neoplastic potential.†

Third, this finding of *in vitro* transformation corresponding to induction of malignancy *in vivo* in hamsters with a virus which also induces *in vitro* transformation in human renal cells may serve to extend the technique suggested by Syverton[14] for the identification of viruses with oncogenic potential for human cells. Syverton proposed that a useful means of screening viruses infectious for primates for such potential would be to determine their capacity to transform human cells *in vitro*.[14] Since it has now been shown that SV40 transforms both human and hamster cells *in vitro* and is oncogenic for the hamster *in vivo*, the demonstration of these effects taken together would seem to provide a more reliable basis for regarding a given virus as potentially oncogenic for man than any one of them taken separately. It would, therefore, be of considerable interest to determine whether adenovirus type XII of human origin, which has been shown by Trentin *et al.*[15] to induce tumors in hamsters, is capable of transforming *in vitro* cells of this species as well as those of human origin.

Summary.—Induction by simian virus 40 of a reproducible transformation in primary cultures of newborn Syrian hamster renal tissues is described. The transformation is characterized by altered cell morphology, abnormal growth pattern, and a greatly accelerated growth rate. Attempts to demonstrate infective virus in subcultures of transformed cells were unsuccessful. Inoculated cultures did not exhibit at any stage cytolytic CPE or intranuclear inclusions characteristic of SV40 infection in human and simian renal cell cultures. The transformed cell types included epithelioid, syncytial, and fibroblastoid forms.

The authors wish to express their appreciation to John Carabitses for microphotography.

* Supported in part by research grants E-1992 and C-4965, U.S. Public Health Service.

† *Note added in proof:* After this communication was submitted for publication, tumorous masses were observed in the cheek pouches of hamsters inoculated 7 weeks earlier with transformed cells. On removal 1 week later, tumors from 4 of the animals were sectioned, stained, and examined microscopically. In all, the histological picture was that of adenocarcinoma of varying degree of differentiation. These findings will be described in detail in a later report. Relevant to these observations is the report of Rabson and Kirchstein (*Proc. Soc. Exp. Biol. Med.*, **111**, 323 (1962)) that appeared after this communication was submitted. They noted the development of tumors in hamsters following intracerebral and subcutaneous inoculation of cells derived from explants of newborn hamster kidney infected with SV40. Histologically, tumors consisted of undifferentiated carcinoma, adenocarcinoma and epidermoid carcinoma with some sarcomatous areas. No tumors, however, developed following cheek-pouch inoculation of the cells.

[1] Shein, H. M., and J. F. Enders, *Proc. Soc. Exp. Biol. Med.*, **109**, 495 (1965).

[2] Shein, H. M., and J. F. Enders, these PROCEEDINGS, **48**, 1164 (1962).

[3] Shein, H. M., J. F. Enders, and J. D. Levinthal, these PROCEEDINGS, **48**, 1350 (1962).

[4] Koprowski, H., J. A. Ponten, F. Jensen, R. G. Ravdin, P. Moorhead, and E. Saksela, *J. Cell. and Comp. Physiol.*, **59**, 281 (1962).

[5] Eddy, B. E., G. S. Borman, G. E. Grubbs, and R. D. Young, *Virology*, **17**, 65 (1962).

[6] Girardi, A. J., B. H. Sweet, V. B. Slotnick, M. R. Hilleman, *Proc. Soc. Exp. Biol. Med.*, **109**, 649 (1962).
[7] Sweet, B. H., and M. R. Hilleman, *Proc. Soc. Exp. Biol. Med.*, **105**, 420 (1960).
[8] Gaylord, W. H., Jr., and G. D. Hsuing, *J. Exp. Med.*, **114**, 987 (1961).
[9] Shein, H. M., and J. D. Levinthal, *Virology*, **17**, 595 (1962).
[10] Foley, G. E., A. H. Handler, R. A. Adams, and J. M. Craig, *National Cancer Institute Monograph No.* **7** (1962), pp. 173, 204.
[11] Vogt, M., and R. Dulbecco, these PROCEEDINGS, **46**, 365 (1960).
[12] Vogt, M., and R. Dulbecco, *Virology*, **16**, 41 (1962).
[13] Melnick, J. L., *Science*, **135**, 1128 (1962).
[14] Syverton, J. T., in *Perspectives in Virology*, ed. M. Pollard (Minneapolis: Burgess Publishing Co., 1961), vol. 2, p. 195.
[15] Trentin, J. J., Y. Yabe, and G. Taylor, *Science*, **137**, 835 (1962).

ON A PLANE ISING LATTICE WITH FIRST AND SECOND INTERACTIONS

BY A. PAIS

INSTITUTE FOR ADVANCED STUDY, PRINCETON

Communicated November 20, 1962

For a number of plane Ising lattices with first (nearest-neighbor) interaction and no magnetic field, it has been shown how to evaluate rigorously the partition sum.[1] Next in complexity to the exactly solved problems come plane lattices with first and second (next to nearest-neighbor) interactions. Low and high temperature expansions for this case have been given by Domb and Potts.[2] In this note, we establish an identity between the square of the partition sum for a square lattice with first interaction only and the partition sum for a similar lattice with first and second interactions (equation (13) below). The identity, though limited to quite special coupling conditions, is perhaps not entirely without interest as, to date, the qualitative insight into the problem is limited.

Consider a square lattice with first interaction $\mu_i\mu_k V$ only ($\mu_i = \pm 1$). The partition sum is

$$Z_n(K) = S \prod \exp \mu_i\mu_j K, \qquad K = -V/kT. \tag{1}$$

$\prod$ denotes the product over all pairs of nearest neighbors, S is the summation over the values ± 1 of all μ_i, and n is the total number of lattice points.

Label each lattice point by a pair of integers (p, q). The sets (p, q) both even or both odd form sublattices called α- and β-lattice respectively. The nearest neighbors α_1, α_2, α_3, α_4 of an α-point are β-points. In the exponential of equation (1) one can group together the four first interactions of each α-point, to get the equivalent form of $Z_n(K)$ (neglect boundary effects):

$$Z_n(K) = S \prod_{\alpha} \exp \mu_\alpha s_\alpha K, \qquad s_\alpha = \mu_{\alpha_1} + \mu_{\alpha_2} + \mu_{\alpha_3} + \mu_{\alpha_4}, \tag{2}$$

where, as indicated, the product operation is now taken with respect to the α-points only.

The function $\mu_\alpha s_\alpha$ takes on the five distinct values $(\mu_\alpha s_\alpha)_A = \pm 4, \pm 2, 0$ only. Thus, we may put in equation (2)

$$\exp \mu_\alpha s_\alpha K = 1 + \mu_\alpha s_\alpha x + s_\alpha{}^2 y + \mu_\alpha s_\alpha{}^3 z + s_\alpha{}^4 u, \tag{3}$$

where x, y, z, u are the solutions of

$$\exp (\mu_\alpha s_\alpha)_A K = 1 + (\mu_\alpha s_\alpha)_A x + (s_\alpha)_A{}^2 y + (\mu_\alpha s_\alpha)_A{}^3 z + (s_\alpha)_A{}^4 u. \tag{4}$$

The spin μ_α occurs only in the factor $\exp \mu_\alpha s_\alpha K$ in equation (2). (Not so for the spins μ_{α_i}.) Insert equation (3) into equation (2) and perform the S-operation on the α-points, which gives

$$Z_n(K) = 2^{n/2} S' \prod_\alpha (1 + s_\alpha{}^2 y + s_\alpha{}^4 u), \tag{5}$$

where S' is the spin sum over the β-lattice only.

$s_\alpha{}^2$ has the three distinct values 16, 4, 0. Thus, we may put

$$1 + s_\alpha{}^2 y + s_\alpha{}^4 u = \exp (h_2 s_\alpha{}^2 + h_4 s_\alpha{}^4). \tag{6}$$

With the help of equation (4), h_2 and h_4 are expressed in terms of K as follows:

$$\left.\begin{aligned} \cosh 2K &= 1 + 4y + 16u = \exp (4h_2 + 16h_4), \\ \cosh 4K &= 1 + 16y + 256u = \exp (16h_2 + 256h_4). \end{aligned}\right\} \tag{7}$$

From equation (2),

$$\left.\begin{aligned} s_\alpha{}^2 &= 4 + 2(M_\alpha + D_\alpha), \\ s_\alpha{}^4 &= 40 + 32(M_\alpha + D_\alpha) + 24 Q_\alpha, \end{aligned}\right\} \tag{8}$$

with

$$\left.\begin{aligned} M_\alpha &= \mu_{\alpha_1}\mu_{\alpha_2} + \mu_{\alpha_2}\mu_{\alpha_3} + \mu_{\alpha_3}\mu_{\alpha_4} + \mu_{\alpha_4}\mu_{\alpha_1}, \\ D_\alpha &= \mu_{\alpha_1}\mu_{\alpha_3} + \mu_{\alpha_2}\mu_{\alpha_4}, \\ Q_\alpha &= \mu_{\alpha_1}\mu_{\alpha_2}\mu_{\alpha_3}\mu_{\alpha_4}. \end{aligned}\right\} \tag{9}$$

M_α is the "first interaction operator" for that cell of the β-net which is labeled[3] by the particular center point α. D_α is the "second interaction operator" and Q_α is a four-spin operator for that cell.

Insert equation (8) into equation (5). In the latter, we are still taking products with respect to the cells of the β-net. Each one of the four terms in M_α occurs in two such cells with an edge in common; but D_α and Q_α occur only once. Hence, equation (5) can be written as

$$Z_n(K) = [2(\cosh 4K)^{1/2}]^{n/2} Z_{n/2}{}^{(2)}(H, H_Q), \tag{10}$$

$$Z_{n/2}{}^{(2)}(H, H_Q) = S' \Pi' \exp [(\mu_i\mu_j)_1 H + (\mu_i\mu_j)_2 \frac{H}{2} + \{(\mu_i\mu_j\mu_k\mu_l)_q - 1\} H_Q]. \tag{11}$$

In equation (11), the meaning of the symbols is as follows. $(\mu_i\mu_j)_1$ and $(\mu_i\mu_j)_2$ are the products of a pair of nearest-neighbor spins and next to nearest-neighbor spins respectively (in the original β-lattice). $(\mu_i\mu_j\mu_k\mu_l)_q$ is the product of four spins which lie on a square. Π' denotes the product over all possible pairs and quadruples as they occur in the exponent. Finally, $H = 4h_2 + 64h_4$, $H_Q = 24h_4$ or, according to equation (7),

$$H = \frac{1}{4} lg \cosh K \geq 0, \qquad H_Q = -\frac{1}{4} lg \cosh 2H \leq 0. \tag{12}$$

The subscript $n/2$ on $Z^{(2)}$ serves to remind that we are dealing with $n/2$ spins on a square lattice. Define $Z(K) = \lim_{n \to \infty} [Z_n(K)]^{1/n}$, $Z^{(2)}(H, H_Q) = \lim_{n \to \infty} [Z_n^{(2)}(H,H_Q)]^{1/n}$. We have the identity

$$Z^{(2)}(H, H_Q) = \frac{[Z(K)]^2}{2[\cosh 4K]^{1/2}}. \tag{13}$$

$Z(K)$ is the partition sum per particle for the well-known case of first interaction only. $Z^{(2)}$ is the partition sum per particle for a square net with the following properties. There is a first interaction HkT, a second interaction of half that strength. Both these couplings are necessarily ferromagnetic in accordance with the inequality sign in equation (12). Observe that this inequality is independent of the sign of V in equation (1), so that we cannot come close to the corresponding antiferromagnetic case by such arguments as used here. Likewise, H_Q is an antiferromagnetic four-particle correlation which modifies the spectrum due to the two H-couplings as follows. It vanishes in the ground state.[4] Excited states either are lowered or remain unchanged by H_Q.

$Z(K)$ has a transition point for $K = K_C$, $|\sinh 2K_C| = 1$. From equation (12), $Z^{(2)}$ has a transition point for $H = H_C$, $H_Q = H_{QC}$,

$$H_C = \frac{lg\,3}{4} = 0{,}274, \qquad H_{QC} = \frac{lg\,3}{8} - \frac{lg\,2}{4} = -0{,}036. \tag{14}$$

However, the H_Q-interaction has a disagreeable property. It follows from equation (12) that the four-particle correlation is temperature-dependent.[5] It would therefore be much more interesting if we could say something about the transition point in the presence of H- but absence of H_Q-interaction. Call $Z^{(2)}(H)$ the corresponding partition sum.

Now the antiferromagnetic property of H_Q holds true for all T. For a large T-region H_Q is a perturbation compared to H. For high T, $H \ll 1$, so $H_Q \simeq -{}^1/_2H^2$ is small of second order and from equation (14) we see that this relation is still very nearly valid at the C-point. As $T \to 0$, $H_Q \to -{}^1/_2H$, so ferromagnetism still predominates. It is therefore very plausible that if we discard H_Q we raise the Curie-temperature, so that

$$\text{for } Z^{(2)}(H): H_C < \frac{1}{4}\, lg\, 3. \tag{15}$$

Further corroboration of the result shown by equation (15) comes from numerical estimates by Domb and Potts[6] which gives values of H_C varying from 0.23–0.25.

The bound given in equation (15) is no doubt correct. However, one would wish to have a proof (not given here) which shows how the Curie point moves due to variations in lattice constants. Presumably, one possible tool for this is the behavior of the long-range order $I(T)$ with T. One would expect that if a lattice 1 has ordering forces which are somewhat weakened so as to get a situation 2, then $I_1(T) > I_2(T)$ for all T which implies $T_{C1} > T_{C2}$. A general proof (which must involve limitations on the degree of perturbation) does not seem easy. Let us, however, demonstrate this behavior by a beautiful example. Consider a plane triangular ferromagnetic lattice with constants V_1, V_1, V_2. Let $x = \exp(-2V_1/$

kT), $y = \exp(-2V_2/kT)$. Then[7] $I(x, y) = [1 - 16x^4y^2(1 - x^2)^{-2}\{(1 + x^2)^2 - 4x^2y^2\}]^{1/4}$. $y = 1$, x correspond to the symmetric square and triangular lattices respectively. One can go from the former to the latter by introducing a second interaction in the square lattice along *one* diagonal direction only and which grows from zero to its appropriate value, corresponding to the range $1 \geq y \geq x$. One will expect the Curie point to rise continuously, and it does as $I(x, y_1) < I(x, y_2)$ for $1 \geq y_1 \geq y_2 \geq x$.

The symmetric triangular lattice has a transition point $H_C = \frac{1}{4} lg\, 3$(!). In view of equation (14) it is therefore interesting to compare the low T-expansion of $I(x, x)$ with the one for $I^{(2)}$, the long-range order for $Z^{(2)}(H)$. One has

$$I(x, x) = 1 - 2x^6 - 12x^{10} + 2x^{12} - 78x^{14} + 24x^{16} + 0(x^{18}), \tag{16}$$

$$I^{(2)}(x) = 1 - 2x^6 - 8x^{10} - 8x^{11} + 18x^{12} - 24x^{13} - 20x^{14} - 48x^{15} + 44x^{16} + 0(x^{17}). \tag{17}$$

Certainly for $x \leq 1/2$, $I^{(2)}(x) > I(x, x)$ as one would guess in view of the relative positions of the Curie points.

It is also instructive to follow the behavior of I with variable second interaction, as was done by Domb and Potts.[2] Thus let H and H' be ferromagnetic first and second interactions and $x = \exp(-2H)$, $w = \exp(-2H')$.

$$\begin{aligned} I(x,w) = 1 &- 2x^4w^4 - 8x^8w^6 - (8x^6 - 18x^8 + 36x^{12} + 8x^{16})w^8 - \\ &(24x^8 + 48x^{10} - 168x^{12} + 144x^{16} + 80x^{20} + 24x^{24})w^{10} - \\ &(20x^8 - 80x^{10} + 364x^{12} + 288x^{14} - 1160x^{16} + 40x^{18} + 340x^{20} + \\ &480x^{24} + 308x^{28} + 96x^{32} + 18x^{36})w^{12} + O(w^{14}x^{10}). \end{aligned}$$

Both $I(x, 1)$ and $I(1, w)$ correspond to first interaction only in a square lattice. Again the low-T behavior of $I(x, w)$ with variable H, H' is as expected from the conjectured long-range order inequality. The square lattice with only first interaction serves as a comparison.

The relation between $Z^{(2)}(H)$ and the case of the symmetric triangular net is as follows. In the latter case, one has a coupling H along one diagonal direction in a square net; in the former, one has $H/2$ along either diagonal direction and this partition apparently increases the order. It is therefore of interest to know how the Curie point moves if we partition γH along one, $(1 - \gamma)H$ along the other diagonal, $0 \leq \gamma \leq 1$. For this purpose, consider the long-range order for asymmetric second interactions. Let $x = \exp(-2H)$ refer to the first, and $y = \exp(-2K)$, $z = \exp(-2L)$ to the two second interactions.

$$\begin{aligned} I(x, y, z) = 1 - 2x^4y^2z^2 - 8x^6y^4z^4 - \\ 2x^8y^2z^2[2(y^2 + z^2)(1 + 3y^2z^2) - 9y^2z^2]\ldots \end{aligned} \tag{18}$$

$y = x$, $z = 1$ gives equation (16), $y = x = z^{1/3}$ gives equation (17), in either case correct to $O(x^{14})$. The partition for varying γ is obtained by putting $yz = x$. From the relative position of $I(x, y, xy^{-1})$ for varying y, one surmises that $\gamma = 1/2$ is that partition which gives the highest Curie point within the γ-range considered.

I am indebted to M. Kac for stimulating discussions and to M. Fisher for an interesting correspondence.

[1] For a recent survey see C. Domb, *Advances in Physics*, **9**, 149, 245 (1960).

[2] Domb, C., and R. Potts, *Proc. Roy. Soc.*, **A210**, 125 (1952).

[3] The sub-subscript sequence 12341 traces a square of the β-net.

[4] This is due to the term -1 in the cofactor of H_Q in equation (11). This term, which is thermodynamically insignificant, has been put there to facilitate the comparison of the spectra in the respective presence or absence of H_Q.

[5] A four-particle interaction with similar properties was encountered in the study of super exchange in an Ising lattice by Fisher, M., *Proc. Roy. Soc.*, **A254**, 66 (1960), see especially p. 85.

[6] See reference 2. I used their curves, Figure 7, with $J_w/|J_x| = 1/2$, and also Figure 10.

[7] Potts, R., *Phys. Rev.*, **88**, 352 (1952).

---

*NOTE ON THE SQUARE-INTEGRABILITY OF THE KERNEL OF THE LINEARIZED BOLTZMANN INTEGRAL EQUATION FOR RIGID SPHERE MOLECULES**

By C. L. Pekeris

DEPARTMENT OF APPLIED MATHEMATICS, THE WEIZMANN INSTITUTE, REHOVOT, ISRAEL

Communicated November 3, 1962

Introduction.—The linearized Boltzmann integral equation for the case of a gas of rigid spheres leads to an eigenvalue problem[1-3]

$$\psi(\mathbf{r}) = (\lambda/\pi) \int K(\mathbf{r},\mathbf{r}_1)\psi(\mathbf{r}_1)d\mathbf{r}_1, \tag{1}$$

where the kernel $K(\mathbf{r},\mathbf{r}_1)$ depends only on the lengths r,r_1 and $\rho = |\mathbf{r} - \mathbf{r}_1|$ of the triangle, and is symmetrical in r and r_1. We have[4]

$$K(\mathbf{r},\mathbf{r}_1) = G(\mathbf{r},\mathbf{r}_1)/[k(r)k(r_1)]^{1/2}, \tag{2}$$

$$G(\mathbf{r},\mathbf{r}_1) = 2\pi[(2/\rho)e^{-A/4} - e^{-\frac{1}{2}(r^2 + r_1^2)}], \tag{3}$$

$$k(r) = 2\pi^2 \left\{e^{-r^2} + [2r + (1/r)] \int_0^r e^{-x^2} dx\right\}, \tag{4}$$

$$A = [\rho^2 + (r^2 - r_1^2)^2/\rho^2], \tag{5}$$

$$k(0) = 4\pi^2, \quad \dot{k}(r) \geqslant 0, \quad k(r) \to 2\pi^{3/2}r, \tag{6}$$

as $r \to \infty$.

In connection with the question of the applicability of the classical theory of integral equations to (1), it is of interest to establish whether K^2 is integrable. Hecke states[3] without proof that K^2 is *not* integrable: that while K^2 is integrable in $d\mathbf{r}_1$, the second integration in $d\mathbf{r}$ diverges. Since some doubt has been expressed about this, we give here a proof of the nonintegrability of K^2.

Proof of the Nonintegrability of K^2.—In the expression,

$$K^2 = \frac{4\pi^2}{k(r)k(r_1)}\left[\frac{4}{\rho^2}e^{-A/2} - 4e^{-A/4 - \frac{1}{2}(r^2 + r_1^2)} + \rho^2 e^{-(r^2 + r_1^2)}\right], \tag{7}$$

the second and third terms in the brackets are integrable, so that it suffices to examine only the first term. That this term may not be integrable is suggested by the fact that the minimum value of A in (5) is $(2r^2 - 2r_1^2)$, a circumstance which

weakens the exponential control of the integrand in the region of integration where $r_1 \to r$, and r is large. Since the doubtful region is where r and r_1 are large, we will use the asymptotic expression $4\pi^3 r r_1$ for $k(r)k(r_1)$. The singularity thus introduced at $r_1 = r = 0$ is integrable. We are thus led to examine the convergence of the integral

$$I = \int d\mathbf{r} \int d\mathbf{r}_1 \frac{e^{-A/2}}{\rho^2 r r_1} . \tag{8}$$

We have

$$I = 8\pi^2 \int_0^\infty dr \int_0^\infty dr_1 \int_{|r-r_1|}^{(r+r_1)} \frac{d\rho}{\rho} e^{-A/2} =$$

$$16\pi^2 \int_0^\infty dr \int_0^r dr_1 \int_{(r-r_1)}^{(r+r_1)} \frac{d\rho}{\rho} \exp\left[-\frac{1}{2}\rho^2 - (r^2 - r_1^2)^2/2\rho^2\right]. \tag{9}$$

Let
$$s = r^2 + r_1^2, \quad t = r^2 - r_1^2, \quad r_1 \leqslant r, \tag{10}$$

$$dr dr_1 = \frac{ds dt}{8 r r_1} = \frac{ds dt}{4(s^2 - t^2)^{1/2}}, \tag{11}$$

$$I = 4\pi^2 \int_0^\infty ds \int_0^s \frac{dt}{(s^2 - t^2)^{1/2}} L(s,t), \tag{12}$$

where
$$L = \int_{(r-r_1)}^{(r+r_1)} \frac{d\rho}{\rho} \exp\left[-\frac{1}{2}\rho^2 - t^2/2\rho^2\right]. \tag{13}$$

Putting
$$\rho^2 = te^x, \quad \tau = \ln[(r + r_1)/(r - r_1)], \tag{14}$$

we get

$$L = {}^1/_2 \int_{-\tau}^{\tau} e^{-t\cosh x} dx = \int_0^\tau e^{-t\cosh x} dx = \int_0^\infty e^{-t\cosh x} dx - M = K_0(t) - M. \tag{15}$$

$$M = \int_\tau^\infty e^{-t\cosh x} dx = \int_{(r^2 + r_1^2)}^\infty \frac{e^{-z} dz}{(z^2 - t^2)^{1/2}} \to \frac{e^{-r^2 - r_1^2}}{2rr_1}\left[1 - \frac{(r^2 + r_1^2)}{4r^2 r_1^2} + \ldots\right]. \tag{16}$$

The integral over M in (12) converges because of the asymptotic exponential behavior shown in (16), so that we need to use only $K_0(t)$ for L in (12). We have

$$\int_0^\infty ds \int_0^s \frac{dt}{(s^2 - t^2)^{1/2}} K_0(t) = (\pi/2) \int_0^\infty ds I_0({}^1/_2 s) K_0({}^1/_2 s). \tag{17}$$

The last integral in (17) diverges logarithmically because

$$I_0({}^1/_2 s) K_0({}^1/_2 s) \to 1/s, \tag{18}$$

as $s \to \infty$. It follows that the kernel K in the integral equation (1) is *not* square-integrable.

Summary.—It is shown that the kernel of the linearized Boltzmann integral equation for rigid sphere molecules is *not* square-integrable.

* This research was supported by the Cambridge Research Laboratories, OAR, through the European Office, Aerospace Research, U. S. Air Force.

[1] Pekeris, C. L., Z. Alterman, L. Finkelstein, and K. Frankowski, "Propagation of sound in a gas of rigid spheres," *The Physics of Fluids*, **5**, 1608 (1962).

[2] Carleman, T., *Problèmes Mathématiques dans la Théorie Cinétique de Gaz*, (Uppsala: Almqvist and Wiksells, 1957), p. 70.

[3] Hecke, E., *Math. Z.*, **12**, 277 (1922).

[4] We shall use the notation of reference 2.

---

*ON THE EFFECT OF SODIUM-FREE SOLUTIONS UPON ISOLATED, SINGLE FROG NERVE FIBERS**

BY V. HONRUBIA† AND R. LORENTE DE NÓ

THE ROCKEFELLER INSTITUTE

Communicated October 18, 1962

Figure 1 illustrates observations made with an isolated, single frog nerve fiber, with the use of sodium-free glucose Ringer's (220 mM glucose, 4 mM potassium phosphates buffer, 1.2 mM calcium chloride, and 2 mM magnesium chloride).

Before describing the observations, it should be noted that the introduction of glucose in the central chamber causes a very rapid downward displacement of the base line, which is referable to the change in the potential of one of the recording silver-silver chloride electrodes and to the appearance of diffusion potentials at the junctions, at the margins of the central chamber, of the glucose solution and the Ringer's solution outside the internodal segments in the air gaps. If only physical conditions were involved, the base line would become stable within a very short period of time. As a matter of fact, however, the initial rapid displacement of the base line is followed by a slower displacement in the same direction, which is referable to the increase in the resting membrane potential caused by the immersion of the fiber in a poorly ionized medium. This phenomenon has long been known.[1]

Fully ionized sodium-free media, i.e., Ringer's solution in which the sodium chloride has been replaced by ethanol-trimethyl-ammonium (choline) or diethanol-dimethyl-ammonium chloride do not cause an increase in the value of the resting membrane potential. But all sodium-free media cause an increase in the apparent resistance of the nerve membrane, which is measured by the increase in the height of the electrotonic potential produced by the applied current. This increase in the apparent resistance of the membrane, for both the inward and the outward current, is a consequence of loss of internal sodium by the nerve fibers.

Rapidly, but not instantaneously, the sodium-free solution caused a decrease in the height of the action potential (Fig. 1, *2*). Within one minute, the action potential disappeared (Fig. 1, *3*), but this effect was referable solely to an increase in the threshold of stimulation. When the stimulating current was increased, the fiber again produced an action potential, and, as was expected, the all-or-nothing law had become invalid: the height of the action potential increased with the magnitude of the stimulating current (Fig. 1, *4*). At this stage of the experiment, restoration by Ringer's solution was fairly rapid (Fig. 1, *6*).

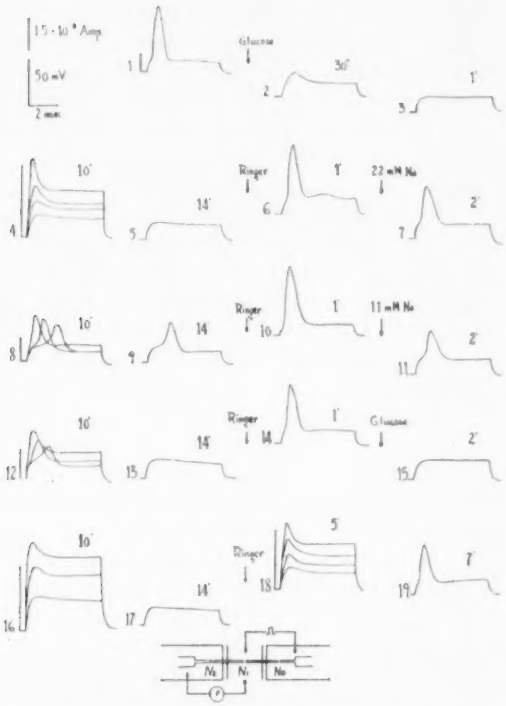

FIG. 1.—Tracings of oscillograph records obtained with an isolated, single frog nerve fiber. The experimental arrangement is indicated in the diagram at the bottom. The segments of the fiber including the exposed nodes N_0 and N_2 were kept in a 5 mM solution of xylocaine. The segment including node N_1 was successively immersed in the indicated solutions. The times given on the right-hand side of the records are the times of action of each solution.

The time calibration, 2 msec, and the potential calibration, 50 mv, apply to all records. The calibration of the stimulating current, 1.5×10^{-8} amp, also applies to all the records. Unless otherwise indicated, all the records were obtained with the same stimulating current, the magnitude of which is given by the vertical bar to the left of record *1*. Records *4*, *8*, *12*, *16*, and *18* were obtained with currents of progressively increasing magnitude. The vertical bar to the left of each record gives the magnitude of the largest current used.

The observations were repeated with solutions containing moderate amounts of sodium ions, which were prepared by mixing the appropriate amounts of sodium Ringer's and glucose Ringer's. These sodium-deficient solutions produced effects similar to those which the sodium-free solution had produced, the differences consisting only in that the reduction in the height of the maximal action potential and the increase in the stimulation threshold were smaller (Fig. 1, *7* to *13*).

After a third restoration by Ringer's solution (Fig. 1, *14*), the central chamber was filled again with glucose Ringer's, which solution once more failed to abolish the ability of the fiber to produce action potentials of graded height (Fig. 1, *16*). The following restoration by Ringer's solution developed at a markedly low rate. After 5 minutes the maximal action potential still had a subnormal height and the height of the action potential still was dependent upon the magnitude of the stimulating current (Fig. 1, *18*). After two additional minutes the action potential has re-

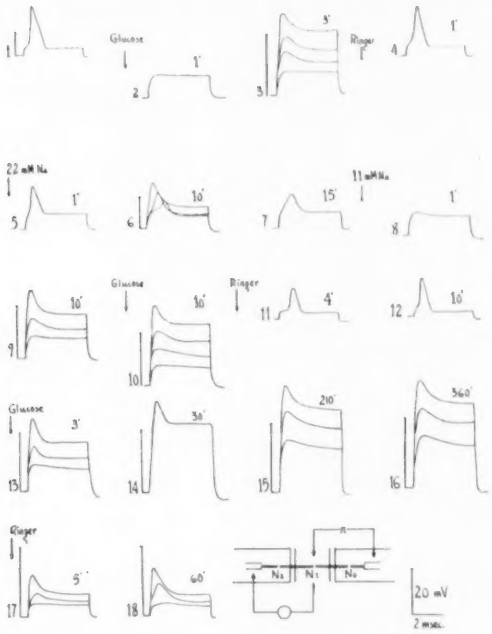

FIG. 2.—(See explanation of Fig. 1.) Nodes N_0 and N_2 were kept immersed in a fully ionized sodium-free medium. In this experiment, the absolute values of the stimulating current were not measured. The relative values are given by the heights of the vertical bars to the left of the records. Absence of a vertical bar indicates that the record had been obtained with the same current as record *1*.

gained a considerable height (Fig. 1, *19*) and the all-or-nothing law became approximately valid.

Similar observations were made in the experiment illustrated by Figure 2. The segment of the fiber enclosed in the central chamber was first placed in contact with glucose Ringer's (Fig. 2, *2*, *3*) and after restoration by sodium Ringer's (Fig. 2, *4*), that segment was successively placed in contact with a solution containing 22 mM sodium ions (Fig. 2, *5* to *7*), with a solution containing 11 mM sodium ions (Fig. 2, *8*, *9*), and with sodium-free glucose Ringer's (Fig. 2, *10*). At this stage of the experiment, restoration by sodium Ringer's already had become a very slow process (Fig. 2, *11*, *12*).

Finally, the central segment of the nerve fiber was again immersed in sodium-free glucose Ringer's and was kept in this solution for six hours, during which time the glucose solution was renewed several times. As can be seen in Figure 2, *13* to *16*, the nerve fiber permanently retained its ability to produce action potentials of graded height in response to stimulation by currents of progressively increasing magnitude.

Replacement of the glucose solution by sodium Ringer's brought about a recovery which not only was very slow but also failed to become complete. After the central segment of the nerve fiber had been kept in sodium Ringer's for 5 minutes the maximal action potentials still had approximately the same height as they had with the

fiber immersed in glucose Ringer's (Fig. 2, *17*). In addition, the threshold of stimulation still was very high. Indeed, the only clear sign of recovery was the marked decrease in the apparent resistance of the membrane and therefore in the height of the electrotonic potential. After 60 min in sodium Ringer's, it was found that the maximal action potential had increased somewhat in height, but it still was markedly subnormal. It was also found that the stimulation threshold still was exceedingly high (Fig. 2, *18*). The observations were continued for one additional hour. No further improvement in the state of the nerve fiber took place.

At this point, an important remark must be made. The action potentials that appear in Figures 1 and 2 are monophasic because the threshold of stimulation of node N_2 had been raised by 5 mM xylocaine in the case of Figure 1 and by a fully ionized sodium-free medium in the case of Figure 2. If the chamber containing node N_2 is kept filled with sodium Ringer's, the action potentials initiated at node N_1 in the sodium free central chamber, when they are caused to be sufficiently large, do initiate action potentials at node N_2, whereby the recorded response becomes diphasic.

Similar results have been obtained in other experiments done with the use of fully ionized sodium-free media, i.e., media in which the sodium chloride of Ringer's solution had been replaced by diethanol-dimethyl-ammonium chloride. In experiments in which the segment of the isolated fiber in the central pool is kept immersed in the sodium-free medium for extended periods of time, however, the results are much more spectacular when glucose Ringer's is used.

The reason for this difference is important. According to the indeed very numerous determinations made in this laboratory of sodium and potassium contents of nerves that had been kept in various sodium free Ringer solutions for varying periods of time, the potassium content remains practically constant at the same time that all the interstitial sodium and a large part of the internal sodium of the nerve fibers is being lost to the medium. (The results of the analyses will be presented in a forthcoming communication.) In fully ionized sodium free media, the internal sodium may escape from inside the nerve fibers in exchange for ethanol-trimethyl-ammonium (choline) or for diethanol-dimethyl-ammonium. In glucose Ringer's, the internal sodium can escape from the nerve fibers only when it is accompanied by an equivalent amount of anions. Consequently, while the initial phase of the loss of sodium by the nerve has approximately equal temporal courses in fully ionized and in poorly ionized sodium-free media, the later phase of loss of internal sodium by the nerve fibers has a markedly slower course in glucose Ringer's than in fully ionized sodium-free media.

The exact relation between the internal sodium content and the height of the maximal action potential that the nerve fibers are capable of producing is not known. In a first approximation, however, it may be said that, other conditions being equal, with the nerve fibers in a sodium-free medium the height of the maximal action potential becomes more or less proportional to the internal sodium content of the fibers. For this reason, after the nerve fibers have been kept for some time in a sodium-free medium, the maximal action potential is permanently higher in glucose Ringer's than in fully ionized sodium-free media.

No attempt will be made to ascertain the cause of the errors contained in the statement made by Huxley and Stämpfli[3, 4] that when isolated, single frog nerve

fibers are immersed in a sodium-free medium, the action potential is abolished instantaneously. It must be emphasized, however, that the errors have had serious consequences.

In 1944, Lorente de Nó[5] gave the first valid proof that sodium is necessary for the maintenance of the ability of nerve fibers to conduct action potentials. Overton[6] had been able to demonstrate that need only with muscle fibers. After having carried out an intensive research, extending throughout several years, Lorente de Nó[1, 7] reached the conclusion that the presence of sodium ions outside the nerve fibers is not necessary for the production and the conduction of the action potential. In those processes, only the sodium that is present inside the nerve fibers can play a specific role.

Later, however, Hodgkin and Katz[8] came to a diametrically opposite conclusion. According to Hodgkin and Katz, the external sodium plays a direct and essential role in the production of the action potential, for which reason the nerve fibers cannot produce action potentials after they have been immersed in a sodium-free medium. Moreover, according to Hodgkin and Katz, the height of the action potential is directly determined by the logarithm of the external sodium concentration. The sodium hypothesis of Hodgkin and Katz was later elaborated by Hodgkin and Huxley (cf. Hodgkin[9]) into what is usually known in the literature under the name of ionic hypothesis.

It appears now that isolated, single frog nerve fibers immersed in a sodium-free medium behave in essentially the same manner as, for many years, the fibers of nerve trunks with sheath or sheathless, have been known to behave, at least in this laboratory.[1, 2, 7] They are able to produce action potentials for many hours, in the total absence of sodium from their external medium. Consequently, the ionic hypothesis is incorrect—a conclusion which is in agreement with results of work done in other laboratories.

Mauro,[10] working with one of the giant fibers of the lobster with the use of internal microelectrodes, found that the fiber is still capable of producing action potentials of graded height after the fiber has been immersed in a sodium-free medium for an extended period of time.

Koketsu[11] has marshalled an important array of experimental evidence—much of which was obtained in work done with the use of microelectrodes introduced into spinal ganglion cells by Koketsu, Cerf, and Nishi—showing that the production of the action potential is not directly dependent upon the presence outside of the ganglion cells of sodium ions or of other ions at specific concentrations, or, indeed, at any concentration.

While the manuscript of this communication was being prepared, an important paper by Van der Kloot and Rubin[12] has appeared. These authors have shown that frog heart muscle can produce action potentials for extended periods of time in sodium-free glucose Ringer's.

Summary.—Sodium-free solutions do not abolish the action potential of isolated, single frog nerve fibers. They only increase the threshold of stimulation and reduce the height of the maximal action potential that the nerve fibers are capable of producing. With nerve fibers in a state of sodium-deficiency, the all-or-nothing law is not even approximately valid. The height of the action potential increases with the magnitude of the stimulating current. The presence of sodium ions outside the

nerve fibers is not necessary for the production of the action potential. In this process, only the internal sodium can play a specific role.

* This research was supported in part by a grant (B-2650) from the U.S. Public Health Service.

† Postdoctoral Research Fellow of the U.S. Public Health Service.

[1] Lorente de Nó, R., *A Study of Nerve Physiology*, Studies from the Rockefeller Institute (New York, 1947), vols. 131 and 132.

[2] Lorente de Nó, R., in *Bioelectrogenesis*, Proceedings of the Symposium on Comparative Bioelectrogenesis, Rio de Janeiro, 1959, ed. Chagas and Paes de Carvalho (New York: Elsevier, 1961), p. 229.

[3] Huxley, A. F., and R. Stämpfli, 1949, quoted in reference 8.

[4] Huxley, A. F., and R. Stämpfli, *J. Physiol.*, **112**, 496 (1951).

[5] Lorente de Nó, R., *J. Cell. Comp. Physiol.*, **24**, 85 (1944).

[6] Overton, E., *Arch. ges. Physiol.*, **92**, 346 (1902).

[7] Lorente de Nó, R., *J. Cell. Comp. Physiol.*, **33**, Suppl. (1949).

[8] Hodgkin, A. L., and B. Katz, *J. Physiol.*, **108**, 37 (1949).

[9] Hodgkin, A. L., *Proc. Roy. Soc. London*, **B148**, 1 (1957).

[10] Mauro, A., quoted in reference 2.

[11] Koketsu, K., in *Biophysics of Physiological and Pharmacological Actions* (Washington: American Association for the Advancement of Science, 1961).

[12] Van der Kloot, W. G., and N. S. Rubin, *J. Gen. Physiol.*, **46**, 35 (1962).

---

*ACTION SPECTRUM FOR PALING (DECREASE IN REFRACTIVE INDEX) OF ULTRAVIOLET-IRRADIATED CHROMOSOME SEGMENTS**

BY RAYMOND E. ZIRKLE AND ROBERT B. URETZ

COMMITTEE ON BIOPHYSICS, UNIVERSITY OF CHICAGO

Communicated November 5, 1962

Chromosome paling, as a result of ultraviolet partial-cell irradiation, has been dealt with in earlier papers from this laboratory,[1-5] and its main features have been summarized.[6] The phenomenon is called paling because, whereas nonirradiated chromosomes appear black by medium-dark phase microscopy, suitably irradiated portions of living chromosomes become gray or even clear (Fig. 1), depending upon amount of exposure. This change in appearance is due to decrease in refractive index, and the latter in turn appears to be due to loss of nonaqueous material, since no change in volume of the irradiated chromosome portions can be detected and, moreover, selective loss of a definite electron-microscopic component[4] is correlated with the paling. To gain some idea of the mechanism by which this disassembly of a living chromosome is brought about, we have worked out an action spectrum for the process.

Methods.—Studies on paling can be made only with partial-cell irradiation. The efficiency of UV radiation, per unit of energy incident on unit area, *decreases* as more and more of the total chromosome complement is bombarded.[3, 5] In particular, when the entire complement (or the entire cell) is irradiated, no paling can be detected; this explains why the phenomenon was not discovered with total-cell irradiation many years ago. Moreover, paling is produced only by direct irradiation of chromosomal material; prolonged exposure that barely misses a chromosome produces no paling.

FIG. 1.—Paling of chromosomes in a metaphase cell of newt heart in tissue culture. (Round pale region is just below center of photograph.) Spindle axis from left to right. Diameter of microbeam, 8μ. Medium-dark phase-contrast microscopy, 1,000 $\times$. (Black isodiametric objects are inclusions, not chromosomes.)

In the present work, partial-cell irradiations were performed with UV microbeams produced by an apparatus similar to the one described by Uretz *et al.*[1, 7] Radiation from a General Electric A-H6 lamp was dispersed with a grating monochromator (Bausch & Lomb 250 mm), and wavelength bands 40 Å in width were introduced into the microbeam apparatus. The midpoints of the bands were 2,250, 2,400, 2,500, 2,600, 2,700, 2,800, and 3,000 Å. The microbeams were conical, with half-angle of about 25°, and the diameter of the focal "hot spot" was 8μ. The total power (ergs/sec) in the various microbeams was measured frequently throughout the experiments by means of a photomultiplier apparatus.[7]

Cultures of newt heart (*Triturus viridescens*) were made,[4] kept, and used at 23°C. Mitotic cells were selected that grew immediately below and adherent to the quartz cover slip. These "naturally" flattened cells were especially favorable for microscopic examination, for photography, and for UV microbeam irradiation. Since the investigation required some hundreds of cells in, as nearly as possible, the same physiological condition, we used only metaphases that had been watched until the chromosomes had their kinetochores on the equatorial plate (Fig. 1). Since every cell was flattened, the axis of the spindle was always perpendicular to that of the microscope, and the chromosomes, with their kinetochores forming a ring around the spindle equator and their arms extending into the cytoplasm, collectively presented a configuration that, for obvious reasons, was referred to as the "butterfly." The target for the 8μ microbeam was the middle of one of the "wings." Since the "wing" was not a single layer of chromosomes, the bombardment microscope was kept focused on the topmost chromosomes in the target area. Since these received the greatest exposure in any given irradiation, they were the ones that would exhibit paling if any did.

At each of the seven wavelengths, samples of cells were given graded incident exposures, a different cell being used for every exposure. Each cell was observed by direct phase-contrast microscopy and by means of time-lapse cinematography (15 frames/sec), which was started a few minutes before irradiation and was continued, with a few minutes out for irradiation, until anaphase movement was complete. Each cell was scored as affected or not affected, the criterion for a positive score being any visually detectable paling, seen either in the living cell or in the film. At the high end of the exposure range, paling was readily seen within a few minutes after irradiation, as in Figure 1, and occurred in all cells of the samples. At the low end, none of the cells scored positive, whereas in the important intermediate part of the range some scored positive and some negative. Here, the anaphase observations were indispensable. Since a chromosome that receives a paling dose is practically certain to exhibit also the phenomenon of stickiness,[2, 6] there is a period of several minutes in anaphase when the bombarded portions of daughter chromosomes are stretched across the equatorial region, the nonirradiated ones having already approached the poles of the spindle. Thus, if paling is present, this is the best time to detect it without visual interference from the other chromosomes. Two observers, working with the time-lapse film, made independent judgments of presence or absence of paling. If both judged it to be present, the cell was scored positive. Differences in judgment were rare and appeared to be random.

Since a total of some 460 cells was used and the number irradiated in one day varied between five and fifteen, the experiments extended over several months and some dozens of batches of cultures. This necessitated suitable randomization of exposure and wavelength over the entire experimental period. For each wavelength, exposures were graded by factors of 2 and were performed in from 2 to 120 sec. These exposures, expressed as total photons incident on the cell, are set forth, with other data, in the wide column 2 of Table 1. At the "hot spot" of the conical microbeam, where the experimental chromosome segment was situated, these photons were incident on an area 8μ in diameter, i.e., about 50μ^2.

The incident energy was not corrected for absorption in the cytoplasm lying between cover slip

and topmost chromosome. This layer could be at most 2 or 3μ thick, and Perry's measurements[5] show that a 2μ thickness absorbs no more than 5 or 6 per cent between 2,400 and 3,000 Å. At 2,250 Å the absorption, although likely to be higher because of cytoplasmic proteins, would be quite unlikely to reduce the incident energy more than a factor of 2; the resulting doubling of relative effectiveness at this wavelength would not invalidate the conclusions drawn later. Of probably greater concern is the absorbance of the chromosome itself. Since it varies with wavelength and is quite appreciable at some values,[5] it is necessary to compare the energy I_0 incident on the top of the chromosome (column 2, Table 1) with an average energy I_{av} incident on material located at various depths. Assuming uniform optical density throughout the chromosome, an approximation for mean incident energy is obtained from the relation

$$\frac{I_{av}}{I_0} = \frac{1}{t}\int_0^t \exp(-kx)dx = \frac{1-(I_t/I_0)}{2.3\log(I_0/I_t)}, \quad (1)$$

where x, the depth, has the maximal value t (actually about 2μ), and k is the linear absorption coefficient. Thus I_{av}/I_0 is readily calculated from $\log(I_0/I_t)$:

Wavelength (Å)	2,250	2,400	2,500	2,600	2,700	2,800	3,000
$\log(I_0/I_t)$	(0.17) (0.5)	0.22	0.28	0.34	0.28	0.21	0.02
I_{av}/I_0	(0.8) (0.6)	0.78	0.73	0.70	0.73	0.79	0.99

The various values of $\log(I_0/I_t)$ were obtained as follows: Those tabulated for 2,400, 2,600, 2,800, and 3,000 Å were measured by Perry.[5] Since his relative values confirm the prevalent assumption that, between 2,400 and 2,800 Å, chromosomal absorption is predominantly due to DNA, the values for 2,500 and 2,700 Å were obtained by interpolation with the aid of a DNA absorption spectrum (Fig. 2*B*). For 2,250 Å, two values were estimated by less direct means. The smaller, 0.17, is calculated from those at 2,400, 2,600, and 2,800 Å on the assumption that DNA absorption predominates at 2,250 Å also. This estimate is certainly a lower limit, since protein absorption, relative to DNA, is many times higher at 2,250 than at 2,600 Å (e.g., Fig. 2*A*, 2*B*), the major relevant chromophores being the peptide bond and also the phenolic ring if tyrosine is present. In the absence of accurate data on relative amounts and optical densities of protein and DNA, we cannot set a correspondingly definite upper limit. The tabulated value 0.5 is derived from 0.17 by setting the protein absorbance for 2,250 Å at twice that of the DNA present. This absorbance ratio follows from use of 300, 7,800, and 3,000 as the respective molecular extinction coefficients for the peptide bond,[16] the tyrosine residue,[16] and the average nucleotide in native DNA[11] and from the assumptions that the chromosomal protein is three times the DNA by weight and that 5% of the amino acid residues are tyrosine.[17] The assumption that protein/DNA = 3 implies, in the living chromosome, a concentration of DNA and protein totaling roughly 400 gm/l, since the value 0.34 for $\log(I_0/I_t)$ at 2,600 Å, if ascribed entirely to DNA, corresponds to a DNA concentration of about 100 gm/l. Thus, since a higher concentration of total nonaqueous material seems unlikely, the value 0.5 for $\log(I_0/I_t)$ appears to be conservatively high. The significance of all the I_{av}/I_0 ratios is considered under *Results and Conclusions.*

Results and Conclusions.—From the experimental data given in the wide second column of Table 1, the 50 per cent effective exposure (EE50) was calculated for each wavelength in photons/cell (column 3). Reciprocals of these EE50's, multiplied by 10^{12} to obtain convenient numbers, are taken as values of relative effectiveness (column 4). This simple procedure is permissible since the seven exposure-effect curves, not shown here but obtainable from column 2 by plotting for each wavelength the "per cent paling" against the logarithm of "exposure," are all of the same shape within experimental error. To visualize the action spectrum, the numbers in column 4 are plotted against wavelength (Fig. 2, curve *A*). It will be noted that the relative effectiveness per incident quantum varies by a factor of about 100 between 2,250 and 3,000 Å and that there is a broad maximum with midpoint

TABLE 1

RELATIONS BETWEEN INCIDENT ENERGY AND PALING AT VARIOUS WAVELENGTHS

Wavelength (Å) (1)	Experimental data: exposure in units of 10^3 incident photons per cell; number of cells used; fraction of cells that showed paling (2)							EE50 (10^3 photons per cell*) (3)	Relative Effectiveness in Terms of: Incident flux at top of chromosome† (4)	Relative Effectiveness in Terms of: Average flux through chromosome‡ (5)
2,250	Exposure	0.38	0.75	1.5	3	6	12	4.6 ± 0.9	220	(200)
	Cells	2	4	5	5	4	2			(270)
	Per cent paling	0	0	0	40	50	100			
2,400	Exposure	3.3	6.5	13	26	53	106	33 ± 6	30	28
	Cells	4	8	10	7	6	2			
	Per cent paling	0	0	20	43	67	100			
2,500	Exposure	9.5	19	38	75	150	300	99 ± 23	10	10
	Cells	11	9	13	9	6	2			
	Per cent paling	0	0	8	22	83	100			
2,600	Exposure	5	10	20	40	80	160	63 ± 5	16	17
	Cells	15	13	32	33	26	6			
	Per cent paling	0	0	6	24	54	100			
2,700	Exposure	5.5	11	22	44	88	175	53 ± 5	19	19
	Cells	6	19	24	18	12	5			
	Per cent paling	0	0	8	22	94	100			
2,800	Exposure	7.5	15	30	60	120	240	64 ± 6	16	15
	Cells	14	13	18	17	18	6			
	Per cent paling	0	0	0	65	78	100			
3,000	Exposure	36	73	145	290	580	1160	450 ± 180	2.2	1.7
	Cells	4	11	10	9	6	2			
	Per cent paling	0	0	0	11	67	100			

* EE50's (50% effective exposures) and standard errors were calculated by Kärber's method as described by Finney.[3]

† Effectiveness is inversely proportional to EE50. The tabulated values are reciprocals of the numbers in column 3, multiplied by 10^{12} for convenience.

‡ Each tabulated value is derived from the corresponding one in column 4 by dividing by the appropriate value of I_{av}/I_0 (see *Methods*) and then normalizing with respect to 2,700 Å by multiplying by 0.73, the I_{av}/I_0 ratio for that wavelength. The two values given for 2,250 Å correspond to the two for I_{av}/I_0 tabulated under *Methods*.

at 2,700 Å and with a height that is logarithmically about midway between the values at 2,250 and 3,000 Å.

In comparing the action spectrum with various available absorption spectra, we may start with the intact chromosome. Although good absorption data for this material are available only for 2,400, 2,600 and 2,800 Å (Fig. 2, curve *B*), it can readily be seen, by comparing the three absorbance values against the three corresponding points on the action spectrum, that there can be no reasonable approach to parallelism.

We accordingly turn to molecular components of the chromosome. We first assume: (*a*) that paling results from UV absorption in only one molecular species; (*b*) that all UV photons absorbed by that species have the same probability of contributing to paling, i.e., that the quantum efficiency is invariant with wavelength. Also, since most of the absorption spectra of interest are dependent on pH and no direct measurement of this quantity for a metaphase chromosome is available, we assume (*c*) that pH 7 is a reasonable value.

Of various molecular species, DNA is a prominent and abundant component of the chromosome. Unfortunately, not much is directly known about *newt* DNA. However, with regard to UV absorption, calf-thymus DNA, which has been extensively studied, can be considered a fairly safe substitute for newt DNA, since

the proportions of the various purines and pyrimidines are similar for all those mammals, amphibia, and fish for which data are available.[9, 10] In Figure 3*B*, the action spectrum for paling is shown with a typical absorption spectrum for calf-thymus DNA.[11] It will be noted that the agreement is quite poor. It is therefore evident that, if the chromophores relevant to paling are located in the DNA molecule, they must be only a fraction of the various kinds that contribute to the DNA absorption spectrum. Accordingly, we turn to the various nucleotides, for which extensive absorption data have recently been published.[12] The only one which fits the action spectrum substantially better than DNA is deoxycytidylic acid, and it fits best at pH 7. The absorption spectrum in Figure 3*D* is thus the best fit that we have been able to find in the literature for any DNA constituent under any conditions. The parallelism to the action spectrum is good from 2,500 to 3,000 Å, but there is great deviation at the lowest wavelengths.

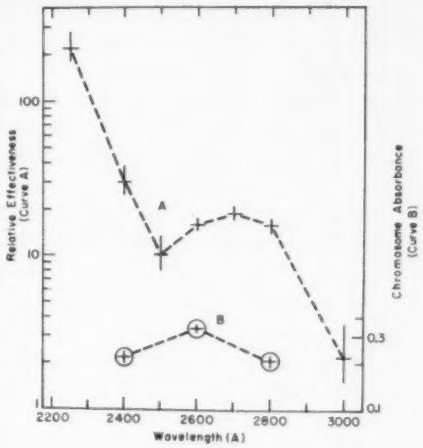

FIG. 2.—(*A*) Action spectrum for chromosomal paling produced by UV microbeams. Values of relative effectiveness are from column 4, Table 1. For each experimental point, the horizontal bar designates the 40Å width of the wavelength band used, and the vertical corresponds to the standard error of the EE50 (column 3, Table 1). The dotted line serves merely to guide the eye. (*B*) Absorbance of newt chromosome (Perry).[5]

Like DNA, proteins are prominent and abundant in chromosomes. The literature, as in the case of DNA, yields no direct information concerning the proteins of *newt* chromosomes. Moreover, with chromosomal proteins, very little is known of their relative amino acid content among various animal groups, and it is impracticable on this basis to select "substitutes" for newt proteins. However, it is a striking fact that, on the whole, proteins containing tyrosine (plus tryptophane in some) taken from widely diverse organisms exhibit UV absorption spectra of quite similar shape; among numerous relevant examples, the one for trypsin[13] (Fig. 3*A*) is fairly typical. Although it does not fit all points of the action spectrum within the standard errors, its general agreement throughout the range 2,250–3,000 Å is much better than DNA and is superior to deoxycytidylic acid. Among other proteins containing tyrosine, some of the absorption spectra fit rather worse and some better than that of trypsin. The best-fitting spectra we have found are those of histones from calf thymus. The one providing the curve of Figure 3*C* was isolated by Cruft *et al.*[14] An earlier preparation by Mirsky and Pollister[15] is similar in shape but fits all action points, within the standard errors, from 2,400 to 3,000 Å.

It thus appears that, among the principal known macromolecular components of chromosomes, the action spectrum indicates a protein, possibly a histone, as the molecular species that most likely absorbs the particular photons that are involved in paling. Certainly, DNA would seem to be contraindicated for this role.

The action spectrum plotted in Figures 2 and 3 is based on the energy I_0 incident on the top of the chromosome. It is necessary to inquire concerning any modifica-

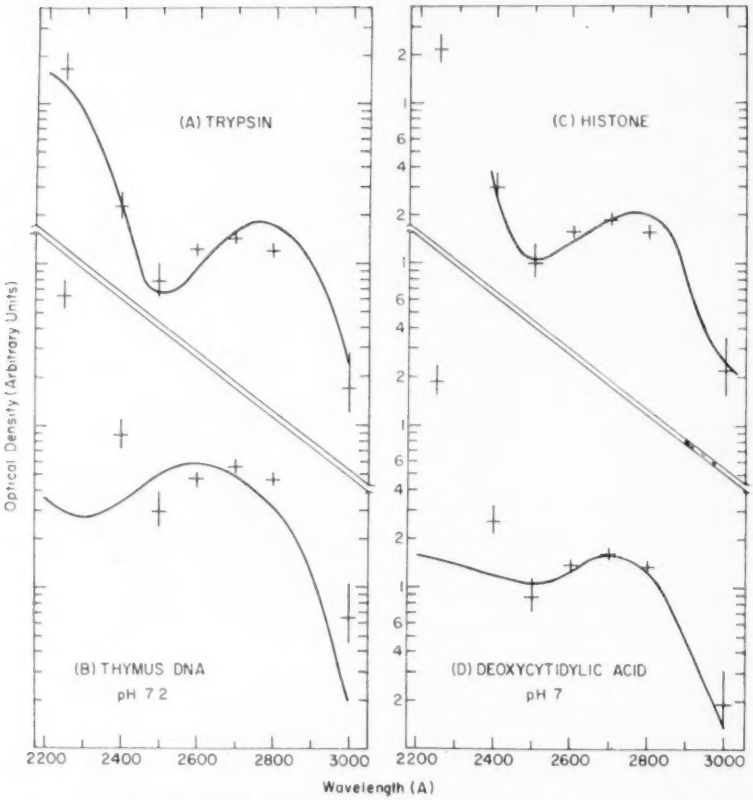

FIG. 3.—Action spectrum for chromosomal paling compared with absorption spectra for trypsin,[13] DNA,[11] histone,[14] and deoxycytidylic acid.[12] In each of the four charts, the seven experimental points are those of Figure 2A, with the ordinates multiplied by a convenient constant, and the optical density of each substance is multiplied by an arbitrary constant that brings the continuous absorption curve into best visual fit with the seven points of the action spectrum.

tion of this spectrum if, instead of I_0, we use I_{av}, the mean energy incident on successive infinitesimal layers of chromosome. Values of I_{av}/I_0 are tabulated under *Methods*, and corresponding values of relative effectiveness based on I_{av} are given in column 5, Table 1. If these numbers are substituted as ordinates in Figure 2A, it is readily seen that the action spectrum is not shifted to any degree that would affect the foregoing comparisons of it with the absorption spectra.

Discussion.—Since, among the chemical constituents of chromosomes, proteins and DNA are predominantly abundant, only these substances will be considered in an attempt to account for paling. The protein/DNA ratio is unknown but very likely lies between 1 and 3.[21] Since we have at present no quantitative relation between the degree of paling seen in the phase microscope and the percentage loss of nonaqueous material,[19] it must be considered quite possible that each of the two substances is relatively abundant enough that the paling could be entirely due to loss of it alone. There is of course the alternative possibility that both are lost in

amounts sufficient to contribute to paling. In trying to deal with these questions, four independent experimental observations are relevant: (1) The "protein-like" shape of the action spectrum reported here. (2) Decrease in chromosome absorbance[5] in paled segments at 2,400, 2,600, and 2,800 Å. This can be ascribed to either loss or alteration of purine and/or pyrimidine side chains of DNA, but some semiquantitative considerations indicate loss as the predominant mechanism.[20] (3) Marked qualitative decrease of Feulgen staining in paled segments,[4] which can be ascribed to either loss or alteration of deoxyribose residues. (4) Clear qualitative decrease in the Alfert-Geschwind reaction in paled segments,[4] indicating either loss or alteration of basic proteins (here, histones).

In Table 2 are listed various hypotheses (column 1) concerning the substance(s) whose loss predominantly accounts for paling. For each such hypothesis, what appears to be the most plausible model(s) for paling are tabulated (column 2). Here the materials assumed lost are shown in parentheses, their relative locations being essential. The chromosome "skeleton" (i.e., that structural residue which survives

TABLE 2

MODELS FOR PALING*

Material assumed lost (1)		Chromosome model (2)	Loss of bases (3)	Decrease in Feulgen (4)	Decrease in A-G stain (5)
Protein only	1*a*.	[DNA, prot]–(*prot*)	−	−	+†
	1*b*.	[DNA, *prot*]–(prot)	−	−	+†
DNA only	2.	[DNA, *prot*]–(DNA)	+	+	−
Both DNA and protein	3*a*.	[DNA, *prot*]–(prot-DNA)	+	+	+†
	3*b*.	[DNA, *prot*]–(DNA-prot)	+	+	+†
	3*c*.	[DNA, prot]–(*prot*-DNA)	+	+	+†

* See text for notation and symbols.
† Will be + if the protein lost includes histone.

paling and always maintains the continuity of the paled segment with the rest of the chromosome) is shown in brackets as containing both protein and DNA (their relative positions not essential), since the presence of neither can at present be ruled out. The dash between brackets and parentheses designates the linkage assumed to be broken, and italics indicate the absorber of the relevant photons. In view of the action spectrum, this absorber is designated as protein in all the models shown. Also, to avoid any need for intermolecular energy transfer, it is assumed that this protein is involved in the linkage that is broken. In columns 3–5 are shown the agreements (+) and/or disagreements (−) of each model with the last three of the four experimental facts listed in the preceding paragraph. It will be noted that models 3*a*, 3*b*, and 3*c* are consistent with all the facts. Each results in loss of both DNA and protein (including histone) and involves two assumptions: (*a*) a single photobreakage of a protein-protein or protein-DNA linkage and (*b*) a combination of some sort between the DNA and protein that are lost. The latter assumption is not startling in view of the established abundance of nucleohistones in cell nuclei.[22] Accordingly, these models would appear preferable to any that require two distinct kinds of photoeffect (e.g., a combination of models 1*b* and 2). It thus seems that the view most compatible with the scanty but striking facts now available is that both protein and DNA are lost from the chromosome, thus accounting for the paling, and are probably lost as some sort of combination which is detached from

the chromosome by photons absorbed in protein, either that which is lost or that which remains in the chromosome "skeleton."

Summary.—In producing paling (loss of nonaqueous material) in ultraviolet-irradiated segments of living chromosomes, the quantum effectiveness at wavelengths 2,250, 2,400, 2,500, 2,600, 2,700, 2,800, and 3,000 Å has the relative values 220, 30, 10, 16, 19, 16, and 2.2 respectively. Thus, the action spectrum more nearly parallels the absorption spectrum of a tyrosine-containing protein than that of DNA or any of its nucleotides. From this finding, along with observations by others that paling is accompanied by decrease in ultraviolet absorption, in Fuelgen reaction, and in Alfert-Geschwind reaction, it is concluded that paling is most likely due to loss of both protein and DNA, possibly as some combination of the two which is detached from the chromosome by photons absorbed by protein.

* Supported by a contract with the U.S. Atomic Energy Commission, by an equipment-loan contract with the Office of Naval Research, and by grants from the U.S. Public Health Service and the Abbott Research Fund, University of Chicago.

[1] Uretz, R. B., W. Bloom, and R. E. Zirkle, *Science*, **120**, 197 (1954).

[2] Bloom, W., R. E. Zirkle, and R. B. Uretz, *Ann. N. Y. Acad. Sci.*, **59**, 503 (1955).

[3] Zirkle, R. E., W. Bloom, and R. B. Uretz, *Proceedings of the International Conference on Peaceful Uses of Atomic Energy*, Geneva (New York: United Nations, 1955, 1956), vol. 11, p. 273.

[4] Bloom, W., and R. J. Leider, *J. Cell Biol.*, **13**, 269 (1962).

[5] Perry, R. P., *Exptl. Cell Res.*, **12**, 546 (1957).

[6] Zirkle, R. E., *Advances in Biol. & Med. Phys.*, **5**, 103 (1957).

[7] Uretz, R. B., and R. P. Perry, *Rev. Sci. Inst.*, **28**, 861 (1957).

[8] Finney, D. J., *Probit Analysis* (2d ed.; Cambridge University Press, 1952).

[9] Sueoka, N., *J. Mol. Biol.*, **3**, 31 (1961).

[10] Allfrey, V. G., A. E. Mirsky, and H. Stern, *Advances in Enzymol.*, **16**, 411 (1955).

[11] Lawley, P. D., *Biochim. Biophys. Acta*, **21**, 481 (1956).

[12] Fredericq, E., A. Oth, and F. Fontaine, *J. Mol. Biol.*, **3**, 11 (1961).

[13] Setlow, R., and B. Doyle, *Biochim. Biophys. Acta*, **24**, 27 (1957).

[14] Cruft, H. J., C. M. Mauritzen, and E. Stedman, *Phil. Trans. Roy. Soc.*, B **241**, 93 (1957).

[15] Mirsky, A. E., and A. W. Pollister, *J. Gen. Physiol.*, **30**, 117 (1946).

[16] Setlow, R. B., and W. R. Guild, *Arch. Biochem. & Biophys.*, **34**, 223 (1951).

[17] Tristram, G. R., in *The Proteins*, ed. H. Neurath and K. Bailey (New York: Academic Press, 1953), pp. 181–233.

[18] Shugar, D., and K. L. Wierzchowski, *Postepy Biochem.*, **4**, 243 (1958).

[19] In our laboratories, interference microscopy has not proved satisfactory as a means of achieving this.

[20] Perry[5] found about 60 per cent reduction in 2,600 Å chromosome absorbance associated with paling of a degree that we have readily obtained with 2,600 Å exposures (I_{av}) of 6×10^9 photons/μ^2. Then since the mean cross section per DNA nucleotide is 2.3×10^{-9} μ^2 for 2,600 Å radiation, the mean number of photons absorbed per nucleotide is about 14. (The protein absorption could reduce this, perhaps 10%.) Then the mean quantum yield required for eliminating the 2,600 Å absorption by the chromosomal nucleotides must be at least 0.6/14 = 0.04 nucleotide/photon. When this is compared with 0.003 and 0.001 for deoxycytidylic and thymidylic acids respectively in solution, while purine nucleotides exhibit even lower values,[18] it seems likely that loss of bases must be invoked to explain the decrease in chromosomal absorbance.

[21] Reasons for 3 as upper bound for the weight ratio are given in last paragraph under *Methods*. That 1 is a reasonable lower bound is indicated by the fact that histones alone are about 70 per cent as abundant as DNA in a wide variety of vertebrate nuclei[14] and outweigh the DNA in isolated DNP.[22]

[22] Zubay, G., and P. Doty, *J. Mol. Biol.*, **1**, 1 (1959).

GENE EXPRESSION IN DIFFERENTIATED CELLS

By E. H. Davidson, V. G. Allfrey, and A. E. Mirsky

THE ROCKEFELLER INSTITUTE

Communicated November 13, 1962

This communication is concerned with the dynamics of gene control over specific biochemical functions in a differentiated cell. Direct experimental access to the intracellular link between gene action and the target cell characters has become feasible with the accumulation of evidence demonstrating that the synthesis of specific RNA's on the genomic DNA template is the actual primary mechanism of gene function in the cell and with the development of the highly effective inhibitor of that synthetic reaction, actinomycin D. In the experiments to be presented, this agent was used to block nuclear RNA synthesis in a cultured mammalian cell type which has retained *in vitro* a differentiated cellular activity. The effect of actinomycin treatment on this cell function and on a specific mitochondrial enzyme activity was then followed. Actinomycin treatment was found to inhibit the specific cell function immediately, while, in contrast, the mitochondrial enzyme activity appeared to remain impervious to the effects of this agent for long periods.

The cell line whose development made possible these studies is of connective tissue origin. Termed ARE-2-60 and described in detail elsewhere,[1] its differentiated property consists of the continuous synthesis and secretion into the culture medium of acid mucopolysaccharides characteristic of connective tissue. The major advantages of experimental material of this nature are twofold: it permits study of cellular differentiation as a genetically inherited or genomically specified cell property, and it provides for the expression of such properties an environment which is devoid of complex (i.e., variable) tissue-tissue interactions. Since the cells grow in a monolayer on a glass substratum, even cell-cell interactions are strikingly reduced as compared to the case in normal tissue, organ culture, or artificial cell aggregates.[2]

Differentiated cellular properties are determined ultimately by information carried in the cell genome. The well-known Mendelian transmission of variant hemoglobin forms serves as a classic illustration of this fact, for hemoglobin is a protein whose mass production constitutes the end-product of a highly specialized cell, the reticulocyte. The particular question to which this investigation is directed is the degree of immediate control exercised by the active genes in another differentiated system. Does a specific cytoplasmic function such as the secretion of some histospecific cell product proceed independently once the synthesizing machinery is set up, or is continuous gene action a requisite for the maintenance of differentiated activity?

*Origin and Characterization of the ARE-2-60 Cell Line.**—The cultured cell line used in these experiments originated three years ago as one of a series of primary monolayer cultures arising from explanted fragments of 1–4 day old weanling rat eye connective tissue. All details of the procedures by which the cultures were initiated and handled are given elsewhere.[1]

The ARE cell line behaves as a typical permanent cell line with respect to growth rate (mean generation time is 22.6 hr), plating efficiency ($\geqslant 52\%$), and karyotype (heteroploid, modal chromosome number near $3n$). All ARE cells are descended from one culture in which a characteristic tissue culture transformation event was observed to occur about four months after explantation of the primary fragments. The useful property of the ARE line, AMPS secretion, was detected

before transformation and has been maintained without quantitative variation since. Eleven clonal strains have been obtained,[1] all of which possess this histospecific property, thus clearly demonstrating the inheritance of a specialization initially set up during the histogenesis of the ancestral tissue of origin.

Connective tissue fibroblasts are known to secrete large quantities of hyaluronic acid and chondroitin sulfates.[3, 4] The major AMPS product synthesized and secreted by the ARE cell line appears to be hyaluronic acid, though other AMPS are not excluded.[1] In this respect, ARE-2-60 resembles fibroblast cell lines described by C. C. Morris[5] and also by Daniel *et al.*[6] In the experiments which are now to be presented, it was cell-bound rather than secreted AMPS synthesis which was measured. Details of the procedures employed are given in reference 1; in brief, ARE cells were planted on glass coverslips, exposed to N-acetylglucosamine-1-C^{14}, and fixed, and the radioactivity in the cells was counted directly in a low-background gas-flow counter.[7] The coverslips were then exposed to a solution of testicular hyaluronidase and recounted. Counts lost from the fixed cells during the hyaluronidase treatment can be considered to represent newly synthesized AMPS.[1]

In monitoring ARE cell function under various conditions, it was found that the per cell rate of AMPS synthesis was exceedingly sensitive to conditions affecting the general rate of protein synthesis. Thus, in experiments utilizing low doses of the protein synthesis inhibitor puromycin, it could be shown that even at levels of puromycin inhibition so mild that some net cell increase occurred during the 24-hr period of the experiment, AMPS synthesis and secretion were inhibited 80–90 per cent. This result set the stage for the experiments which now follow, for it suggested the possibility that in this continuously growing cell type active nuclear mediation might be required for the maintenance of the rate of protein synthesis on which the AMPS production system depends.

Effect of Actinomycin D on Synthesis of RNA, Protein, and Cell-Bound AMPS.—It is known that actinomycin functions by suppressing RNA-DNA polymerase activity,[8] apparently by complexing specifically and firmly with the DNA primer,[9, 10] and it has been shown in other tissue culture systems that actinomycin inhibits almost completely the synthesis of all cell RNA.[11, 12] The small amount of RNA synthesized in cells 95 per cent inhibited by actinomycin treatment does not resemble cell DNA in base composition[8] and in fact appears to consist mainly of s-RNA.[11] The irreversible nature of actinomycin action makes it possible to consider cells which have been exposed to the drug and then transferred to actinomycin-free medium as "chemically enucleated" cells.

In Figure 1 are presented the pooled results of several experiments in which RNA synthesis and AMPS synthesis were measured simultaneously in replicate coverslip preparations incubated for one hr with the respective C^{14} precursors at given intervals following a 20-min actinomycin treatment. The result of the experiments summarized in Figure 1 is clearcut: when 97 per cent of all cell RNA synthesis is blocked by actinomycin D, the rate of AMPS synthesis begins to decline immediately, without appreciable lag, and it continues to decline as long as it is followed. It is evident that in order for this differentiated trait to be expressed, *continuous nuclear activity* is required in the form of DNA-dependent RNA synthesis. This system is therefore characterized by immediate nuclear control. Parallel experiments were conducted to measure the uptake of C^{14}-L-leucine into protein at various intervals after actinomycin treatment. It was found that rate of total protein synthesis (CPM/coverslip/one-hr incubation) declined at essentially the same rate as does AMPS synthesis (Fig. 2). Franklin and Baltimore have published essentially

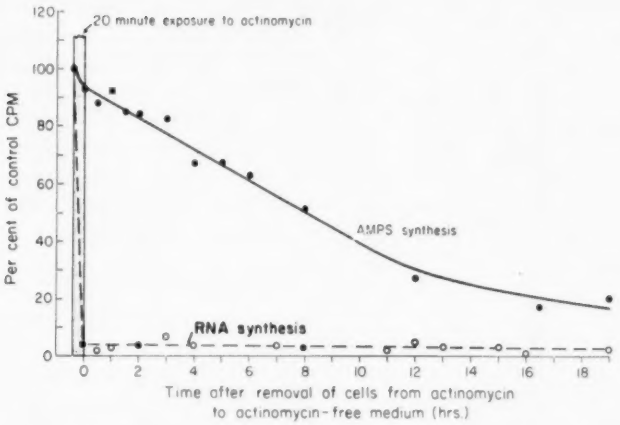
20 minute exposure to actinomycin
Per cent of control CPM
AMPS synthesis
RNA synthesis
Time after removal of cells from actinomycin to actinomycin-free medium (hrs.)

FIG. 1.—Effect of actinomycin D on synthesis of RNA and cell-bound AMPS. After exposure to actinomycin D for 20 min, coverslip cultures were transferred to actinomycin-free medium where they remained for the periods of time given along the abscissa. They were then incubated with C^{14}-N-acetylglucosamine or C^{14}-orotic acid for one hr, rinsed, fixed, and counted as described in text. Heavy black dots represent an average of three or four independent determinations, each in duplicate; open circles represent single determinations.

similar data showing the effects of actinomycin D on total protein synthesis in L-cells.[12]

In these experiments, isotopic labeling was carried out in actinomycin-free medium containing 5 μC/ml C^{14}-orotic acid (for RNA), 1 μC/ml C^{14}-L-leucine (for protein), or 5–10 μC/ml N-acetylglucosamine-1-C^{14} (for AMPS). Ninety-nine per cent of the counts incorporated from orotic acid were removable by incubation in 0.1 per cent crystalline RNAase. Protein samples were fixed in cold TCA in the same way as RNA samples. Twelve to sixteen hr after planting (7×10^5 cells/coverslip), the cells adhering to the coverslip surface were exposed for 20 min to actinomycin D, at a final concentration of 5 μg/ml, then rinsed free of the agent and transferred to clean medium. No cell division occurs in the period between planting and exposure to actinomycin.

Protein Turnover and Cell-Bound AMPS Synthesis Rate.—The effect of actinomycin on AMPS synthesis could be due to its interference with protein synthesis, in particular to interference with the synthesis of the enzymes which construct the AMPS polymers (or their components). If this were the case, then a parallel experiment to those of Figure 1, but where protein synthesis itself (rather than RNA synthesis) is blocked, should cause a sharper fall in AMPS synthesis rates than was found in the actinomycin-treated cells. Such was in fact the result (Fig. 2) when the effect of 50 μg puromycin/ml on AMPS synthesis was tested. At this dose, over 96 per cent of the normal protein synthesis was obliterated. Since puromycin inhibition is not irreversible, the 50 μg/ml concentration was maintained in the isotope-containing media. AMPS synthesis in the one-hr incubation periods with N-acetylglucosamine-1-C^{14} at the given time intervals after the start of puromycin treatment drops about five times faster than it does if RNA synthesis is blocked instead. The short rise in AMPS synthesis at 15 min and 30 min above the control values (Fig. 2) is not understood.

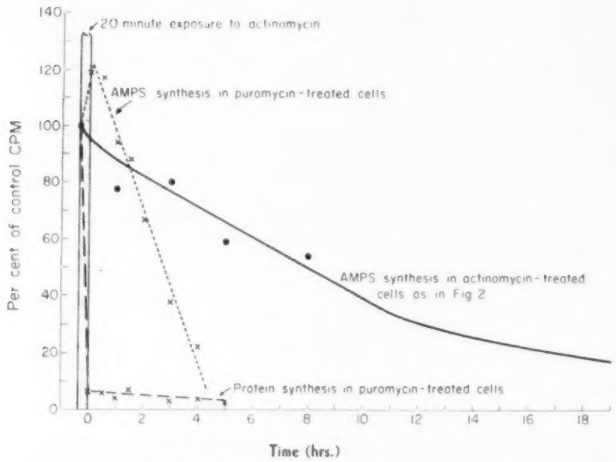

FIG. 2.—Comparison between the effect of actinomycin and the effect of puromycin on cell-bound AMPS synthesis. Heavy black dots represent the relative uptake of C^{14}-leucine into cell protein at various times following 20-min exposure to actinomycin. AMPS synthesis and protein synthesis in puromycin-treated cells were measured as described in the text from uptake of N-acetylglucosamine-1-C^{14} and C^{14}-leucine after various periods of exposure to 50 μg/ml puromycin.

It would thus appear that the turnover of one or several key enzymes constituting the AMPS synthesizing apparatus is so high that it must be continuously resynthesized to maintain the normal AMPS synthesis rate. This is in line with the finding that total protein turnover even in these rapidly growing cells is very high. At the rate of protein turnover characteristic of ARE cells,[1] half the protein present at any given time would have been replaced within three days, despite the rapid accretion of new protein occurring simultaneously as a function of the characteristically high rate of cell proliferation. Using another tissue culture cell line growing at comparable rates, Eagle *et al.* reported the very similar value of 1.0 per cent protein turnover/hr.[13] Since these turnover values refer to total cell protein, specific protein constituents are probably characterized by much higher turnover rates. Fast turnover of the AMPS-synthesizing machinery associated with a constant flow of apparently short-lived, newly synthesized RNA molecules is the simplest explanation of the results presented in Figures 1 and 2.

It is in any case evident that those RNA molecules on which AMPS synthesis depends must turn over at a high rate, since decreased AMPS production is detected within 20 min of actinomycin treatment (the shortest time the resolution of the method permits). As total protein synthesis appears to fall at about the same rate as AMPS synthesis in ARE cells and shows no lag before fall-off of synthesis rate in similarly treated L-cells,[12] the result obtained with the specific AMPS marker has a certain generality. Little is known about the rates of turnover of RNA molecules synthesized by RNA-DNA polymerase in nucleated cells. One system from which information bearing on this question has been derived is that of the isolated calf thymus lymphocyte nucleus. In this nucleus, the bulk of the RNA synthesized in a given period of time is messenger-type RNA, resembling cell DNA in base composition.[14] The evidence suggests that this RNA retains its activity to

stimulate nuclear protein synthesis for only about 20 min from the time of its own construction.[15] Thus, thymus lymphocyte messenger RNA would appear to possess a high turnover rate, since it is rapidly synthesized and rapidly inactivated. However, it is not profitable to speculate on which RNA component is the critically affected one in actinomycin-treated ARE cells. As Allfrey and Mirsky have pointed out,[17] both messenger and ribosomal RNA appear to be synthesized from a DNA template, and in rapidly growing cells both are synthesized at a high rate so that empirical distinctions between them tend to blur.

The Effect of Actinomycin on Succinic Dehydrogenase Activity.—In order to gain a better perspective on the immediacy of nuclear control in ARE cells, it was decided to test the effect of actinomycino n an enzymic activity of a different type. The widely distributed mitochondrial enzyme succinic dehydrogenase was chosen, since if there is some component of the cellular machinery which is not so immediately dependent on nuclear control, it might well be sought in a cytoplasmic organelle such as the mitochondrion. The idea that mitochondria are to be regarded as cell organelles is an old one.[16] Recent support for the view that mitochondria are relatively autonomous cytoplasmic units (i.e., cell organelles) derives from studies of Fletcher and Sanadi[18] on mitochondrial turnover. These authors labeled rat liver mitochondria with methionine S^{35} and acetate C^{14} and then followed the loss of label from cytochrome C and several other mitochondrial components. They found that radioactivity in all the mitochondrial fractions declined at the same rate, with a half-life of 10 days, almost twice the half-life known for total liver cell proteins.[19, 20] As the authors note, the picture obtained is that of breakdown (and synthesis) of the whole mitochondrial entity at once, and this result is in accord with the organelle theory. The report by Chevremont *et al.*[21] that mitochondria in chick fibroblasts will display under certain conditions a feulgen-positive material which becomes labeled with thymidine-H^3 (DNA) might also be regarded as oblique support for the organelle thesis.

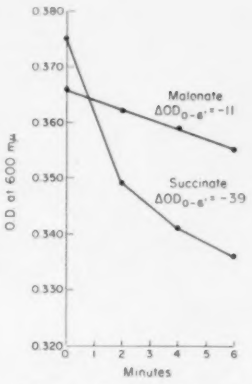

FIG. 3.—Succinic dehydrogenase activity of cell homogenates. The reaction cuvettes each contained 24.5 μM succinate, 6 μM KCN, 30 μg EDTA, 11.2 μg dichlorophenol indophenol, and 500 μg crystalline bovine serum albumin, besides the cell extract to be tested for succinic dehydrogenase activity. The exact composition of the stock solutions was as in Rogers.[25] The procedure was as follows: 0.50 ml KCN EDTA-BSA solution and 1.55 ml 0.01 *M* Na succinate solution or 0.01 *M* Na succinate containing 0.14 *M* malonate were mixed and allowed to equilibrate for 3 min in the Beckman spectrophotometer. The dye was then added (0.075 ml), the contents were mixed rapidly, and a zero-time reading of *OD* at 600 mμ was taken. Readings were taken at 2, 4, and 6 min thereafter, preceded in each case by stirring within 15 sec.

Mitochondria, however, are also subject to central genomic control. Ephrussi and co-workers[22] have demonstrated single-factor Mendelian transmission of mitochondrial respiratory enzyme systems in yeast. C. Raut has described other yeast mutants in which specifically mitochondrial cytochrome enzymes are shown to be controlled by a single Mendelian factor.[23, 24] In another organism, Neurospora, cytochrome-free genetic mutants have also been identified.[25] Measurement of succinic dehydrogenase activity in actinomycin-treated ARE cells would indicate

whether genomic control over this mitochondrial enzyme is characterized by the same immediacy as shown for AMPS and total protein synthesis in these cells.

Twelve to sixteen hr after planting, replicate ARE cultures were thus exposed to 8 μg/ml actinomycin for 20 min, the monolayer was rinsed and covered with fresh medium, and at given intervals thereafter the cells were harvested. Cell homogenates were then prepared as described below. Parallel coverslip cultures with the same ratio of actinomycin to cells were used to monitor RNA synthesis throughout the experiment with the same procedures as utilized in the experiment of Figure 1. The results of two experiments measuring succinic dehydrogenase in actinomycin-treated cells are shown in Table 1, expressed as mμM succinate reduced per mg of protein.

TABLE 1

SUCCINIC DEHYDROGENASE ACTIVITY AND RNA SYNTHESIS AFTER ACTINOMYCIN TREATMENT

Time after actinomycin	Experiment I		Experiment II	
	Per cent of control RNA synth.	mμM succinate reduced/mg P	Per cent of control RNA synth.	mμM succinate reduced/mg P
Control (0 hours)	100	75.6	100	75.2
2	1.8	147.6	4.8	120.8
8	2.6	90.0	3.3	
12			3.9	114.8
17	1.8	142.0		
23			3.6	105.2

Each value is based on duplicate determinations carried out on two independent replicate cultures.

It is evident from the data of Table 1 that the specific activity of succinic dehydrogenase shows no decline in cells suffering near-total blockage of nuclear RNA synthesis for many hours. In fact, succinic dehydrogenase activity has increased somewhat in the actinomycin preparations, perhaps as a by-product of the general derangement of synthetic metabolism wrought by the actinomycin treatment (total protein/10^6 cells remained constant throughout the experiment).

Succinic dehydrogenase activity was measured with a method adopted from the procedure of K. Rogers[26] originally intended for the estimation of succinate. This method depends on succinic dehydrogenase-mediated electron transport between succinate and the blue dye 2,6-dichlorophenol in the presence of cyanide to block further cytochrome-mediated transport pathways. Succinic dehydrogenase is specifically inhibited by malonic acid, and the activity of this enzyme was expressed as the *difference* in the decline in OD at 600 mμ of the contents of two Beckman cuvettes, identical except for the presence of about 10 times as much malonate as succinate in one of the cuvettes. Details of the assay procedure are given in the legend to Figure 3. The cell extracts used for the enzyme activity measurements were prepared as follows: Several million cells were washed in the cold in 0.06 *M* Na/K phosphate buffer, and, after standing at 0–2° for 30 min under these hypotonic conditions, they were 100 per cent broken by three min of motor-driven homogenization in a 2 ml Tenbroek homogenizer. Homogenates were then dialyzed at 0–2° against four 1:50 volumes of 0.06 *M* pH 7 phosphate buffer containing 0.01 *M* Na succinate. Duplicate 0.40 ml samples were taken for protein analysis by the Lowry procedure,[27] and the remaining homogenate was kept in the cold until 15 min before measurement of enzyme activity. Figure 3 shows curves typical for such preparations. According to a linear standard curve for these reaction conditions,[28] an OD change of 0.010 represents the disappearance of 4 mμM succinate, and thus, in the case portrayed in Figure 3, the succinic dehydrogenase in the preparation catalyzed the reduction of 11.2 mμM of succinate during the six min of observation.

Discussion.—The fact that AMPS production by ARE cells falls without lag when DNA-dependent RNA synthesis is blocked serves as a demonstration that AMPS synthesis is a genomically controlled cell character. The use of actinomycin D thus constitutes a novel method for showing the dependence of specific cellulular

functions on gene action, one which is complementary to the classical methods.

The main focus of attention in this paper is the degree of immediacy which characterizes genomic control over specific cell functions. AMPS synthesis, an inherited differentiated character of the ARE-2-60 cell line, has been shown to cease when gene action is discontinued, as does the total protein synthesis of these cells. The apparent decay of AMPS synthetic activity in actinomycin-treated ARE cells displayed a half-time of eight hr, and, since AMPS synthesis was shown to be directly dependent on protein synthesis, that value constitutes a quantitative index of the immediacy of gene control over this cellular function. In the same cell, however, it was found that as long as 23 hr after obliteration of RNA synthesis the specific activity of the mitochondrial enzyme succinic dehydrogenase remains undiminished. Thus, gene action determining this enzyme system is characterized by a low degree of immediacy. Nonetheless, it is to be stressed that the evidence available at this time demonstrates clearly the existence of an ultimate genetic control over mitochondrial systems though it also suggests a large degree of mitochondrial autonomy. In considering the vital dynamics of intracellular function, the *immediacy* with which a given cell character is controlled by its genomic determinants is one of the main pieces of information necessary for understanding the manner in which that character is integrated into cellular metabolism. It is therefore of considerable interest to find that highly diverse degrees of immediacy in gene control coexist within the same cell.

Turning to what is known about immediacy of gene control in other systems, the main example among the cells of vertebrates is the reticulocyte. Hemoglobin synthesis in the mammalian reticulocyte remains active for days after loss of the cell nucleus, thus proving the existence of ribosomal protein synthesis systems[29] which do not require immediate gene action in order to maintain function, although it is well known that hemoglobin synthesis is under genetic control. Of added interest here is a recent observation that actinomycin D does not affect reticulocyte hemoglobin synthesis.[11] Whether the reticulocyte model is analogous to the succinic dehydrogenase system studied here depends on whether the latter enzyme was being synthesized in the course of the experiment, which is unknown. On the basis of present information, the situation is different in bacteria. Time lag between gene action and the appearance of the target character has been studied in various ways in bacteria and has been found to be of exceedingly short duration. For example, β-galactosidase production in *E. coli* zygotes was detected within two min of the introduction of the gene for β-galactosidase in a mating experiment of Riley *et al.*[30] In another case, Lacks and Hotchkiss studied amylomaltase formation in pneumococcus mutants constitutively lacking this enzyme, following introduction of the gene for its synthesis by wild type transforming DNA, and it was found that amylomaltase formation began after a lag of only six min.[31] Other examples involving virus-induced enzyme synthesis could be cited, e.g., the appearance of deoxycytidylate hydroxymethylase in T-2 infected *E. coli*.[32] All of these microbial systems illustrate an extreme of immediacy in gene control over the respective cell functions, compared to the case in the differentiated vertebrate cells studied. The contrast serves to draw attention to one of the fundamental properties of nucleated differentiated cells, the existence of mechanisms moderating and controlling the inherited genomic potentialities carried by these cells. We know that genomic

control is exercised through the selective repression and activation of certain genetic loci in certain cells. It is apparent that an even more subtle mode of genomic control exists, represented by variations in the immediacy with which gene action is reflected in the target cell activities. Since cell differentiation is the result of these processes of genomic specialization and modulation, investigation into their nature and mechanism is among the fundamental problems in developmental biology; for it is now known that gene activity may be necessary for the maintenance of a char acter as well as for its first appearance.

Summary.—Actinomycin D was used to study gene control over specific cellular activities in an established cultured cell line preserving a differentiated biosynthetic function *in vitro*. It was found that the specific biosynthesis characteristic of these cells was subject to immediate genomic control, while, by contrast, specific activity of a mitochondrial enzyme was not affected by actinomycin treatment.

* This nomenclature is conventional. "ARE-2-60" denotes a culture line initiated February 1960 and constituted of altered rat eye cells.

[1] Davidson, E. H., in preparation (1962).

[2] Moscona, A., *Eighteenth Symposium of the Society for the Study of Development and Growth* (1960), p. 45.

[3] Godman, G. C., and K. R. Porter, *J. Cell Biol.*, **8**, 719 (1960).

[4] Grossfeld, H., K. Meyer, and G. Godman, *Proc. Soc. Exp. Biol. Med.*, **88**, 31 (1955).

[5] Morris, C. C., *Ann. N. Y. Acad. Sci.*, **86**, 878 (1960).

[6] Daniel, M. R., J. T. Dingle, and J. A. Lucy, *Exp. Cell Res.*, **24**, 88 (1961).

[7] Baltimore, D., and R. M. Franklin, these PROCEEDINGS, **48**, 1383 (1962).

[8] Hurwitz, J., J. J. Furth, M. Malany, and M. Alexander, these PROCEEDINGS, **48**, 1222 (1962).

[9] Raven, H. M., H. Kersten, and W. Kersten, *Hoppe-Seylers Z. Physiol. Chem.*, **321**, 139 (1960).

[10] Kawamata, J., and M. Imamishi, *Biken's J.*, **4**, 13 (1961).

[11] Reich, E., R. M. Franklin, A. J. Shatkin, and E. L. Tatum, these PROCEEDINGS, **48**, 1238 (1962).

[12] Franklin, R. M., and D. Baltimore, Cold Spring Harbor Symposia on Quantitative Biology, vol. 27, in press.

[13] Eagle, H., K. A. Piez, and R. Fleischman, *J. Biol. Chem.*, **228**, 847 (1957).

[14] Sibatani, A., S. R. deKloet, V. G. Allfrey, and A. E. Mirsky, these PROCEEDINGS, **48**, 471 (1962).

[15] Allfrey, V. G., A. E. Mirsky, and S. Osawa, *J. Gen. Physiol.*, **40**, 451 (1957).

[16] Benda, C., *Ergebnisse der Anatomie und Entwicklungsgeschichte* (Wiesbaden: Merkel and Bonnet, Anatomische Hefte), 2te Abtheilung, 1903.

[17] Allfrey, V. G., and A. E. Mirsky, these PROCEEDINGS, **48**, 1590 (1962).

[18] Fletcher, M. J., and D. R. Sanadi, *Biochim. et Biophys. Acta*, **51**, 356 (1961).

[19] Schapira, G., J. Krub, J. C. Dreyfus, and F. Schapira, *J. Biol. Chem.*, **235**, 1738 (1960).

[20] Tower, H., and L. M. Morse, *J. Biol. Chem.*, **173**, 53 (1948).

[21] Chevremont, M., E. Basslear, and E. Baekeland, *Arch. Biol.* (*Liége*), **72**, 501 (1961).

[22] Chen, S-Y., B. Ephrussi, and H. Hottinguer, *Heredity*, **4**, 337 (1950).

[23] Raut, C., *Exp. Cell Res.*, **4**, 295 (1952).

[24] Raut, C., *J. Cell Comp. Physiol.*, **44**, 463 (1954).

[25] Mitchell, D. F., M. Mitchell, and A. Tissières, these PROCEEDINGS, **39**, 606 (1953).

[26] Rogers, K., *Biochem. J.*, **80**, 240 (1961).

[27] Lowry, O. H., N. J. Rosebrough, A. Lewis Farr, and R. J. Randall, *J. Biol. Chem.*, **193**, 265 (1951).

[28] McEwen, B., unpublished data.

[29] Schweet, R., H. Lamfrom, and E. Allen, these PROCEEDINGS, **44**, 1029 (1958).

[30] Riley, M., A. B. Pardee, F. Jacob, and J. Monod, *J. Molec. Biol.*, **2**, 216 (1960).

[31] Lacks, S., and R. D. Hotchkiss, *Biochem. Biophys. Acta*, **45**, 155 (1960).

[32] Flaks, J. G., J. Lichtenstein, and S. S. Cohen, *J. Biol. Chem.*, **234**, 1507 (1959).

*EFFECTS OF MECHANICAL SHEAR ON GENETIC ACTIVITY OF BACILLUS SUBTILIS DNA**

By Eugene W. Nester,† A. T. Ganesan, and Joshua Lederberg

Department of Genetics, Stanford University Medical Center, Palo Alto, California

Communicated November 26, 1962

DNA molecules in solution can be fragmented by mechanical shearing forces.[1] Such fragmentation disrupts the linkage of genetic markers arrayed on the DNA molecule of the bacteriophage lambda.[2] In *Bacillus subtilis*, the aromatic linkage group carries at least nine genes specifying structural enzymes for steps in aromatic acid biosynthesis and also a histidine marker.[3, 4] This situation affords an unusually favorable opportunity to relate the biological to the physical consequences of shearing forces of DNA in a transformation system.

Materials and Methods.—Pertinent information on the strains carrying the linked mutants is given in Table 1 and linkage map, Figure 1. All loci, except for aro_2 and aro_3, were ordered on

TABLE 1

List of Strains of *Bacillus subtilis*

Strain No.	Genotype[1]	Growth response
23	thr^-	threonine
168	try_2^-	tryptophan
SB19	Reference Prototroph	—
SB25	$his_2^-try_2^-$	histidine + tryptophan
SB70	$his_2^-tyr_1^-$	histidine + tyrosine
SB130	$his_2^-aro_1^-$	histidine + tyrosine + phenylalanine + tryptophan
SB137	$his_2^-aro_2^-$	histidine + shikimic acid
SB148	$his_2^-aro_3^-$	histidine + shikimic acid
SB202	$aro_2^-try_2^-his_2^-tyr_1^-$	shikimic acid + tryptophan + histidine + tyrosine
SB402	$aro_3^-his_2^-aro_1^-$	shikimic acid + histidine + tyrosine + phenylalanine + tryptophan

[1] The nomenclature of genotypes follows the suggestions of Demerec[16] and the abbreviations coincide with the designations given by the editors of the *Journal of Biological Chemistry*.

the basis of three-point crosses on the assumption that the least frequent class results from a quadruple crossover.[4] A two-point map distance (q) can be stated as the ratio of crossover to total transformants with respect to the markers tested.[5] The mapping of the loci by this procedure accords with the ordering based on the three-point tests.

Media—Difco Antibiotic medium 3 = A3; Davis mineral[6] = D. Competency regimen—CHT-1 and CHT-10 with aromatic supplements added.[4]

DNA was assayed at limiting levels: no more than 0.02 μg per ml of 5×10^8 recipient cells.

DNA was initially prepared as previously described.[7] In later experiments, it was prepared

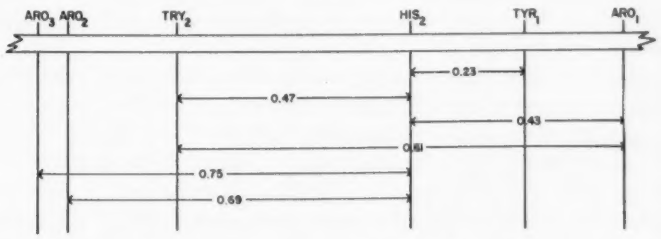

Fig. 1.—Linkage map of loci of aromatic amino acid biosynthesis in *Bacillus subtilis*. Map distance $q = (10 + 01)/(10 + 01 + 11)$.

according to the procedure of Marmur,[8] which includes a minimum of two precipitations of the final ethanol precipitate in 0.54 volumes of isopropanol. The location of the peaks of radioactivity and biological activity was the same for both preparations assayed by sucrose gradient sedimentation. In many preparations, the isopropanol precipitation removed a shoulder of P^{32} activity which was biologically inactive, trailing the major peak and mostly solubilized by RNase.

For the preparation of P^{32}-labeled DNA, bacteria were grown under the conditions described by Young and Spizizen.[9] In some preparations, two aliquots of unlabeled bacteria grown in A3 were added as a carrier immediately prior to the DNA isolation. The behavior of biological activity and P^{32} banding corresponded to preparations when no such carrier was added. The quantities of P^{32} employed resulted in a maximum of 0.6 atoms of P^{32} per 10^5 atoms of P^{31} DNA phosphorus, or 0.2 atoms per DNA molecule of molecular weight 10^7. Bihelix breakage during storage was not detected when samples of a single preparation were centrifuged periodically over four weeks, the longest a preparation was ever used. DNA concentration was routinely determined and expressed as optical absorbance at 260 mμ.

Shearing: Solutions of DNA, with an absorbance of 0.5 in 0.14 *M* sodium chloride + 0.015 *M* sodium citrate, were stirred at 6,000 rpm with a Virtis Homogenizer micropropeller with crossed blades. A volume of 1.3 ml was used in a fluted micro-cup, having a total capacity of 2 ml. The cup was surrounded with an icebath. Varying the DNA concentration between 0.05 and 0.5 absorbance units, or the salt concentration between 0.14 *M* and 2.0 *M* NaCl, in 0.15 *M* sodium citrate did not appreciably affect the kinetics nor extent of biological inactivation.

Viscosity was measured in a single-bulb capillary viscosimeter at 37° employing DNA concentrations of 0.5 absorbance in 0.14 *M* NaCl + 0.015 sodium citrate. Flow time of the diluent was 102.0 sec.

Experimental Results.—Breakage of a DNA molecule may be evidenced biologically as the disruption of genetic linkage, i.e., the loss of multiple cotransfers relative to single transfers. A variety of shearing methods was evaluated by the ratio of single-marker transfer to linkage group cotransfer to SB 190, i.e., try_2 compared to aro_2-his_1: (1) Squirting the DNA solution under pressure through various-sized hypodermic needles,[10] (2) spraying from an atomizer,[11] (3) sonic oscillation,[12] and (4) stirring in a Virtis homogenizer.[2] Each of these techniques showed some discriminating effect for breaking the molecule, but the stirring technique was most effective in our hands and was used exclusively in these studies.

Figure 2 displays the results of a kinetic study of the transfer of the linkage group, aro_3-aro_1 (recipient SB 402) by wild type DNA after progressive shearing. After one min, there is a rapid and progressive decrease in singlet, doublet, and triplet transfers respectively. After 20 min, there is no further decrease in singlet transfer, whereas the activity for the doublets and triplets continues to drop. Like the biological activity, most of the viscosity increment has been reduced by 5 min. The further measurements of the approach to the asymptotic viscosity are too imprecise to justify further comparisons since a small fraction of undegraded DNA molecules would contribute disproportionately to the biological activity as compared with the viscosity.

Although the data in Figure 2 suggest bihelix breakage, the possibility that damage at random sites along the DNA molecule results in inactivation of only portions of the linkage group has not been rigorously excluded. In order to distinguish damage in an intact bihelix from breakage, the biological activity of DNA should be expressed as a function of the size of the DNA molecules.

The physical characteristics of sheared versus intact DNA (both labeled with P^{32}) were studied by sedimentation in a liquid column stabilized by a sucrose density gradient. Fractions were collected and assayed for radioactivity and for biological

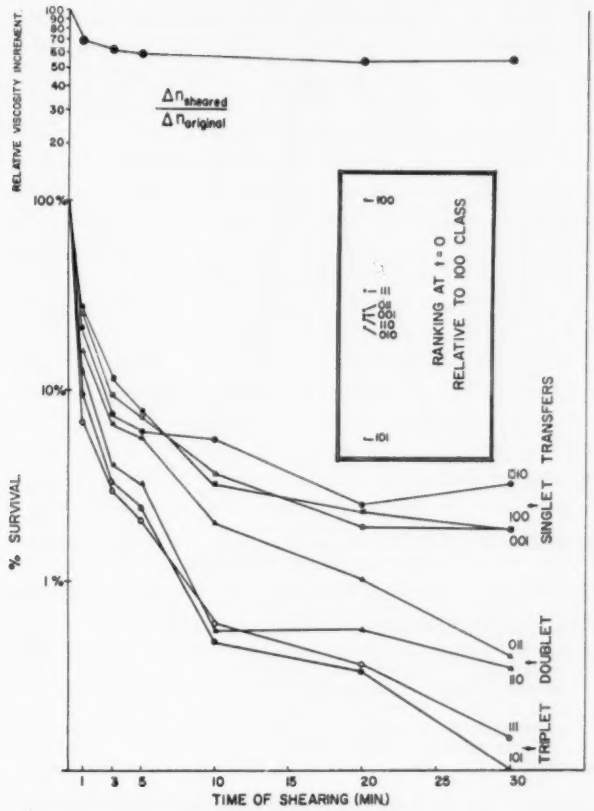

FIG. 2.—Kinetics of the effect of shearing on transforming activity and viscosity. 1.3 ml of SB 19 DNA, 0.5 O.D. units per ml, was sheared at 6,000 rpm for the indicated time. The total sample was assayed for viscosity and an aliquot diluted for the transfer of the linkage group aro_2–aro_1. The platings were done on doubly supplemented media, and in most cases a total of 600 representative colonies of all three primary transformant classes were analyzed for the remainder of their genotype by replicate plating onto appropriately supplemented media. However, because of the reduction in biological activity, 390, 297, and 266 colonies were analyzed for the time periods 10, 20, and 30 min respectively.

activity against the recipient strain SB 202 (aro_2^-, try_2^- his_2^- tyr_1^-). We ask: (1) Are all size classes of DNA equally active in transformation? (2) Does shearing change the sedimentation characteristics of the DNA?

Unsheared sample (Fig. 3): The biological activity of the DNA with respect to try_2^+ transfer varies with the sedimentation constant; the peak for P^{32} (total DNA) is at $S = 6.9$; the peak for biological activity is at $S = 10.0$.[13] This displacement has been observed in every DNA preparation studied, including DNA isolated from exponentially growing cells pulse-labeled for only 10 min, and DNA containing a large fraction of unlabeled carrier DNA.

Sedimentary fractionation of markers in the DNA was investigated by assaying these same fractions for transfer of the aro_2 marker (linked to try_2) as well as four markers unlinked to the try_2 locus and to each other: uracil, histidine, methionine,

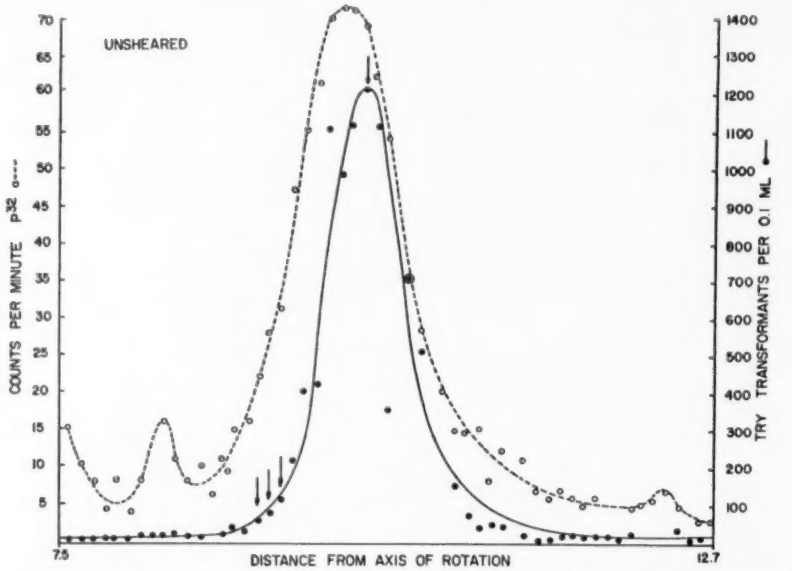

FIG. 3.—Sedimentation of unsheared DNA. 0.1 O.D. units of P^{32}-labeled DNA, prepared by the Marmur procedure, was layered on top of a sucrose gradient column of 24 ml, the sucrose concentration decreasing linearly from 20 per cent wt/vol at the bottom to 5 per cent at the top. The solution was centrifuged for 12 hours at 20,000 rpm at 6 per cent in the SW 25.1 rotor of the Spinco Model L centrifuge. The rotor was allowed to stop without braking, and 0.45-ml samples were collected dropwise through a hole punctured in the bottom of the centrifuge tube. 0.1 ml aliquots were added to 0.9 ml of competent bacteria and transformants assayed as previously described. 0.2 ml were plated on planchets and assayed for radioactivity. The fractions may be numbered, in the order in which they are collected, from right to left. The arrows point to fraction numbers 31 and 38–40.

and phenylalanine. All of these markers sedimented together, indicating that the biologically active DNA comprises only a portion of the total DNA isolated, namely, the larger molecules. The biologically inactive DNA may consist of partially degraded material.

Fractions 30, 31, 32, the tubes of peak biological activity, as well as fractions 38, 39, 40, corresponding to the peak of activity of sheared DNA, were assayed for the cotransfer of aro_2-tyr_1 (recipient strain SB 202). The transfer of this segment of the linkage group is essentially the same in all of these fractions (Table 2) from this preparation.

TABLE 2

COTRANSFER OF aro_2-tyr_1 MARKERS BY UNSHEARED DNA

Fraction No.[1]	No. transformants scored[2]	Try_2^+ Transformant Genotypes (per cent of total transformants)							
		1111[3]	1110	1101	0111	1100	0110	0101	0100
30	200	19	2.5	1	19.5	27	6	1.5	23.5
31	200	21.5	5	1	21.5	22	6	1.5	21.5
32	200	32	6.5	0	17.5	25	3.5	0	16.5
38	100	17	5	1	21	24	4	1	27
39	80	18.7	3.8	0	21.3	28.8	5	3.8	18.7
40	60	23.3	3.3	1.6	15	26.5	1.6	1.6	28.3

[1] Fraction No. refers to designation in Figure 2.
[2] The indicated number of try$^+$ transformants were stroked onto nutrient agar plates with sterile toothpicks (50 per plate). These plates were then replicated to appropriately supplemented media to determine the remainder of the genotype.
[3] The donor markers are designated as 1 and the recipient markers 0.

The unsheared material has also been run through the methylated albumen column described by Mandell and Hershey.[14] In contrast to the results from the previous sedimentation experiments (involving different DNA preparations), some fractionation of molecules according to their capacity for quadruplet versus singlet transfer is indicated, with the genetically smaller fragments eluting at the lower salt concentrations, suggesting their decreased physical size. In concordance with the previous sedimentation results, the peak of biological activity is displaced from the peak of DNA concentration. Again, the genetically longer fragments possess the higher biological activity.

After shearing, the sedimentation diagram shows P^{32} activity at $S = 5.7$ (Fig. 4). No more than a few per cent, at most, of unsheared material at $S = 7.1$ can be seen. Again, the biological activity is biased towards the high S side of the peak of P^{32} activity ($S = 6.5$). To test whether sheared DNA molecules are genetically cleaved, try_2 transformants were scored for the remainder of their genotype (Table 3). There is a marked reduction in the proportionate cotransfer with try_2 of linked markers in the sheared compared with unsheared material. The quadruplet (1111) and triplet (1110) transfers show the most striking responses.

Correlation of map distance and shear effectivity: Shear forces should cleave distant loci while leaving closer genetic loci still intact. Wild type DNA, sheared for 30 min, was assayed for cotransfer of his_2 and a series of markers located at various map distances from it. The furthest markers are more readily separated (Table 4). Different DNA samples often show different absolute values for r/r_s, but the correlation remains.

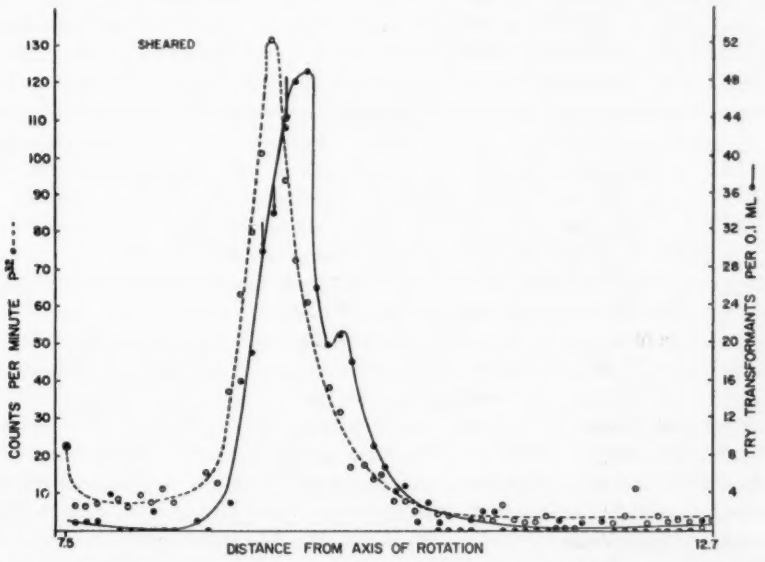

FIG. 4.—Sedimentation of sheared DNA. The DNA preparation used in Figure 3 was sheared for 30 min at 6,000 rpm, resulting in 97 per cent loss in transforming activity of the try_2 marker. 0.05 O.D. units were layered on a sucrose-gradient column, and the remainder of the centrifugation, collection, and assay were done as described under Figure 3. The arrows indicate fractions 40–42.

TABLE 3

COTRANSFER OF aro_2-tyr_1 MARKERS BY SHEARED DNA

Fraction No.[1]	No. transformants scored[2]	Try_2^+ Transformant Genotypes (per cent of total transformants)							
		1111	1110	1101	0111	1100	0110	0101	0100
40	195	2.4	2.6	0	7.2	23.6	10.2	0.5	53
41	175	2.3	2.8	1.1	6.3	22.3	9.8	2.3	53
42	128	0.8	0.85	0	13.2	18.0	6.2	1.56	44

[1] Fraction No. refers to the designation in Figure 4.
[2] The indicated number of try^+ transformants were stroked onto nutrient agar plates with sterile toothpicks(50 per plate). These plates were then replicated to appropriately supplemented media to determine the remainder of the genotype.

TABLE 4

CORRELATION OF COTRANSFER INDEX OF his_2 LINKAGE WITH VARIOUS MARKERS BEFORE AND AFTER SHEARING

Markers	Cotransfer index before shearing, r	Cotransfer index after shearing, r_s	Relative effect of shearing, r/r_s
his_2-tyr_1	0.77	0.23	3.3
his_2-aro_1	0.57	0.12	4.2
his_2-try_2	0.53	0.10	5.3
his_2-aro_2	0.31	0.05	6.2
his_2-aro_3	0.25	0.015	16.7

The DNA preparation was assayed on the indicated double auxotrophs before and after shearing for 30 min at 6,000 rpm. The cotransfer index was calculated from the transformant counts on appropriately supplemented media.

Discussion.—The present observations on the loss of biological activity of DNA degraded by shear forces extend similar work done on pneumococcal DNA after shear degradation. We can also correlate a physical breakage of the DNA bihelix with the disruption of linkage of genetic loci located in nucleotide sequences on either side of the point of breakage.

In the present studies, the DNA extracted from *B. subtilis* has a sedimentation constant of 26.7 measured at 20°C using a DNA concentration of 25 μg per ml and an "Epon" centerpiece in the Spinco Model E analytical ultracentrifuge. This value compares favorably with the sedimentation constant of 30 obtained by Burgi and Hershey[15] for a sample of *E. coli* DNA. This size corresponds to one-quarter molecules of the T2 DNA of molecular weight 120×10^6. In contrast to the phage DNA, the molecules of *B. subtilis* DNA are not of uniform length. Both P^{32} and biological activities yield a disperse band after velocity sedimentation and fractionate into different genetic sizes on the methylated albumin column. A variety of shear forces during DNA isolation have resulted in a product which may represent only a fraction of its molecular weight inside the cell.

The studies of the breakage of T2 and lambda DNA have led to the conclusion that at a critical shear rate the DNA molecule tends to break at a point near the middle of the molecule, resulting in two half-molecules not subject to further degradation at the same shear rate. In the present studies, because of the relatively low molecular weight of the DNA, the critical rate of shear was determined arbitrarily as that rate of shear required to give a distinction in the inactivation of transfer of a single, compared to two, linked markers. At the speeds of stirring necessary to give these rates of shear, the vortex dips into the DNA solution and results in the production of air bubbles and turbulence. The significance of such forces on the phenomena observed is not apparent.

Several observations suggest that the present results may likewise be interpreted as the transverse breakage of DNA bihelices to about half their original size:

1. The displacement of the sedimentation constant for peak biological activity is 0.65 (uncorrected for the gradient of the sucrose), corresponding to a ratio of 0.4 in molecular weight.[12]

2. The shearing reduces the specific viscosity of the DNA by forty per cent.

3. The shearing of DNA resulted in the production of a new population of molecules, more uniform than the original population, indicating a preferential cleavage of the larger molecules.

4. The critical rate of shear can vary within limits—7,500 rpm for 5 min resulted in a DNA preparation equivalent to 6,000 rpm for 30 min in its sedimentation characteristics.

Taken in concert, these data suggest that the molecules of DNA are being broken near the middle.

The kinetics of inactivation does not permit one to distinguish between the disruption of linkage from the separate losses of component markers. In fact, since there is a survivorship of two to three per cent for the single markers at 30 min, the survivorship expected for triplet transfer would be only 10^{-5} if the markers were subject to independent loss. The actual survivorship of 111 is one hundred times higher than this. Therefore, the loss of single markers from triplet transfers cannot occur independently. This would be true if, for example, the breakage of a molecule tended to leave some markers intact in a smaller fragment, which was then relatively insensitive to further shearing. This view would also be consistent with the time course of inactivation and of loss of viscosity.

The study of shearing effects points up a number of problems covering the heterogeneity of "untreated" DNA. This has been studied by two independent techniques: velocity sedimentation and fractionation on a methylated albumin column. Both techniques indicate that the DNA fractions of highest molecular weight are the most likely to become integrated into the recipient genome. However, both techniques might confound complexing with, say, protein with molecular-weight variation.

The heterogeneity of the DNA as now isolated poses delicate problems for rigorous interpretation of the shearing effects. The most plausible model is the disruption of multiplet transforming molecules into smaller fragments having singlet activity. However, the extent of marker inactivation and the frequency of singlet transfer with the initial material make it difficult to prove the essential point that a multiplet has been converted to a singlet unit. Instead, we might argue a selective inactivation of different types of units. This problem is mitigated in the lambda phage system by the initial higher incidence of cotransfer that can be demonstrated in phage infection.

Summary.—DNA, extracted from *Bacillus subtilis* by lysozyme lysis and purified by shaking with chloroform-octanol and ribonuclease treatment, is heterogeneous in its physical and genetic size. The larger fragments appear to have the greatest biological activity. The DNA can be sheared mechanically, resulting in a class of molecules possessing a lower sedimentation value, reduced viscosity, and a decreased genetic complement. Their physical properties suggest that the sheared DNA molecules are one-half their original size.

The authors thank J. Mandell for assistance in the chromatography of the DNA and M. Schafer for capable technical assistance.

* This work was supported by training grant 2G295 and research grant C4496 from the National Institutes of Health and by a grant from the National Science Foundation.

† Present address: Department of Microbiology, University of Washington, Seattle, Washington. Research Fellow of the American Cancer Society, 1959–61.

[1] Levinthal, C., and P. Davison, *J. Mol. Biol.*, **3**, 674–83 (1961).

[2] Kaiser, A. D., *J. Mol. Biol.*, **4**, 275 (1962).

[3] Anagnostopoulos, C., and I. P. Crawford, these PROCEEDINGS, **47**, 378 (1961).

[4] Nester, E. W., M. Schafer, and J. Lederberg, *Genetics* (in press).

[5] Map distance, $q = 1 - r$ (cotransfer index) = (01 + 10)/(11 + 01 + 10) as defined for an experiment 11 (donor) — × 00 (recipient). (See references 4 and 7.)

[6] Lederberg, J., in *Methods in Medical Research*, ed. R. W. Gerard (Chicago: The Year Book Publishers, Inc., 1950), vol. 3, p. 5.

[7] Nester, E. W., and J. Lederberg, these PROCEEDINGS, **47**, 52 (1961).

[8] Marmur, J., *J. Mol. Biol.*, **3**, 208 (1961).

[9] Young, F. E., and J. Spizizen, *J. Bact.*, **81**, 823 (1961).

[10] Davison, P., these PROCEEDINGS, **45**, 1560 (1959).

[11] Cavalieri, L. F., and B. H. Rosenberg, *J. Am. Chem. Soc.*, **81**, 5136 (1959).

[12] Doty, P., B. B. McGill, and S. A. Rice, these PROCEEDINGS, **44**, 432 (1958).

[13] These values for S are only provisional since a single distance at a single time was measured. Corrections have not been made for temperature and the sucrose gradient.

[14] Mandell, J., and A. D. Hershey, *Anal. Biochem.*, **1**, 66 (1960).

[15] Burgi, E., and A. D. Hershey, *J. Mol. Biol.*, **3**, 458 (1961).

[16] Demerec, M., in *Genetic Studies with Bacteria*, Carnegie Institution of Washington Publication 612 (1956).

PHYSICAL PROPERTIES OF MESSENGER RNA OF BACTERIOPHAGE T4

BY EKKEHARD K. F. BAUTZ

INSTITUTE OF MICROBIOLOGY, RUTGERS, THE STATE UNIVERSITY

Communicated by Michael Heidelberger, November 23, 1962

The finding of rapidly labeled RNA fractions in many systems[1–6] has led to the general acceptance of the messenger hypothesis. Most of the predictions made by Jacob and Monod[7] have been experimentally verified[8–11] through investigations carried out by specifically labeling the messenger fractions with radioisotopes. Such studies, however, have not required the separation of messenger RNA from the bulk of ribosomal and soluble RNA, and since optical methods such as the measurement of melting profiles could not be applied to such mixtures of RNA species, little could be said about the physical state of the messenger RNA.

With the selective technique of complex formation between strands of complementary sequences,[13, 14, 18] it has become possible to isolate T4 msRNA* in a highly purified form on a T4 DNA-cellulose column.[15] The biological activity of T4 msRNA isolated in this fashion was established with cell-free extracts of *E. coli*.[12]

The purpose of this paper is to present recent studies on the physical state of T4 msRNA and to discuss possible correlations between its structure and its biological activity.

Materials and Methods.—Escherichia coli B, grown in one-liter batches of minimal medium to a titer of 5×10^8 cells/ml were infected with a total of 3×10^{12} T4 wild type phage particles in the presence of 5 μg/ml of tryptophan. The bacteria

were harvested 8 min after infection as described previously,[15] and the washed cells were frozen in dry ice-methanol. RNA was extracted with sodium dodecylsulfate (SDS) and hot phenol in the presence of polyvinyl sulfate (PVS) as described by Scherrer and Darnell.[6] The T4 DNA-cellulose column and the incubation and elution steps have already been described.[12] Measurements of optical density were performed with a Zeiss spectrophotometer equipped with a heatable cell holder. Melting profiles were measured at 260 mμ, in quartz cells of 3-ml capacity stoppered with special short-stem thermometers purchased from Paracell Inc., N. Y. Pancreatic ribonuclease was purchased from Worthington Biochemicals. Poly A and poly U were purchased from Miles Chemical Company, Clifton, N. J.

Sucrose density gradient centrifugation: The RNA samples were layered on top of a linear gradient ranging from 5–20 per cent sucrose (Merck) solution. The samples and the sucrose solutions were in 1×10^{-2} *M* Tris buffer pH 7.4, containing 1×10^{-3} *M* Mg^{++}. The tubes were spun at 38,000 rpm for 5 hr in a Spinco SW 39 swinging bucket rotor, and after conclusion of the run the tubes were punctured at the bottom and fractions of 10 drops each were collected through a 20-gauge hypodermic needle. To each fraction 1 ml of 1×10^{-2} *M* Tris buffer pH 7.4 was added, the optical density was read, and the RNA was precipitated with 10 per cent trichloroacetic acid (TCA). The precipitates were collected on millipore filters, dried, and counted in a Packard Model EX liquid scintillation counter. The RNA used was labeled with H^3-uracil (New England Nuclear Corporation, specific activity 1 c/m*M*) from 5–8 min after infection with T4 phage particles as described before.

The assays for amino acid incorporation in cell-free extracts contained per ml: 14 μ*M* Mg acetate, 0.1 ml of a preincubated[16] 30,000 × *g* supernatant fraction from *E. coli* B cells (OD_{260} = 240), 1 mg *E. coli* B S-RNA, 0.2 μc C^{14} L-threonine (specific activity = 164 mc/m*M*). The other additions were the same as described by Nirenberg and Matthaei.[16] The samples were incubated for 60 min at 35° and the radioactivity of acid-insoluble protein was determined the following way: After hot TCA (5 per cent) hydrolysis and repeated washing with 5 per cent TCA and ethanol ether (1:1), the precipitates were dissolved in 0.4 ml formic acid, mixed with 15 ml *p*-dioxane scintillation liquid,[17] and counted as described above.

Results.—Size distribution of T4 msRNA before and after infection: Figure 1*a* shows the distribution of H^3-uracil-labeled T4 msRNA after sucrose density gradient centrifugation. When a sample of the total RNA, isolated 8 min after infection, was applied, a substantial portion of the T4 msRNA sedimented with S values considerably higher than those observed by other investigators under similar conditions.[18–20] Centrifugation in the absence of Mg^{++} results in a similar distribution of radioactivity, and the fractions of high molecular weight thus obtained seem not to result from artificial association between smaller molecules brought about by the action of bivalent cations. We attribute this relatively high yield of high-molecular-weight messenger RNA to the hot phenol isolation procedure, which seems to be superior to such methods as the use of lysozyme or SDS plus cold phenol. It also yields messenger RNA of higher activity as judged by amino acid incorporation in cell-free extracts. Figure 1*b* shows the molecular size of purified T4 msRNA as it is eluted from the T4-DNA cellulose column. It shows less heterogeneity in size since the components having S-values above 23 are almost entirely missing. The

question of whether the large-size T4 msRNA, lost during hybridization with T4 DNA, represents a complex between several messenger RNA molecules or between messenger RNA and ribosomal RNA molecules is under current investigation.

Hyperchromicity of T4 msRNA: Incubation of 5 mg of RNA from T4-infected cells for 6 to 8 hr at 51°C on the DNA-cellulose column yielded approximately 100 μg of an RNA fraction which appeared to consist mainly of T4 msRNA. This material shows positive orcinol and negative diphenylamine reactions, it has a ratio of OD 260/280 = 2.04 and OD 240/260 = 0.62, and it shows a hyperchromic effect upon heating in standard saline citrate (Fig. 2). The amount of hyperchromicity

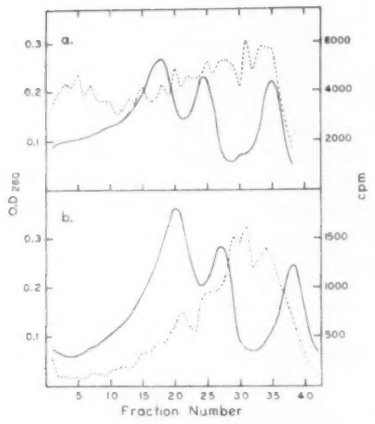

FIG. 1.—Size distribution of T4 msRNA labeled with H^3-uracil from 5–8 min after infection: (*a*) before fractionation on the T4 DNA-cellulose column, (*b*) after fractionation on the T4 DNA-cellulose column. To (*b*) 0.4 mg of *E. coli* RNA was added as carrier. ——— = absorbance at 260 mμ. ---- = radioactivity, given as acid-precipitable counts.

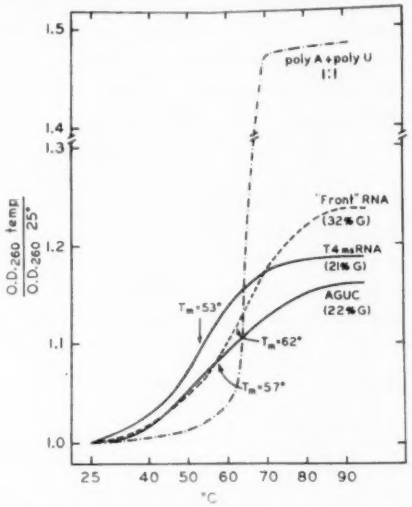

FIG. 2.—Increase in optical density with temperature for the following polynucleotides in 0.15 *M* NaCl + 0.015 Na citrate, pH 7: Purified T4 msRNA as obtained after passage through the DNA-cellulose column. *E. coli* RNA = Front RNA not retained by the DNA column. A random AGUC copolymer, prepared by O. W. Jones, National Institutes of Health, with polynucleotide phosphorylase. A 1:1 mixture of poly A + poly U. The samples were at a concentration of 15 to 30 μg/ml. Upon cooling of the heated samples, the absorbancies returned to the original values. No correction was made for thermal expansion of the solvent.

varies for different RNA preparations (Table 1), but the temperature-midpoint of the helix-coil transition (T_m) proved to be relatively constant for several preparations, especially for those isolated at similar times after infection. Other experiments showed that samples of RNA tested before passage through the DNA-cellulose column and samples not adsorbed onto the column (their major constituent being *E. coli* ribosomal RNA), under the same conditions, show between 23 and 24 per cent hyperchromicity with T_m values of between 62 and 63°C. In comparison, an AGUC copolymer having the base composition: A: 22 per cent, G: 22 per cent, U: 27 per cent, C: 29 per cent (O. W. Jones, personal communication),

TABLE 1

INCREASE IN OPTICAL DENSITY AT 260 mμ FOR SEVERAL T4 msRNA SAMPLES IN 0.15 *M* NaCl + 0.015 *M* Na CITRATE

Preparation	Isolated min after infection	Treatment after elution from DNA column	Per cent hyperchromicity	T_m
a	8	ethanol precipitation followed by dialysis against 1×SSC	19	53
a	8	dialysis against 1×SSC	20	55
b	8	EtOH precipitation	15	52
b	8	dialysis against 1×SSC	16	52
c	8	EtOH precipitation heated and slow cooled	20	52
c	8	EtOH precipitation heated and fast cooled	20	52
d*	16	dialyzed against H_2O	18	55
e*	25†	dialyzed against H_2O	20	54

* Found to be as active in stimulating incorporation of C^{14}-threonine in a cell-free system as the RNA isolated 8 min after infection.
† At 5 minutes after infection, chloramphenicol was added at a concentration of 100 μg/ml.

shows 16 per cent hyperchromicity with $T_m = 57°C$ (Fig. 2). It was observed furthermore that, with all T4 msRNA samples tested, the optical density profiles obtained by heating and cooling are identical.

Kinetics of ribonuclease digestion: The hyperchromic effect on RNA upon heating can also be observed following digestion with ribonuclease. Figure 3 shows the change in optical density of T4 msRNA and *E. coli* RNA as a function of time of incubation with 0.2 μg/ml of pancreatic ribonuclease. In the presence of monovalent cations, T4 msRNA is degraded at a rate slightly greater than is ribosomal RNA. At 10^{-2} *M* Mg^{++}, the difference is much more pronounced.

Heat inactivation of T4 msRNA: When tested in the Nirenberg system,[16] T4 msRNA, isolated on the DNA column, actively stimulates amino acid incorporation into acid-insoluble proteins.[12] The specific messenger activity of this material is about eight times as high as the activity of the unfractionated RNA. The melting profile and also the kinetics of ribonuclease digestion indicate that the T4 messenger in its active form consists of a single polynucleotide chain. Heat-inactivation studies given in Figure 4 confirm this indication, since the T4 msRNA can be heated for short periods of time well above the apparent midpoint of helix-

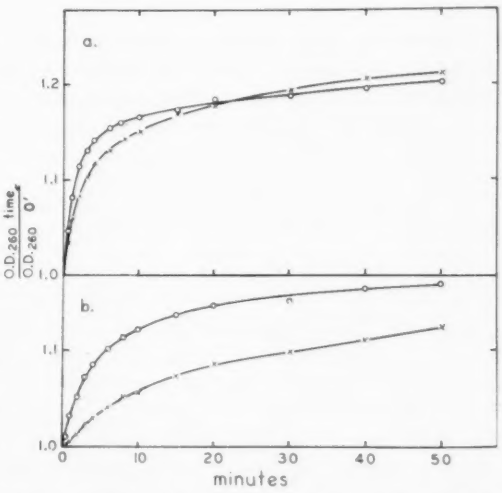

FIG. 3.—Kinetics of digestion by ribonuclease of RNA isolated 8 min after T4 infection = X, and of purified T4 msRNA = 0; (*a*) in 0.08 *M* phosphate buffer pH 7.0, (*b*) in 0.01 *M* Tris Mg^{++} buffer pH 7.4. At zero time 0.2 μg/ml ribonuclease was added.

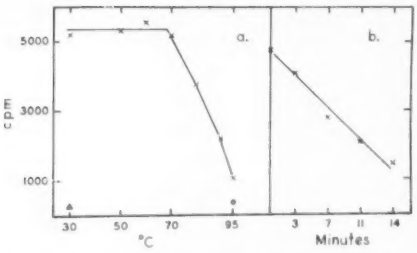

FIG. 4.—Heat-inactivation of T4 msRNA. (*a*) Samples of 15 μg of T4 msRNA were incubated for 10 min at a given temperature in 0.1 *M* Tris pH 7.6 + 0.01 *M* Mg^{++} and after rapid cooling the promotion of C^{14} L-threonine incorporation into acid-insoluble protein was determined as described in *Materials and Methods*. × = incorporation with RNA added. △ = blank (no RNA added). ⊙ = same as X, but cooled slowly. (*b*) Samples of 12 μg of T4 msRNA were heated at 90°C for given times. Experimental conditions as in 4*a*.

coil transition. Since the time curve of inactivation at 90°C follows roughly a single-hit curve (Fig. 4*b*), the decrease in activity above 70°C (Fig. 4*a*) seems to be caused by thermal scission of the polymer. Heating of a T4 msRNA sample to 95°C for 10 min, followed by slow cooling, inactivates the RNA to a greater extent than heating followed by fast cooling (Fig. 4*a*), a result which again indicates the active messenger to be a single-stranded polynucleotide.

Discussion.—Doty *et al.*[21] have found that upon heating of polynucleotides in solution the observed increase in absorbance shows complete correlation with the decrease in optical rotation, a finding that could only be explained by the transition from an ordered helix to a random coil. The helical content of a polynucleotide was found to vary between 0 per cent for poly U and 100 per cent for an equimolar mixture of poly A + poly U or for DNA. The helical content of TMV RNA was estimated to be of the order of 60 per cent, while polynucleotides of random sequences could have a helix content as high as 40 per cent.[21, 22] These high values suggest that there need not be a perfect matching of complementary base sequences for the establishment of short helical regions. There seems to be a wide distribution of size and strength of the helical regions, indicated by the broad transition curves obtained for single-stranded polynucleotides (see also Fig. 2). Although the maximal increase in absorbance (Δ OD_{max}) should be a direct measure of helix content, we can only give an estimate in the case of T4 msRNA preparations. However, the frequently observed 20 per cent increase in absorbance seems to represent an upper limit which, taken tentatively as a correct value, would then attribute to T4 msRNA a helix content of

$$\frac{\Delta OD_{max}\ \text{T4 msRNA}}{\Delta OD_{max}\ \text{Poly A + poly U}} = \frac{0.20}{0.48} = 42\ \text{per cent.}$$

It is likely that the relatively low value of T_m for T4 msRNA compared with the T_m of the *E. coli* RNA is mainly due to the difference in guanine content. A similar dependence upon guanine content seems to exist for the susceptibility towards digestion by ribonuclease. T4 msRNA is much more readily attacked than is ribosomal RNA by ribonuclease at a magnesium concentration at which *in vitro* protein synthesis proceeds at maximal rate. Such conditions might be very similar to the physiological, and it therefore seems worth stressing this point in view of the rapid metabolic turnover of msRNA. The relative resistance of ribosomal RNA to attack by nuclease is perhaps one of the factors which have played a strong evolutionary role in selecting for the unique base composition of ribosomal RNA in the most unrelated species.

The question of whether one or both strands of DNA are utilized as templates

for synthesis of msRNA is still unanswered. Studies on DNA-dependent RNA synthesis, catalyzed by a purified enzyme system from *Micrococcus lysodeikticus*, clearly show that, *in vitro*, both DNA strands do function as primers. The product, a high-molecular-weight RNA with DNA-like base composition and complementary base sequences, assumes (possibly during the isolation procedure) the structure of a double-stranded helix.[23] If one accepts the *in vitro* synthesis of RNA as a model system, it seems likely that both strands of DNA may at least potentially serve as templates for msRNA synthesis. On the other hand, there are two findings which could be interpreted best by assuming that *in vivo* only one DNA strand is utilized. One is the fact that in T4 msRNA guanine does not equal cytosine[15] and the other is the observation that only about one-half of the A-T mutant sites in the T4 rII region show an effect with 5-fluorouracil.[24] Whereas the former observation indicates that only one of the two DNA strands mediates RNA synthesis, the latter suggests that only one RNA strand is the active messenger for either the rIIa or the rIIb protein. Although these two arguments support each other, they do not settle the question decisively.

Provided that the complementary strand was not lost during the isolation and purification steps, the results reported here support the view that *in vivo* only one of the two DNA strands serves as a primer for messenger RNA synthesis. However, it should be emphasized that the single-strandedness established for purified T4 msRNA does not eliminate the possibility that the reading alternates between the two DNA strands or that both strands are read, but at different times.

While the solution of these problems will require quantitative studies on the biosynthesis of messenger RNA, from our results it can be concluded that the *active* T4 messenger seems to be a single polynucleotide chain with a helix content of roughly 40 per cent, its melting profile being similar to that of a random copolymer of comparable base composition.

Summary.—Parallel studies on heat denaturation, digestion by ribonuclease, and hyperchromicity of T4 messenger RNA indicate that the messenger RNA molecule in its biologically active form is a single-stranded polynucleotide with a degree of secondary structure similar to that of a random copolymer.

The author is greatly indebted to O. W. Jones, National Institutes of Health, for his generous gift of the polymer. Thanks are due to L. Bautz for performing a substantial part of the experiments. This work was supported by grants from the National Institutes of Health, Division of General Medical Sciences, (10395–01) and from the National Science Foundation (G 23856).

* Abbreviations used throughout this paper: T4 msRNA = phage T4 messenger RNA. (We have found it necessary to designate a two-letter symbol for the term "messenger" since the symbol *m* is already being used in T_m = temperature midpoint of helix-coil transition.) A = adenylate; G = guanylate; U = uridylate; C = cytidylate.

[1] Volkin, E., and L. Astrachan, *Virology*, **2**, 146 (1956).

[2] Astrachan, L., and T. M. Fisher, *Fed. Proc.*, **20**, 359 (1961).

[3] Yčas, M., and W. S. Vincent, these PROCEEDINGS, **46**, 804 (1960).

[4] Hayashi, M., and S. Spiegelman, these PROCEEDINGS, **47**, 1564 (1961).

[5] Sibatani, A., S. R. de Kloet, V. G. Allfrey, and A. E. Mirsky, these PROCEEDINGS, **48**, 471 (1962).

[6] Scherrer, K., and J. Darnell, *Biochem. Biophys. Res. Comm.*, **7**, 486 (1962).

[7] Jacob, F., and J. Monod, *J. Mol. Biol.*, **3**, 318 (1961).

[8] Nomura, M., B. D. Hall, and S. Spiegelman, *J. Mol. Biol.*, **2**, 306 (1960).

[9] Hall, B. D., and S. Spiegelman, these PROCEEDINGS, **47,** 137 (1961).
[10] Brenner, S., F. Jacob, and M. Meselson, *Nature,* **190,** 576 (1961).
[11] Risebrough, R. W., A. Tissières, and J. D. Watson, these PROCEEDINGS, **48,** 430 (1962).
[12] Bautz, E. K. F., *Biochem. Biophys. Res. Comm.*, **9,** 192 (1962).
[13] Marmur, J., and D. Lane, these PROCEEDINGS, **46,** 453 (1960).
[14] Doty, P., J. Marmur, I. Eigner, and C. Schildkraut, these PROCEEDINGS, **46,** 461 (1960).
[15] Bautz, E. K. F., and B. D. Hall, these PROCEEDINGS, **48,** 400 (1962).
[16] Nirenberg, M. W., and J. H. Matthaei, these PROCEEDINGS, **47,** 1588 (1961).
[17] Bray, G. A., *Analytical Biochem.*, **1,** 279 (1960).
[18] Sagik, B. P., M. H. Green, M. Hayashi, and S. Spiegelman, *Biophys. J.*, **2,** 409 (1962).
[19] Ishihama, A., N. Mizuno, M. Takai, E. Otaka, and S. Osawa, *J. Mol. Biol.*, **5,** 251 (1962).
[20] Monier, R., S. Naono, D. Hayes, F. Hayes, and F. Gros, *J. Mol. Biol.*, **5,** 311 (1962).
[21] Doty, P., H. Boedtger, J. R. Fresco, R. Haselkorn, and M. Litt, these PROCEEDINGS, **45,** 482 (1959).
[22] Haselkorn, R., and P. Doty, *J. Biol. Chem.*, **235,** 1479 (1961).
[23] Geiduschek, E. P., J. W. Moohr, and S. B. Weiss, these PROCEEDINGS, **48,** 1078 (1962).
[24] Champe, S. P., and S. Benzer, these PROCEEDINGS, **48,** 532 (1962).

*INSULIN—A PROBABLE GROSS MOLECULAR STRUCTURE**

BY J. RALPH EINSTEIN, A. STEWART MCGAVIN,† AND BARBARA W. LOW

DEPARTMENT OF BIOCHEMISTRY, COLLEGE OF PHYSICIANS AND SURGEONS, COLUMBIA UNIVERSITY

Communicated by David Shemin, August 3, 1962

In an earlier communication,[1] we described two alternative models for the gross structure of the insulin molecule. The models were based on our evidence for rodlike regions of high electron density in the orthorhombic crystal forms and were derived from transform and Patterson studies.

One of the crystal forms of insulin (a shrinkage stage, type C) has the space group $I2_12_12_1$ with one molecule per asymmetric unit. In this form, the two molecules of the dimer are related by a crystallographic twofold rotation axis parallel to *a*, whereas in the other forms (space group $P2_12_12_1$) the twofold axis is noncrystallographic. The restrictions imposed by the body-centering on the models and on their intermolecular arrangement have been discussed, and the arrangements of the models in the *a*-plane projection of the type C form have been defined.[1]

This paper describes our further studies with the C form in an attempt to refine the models and to choose between them. The models were described as arrays of rodlike units parallel or nearly parallel to *a* and, in one model, of overlapping units of unspecified configuration, which give rise to comparable regions of high density in the *a*-plane projection. In the model termed arrangement (1), there are two rods (A + B) per molecule; the projected positions of the rodlike units on the *a*-plane are shown in Figure 1*a;* a complete unit-cell projection is shown in Figure 2*a*, and an illustration in three dimensions of the model is shown in Figure 3*a*. The model termed arrangement (2) consists of one rodlike unit, B, and two units of unspecified configuration, A and C. The projected positions of these units are shown in Figure 1*b;* a complete unit-cell projection is shown in Figure 2*b* (unit C omitted for clarity of presentation); an illustration in three dimensions of the model is shown in Figure 3*b* (unit C again omitted).

If the models are associated with the known primary structure of insulin, then in arrangement (1) each rod (A or B) would correspond to a part of one peptide chain. The limiting length for rods parallel to a is 26 Å (a = 52 Å). In terms of the probable α-helix configuration for the rods,[1] this length would correspond to a maximum of about 14 residues (21 Å) per rodlike region, allowing for continuity with contiguous regions of peptide chain. A single molecule would then be represented by two α-helical segments (one per chain), parallel and adjacent to each other, but separated by a translation along their axial direction so that they lie side by side for a length of only five residues (see Fig. 3a). In arrangement (2), the rod B would correspond to the whole or a large part of one of the two polypeptide chains in the α-helix configuration. The presence of the intra-chain disulfide bond in the A chain prevents the whole chain from being coiled into one continuous α-helix. It appeared most plausible to us to associate rod B with the whole or a large part of the polypeptide chain B. The units A and C may represent small regions of unspecified configuration in either the A or the B chain.

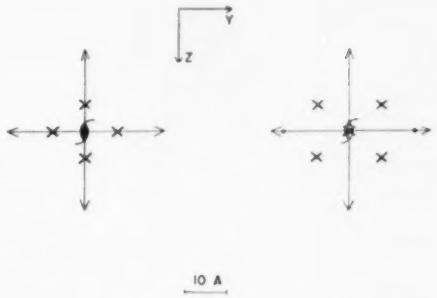

FIG. 1.—Elementary arrangement of points corresponding to projected positions on the a-plane of units of the two models. (a) Left: arrangement (1), (b) Right: arrangement (2). In arrangement (2), the crosses mark high-weight positions, and the dots, low-weight positions. The cross on the 2_1 axis represents the position of four overlapping units A; each of the other crosses represents one unit B; each of the two dots represents the position of two overlapping units C.

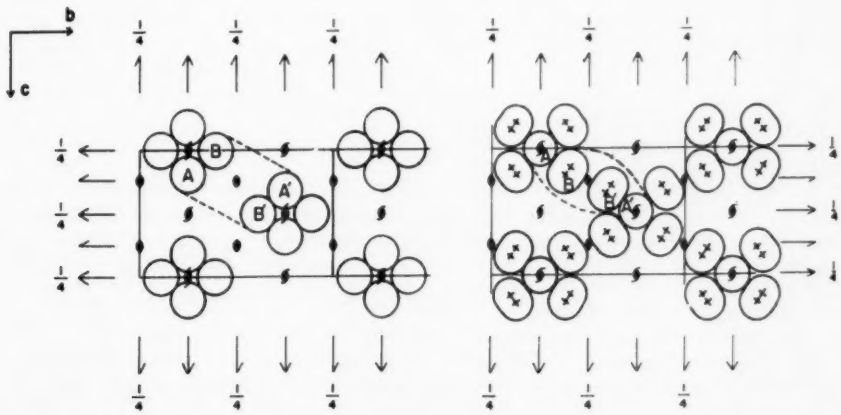

FIG. 2.—Unit-cell projections on the a-plane for the two models. (a) *Left:* model corresponding to the point set of arrangement (1), Figure 1a. Each circle represents two equivalent rodlike units, end-to-end, of high electron density. (b) *Right:* model corresponding to the point set of Figure 1b (unit C omitted). The elongated figures represent rodlike units tilted slightly with respect to a. Each circle on a 2_1 axis represents the overlapping in projection of four equivalent units. In both (a) and (b), the dashed lines enclose a single insulin dimer ABB′A′, as seen in projection.

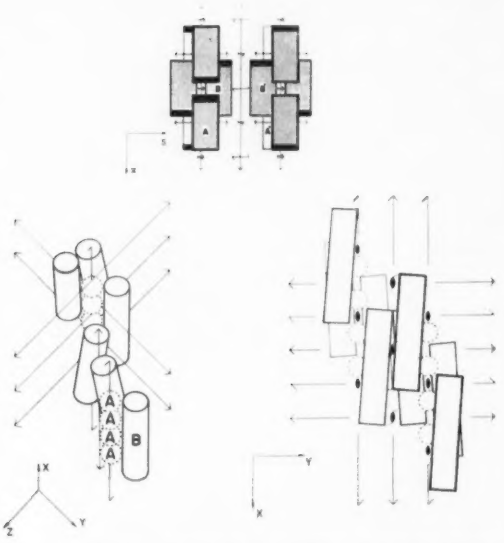

FIG. 3.—Three-dimensional illustrations of the two models. (*a*) Above: model corresponding to arrangement (1), Figures 1*a* and 2*a*. The letter *s* designates the vector [011]. Both rodlike units A and B are arbitrarily assigned a zero tilt and a length of 21 Å. The rods ABB′A′ represent part of one insulin dimer. (*b*) and (*c*) Below: two views of a model corresponding to arrangement (2), Figures 1*b* and 2*b* (low-weight positions omitted). The intersections of the units A, of unspecified gross structure, with the 2_1 axis are represented by dashed spheres, the centers of which are assigned a separation of $a/4$ along the axis. Arbitrarily assumed values for the unknown parameters for the rodlike units B are: tilt, 6°; length, 45 Å; *x*-coordinates of rod centers, $a/8$ and symmetry-related positions.

Experimental.—The models were refined using a modified least-squares program for the IBM 7090.[2] The IBM 7090 was also employed for the calculation of Fourier series. Structure factors were calculated in the following way. A unit which represents a rodlike region in end-on projection was represented as a circular region of constant density, as it was in the optical transform method.[1] The use of a digital computer made possible the employment of more sophisticated models, but none seemed warranted. The diameter of the circle was taken to be 6 Å; the Fourier transform of the circle then agrees fairly closely, for spacings out to 3.5 Å, with that of an α-helix in end-on projection. A unit which was assumed to represent a rodlike region tilted slightly with respect to the *a* axis was represented by five overlapping 6 Å circles. The two components of the vector between centers of neighboring circles were called the two "tilt" parameters for the unit. This method of representing a tilted rod is more accurate than the elongated apertures of the optical masks in that the density is greater at the center of the unit than at the ends, instead of being everywhere constant. Further, the total weight of each unit can easily be varied independently of its shape. In arrangement (2), the common projection of four units A, and the common projection of two units C, were each represented by a single circle of 6 Å diameter.

Before least-squares refinement, a large number of sets of parameters was tested, for each arrangement, to secure a good set of starting parameters. In the least-squares refinements, the parameters refined included the scale and temperature parameters for the observed data, and positional, tilt and weight parameters for the units. The scale and temperature parameters were refined separately from the other parameters, in alternate cycles. Structure amplitudes for the 0*kl* reflections out to 3.5 Å were used.

Four different weighting functions were employed. The first, w_1, depended only on $\sin\theta/\lambda$, with a maximum value of 1.0 at 10 Å spacing, a minimum of zero at 5 Å spacing, and a value of 0.5 at 3.3 Å spacing. The form factor for the units is zero near 5 Å spacing. The second, w_2, was w_1 multiplied, for each reflection, by the structure amplitude $|F(0kl)|$. The third, w_3, depended only on $\sin\theta/\lambda$; it decreased smoothly from a maximum 1.0 at 10 Å spacing, with a value of 0.5 at 4 Å spacing. The fourth, w_4, was w_3 multiplied, for each reflection, by the structure amplitude $|F(0kl)|$. At each stage of refinement a reliability index was calculated. The value of the reliability index depended rather markedly on the weighting function used. These indices have clearly no more than comparative significance.

Least-Squares Refinement.—In the refinements of arrangement (2), unit B alone

was permitted to tilt; unit A was confined to the position 0, 0, and unit C to the position y,0. The parameters refined, with slight changes from their initial values, to nearly the same values with each of the weighting functions. In the refinement of arrangement (1), when both units were permitted to tilt, their parameters changed markedly, and the final models obtained with the four weighting functions were markedly different. Three of the resulting models, in which the units developed excessive tilt, were incompatible with the basic hypothesis. The fourth, obtained with weighting function w_3, is similar to the model discussed in the following paragraph.

With an earlier version of the refinement program in which all the parameters, including scale and temperature factors, were refined together, another set of parameters had been obtained for arrangement (1). These parameters were very different from the initial ones. One unit moved and tilted to such an extent that, with overlap due to symmetry, it represented both of the original units connected by a bridge. The other unit moved, and its weight became negative—i.e., it represented a negative deviation from the average projected density. When these parameters were used as the starting values in the final version of the program, they refined, with relatively small changes, to substantially the same values with all the weighting functions. This model will be called "arrangement (1) with tilt." For comparison, refinements were done for arrangement (1) in which the units were confined to positions y,0 and 0,z, and were not permitted to tilt. The parameters of this model, which will be called "arrangement (1) without tilt," refined to nearly the same values with all the weighting functions.

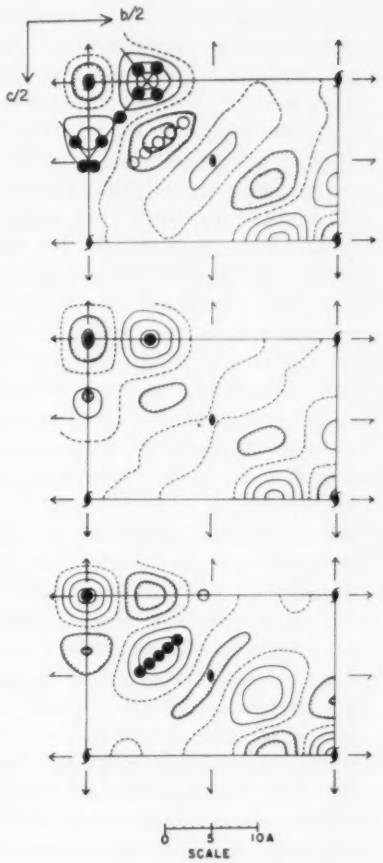

FIG. 4.—Final refined positions, in projection, of units in arrangements (1) and (2). (*a*) Top: refinement of arrangement (1) where tilt is permitted. (*b*) Center: refinement of arrangement (1) where units are without tilt and are confined to positions over twofold axes. (*c*) Bottom: refinement of arrangement (2). In the figures, the axis of a tilted unit is represented by five equi-spaced points. Black circles (single or set of five) represent units of high relative weight; shaded circles, units of low relative weight; open circles, unit of negative weight. In each figure, the unit positions are superimposed on a Fourier synthesis obtained using the observed structure amplitudes and signs from the refined model. In the Fouriers, the dashed lines represent the "zero" contour, and the marked lines, "negative" contours. Contours are at equal arbitrary intervals.

The final reliability indices for arrangement (1) with tilt were, with w_1, w_2, w_3, and w_4, 0.35, 0.07, 0.38, and 0.09, respectively. The corresponding indices for arrangement (1) without tilt were 0.55,

0.24, 0.66, and 0.29. For arrangement (2), they were 0.32, 0.10, 0.37, and 0.13.

Fourier projections were then calculated ($F(000)$ omitted), using observed structure amplitudes and signs from three refinements: arrangement (1) with tilt, arrangement (1) without tilt, and arrangement (2). The coefficients employed in the Fourier series were for reflections having a minimum spacing of 7 Å: at 7 Å, the form factor of the units has a value 0.4 of its value at $\sin\theta/\lambda = 0$; it falls to zero at about 5 Å spacing. Terms for which $|F_{calc.}| \leq 1/2\,|F_{obs.}|$ were omitted. For none of these arrangements did the weighting functions employed change the calculated signs for more than three of the weakest reflections. From a possible 17 terms, arrangement (1) with tilt (weighting function w_2) gave signs for all the terms, arrangement (1) without tilt for 16 terms, and arrangement (2) for 15 terms. The final positions for the models are shown in Figure 4 superimposed over the corresponding Fourier projections.

The signs for the strong reflections, as calculated for arrangement (1) with tilt and for arrangement (1) without tilt, are the same, and opposite to the signs for these reflections calculated for arrangement (2). This relationship, which also holds for most of the weaker reflections, is illustrated by the Fourier projections based on these signs.

We note that arrangements (1) and (2), as initially defined, were in a general way the negatives of each other (referred to their average values): that is, the units of arrangement (1) fell initially directly between those of arrangement (2) (Fig. 1*a* and *b*). Both refined models of arrangement (1) appear as approximate negatives of arrangement (2), and in particular the negative unit resulting from the refinement of arrangement (1) with tilt (Fig. 4*a*) coincides in position with the tilted positive unit of arrangement (2) (Fig. 4*c*). Arrangement (1) with tilt represents a refinement of arrangement (1) without tilt, as shown by comparison of their reliability indices. In the following discussion, therefore, we shall consider only the better refinement of arrangement (1).

Given our basic hypothesis,[1] one model represents the true structure, and the other represents approximately the negative of the true structure (referred to its average value). Clearly, only arrangement (2) is valid, as may be demonstrated by the following considerations.

(1) The refinement of arrangement (1) with tilt is largely incompatible with our basic hypothesis, for, considered simply as a model, it includes a broad, moderately high plateau relative to the negative region, thus implying that the rodlike regions are not very prominent features of the structure.

(2) A valid model must satisfy the chemical criterion that there be a minimum at the twofold rotation axis parallel to *a*. No atom which is part of a protein molecule may lie on a twofold axis; few atoms could be expected to lie closer than a distance of 2 Å from the axis. The minimal diameter of the low-density region about this axis (mainly mother liquor) must be a few Angstrom units. Arrangement (2) satisfies, and arrangement (1) with tilt fails to satisfy, the above criterion; their opposite behavior at the twofold axis is a consequence of their negative relationship. In arrangement (1) with tilt, there is a peak at the twofold axis with respect to the neighboring negative units, and in the Fourier for this arrangement there is a maximum at this position. On the other hand, both in the model and in the Fourier for arrangement (2) there is a pronounced trough at the twofold axis.

In the Fourier projection, this is not the deepest minimum, but considering the probable effects of errors in intensity measurements and in calculated signs, and the resolution of the projection, one may say that this feature of the Fourier does agree with the expected electron-density distribution.

(3) We may note that in the initial model of arrangement (1) (Fig. 2*a*) the principal rodlike regions of the dimer were about 20 Å from each other. This model might have represented a plausible first approximation for the insulin dimer if and only if, in a refined model, most of the region between the rods were to be "filled in"—that is, if it were to represent a relatively high plateau with respect to the lowest projected electron density. (There would necessarily have to be a "hole" in this plateau at the twofold axis.) If one were to consider the Fourier for arrangement (1) with tilt to be an approximation of the correct density function, then this requirement is clearly unsatisfied. The deep troughs adjacent to the rodlike units would necessarily represent the minimum projected density of the Fourier. Further, one would have to assume the maximum at the twofold axis to be due to errors, and/or to represent a narrow ring of density which was unresolved—both highly unlikely assumptions. Then the entire region about the twofold axis, extending from one of the troughs to the other, would have minimal or near-minimal density. In the dimer unit, the association between the two molecules would depend, at best, on a few intermolecular contacts in this region.

Only one fact appears slightly inconsistent with the conclusion that arrangement (2) is the correct one: the reliability indices for arrangement (1) with tilt, obtained with weighting functions w_2 and w_4, are a little lower than the corresponding indices for arrangement (2). This can be explained, however, as a consequence of the fact that arrangement (1) with tilt has two more parameters to be refined than does arrangement (2).

Both arrangement (1) and also its related Fourier projection having been eliminated, the final model is that shown, schematically, superposed over the Fourier of Figure 4*c*, and, ignoring unit C, illustrated in three dimensions in Figure 3*b* and *c*. The refined weights (obtained with weighting function w_2) of the units of this model are, on a relative scale: unit A, 1.0; unit B, 1.7; unit C, 0.5. The relative weights per molecule are then: unit A, 0.25; unit B, 1.7; unit C, 0.25. Thus, in one molecule the rodlike unit B has a weight approximately seven times that of each of the other two units.

Conclusion.—Re-examination of the experimental data and of the hypothesis on which these results are based leads to the following conclusions:

(1) It is possible that all the evidence[1] presented for the existence of rodlike regions of electron density, parallel or nearly parallel to *a* in the B, P, and C crystal forms, is invalid. Even an interpretation, such as we have made, of the three-dimensional vector structure of so complicated a structure is fraught with peril. If our fundamental premise is incorrect, then we may draw no conclusion whatever from these further studies.

(2) The evidence from various sources for the existence and orientation of rodlike regions of electron density, considered as a whole, is strong. If it is valid, then we may conclude:

(*a*) A solution of the 0*kl* electron-density projection must provide information about the positions of the rods.

(*b*) The Fourier (Fig. 4*c*) is an approximation at low resolution of the true *a*-plane electron-density projection.

(*c*) In the structure of a single insulin molecule there is a rodlike region of high electron density (unit B of Figures 2*b* and 3*b*) which very probably corresponds to a large part (15–30 residues) of the B polypeptide chain in the α-helix configuration, and two other regions, unit A and unit C, which show up in projection because of overlapping, correspond to 3–6 residues each in unspecified configuration. Both units A and C could correspond to regions of either polypeptide chain A or B, depending on the number of residues in unit B. We have no evidence concerning the structure of the remaining parts of the molecule; they most probably occupy positions of moderately high density in the Fourier (see Fig. 4*c*).

(*d*) The two principal rodlike units (B) of the dimer are adjacent to the dimer twofold axis and somewhat crossed. In the projection (Fig. 2*b*), the A and B units of the dimer, ABB′A′, are shown enclosed within the broken line.

We note that the requirement for two inter-chain disulfide bonds per molecule does not conflict with our tentative structure as described: the relative heights along the *a* axis have not been defined. Even if both units A and C are parts of the A polypeptide chain, and if two disulfide bridges are required to connect unit B with units A and C, these most restrictive requirements may be met.

Several model structures have previously been described for insulin. In the detailed model structures described by Lindley and Rollett[3] and by Linderstrøm-Lang,[4] the whole or a part of the polypeptide chain B is in the α-helix configuration; there is no conflict here. The detailed structures described for the polypeptide chain A are incompatible with our results. The model structure described by Low[5] is invalid for nonerystallographic reasons (excess left-handed helix).

Our evidence for the symmetry of the dimer unit led us earlier to suggest[6] (*a*) that the dimer as an asymmetric unit with point group 2 might be found in the rhombohedral zinc insulin crystals, space group R3, with 2 molecules in the asymmetric unit,[7] (*b*) that the point group of the hexamer might be 32 with the three twofold rotation axes lying in a plane normal to, and intersecting, the threefold axis, and thus at 120° to each other, and (*c*) that in principle the presence of a nonerystallographic twofold axis should be detectable by analysis of the vector structure. Rossmann and Blow[8] have developed an elegant new method of vector structure analysis, and they have found that in rhombohedral zinc insulin[9] there are nonerystallographic twofold axes lying in a plane normal to the trigonal axis, implying that the dimer as an asymmetric unit has the point group 2. They have not established whether the three twofold axes intersect at a threefold axis (as required for the point group 32).

The earlier studies of Low[10] led her to conclude that long ($\approx$44 Å) rods of insulin, corresponding to the whole of the B chain in the α-helix configuration, would pack in the unit cell of the rhombohedral crystals with the rods oriented approximately perpendicular to the trigonal axis. The present model would also suggest this general packing arrangement for the rodlike regions of chain. If our model structure is correct, and if the dimer has the same structure in the rhombohedral form as in the orthorhombic forms, then the findings of Rossmann and Blow would establish this orientation of the rods. It should be noted, however, that although the dimer unit, as predicted, has the point group 2 in the rhombohedral zinc insulin

crystals, and there is evidence for invariance of the dimer unit in the orthorhombic forms, these findings are not sufficient evidence for complete structure invariance. It is still formally possible that the specific stereochemistry of a single insulin molecule in the rhombohedral form differs from that in the orthorhombic forms.

Our trial-and-error studies may be continued in three dimensions, as an adjunct to the isomorphous-replacement studies.

Summary.—Trial-and-error studies using Patterson and Fourier-transform methods, based on the evidence for rodlike regions of high electron density in the orthorhombic crystal forms of insulin, have led to the description of a model for the gross structure of a major part of the insulin molecule[11] and to the elimination of the one other initially plausible model described earlier.[1] The arrangement of the units of the model in the type C orthorhombic insulin crystals has been defined in two dimensions. The nature and degree of our confidence in this model structure have been discussed. Although the demonstrated agreement is very encouraging, the model should not, without further proof, be considered established.

* This investigation was supported by a Senior Research Fellowship SF-246C to one of us (B. W. L.) from the Public Health Service, in part by a Public Health Service Research Grant A1320 C from the National Institute of Arthritis and Metabolic Diseases, Public Health Service, and in part by a research grant G3347 from the National Science Foundation. We are grateful to the Watson Scientific Computing Laboratory for IBM 7090 computing facilities.

† Present address: Department of Radiation Biology and Physics, Queen's College, University of St. Andrews, Dundee, Scotland.

[1] McGavin, A. S., J. R. Einstein, and B. W. Low, these PROCEEDINGS, **48,** 2150 (1962).

[2] Program written by R. A. Sparks, P. K. Gantzel, and K. N. Trueblood and modified by one of us (J. R. E.).

[3] Lindley, H., and J. S. Rollett, *Biochim. Biophys. Acta*, **18,** 183 (1955).

[4] Linderstrøm-Lang, K., in *Peptide Chemistry: Report of a Symposium Held by the Chemical Society* (London: The Chemical Society, 1955), Special Pub. No. 2.

[5] Low, B. W., in *Currents in Biochemical Research*, ed. D. E. Green (New York: Interscience, 1956), p. 422.

[6] Low, B. W., and J. R. Einstein, *Nature*, **186,** 470 (1960).

[7] Crowfoot, D., *Proc. Roy. Soc.* (*London*), **A164,** 580 (1938); Crowfoot, D., and D. Riley, *Nature*, **144,** 1011 (1939).

[8] Rossmann, M. G., and D. M. Blow, *Acta Cryst.*, **15,** 24 (1962).

[9] Rossmann, M. G., and D. M. Blow, private communication, using unpublished data of D. M. Crowfoot Hodgkin.

[10] Low, B. W., *Nature*, **169,** 955 (1952).

[11] An earlier description of a model substantially the same as the final model described here, except for the absence of the unit C, was presented at the Fifth International Congress of the International Union of Crystallography, Cambridge, England, in 1960; see published abstract (Low, B. W., A. S. McGavin, and J. R. Einstein, *Acta Cryst.*, **13,** 1056 (1960)).

*STUDIES ON POLYNUCLEOTIDE-STIMULATED AMINO ACYL TRANSFER FROM SOLUBLE-RNA TO RAT LIVER RIBOSOMES**

By June M. Fessenden,† Judith Cairncross, and Kivie Moldave

DEPARTMENT OF BIOCHEMISTRY, TUFTS UNIVERSITY SCHOOL OF MEDICINE, BOSTON

Communicated by Severo Ochoa, November 16, 1962

Recent evidence has provided experimental support for the concept of a "messenger RNA" concerned with the transmission of information from DNA to protein.[1–5] The demonstrations that biosynthetically prepared polyribonucleotides of varying base compositions stimulate the incorporation of individual amino acids in an amino acid-incorporating system from *E. coli*[6–15] suggest that such polymers act as synthetic "messengers." These results have provided an experimental approach to the problem of "coding" in protein synthesis whereby a certain sequence of nucleotides in RNA can determine the sequence of amino acids in a polypeptide chain. The relative agreement between some of the assigned nucleotide "code" units derived from studies with *E. coli* and amino acid replacement data from a number of species[12, 13, 16–19] and other studies [20, 21] suggest that the "genetic code" might apply to more than one species. This study was initiated since it appeared of considerable importance to determine whether comparable evidence could be obtained in mammalian cells. The use of a highly purified rat liver system, available in this laboratory,[22, 23] that catalyzes the transfer of amino acids from amino acyl *s*-RNA to ribosomal protein was considered since it is relatively free of interfering reactions which are also involved in protein synthesis. The amino acyl transfer reaction represents an isolated reaction, dissociated from amino acid activation and the synthesis of *s*-RNA amino acid, which leads to the incorporation of amino acids into proteins. This communication describes the characterization of such a system which responds markedly to addition of various polynucleotides. While this work was in progress, several reports appeared which demonstrated that the incorporation of free amino acids in crude sub-cellular mammalian systems was stimulated by polynucleotide preparations.[24–27]

Materials and Methods.—The preparation of amino acyl *s*-RNA labeled with C^{14}-amino acids, deoxycholate-extracted ribosomes, pH 5 supernatant, and two purified soluble protein factors, designated amino acyl transferases (or polymerases) I and II, from rat liver has been described previously.[22, 23] The resolution of transferases I and II from the pH 5 supernatant fraction and the purification of transferase II, which has also been obtained from microsomal extracts,[23, 28] will be described in detail in a subsequent communication. Polyuridylic acid (poly U), polycytidylic acid (poly C), polyuridylic-guanylic acid (poly UG, 5:1), polyuridylic-cytidylic acid (poly UC, 5:1), and polyuridylic-adenylic acid (poly UA, 5:1) were obtained from Dr. Severo Ochoa and his colleagues; their generous gifts are gratefully acknowledged.

Incubation procedures are described in detail below. At the end of the incubation, the perchloric acid-insoluble fraction was prepared and the residual protein was obtained from it after several washes including two extractions with 5 per cent trichloroacetic acid at 90°. The residual proteins were plated directly and were

counted long enough to achieve at least a 10 per cent precision; appropriate corrections for self-absorption and background (1.6 to 2.0 cpm) were applied.

Results and Discussion.—Previous studies demonstrated the requirements for GTP and a soluble fraction of the cell for amino acyl transfer to cytoplasmic ribonucleoprotein particles.[22, 23] Recent reports from this laboratory[23, 28] have presented evidence indicating the presence of two activities essential for amino acyl transfer. One of these, transferase I, catalyzes amino acyl transfer to intact microsomes, but is inactive in experiments with purified ribosomes. The other activity, transferase II, has been obtained from the soluble portion of the cell and from deoxycholate-soluble extracts of microsomes and is required, in addition to transferase I, for amino acyl transfer to ribosomes. Thus, amino acyl transfer is obtained with crude soluble preparations after removal of the amino acid-activating enzymes (pH 5 supernatant) or with the two purified factors (amino acyl transferases I and II) in the presence of GTP and glutathione.

The effect of polyuridylic acid on amino acyl transfer was examined with two concentrations of ribonucleoprotein (Table 1). Addition of poly U to incubations of pH 5 supernatant with high concentrations of ribosomes (experiment A) resulted in slightly higher incorporation of phenylalanine as compared to controls without poly U. Incubations in the presence of transferases I and II did not reveal any stimulation on addition of poly U. When similar incubations were carried out with relatively low concentrations of ribosomes (experiment B), addition of poly U in the presence of pH 5 supernatant led to a marked (2–4 fold) stimulation of phenylalanyl transfer. In contrast to the marked stimulation observed in incubations with pH 5 supernatant, slight but significant increases were observed on addition of poly U to incubations with combined transferases I and II.

Since the possibility existed that endogenous "messenger RNA" on rat liver ribosomes might interfere with the interaction of exogenous polynucleotide with ribosomal particles, preincubation procedures were assayed in attempts to facilitate such interactions. As shown in Table 2, preincubation of both high (experiment A) and low (experiment B) concentrations of ribosomes in the presence of pH 5 supernatant led to a drastic decrease in phenylalanine incorporation as compared to the results obtained without a preincubation period (Table 1). Ribosomes preincubated with transferases I and II did not exhibit such a loss of activity. The addition of poly U to ribosomes preincubated with pH 5 supernatant resulted in a marked stimulation of amino acyl transfer, particularly in experiments with less

TABLE 1

THE EFFECT OF POLYURIDYLIC ACID ON AMINO ACYL TRANSFER

Enzyme preparation	Poly U additions	Cpm Incorporated into Protein	
		Experiment A	Experiment B
None	−	100	44
None	+	114	−
pH 5 supernatant	−	734	461
" " "	+	858	1,144
Transferases I and II	−	612	327
" " " "	+	565	433

Incubations contained 0.08 mg (2,500 cpm) of C^{14}-phenylalanyl s-RNA, ribosomes, 1.2 μmoles of GTP·$MgCl_2$, 10 μmoles of glutathione, and 10 mg of pH 5 supernatant protein or 0.003 mg of transferase I plus 4 mg of soluble transferase II protein where indicated, in a total volume of 2.5 ml. Poly U additions, indicated by + signs, consisted of 0.2 mg of polyuridylic acid. Experiment A was carried out with 7 mg of ribosomes and experiment B with 0.7 mg of ribosomes per flask. Incubations were carried out for 20 min at 37°.

TABLE 2

EFFECT OF PREINCUBATION AND POLYURIDYLIC ACID ON AMINO ACYL TRANSFER

Preincubation components	Incubation additions	Cpm Incorporated into Proteins Experiment A	Experiment B
Ribosomes	s-RNA-Phe-C^{14}	119	9
"	" + poly U	125	0
" + pH 5 supernatant	"	255	75
" "	" + poly U	817	1,165
" + Transferases I & II	"	883	274
" " "	" + poly U	850	372

Ribosomes, 1 μmole of GTP·$MgCl_2$ and 10 μmoles of glutathione were incubated at 37° as such, in the presence of 10 mg of pH 5 supernatant protein, or with 0.003 mg of transferase I plus 4 mg of soluble transferase II protein. After an 8-min preincubation, 0.08 mg (2,500 cpm) of C^{14}-phenylalanyl s-RNA and, where noted, 0.2 mg of polyuridylic acid were added and the incubation was continued for an additional 20 min. Experiment A was carried out with 7 mg of ribosomes and Experiment B with 0.7 mg of ribosomes, in a final volume of 2 ml.

than 1 mg of ribosomes. Preincubation in the absence of transferring preparations led to irreversible inactivation. The loss of activity on preincubation and the marked recovery on addition of poly U are consistent with the degradation of an endogenous ribosomal component and its replacement by the synthetic polynucleotide. It is interesting to note that the purified transferases I and II do not catalyze the decrease in ribosomal activity and subsequently fail to exhibit a significant poly U effect, suggesting the presence of an additional factor in the pH 5 supernatant responsible for this effect. Studies on the nature of this factor are presently in progress and will be reported subsequently.

As discussed above, the poly U-dependent stimulation of amino acyl transfer is more apparent with lower concentrations of ribosomes. Similar results are presented in Figure 1. Although the stimulatory effect of poly U on amino acyl transfer was more marked at lower ribosomal concentrations, optimal incorporation in the presence of poly U was observed in incubations containing 0.7 mg of preincubated ribosomes. With increasing ribosomal concentrations, the poly U-dependent incorporation was decreased while endogenous incorporation increased.

The effect of varying concentrations of pH 5 supernatant on ribosomal preincubations is shown in Figure 2. The values obtained with ribosomes preincubated with 1 to 2.5 mg of pH 5 supernatant protein, in the presence and absence of poly U, are quantitatively similar to those obtained in nonpreincubated experiments (Table 1); higher concentrations led to lower incorporation values in the absence of poly U, and the response to poly U also appeared to be proportional to the concentration of pH 5 supernatant.

Figure 3 shows the dependence of phenylalanyl transfer to preincubated ribosomes on the concentration of poly U. Significant stimulation was observed with 0.02 mg of polynucleotide per ml of incubation fluid and maximal incorporation was observed with approximately 0.1 mg per ml. The addition of poly C over a similar concentration range had no effect on this process. Possibilities existed that the extent of polynucleotide-stimulated amino acyl transfer observed above might reflect less than maximal incorporation due to the degradation of C^{14}-amino acyl s-RNA or added polynucleotide or to the inactivation of transferring enzymes or ribosomes during the incubation. Alternatively, the amino-acid acceptor sites on the ribosomal particle might have become saturated, thus causing incorporation to cease. The experiments described in Figure 4 represent an attempt to examine these possibilities. Amino acyl transfer was completed within 5 min of incubation

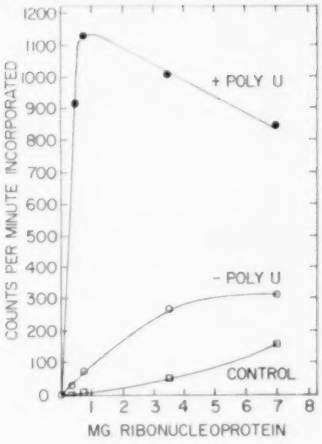

FIG. 1.—Effect of polyuridylic on amino acyl transfer to varying concentrations of preincubated ribosomes. Ribosomes (0.3 to 7 mg) were incubated at 37° in the presence of 1 μmole of GTP·$MgCl_2$, 10 μmoles of glutathione, and 10 mg of pH 5 supernatant protein in a total volume of 1.6 ml. After 8 min of preincubation, 0.08 mg of C^{14}-phenylalanyl *s*-RNA with (closed circles, + Poly U) or without (open circles, − Poly U) 0.2 mg of polyuridylic acid was then added and incubated for an additional 20 min in a total volume of 2 ml. The control (squares) represents incubations carried out in a similar manner, in the absence of pH 5 supernatant.

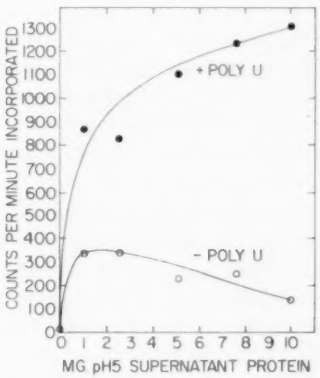

FIG. 2.—Effect of polyuridylic acid on amino acyl transfer to ribosomes preincubated with varying concentrations of pH 5 supernatant protein. Approximately 0.7 mg of ribosomes were incubated at 37° for 8 min in the presence of GTP, glutathione, and the concentrations of pH 5 supernatant protein shown, as described in Figure 1. C^{14}-phenylalanyl *s*-RNA with (closed circles, + Poly U) or without (open circles, − Poly U) polyuridylic acid was then added and incubated for an additional 20 min.

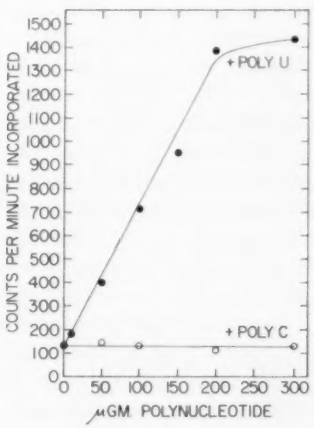

FIG. 3.—Effect of polyuridylic acid concentration of amino acyl transfer to preincubated ribosomes. Approximately 0.7 mg of ribosomes were incubated at 37° for 8 min in the presence of GTP, glutathione, and pH 5 supernatant as described in Figure 1. C^{14}-Phenylalanyl *s*-RNA and varying concentrations of polyuridylic acid (closed circles, + Poly U) or polycytidylic acid (open circles, +Poly C) were then added and incubated for an additional 20 min.

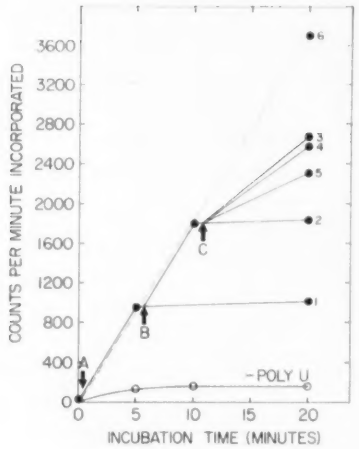

FIG. 4.—The effect of multiple additions on amino acyl transfer to preincubated ribosomes. Approximately 0.7 mg of ribosomes were preincubated for 8 min as described in Figure 1. Series 1 received 0.08 mg of C^{14}-phenylalanyl *s*-RNA and 0.2 mg of polyuridylic acid at the end of the preincubation period, A, and were assayed after 5 and 20 min of incubation. Series 2 received polyuridylic acid at A and C^{14}-phenylalanyl *s*-RNA at A and B. Series 3 received polyuridylic acid at A, and C^{14}-phenylalanyl *s*-RNA at A, B, and C. Series 4 received polyuridylic acid at A and C, and C^{14}-phenylalanyl *s*-RNA at A, B, and C. Series 5 received polyuridylic acid at A and C, and C^{14}-phenylalanyl *s*-RNA at A and B. Experiment number 6 represents an incubation with 0.24 mg of C^{14}-phenylalanyl *s*-RNA added at A. A control series in the absence of polyuridylic acid (open circles, – Poly U) received C^{14}-phenylalanyl *s*-RNA at 0, 5, and 10 min of incubation.

(Figure 4, series 1). Addition of a second dose of C^{14}-phenylalanyl *s*-RNA to the labeled suspensions, after 5 min of incubation (point B), resulted in the further incorporation of amino acid into protein as shown in series 2. The extent of incorporation during the second 5-min labeling period was quantitatively similar to that observed during the first 5 min. A third addition of C^{14}-phenylalanyl *s*-RNA was made after 10 min of incubation (point C); again, the extent of incorporation during this third labeling period was quantitatively similar to those observed during the first and second 5-min incubations. The addition of poly U and C^{14}-phenylalanyl *s*-RNA at point C (series 4) did not lead to a greater increase in ribosomal labeling than that observed with C^{14}-phenylalanyl *s*-RNA alone and the addition of Poly U only (series 5) was not as effective. The results presented here indicate that the limiting component in the incubation system is the labeled substrate, C^{14}-phenylalanyl *s*-RNA, probably due to the degradation of *s*-RNA-amino acid under these conditions. It would also appear that the poly U responsible for the enhanced incorporation, perhaps ribosomal-bound polynucleotide, is not excessively broken down during these incubations. Further, ribosomal amino acid-acceptor sites do not appear to be saturated, as evidenced also by incubation series 6 which received three times the usual dose of C^{14}-phenylalanyl *s*-RNA at the beginning of the incubation.

The effects of several polymers on the transfer of various *s*-RNA-bound C^{14}-amino acids are summarized in Table 3. Although the specific radioactivities of the C^{14}-amino acyl *s*-RNA preparations varied between 18,000 cpm and 40,000 cpm per mg of *s*-RNA, approximately 3,000 cpm of each was used per incubation. Amino acyl transfer in the absence of polynucleotides was less than 10 per cent of that observed in control flasks which were not preincubated. The results obtained here indicate that the transfer of individual *s*-RNA-bound amino acids is stimulated by specific polynucleotide preparations. For example, incorporation of phenylalanine under these conditions is stimulated by all of these polymers, glycine by poly UG, and serine by poly UC. These partial results appear to be in general

TABLE 3

THE EFFECT OF VARIOUS POLYNUCLEOTIDES ON THE TRANSFER OF INDIVIDUAL *s*-RNA-BOUND AMINO ACIDS

s-RNA-bound C^{14}-amino acid	Control	Polynucleotide Added				
		None	Poly U	Poly UG (5:1)	Poly UC (5:1)	Poly UA (5:1)
Glycine	390	0	0	*85*	0	0
Isoleucine	798	24	12	16	16	*45*
Leucine	2,625	24	33	*320*	*403*	*108*
Lysine	1,020	24	8	0	12	9
Phenylalanine	594	42	*3,449*	*1,056*	*1,872*	*182*
Serine	381	20	0	8	*125*	0
Threonine	522	0	0	0	0	0
Tyrosine	207	8	0	0	0	*20*
Valine	315	0	28	*535*	0	0

Approximately 0.7 mg of ribosomes were incubated at 37° for 8 min in the presence of GTP, glutathione, and pH 5 supernatant as described in Figure 1. After 8 min, C^{14}-amino acyl *s*-RNA and 0.3 mg of the polynucleotide noted were added and incubated for an additional 20 min. In this experiment, the Poly U used was purchased from Miles Laboratories. The results are expressed as increase in specific radioactivity (cpm per mg) of ribosomal protein; values obtained in the presence of polynucleotides have therefore been corrected by subtracting the values obtained in the absence of polynucleotide (None). The control values refer to amino acyl transfer to ribosomes, in the absence of polynucleotide and a preincubation period, as described in Table 1.

agreement with those obtained with *E. coli*.[6–15] The relative incorporation obtained here with poly UA, however, does not appear to be as marked as in the *E. coli* system or as with other active polymers in this system. It should be emphasized that Poly C had no effect on the incorporation of any of the amino acids tested. These data further suggest that the polynucleotide-enhanced incorporation is specific for individual amino acids and does not involve the simultaneous transfer of all of the *s*-RNA-bound amino acids; the C^{14}-amino acyl *s*-RNA preparations were similar with respect to endogenous, bound amino acids and differed only in the nature of the radioactive amino acid.

The low level of endogenous amino acid incorporation obtained with preincubated ribosomes and the marked stimulation observed in the presence of synthetic polymers reflect polynucleotide effects comparable to those obtained with free amino acids and markedly higher than those reported previously for amino acyl transfer[9] in *E. coli* systems. The observations described above suggest that this mammalian system is particularly well suited for studies designed to investigate the "universality" of the genetic code.

Summary.—A rat liver system that catalyzes amino acyl transfer from amino acyl *s*-RNA to ribosomal protein is stimulated by the addition of polyuridylic acid. The stimulation is markedly greater when ribosomes are preincubated with pH 5 supernatant, particularly in experiments with low concentrations of ribosomes. When amino acyl transfer is examined with several polynucleotide preparations, varying in base composition, the incorporation of individual *s*-RNA-bound amino acids appears to be enhanced in the presence of specific polynucleotides. Partial characterization of this polynucleotide-stimulated mammalian system has been carried out. The results suggest that on preincubation, a component of ribosomes, possibly messenger RNA, is removed by a soluble factor which is different from the amino acyl transferring enzymes. The stimulation observed on addition of polynucleotides to preincubated ribosomes suggests that the natural messenger RNA is replaced by these synthetic messenger molecules.

* Supported in part by research grants from the American Cancer Society (P-177) and the U.S. Public Health Service (A-1397 and GM-K3-4124). We would like to acknowledge the many helpful discussions with Albert J. Wahba.

† Predoctoral Research Fellow of the U.S. Public Health Service.

[1] Volkin, E., and L. Astrachan, *Virology*, **2**, 149 (1956).

[2] Jacob, F., and J. Monod, *J. Mol. Biol.*, **3**, 318 (1961).

[3] Brenner, S., F. Jacob, and M. Meselson, *Nature*, **190**, 576 (1961).

[4] Gros, F., H. Hiatt, W. Gilbert, C. G. Kurland, R. W. Riseborough, and J. D. Watson, *Nature*, **190**, 581 (1961).

[5] Sibatani, A., S. R. deKloet, V. G. Allfrey, and A. E. Mirsky, these PROCEEDINGS, **48**, 471 (1962).

[6] Nirenberg, M. W., and J. H. Matthaei, these PROCEEDINGS, **47**, 1588 (1961).

[7] Lengyel, P., J. F. Speyer, and S. Ochoa, these PROCEEDINGS, **47**, 1936 (1961).

[8] Speyer, J. F., P. Lengyel, C. Basilio, and S. Ochoa, these PROCEEDINGS, **48**, 63 (1962).

[9] Nirenberg, M. W., J. H. Matthaei, and O. W. Jones, these PROCEEDINGS, **48**, 104 (1962).

[10] Martin, R. G., J. H. Matthaei, O. W. Jones, and M. W. Nirenberg. *Biochem. Biophys. Research Comm.*, **6**, 410 (1962).

[11] Lengyel, P., J. F. Speyer, C. Basilio, and S. Ochoa, these PROCEEDINGS, **48**, 282 (1962).

[12] Speyer, J. F., P. Lengyel, C. Basilio, and S. Ochoa, these PROCEEDINGS, **48**, 441 (1962).

[13] Basilio, C., A. J. Wahba, P. Lengyel, J. F. Speyer, and S. Ochoa, these PROCEEDINGS, **48**, 613 (1962).

[14] Matthaei, J. H., O. W. Jones, R. G. Martin, and M. W. Nirenberg, these PROCEEDINGS, **48**, 666 (1962).

[15] Wahba, A. J., C. Basilio, J. F. Speyer, P. Lengyel, R. S. Miller, and S. Ochoa, these PROCEEDINGS, **48**, 1683 (1962).

[16] Tsugita, A., and H. Fraenkel-Conrat, these PROCEEDINGS, **46**, 636 (1960).

[17] Wittmann, H. G., *Naturwissenschaften*, **48**, 729 (1961).

[18] Smith, E., these PROCEEDINGS, **48**, 677 (1962).

[19] Smith, E., these PROCEEDINGS, **48**, 859 (1962).

[20] von Ehrenstein, G., and F. Lipmann, these PROCEEDINGS, **47**, 941 (1961).

[21] Tsugita, A., H. Fraenkel-Conrat, M. W. Nirenberg, and J. H. Matthaei, these PROCEEDINGS, **48**, 846 (1962).

[22] Grossi, L. G., and K. Moldave, *J. Biol. Chem.*, **235**, 2370 (1959).

[23] Fessenden, J. M., and K. Moldave, *Biochemistry*, **1**, 485 (1962).

[24] Arnstein, H. R. V., R. A. Cox, and J. A. Hunt, *Nature*, **194**, 1042 (1962).

[25] Maxwell, E. S., these PROCEEDINGS, **48**, 1639 (1962).

[26] Weinstein, B., and A. N. Schechter, these PROCEEDINGS, **48**, 1686 (1962).

[27] Griffin, A. C., and M. A. O'Neal, *Biochim. et Biophys. Acta*, **61**, 469 (1962).

[28] Fessenden, J. M., and K. Moldave, *Biochem. Biophys. Research Comm.*, **6**, 232 (1961).

---

*RIBONUCLEIC ACID POLYMERASE OF AZOTOBACTER VINELANDII, I. PRIMING BY POLYRIBONUCLEOTIDES**

BY JOSEPH S. KRAKOW† AND SEVERO OCHOA

DEPARTMENT OF BIOCHEMISTRY, NEW YORK UNIVERSITY SCHOOL OF MEDICINE

Communicated November 29, 1962

The initial investigations[1–5] on RNA polymerase demonstrated that DNA[6] primes and directs the synthesis of RNA. Subsequently it was shown that native DNA is a more effective primer than is the heat denatured, single stranded form.[7] Recently Nakamoto and Weiss[8] reported that poly C and turnip yellow mosaic virus RNA could direct the synthesis of polyribonucleotides with polymerase preparations from *Micrococcus lysodeikticus*. The effect of polyribonucleotides has been confirmed and extended with a 500-fold purified RNA polymerase from

Azotobacter vinelandii. These studies are the subject of the present communication.

Methods and Materials.—C^{14}-labeled ribonucleoside di- and triphosphates were obtained from the Schwarz BioResearch Inc., Orangeburg, N. Y. Nonlabeled ribonucleoside triphosphates were from the Schwarz BioResearch Inc. and the Pabst Laboratories, Milwaukee, Wisconsin. Calf thymus DNA was obtained from the Worthington Biochemical Corporation, Freehold, New Jersey, and creatine kinase from the California Foundation for Biochemical Research, Los Angeles. We are greatly indebted to Dr. Carlos Basilio for preparing the polyribonucleotide polymers and to Dr. C. A. Knight for generous gifts of TMV RNA. Oligodeoxythymidylic acid was kindly provided by Dr. H. G. Khorana, University of Wisconsin. We are also indebted to Dr. E. Alpert of Merck, Sharp and Dohme, West Point, Pennsylvania, for a gift of actinomycin D. *Azotobacter* RNA polymerase was purified and assayed for nucleotide incorporation as previously described.[9] In assay A (DNA-primed reaction) each incubation mixture (0.25 ml) contained (in μmoles), Tris-HCl buffer, pH 8.5, 20; $MgSO_4$, 5; mercaptoethylamine, 8; CTP, 0.5; UTP, 0.5; GTP, 0.5; C^{14}-ATP (2.1×10^5 cpm/μmole), 0.5; calf thymus DNA; and enzyme. In assay B (polyribonucleotide-primed reaction) each incubation mixture (0.2 ml) contained (in μmoles), Tris-HCl buffer, pH 7.1, 20; $MgCl_2$, 2; $MnSO_4$, 0.5; mercaptoethylamine, 8; ribonucleoside triphosphate ($2.1–2.6 \times 10^5$ cpm/μmole), 0.2; polyribonucleotide; and enzyme.

Results.—Effect of polyribonucleotides: In agreement with the results of Nakamoto and Weiss[8] with *M. lysodeikticus* enzyme, RNA polymerase from *A. vinelandii* utilized poly C to prime the synthesis of poly G (Table 1). Moreover, both poly U

TABLE 1

EFFECTIVENESS OF VARIOUS POLYNUCLEOTIDES AS PRIMERS*

Polynucleotide	Nucleotides added	Nucleotides incorporated (milliμmoles)
Calf thymus DNA, native	C^{14}-GTP, ATP, UTP, CTP†	13.0‡
Calf thymus DNA, denatured	" " " "	3.2‡
TMV RNA	" " " "	0.5‡
Poly U	C^{14}-ATP	6.5
Poly A	C^{14}-UTP	4.2
Poly C	C^{14}-GTP	4.1
Poly I	C^{14}-CTP	0.2

* Assay A was used with DNA as primer; assay B with polyribonucleotides as primers. The reaction mixtures contained 10 μg of the indicated polynucleotide and 10 μg of RNA polymerase. Incubation, 10 min at 37°.

† The incorporation of the labeled nucleotide was dependent on the presence of a full complement of ribonucleoside triphosphates.

‡ Based on total nucleotide incorporated, calculated from base ratio of primer.

and poly A primed the synthesis of their complementary polyribonucleotides. The priming ability of the three homopolymers was similar but poly U was the most active. These polymers directed the synthesis of polyribonucleotide to the extent of 30–50 per cent that obtained with native calf thymus DNA as primer. In marked contrast to the priming effect of these homopolymers was the poor activity of poly I and of TMV RNA (Table 1). Transfer RNA and ribosomal RNA were also essentially inactive.

The homopolymers directed specifically the synthesis of their complementary polyribonucleotides. Thus, poly U promoted the incorporation of ATP but not that of CTP, UTP, or GTP (Table 2). There was no requirement for a full complement of ribonucleoside triphosphates; addition of CTP, UTP, and GTP to the samples containing poly U and C^{14}-ATP inhibited to some extent the incorporation of AMP from the latter compound. Substituting C^{14}-ADP for C^{14}-ATP resulted in negligible incorporation of AMP. However, incubation of poly U and C^{14}-

TABLE 2
PRIMING OF POLY A SYNTHESIS BY POLY U*

Additions	Labeled nucleotide incorporated (milliμmoles)
C^{14}-ATP	13.4
C^{14}-UTP	<0.05
C^{14}-CTP	<0.05
C^{14}-GTP	<0.05
C^{14}-ADP	0.12
C^{14}-ADP + creatine kinase (10 μg) and creatine phosphate (7 μmoles)	14.0

* Assay B with 17 μg of poly U and 16 μg of RNA polymerase. Incubation, 5 min at 37°.

ADP, in the presence of creatine kinase and creatine phosphate, gave the same result as incubation with C^{14}-ATP (Table 2).

That poly A directed the incorporation of UMP was further demonstrated by utilizing the poly A synthesized with poly U as primer to prime the incorporation of UMP from C^{14}-UTP into polymer (Fig. 1). Addition of UTP to mixtures containing C^{14}-ATP and poly U decreased the incorporation of AMP from C^{14}-ATP (▽-▽-▽). This suggested that nonlabeled poly U was formed from UTP with newly synthesized C^{14}-poly A as template. In accordance with this interpretation UMP was incorporated from C^{14}-UTP, in the presence of poly U and nonlabeled ATP (•-•-•). This incorporation followed an autocatalytic course as would be expected from the gradual increase in poly A primer formed from ATP in the presence of poly U. In similar experiments with poly C, GTP, and C^{14}-CTP there was no incorporation of C^{14}-CMP into the acid insoluble fraction, indicating that under these conditions, the newly synthesized poly G could not prime the synthesis of poly C.

Although poly A and poly U were poor primers with *M. lysodeikticus* enzyme, the 1:1 poly A + poly U complex primed the incorporation of either AMP or UMP.[8] With *Azotobacter* RNA polymerase the 1:1 poly A + poly U complex was not very different from poly A in its ability to prime UMP incorporation. However, the complex was a much poorer primer of poly A synthesis than was poly U (Table 3, experiment 1). The effectiveness of the A + U complex with UTP and its poor activity with ATP might be due to its ability to add only one other strand of poly U resulting in the formation of the triple stranded complex A + 2U.

In agreement with the results of Nakamoto and Weiss[8] with *M. lysodeikticus* enzyme, *Azotobacter* RNA polymerase catalyzed the synthesis of either poly A

TABLE 3
PRIMING OF NUCLEOTIDE INCORPORATION BY COPOLYMERS CONTAINING AMP AND UMP*

Experiment No.	Primer	Substrate	Labeled nucleotide incorporated (milliμmoles)
1	Poly A (5 μg)	C^{14}-UTP	1.8
	Poly U (5 μg)	C^{14}-ATP	2.8
	Poly A (5 μg) + poly U (5 μg)	C^{14}-UTP	2.2
		C^{14}-ATP	0.2
2	Random poly AU 1:1 (20 μg)	C^{14}-UTP	2.2
		C^{14}-ATP	3.7
		C^{14}-UTP + ATP	1.5
		C^{14}-ATP + UTP	1.3
3	Alternating poly AU (15 μg)	C^{14}-ATP	<0.05
		C^{14}-UTP	<0.05
		C^{14}-ATP + C^{14}-UTP	<0.05

* Assay B with 10 μg of RNA polymerase. Incubation, 10 min at 37°.

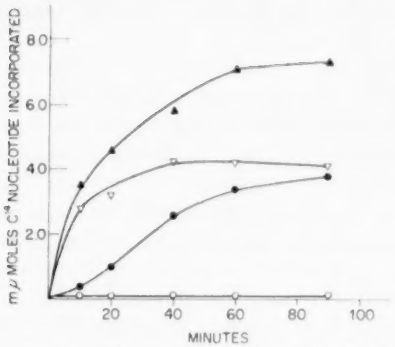

FIG. 1.—Priming of poly U synthesis by poly A synthesized *in situ*. Each point on the curves represents an assay B incubation containing 5 μg of poly U, 4 μg of RNA polymerase, and substrate as follows: C¹⁴-ATP, ▲–▲–▲; C¹⁴-ATP + UTP, ▽–▽–▽; C¹⁴-UTP + ATP, ●–●–●; and C¹⁴-UTP, ○–○–○. Incubation at 37°.

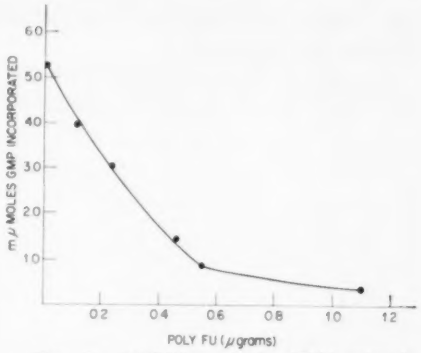

FIG. 2.—Inhibition of the DNA-primed synthesis of RNA by poly FU. Each point on the curve represents an assay A incubation with 50 μg of native calf thymus DNA, 10 μg of RNA polymerase, and poly FU as indicated. Labeled substrate, C¹⁴-GTP. Incubation, 5 min at 37°.

or poly U with a random AU (1:1) copolymer (Table 3, experiment 2). Moreover, the incorporation of UMP from C¹⁴-UTP was not increased by the presence of cold ATP or *vice versa*. On the other hand, alternating poly AU, prepared with the *Azotobacter* polymerase with poly dAT as template,[10] did not prime the incorporation of UMP or AMP (from C¹⁴-UTP and C¹⁴-ATP, respectively) whether singly or in combination (Table 3, experiment 3).

Effect of polynucleotides containing uracil analogs: Several homopolymers containing analogs of uracil were tested for AMP incorporation from C¹⁴-ATP; none of them had priming activity (Table 4). The copolymer, poly UFU (1:1), had approximately 60 per cent of the priming activity of poly U. Poly thio U or poly N-methyl U did not interfere with the priming by poly U but poly FU was very inhibitory. Addition of poly FU (10 μg) to mixtures containing 10 μg of poly U resulted in 97 per cent inhibition of poly A synthesis; smaller amounts of poly FU still showed marked inhibition of AMP incorporation. Poly FU inhibited even more strongly the DNA-primed synthesis of RNA. In the presence of 50 μg of

TABLE 4

EFFECT OF POLYMERS CONTAINING URACIL ANALOGS ON THE SYNTHESIS OF POLY A*

Polymer added	AMP incorporated (milliμmoles)
Poly U	10.7
Poly N-methyl U	0.1
Poly thio U	0.5
Poly FU	0.2
Poly UFU 1:1	6.8
Poly N-methyl U + poly U	10.1
Poly thio U + poly U	10.6
Poly FU (1 μg) + poly U	7.3
Poly FU (5 μg) + poly U	1.9
Poly FU (10 μg) + poly U	0.4

* Assay B with 10 μg of RNA polymerase. Unless otherwise stated 10 μg of polymer were added. Substrate, C¹⁴-ATP. Incubation, 10 min at 37°.

calf thymus DNA, addition of 1.1 μg of poly FU caused 90 per cent inhibition of RNA synthesis (Fig. 2).

Competition between polyribonucleotides and DNA: Inhibition by polyribonucleotides of the DNA-primed synthesis of RNA was not restricted to poly FU. As shown in Table 5, poly U (40 μg) inhibited 66 per cent. Inhibition by poly A and by the 1:1 poly A + poly U complex was much less pronounced. It is of interest to note that the poly C-primed synthesis of poly G was inhibited by DNA. Addition of an equal amount of DNA resulted in 56 per cent inhibition of GMP incorporation (Fig. 3).

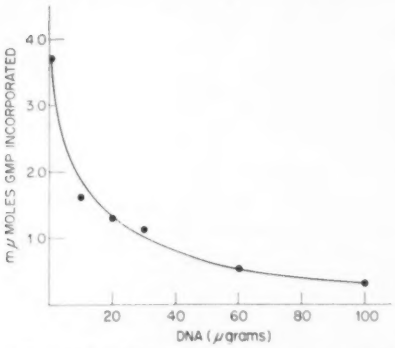

FIG. 3.—Inhibition of the poly C-primed synthesis of poly G by DNA. Each point on the curve represents an assay B incubation with 10 μg of poly C, 10 μg of RNA polymerase, and native calf thymus DNA as indicated. Labeled substrate, C^{14}-GTP. Incubation, 10 min at 37°.

Effect of actinomycin D: The antibiotic polypeptide actinomycin D has been shown to inhibit RNA polymerase *in vitro*[11, 12] and to produce almost complete inhibition of RNA synthesis *in vivo*.[12–15] It was therefore of interest to compare the effect of actinomycin D on RNA polymerase when primed by either DNA or polyribonucleotides. As seen in Table 6, actinomycin D was a very effective inhibitor of the DNA-primed reaction but it did not inhibit polyribonucleotide-primed synthesis or the synthesis of poly A or poly U which, to a relatively small extent, occurs in the presence of DNA.

Discussion.—The *Azotobacter* RNA polymerase used in this work was purified 500 fold and was approximately 90 per cent homogeneous in the ultracentrifuge. Sucrose gradient centrifugation of the preparation showed that both the DNA- and poly U-primed activities were associated with the protein having the sedimentation characteristic of the major component in the RNA polymerase preparation.[16] Although it is not possible to rule out conclusively the presence of separate enzymes with very similar properties, these results suggest that a single enzyme is involved. The demonstration that the polyribonucleotides inhibited the DNA-primed synthesis of RNA and, conversely, that DNA inhibited the polymer-primed reaction also suggests a single enzyme. A single enzyme is also strongly suggested by the fact that the ratio of activities with DNA or with poly A as primer remained con-

TABLE 5

EFFECT OF POLY U AND POLY A ON THE DNA-PRIMED SYNTHESIS OF RNA*

Polyribonucleotide added	C^{14}-GMP incorporated (milliμmoles)
None	5.2
Poly U (10 μg)	2.6
Poly U (20 μg)	2.4
Poly U (40 μg)	1.7
Poly A (10 μg)	4.2
Poly A (20 μg)	4.4
Poly A (40 μg)	4.3
Poly A + poly U (each 10 μg)	3.8

* DNA-primed reaction with 50 μg of native calf thymus DNA. Assay A with C^{14}-GTP as the labeled substrate and 10 μg of RNA polymerase. Incubation, 5 minutes at 37°.

TABLE 6

EFFECT OF ACTINOMYCIN D ON RNA POLYMERASE PRIMED BY DNA OR BY POLYRIBONUCLEOTIDES*

Primer	Substrate	Actinomycin (μmoles/liter)	C^{14}-nucleotide incorporated (milliμmoles)
DNA	C^{14}-ATP, UTP, GTP, CTP	...	5.6
		0.1	2.8
		1.0	1.0
DNA	C^{14}-ATP	...	2.2
		20.0	2.4
DNA	C^{14}-UTP	...	1.4
		20.0	1.3
Poly U	C^{14}-ATP	...	5.5
		25.0	5.3
Poly A	C^{14}-UTP	...	3.0
		25.0	2.0
Poly C	C^{14}-GTP	...	2.9
		25.0	3.1

* Assay A was used for the DNA-primed reactions (with 20 μg of native calf thymus DNA). Assay B was used for the polyribonucleotide-primed reactions with 10 μg of polymer. Samples contained 10 μg of RNA polymerase. Incubation, 10 min at 37°.

stant throughout purification.[16] The poor priming ability of TMV RNA suggests that RNA polymerase does not copy RNA *in vivo*. The ability to use polyribonucleotides as primers may only reflect a lack of specificity with regard to the primer. There also seems to be a lack of specificity with regard to the substrate for, in a dAT-primed reaction, RNA polymerase catalyzed the synthesis of a poly deoxy A ribo U copolymer when dATP and UTP were used as substrates.[16] This synthesis proceeded at a rate approximately 2 per cent that obtained with ATP and UTP as substrates.

Although with DNA the highly ordered, double stranded molecule is the primer of choice, the opposite appears to be true with respect to the polyribonucleotides. The ordered 1:1 poly A + poly U complex was a poor primer for AMP incorporation although still able to direct the synthesis of poly U. The highly ordered poly AU (alternating) showed no priming activity at all. In contrast, the random poly AU (1:1) which has only intermittent helical content[17] primed the incorporation of both AMP and UMP. Poly I, which probably exists as a triple stranded complex, was unable to prime the incorporation of CMP. Thus, native DNA which is highly ordered is an effective primer whereas the ordered polyribonucleotides tested do not prime. In this regard it is of interest to note that the 1:1 (by weight) poly A + oligodeoxy T complex primes equally well the synthesis of poly A and poly U.[16]

Poly FU was a very effective inhibitor of RNA polymerase, whether primed by DNA or by polyribonucleotides. The inhibition seems to be a consequence of the poly FU binding to the primer site on the enzyme. From the effect of poly FU on the DNA-primed reaction it is possible to calculate that from 30 to 40 molecules of RNA polymerase are bound per molecule of poly FU. The ability of the copolymer, poly UFU, to direct the incorporation of AMP suggests that long runs of FUMP are required for inhibition. In contrast to poly FU, actinomycin D which, as previously shown[11, 12] is a very potent inhibitor of the DNA-primed reaction, was virtually without effect on the reaction primed by polyribonucleotides. These results substantiate the conclusion[12] that actinomycin D acts by binding specifically to the DNA primer and not to the RNA polymerase.

Summary.– RNA polymerase, purified 500 fold from extracts of *Azotobacter vinelandii*, used polyribonucleotides (poly A, poly U, poly C) in addition to DNA as primers. Priming by homopolynucleotides directed the incorporation of the complementary nucleotides. There was competition between the various primers suggesting that a single enzyme is involved in the reactions studied. Poly fluorouridylate was an effective inhibitor of both the DNA- and polyribonucleotide-primed reactions but actinomycin D, which inhibits the reaction primed by DNA, had no appreciable effect on the polyribonucleotide-primed reaction.

* Aided by a grant from the National Institute of Arthritis and Metabolic Diseases (Grant A-1845) of the U.S. Public Health Service.

† Postdoctoral Fellow of the National Institutes of Health, U.S. Public Health Service.

[1] Hurwitz, J., A. Bresler, and R. Diringer, *Biochem. Biophys. Res. Comm.*, **3**, 15 (1960).

[2] Weiss, S. B., and T. Nakamoto, *J. Biol. Chem.*, **236**, PC 18 (1961).

[3] Stevens, A., *J. Biol. Chem.*, **236**, PC 43 (1961).

[4] Ochoa, S., D. P. Burma, H. Kröger, and J. D. Weill, these PROCEEDINGS, **47**, 670 (1961).

[5] Chamberlain, M., and P. Berg, these PROCEEDINGS, **48**, 81 (1962).

[6] The abbreviations used in this paper are: RNA and DNA, ribo- and deoxyribonucleic acid, respectively; TMV, tobacco mosaic virus; dAT, deoxyadenylate-thymidylate copolymer; ATP, GTP, UTP, and CTP, the 5′-triphosphates, and AMP, GMP, UMP, and CMP, the 5′-monophosphates, respectively, of adenosine (A), guanosine (G), uridine (U), and cytidine (C); ADP, adenosine 5′-diphosphate; dATP, deoxyadenosine 5′-triphosphate; Tris, tris(hydroxymethyl) aminomethane. In polynucleotide chains the capital letters A, G, U, C, T, I, and FU are used for the above nucleosides plus thymidine, inosine, and fluorouridine, respectively.

[7] Burma, D. P., H. Kröger, S. Ochoa, R. C. Warner, and J. D. Weill, these PROCEEDINGS, **47**, 749 (1961).

[8] Nakamoto, T., and S. B. Weiss, these PROCEEDINGS, **48**, 880 (1962).

[9] Krakow, J. S., and S. Ochoa, in *Methods in Enzymology* (New York: Academic Press), vol. 6 (in press).

[10] Furth, J. J., J. Hurwitz, and M. Goldmann, *Biochem. Biophys. Res. Comm.*, **4**, 431 (1961).

[11] Goldberg, I. H., and M. Rabinowitz, *Science*, **136**, 315 (1962).

[12] Hurwitz, J., J. J. Furth, M. Malamy, and M. Alexander, these PROCEEDINGS, **48**, 1222 (1962).

[13] Kirk, J. M., *Biochim. et Biophys. Acta*, **42**, 167 (1960).

[14] Reich, E., R. M. Franklin, A. J. Shatkin, and E. L. Tatum, *Science*, **134**, 556 (1961).

[15] Reich, E., R. M. Franklin, A. J. Shatkin, and E. L. Tatum, these PROCEEDINGS, **48**, 1238 (1962).

[16] Krakow, J. S., and S. Ochoa, unpublished results.

[17] Steiner, R. F., in R. F. Steiner and R. F. Beers, Jr., *Polynucleotides* (Amsterdam: Elsevier Publishing Company, 1961), p. 195.

---

*THE STRUCTURE OF THE DNA-ACRIDINE COMPLEX**

BY L. S. LERMAN†

DEPARTMENT OF BIOPHYSICS, UNIVERSITY OF COLORADO

Communicated by Theodore T. Puck, November 29, 1962

It has been proposed that acridines and related compounds bind to DNA by intercalation between normally neighboring base pairs in a plane perpendicular to the helix axis (Lerman, 1961); the space is provided by an extension and local untwisting of the helix. To test this hypothesis further, some other properties of the

DNA-acridine complex have been examined in dilute aqueous solution, including the orientation of the plane of the acridine and the effect of complexing on the orientation of the plane of the purines and pyrimidines, both with respect to the DNA helix axis. The results show that the bound acridine is more nearly perpendicular than tangent to the helix axis, and the perpendicularity of the base pairs to the helix axis is not significantly altered. In a separate study of the effect of complexing on the rates of diazotization of amino acidines, and the effect of complexing on the reactivity of purine and pyrimidine amino groups, it is also shown that the amino groups of amino acridines are relatively inaccessible within the complex, and hydrogen bonding between base pairs remains undisturbed (Lerman, 1963).

Experimental Methods.—Polarized fluorescence was measured at 90° to the incident beam in a conventional instrument constructed in this Department of Biophysics. Monochromatic polarized light was obtained from a tungsten or deuterium arc source by means of a Beckman DU monochromator fitted with a rotatable calcite Glan prism. The sample was examined at 25.0°C in either a 1 cm square fused silica cuvette or a fused silica capillary tube. The intensity of the emission was determined through an appropriate long wave-length pass filter and a calcite Glan-Thompson prism by a chilled, low-noise (EMI 9536) photomultiplier, operated as a photon counter. Flow of the DNA solution was effected by a synchronous motor-driven syringe. All measurements represent roughly 10^5 counts or more (about 100 × background), accumulated in one or more ten-second periods. Flow dichroism was measured in a Cary Model 14 spectrophotometer, using the Glan prism. The solution was driven through a short-path cuvette with planar silica windows, separated by 0.0271 cm, perpendicular to the light beam.

All measurements were carried out with chicken erythrocyte DNA isolated from washed nuclei by phenol extraction, similar to the method of Kirby (1958).

Recognition of the Acridine Plane.—If an array of stationary, randomly oriented fluorescent molecules is illuminated with suitable exciting radiation, the emitted light is polarized; that is, the emitted intensity observed through a polarizing prism will depend on the orientation of the prism. Although polarized emission is also observed when the exciting radiation is unpolarized, the degree of polarization of the emitted light is less. All of the following discussion and experimental results will refer to polarized excitation. Where emission is observed at right angles to the exciting beam, it is appropriate to compare intensities found when the analyzing prism is oriented perpendicular and parallel to this plane. When the exciting beam enters along the X axis, and emission is observed along the Y axis, the degree of polarization is given by the difference between the two intensities measured with the plane of polarization of the analyzing prism respectively parallel to Z and to X, divided by the sum of the same intensities. The probabilities of absorption and of emission with a particular polarization are proportional to the square of the cosine of the angle between the electric vector of the absorbed or emitted light and the direction of charge displacement, the transition moment, corresponding to the electronic transition responsible for absorption or emission. It can be shown that the Z intensity is greater and, consequently, the degree of polarization is positive, when the electronic transition moments for absorption and emission are more or less parallel; when they are more nearly perpendicular, the X intensity will be larger and the degree of polarization will be negative (Pringsheim, 1949). Since we shall be concerned only with singlet $\pi - \pi^*$ transitions, the transition moments for both absorption and emission will lie in the plane of the aromatic rings. It has been found, almost without exception, that the spectral distribution of emission from solutions of fluorescent substances is independent of the wavelength of excitation. Thus, the variation of the degree of polarization of emission with the wavelength of excitation corresponds to changes in direction only of the transition moment for excitation. The actual value of the degree of polarization may be taken to reflect the distribution of excitation probabilities between two or more different transitions that can be excited by the same wavelength (Albrecht, 1960). If the fluorescent molecules are allowed to rotate instead of remaining stationary during the interval between absorption and emission, the observed polarization will either disappear or be diminished depending upon the extent of randomization. In sufficiently concentrated solution, the emission may also be depolarized by migration of the excitation to nearby similar molecules. Polarization spectra for dilute solutions of the acridine deriva-

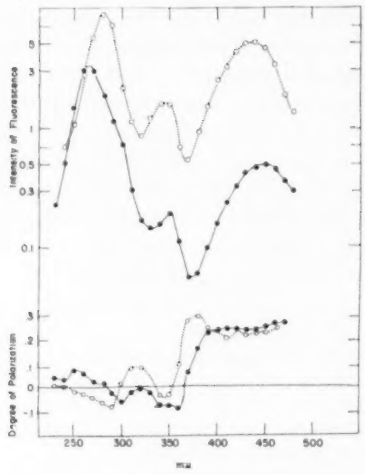

FIG. 1.—Excitation and polarization spectra for quinacrine in sucrose and DNA solution. The upper curves show the relative fluorescence intensities per unit concentration as a function of the wavelength of excitation, uncorrected for the energy distribution in the exciting radiation, for dilute solutions of quinacrine in DNA (solid line) and in 60% sucrose (dotted line). The lower curves show the degree of polarization of the 90° emission at each wavelength. The DNA concentration was about 3.6×10^{-4} *M* in nucleotides. The quinacrine was 2.65×10^{-6} *M* in the DNA solution, corresponding to one dye molecule per 68 nucleotide pairs. In the sucrose solution, the quinacrine was 1.51×10^{-7} *M*.

tive, quinacrine (Atebrin), are shown in Figure 1, together with the corresponding excitation spectra, uncorrected for the energy distribution of the exciting source. Although almost no polarization is observed in simple aqueous solutions, substantial polarization is observed in DNA solution because nearly all of the quinacrine is tightly bound, and DNA, by virtue of its molecular weight and configuration, is characterized by an exceedingly small rotational diffusion constant. (Similarly, the viscosity of a concentrated sucrose solution is sufficient to prevent a large rotational depolarization in the absence of DNA.) It will be noted that the long wave excitation maximum is shifted to somewhat longer wavelengths by attachment to DNA, as is found for the absorption maximum of proflavine (Peacocke and Skerrett, 1956) and other acridines (Mortland *et al.*, 1954). Although the fluorescence yield is generally much less for the bound than the free dye, a relatively increased emission probability can also be seen in the region of ultraviolet absorption by DNA. This presumably corresponds to sensitization of fluorescence and will be treated in a separate communication. From these data the wavelengths of 450 mμ and 300 mμ were selected as providing adequate fluorescence intensities with parallel (∥) and perpendicular (⊥) pairs of transition moments. The directions of these transitions serve to specify the plane of the molecule.

The Effect of Flow.—It will be useful to consider a simplified scheme in which the transition moments for absorption and emission must lie either parallel or perpendicular to the flow axis, and the DNA molecule is assumed to be fully oriented with the helix axis parallel to the flow axis, and randomly rotated around the flow axis. Let us also restrict our attention to just two pairs of prism orientations—both prisms vertical, parallel to flow, and both horizontal, perpendicular to flow.

There are then three ways in which an acridine might be attached to the DNA helix, as indicated by types TL, TS, and P in Table 1 and Figure 2, and a set of four experimental predictions for each. The experimental measurement consists in the comparison of the fluorescence intensities of the flowing and stationary solution, given simply by the relative difference in intensities obtained when the DNA is oriented by flow and when its orientation is random. If a particular transition is that rendered parallel to the relevant prism orientation, the probability of observing transition will increase from the average value for random orientation to the maximum value; if the transition is rendered perpendicular to the prism orientation, it will not be observed at all. It will be seen that where one transition for either absorption or emission is parallel to a prism and the other is perpendicular, the product of the absorption and emission probabilities nevertheless equals zero.

TABLE 1

THE EXPECTED EFFECTS OF FLOW ORIENTATION ON POLARIZED TRANSITION PROBABILITIES ACCORDING TO THE BINDING ARRANGEMENT

		TL	TS	P
	A. Orientation with respect to the helix axis			
1.	type of arrangement	TL	TS	P
2.	plane of dye	tangent	tangent	perpendicular
3.	emission transition	perpendicular	parallel	perpendicular
4.	∥ absorption transition	perpendicular	parallel	perpendicular
5.	⊥ absorption transition	parallel	perpendicular	perpendicular
	B. Difference in intensities, (flow oriented) − (random); both prisms parallel to flow			
6.	absorption only, ∥ transition	−	+	−
7.	absorption only, ⊥ transition	+	−	−
8.	emission only, assuming equal excitation	−	+	−
9.	emission from ∥ absorption	−	+	−
10.	emission from ⊥ absorption	−	−	−
	C. Difference in intensities, (flow oriented) − (random); both prisms perpendicular to flow			
11.	absorption only, ∥ transition	+	−	+
12.	absorption only, ⊥ transition	−	+	+
13.	emission only, assuming equal excitation	+	−	+
14.	emission from ∥ absorption	+	−	+
15.	emission from ⊥ absorption	−	−	+

The signs, + and −, signify that the flow oriented intensity is either greater or less, respectively, than the intensity for nonoriented molecules. If perfect orientation were achieved (infinitely great shear, etc.), all of the − values would approach zero. Lines 6, 7, 11, and 12 indicate changes that can, in principle, be observed as dichroism due to flow. Lines 9, 10, 14, and 15 indicate the net changes due to the product of the absorption and emission probabilities that would be expected in the fluorescence.

Since the functions are nonlinear, the effect of the decline will usually prevail when orientation is incomplete, and a net decrease in intensity will be observed.

Since the DNA molecule in solution appears to be a statistical coil of limited flexibility, only partial orientation can be expected, and the change in intensities induced by flow will be much less marked than the simplified theory predicts. A qualitative interpretation of the experimental results is possible, however, in terms of the direction of each intensity change induced by flow for each transition at each pair of prism orientations, together with an estimate of the degree of orientation of the DNA. Experimental results for quinacrine, presented in Table 2, should be compared with the expectations presented in lines 9, 10, 14, and 15 of Table 1 for the three hypothetical orientations. Since both intensities decrease during flow when the prisms are parallel to flow and both increase when the prisms are perpendicular, the data are compatible only with arrangement P. The extent of orientation indicated here, about 0.3, is substantially greater than the extent of orientation indicated in the flow dichroism studies discussed below and those of Cavalieri *et al.* (1956), for comparable DNA concentrations. However, both measurements agree when account is taken of the differences in geometry and the form of the functions averaged in the two types of measurement.

TABLE 2

FRACTIONAL CHANGE DUE TO FLOW IN THE FLUORESCENCE OF QUINACRINE BOUND TO DNA

Polarization of emission	X	X	Z	Z
Wavelength of excitation	3000	4500	3000	4500 Å
Exciting radiation Y polarized	+0.24	+0.35	−0.12	−0.11
Exciting radiation Z polarized	−0.10	−0.10	−0.26	−0.29

The DNA (as nucleotides) and total quinacrine concentrations were $3.76 \times 10^{-4} M$ and $5.5 \times 10^{-6} M$, respectively, corresponding to one quinacrine molecule per 34 nucleotide pairs. The shear rate during flow (at the walls of the capillary) was about 1.2×10^{4} sec^{-1}. The X and Y polarizations are perpendicular to flow; Z is parallel to flow. The transitions excited at 4,500 Å and 3,000 Å are parallel and perpendicular, respectively, to the transition of emission.

Since the longest wavelength of excitation always corresponds to the same electronic transition as that responsible for emission, it will be possible in general to establish the angle between this transition and the helix axis for any fluorescent molecule that binds to DNA. Perpendicular transitions, however, are not always available at useful intensities, so that complete specification of the orientation of the plane containing the dye is not always possible. For substances having a positively polarized band with a substantially lower degree of polarization than the longest wave-length absorption, the calculation can also be made on the assumption that the lower degree of polarization results from transitions in more than one direction in the plane of the molecule. Acridine yellow, the most powerful mutagen studied by Orgel and Brenner (1961), provides a band at 305 mμ with degree of polarization, 0.10, when bound to DNA, as well as the long wave band in the region of 460 mμ with degree of polarization, 0.35. In flow experiments with acridine yellow like those described above, the fluorescence intensities resulting from excitation of either band again change by the same amount, and in the same directions as found for quinacrine. Since the perpendicular contribution to short wave-length excitation is of course much less, the precision with which the plane can be specified is correspondingly diminished, but the conclusion remains the same; the dye must be nearly perpendicular to the helix axis.

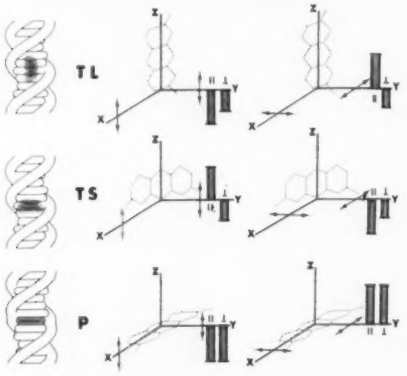

FIG. 2.—Three conjectures for the orientation of acridine bound to DNA. Each arrangement is identified similarly in Table 1. The bar graphs on each set of coordinate axes represent qualitatively the expected change in intensity of fluorescence when the DNA is itself oriented by flow along the Z axis. It is assumed that a beam of monochromatic light along the X axis, polarized as shown in each diagram, is absorbed by a transition in either the long or short axis of the molecule, according to its wavelength, and that the emitting transition is along the short axis. The light emitted in the Y direction is measured through a polarizing prism, directed as shown. The change corresponding to short axis excitation is identified as $\parallel$, and to long axis excitation, as $\perp$. (The acridine skeleton in the figure is that of proflavin.)

Orientation of the Plane of the Base Pairs.—The similarity of the configuration of pure, undenatured DNA in solution to the B structure found in fibers at relatively high humidity is usually accepted on the basis of two kinds of evidence: the continuous swelling of fibers at very high humidities, approaching the dissolved state, without any indication of an abrupt structural transition, and the determinations of mass per unit length and helix radius by low-angle X-ray scattering from liquid crystals and concentrated solutions of DNA (Luzzati *et al.*, 1961a). On this assumption the ambiguity of flow dichroism measurements on simple DNA solutions is resolved, and the determinations can be taken to signify only the extent to which the helix is oriented by flow, rather than the inseparable combination of helix orientation and base pair tilt. The question of tilting of the base pairs is again of interest with respect to the DNA-acridine complex, since strong tilting would lower the mass per unit length enough to allow for a net decrease even after the mass of the bound acridines is added (Lerman, 1961). Since the amount of tilting required,

roughly 45°, abolishes the dichroism of the helix in stretched DNA fibers (Wilkins *et al.*, 1951), the measurement of the flow dichroism of the DNA-acridine complex can be expected to respond sensitively if this structural change is involved in formation of the complex. If, on the other hand, the intercalation hypothesis is more nearly correct, the DNA dichroism should be about the same in the complex as in the pure state, or even somewhat greater because of the straightening of the helix indicated by the viscosity enhancement at low rates of shear (Lerman, 1961). Flow dichroism measurements on DNA and complexes with quinacrine are presented in Table 3. Similar results have also been obtained with proflavine. Dichroism is given as the fractional change in absorbance due to flow, with the polarizing prism either parallel or perpendicular to the flow axis. It should be noted that the geometry is different than that of the flow fluorescence experiments; the flow is between parallel planes (the windows of the cuvette) rather than through a tube of circular cross section. Light will be absorbed in these solutions both by the complex and by unattached quinacrine, which will not contribute to the flow dichroism. Since it was desirable to approach saturation of the binding sites, the concentration of free quinacrine is considerable, and accordingly, it is necessary to deduct its contribution to the absorbance of the solution for correct estimation of the dichroism of the complex. For this purpose, the concentration of bound quinacrine was calculated from the ultraviolet absorption spectra, which differ significantly for the free and bound dye. The dichroism at long wavelengths, due entirely to the dye, will directly indicate the contribution of the dye to the dichroism at 2600 Å, since both transitions are in the plane of the rings. Since the dye accounts for only 0.34 of the absorbance of the complex at 2600 Å, the dichroism due to DNA in the complex must be very nearly the same as that of the dye.

TABLE 3

FLOW DICHROISM OF DNA AND DNA-QUINACRINE

Wavelength	2600	4325	4550 Å
DNA only			
Dichroism, Z polarization	−0.19		
Dichroism, Y polarization	+0.086		
DNA-quinacrine			
Dichroism, Z polarization	−0.24	−0.25	−0.24
Dichroism, Y polarization	+0.11	+0.12	+0.11
Absorbance, DNA contribution	0.654	0.000	0.000
Absorbance, DNA plus bound quinacrine	0.989	0.106	0.100
Absorbance, total	1.422	0.240	0.213

The dichroism is tabulated as the fractional change in absorbance of the DNA or the DNA-quinacrine complex when the solution is subjected to flow. The shear rate at the windows was 1.18×10^4 sec^{-1}. The absorbances in the stationary solution show the distribution of absorption between DNA, bound quinacrine, and the unattached dye. The DNA concentration (as nucleotides) when measured alone was 3.2×10^{-3} *M*, and in the complex, 3.6×10^{-3} *M*. The quinacrine bound to DNA was 0.661×10^{-3} *M*, or one quinacrine molecule per 2.7 nucleotide pairs. The Y and Z axes are perpendicular and parallel, respectively, to the direction of flow.

Thus, all strongly tilted models are excluded since DNA is more, rather than less, dichroic in the complex than alone. Also, the close similarity of the dichroism values for the quinacrine and the DNA itself demonstrates that the plane of the purine and pyrimidine pairs must be parallel to the direction of the long wave-length transition of the quinacrine. In view of the preceding considerations, the planes of both must be parallel.

Structure of the Complex.—The fluorescence and dichroism results require that

both the base pairs and the acridine lie substantially perpendicular to the molecular axis, but do not necessarily specify the intercalated configuration. The additional restriction that the mass per unit length of the complex is less than that of DNA alone (Luzzati *et al.*, 1961*b*, Lerman, 1961) is in agreement with the properties of the intercalated model; it could be reconciled with arrangements based on external edgewise attachment of the acridine by the *ad hoc* supposition that gaps, filled with solvent, are generated in the stack of base pairs. Roughly one such gap, the thickness of a base pair, would be required for each acridine bound, so that at the saturation region for strong binding of proflavine there would be a gap for every two base pairs. This model is, of course, energetically highly implausible, and the supposition of an almost totally aqueous environment for the acridine is incompatible with the properties of the complex as determined by reaction rate studies (Lerman, 1963). The comparison of the rates of diazotization of the amino groups of proflavine and other acridines when bound to DNA and free in solution shows a severe restriction on the accessibility of the amino groups to attack by the nitrosating reagents. This restriction is not found when the amino acridines are bound to other anionic polymers, even where there is a broad aromatic moiety for face to face contact with acridine. The intercalated structure remains as the only hypothesis fully compatible with the diverse experimental evidence.

A Conjectural Mechanism for Mutagenesis.—A mechanism based on the intercalation of an acridine into a single strand of the DNA molecule, as proposed by Brenner *et al.* (1961) for generating insertion and deletion mutations during DNA synthesis, demands a somewhat different structural basis than the model proposed here, in order to accommodate the pairing of an extended strand containing the acridine with a nonextended strand containing one additional base. It has seemed more useful to consider whether a mechanism might be devised on the basis of the simple intercalated model, and taking into account also some of the other characteristic properties of acridine mutagenesis. Aside from the presumably irrelevant induction of mutations by photodynamic action of the acridines, it appears clear that there is a potent mutagenic effect in the reproduction of the T-even phages, and that there is no significant mutagenic effect on *Escherichia coli* during vegetative growth (as shown by our own observations and other investigators). There are at least two differences between the multiplication of bacteria and the multiplication of phage; the phage DNA contains hydroxymethyl cytosine instead of cytosine, and phage multiplication is accompanied by extensive genetic recombination. It is difficult to attribute any particular significance to the presence of the substituted cytosine that might be relevant to the acridine effect. (We have observed the usual viscosity enhancement in T2 DNA mixed with proflavine.) However, it is easy to attribute a role in mutagenesis to the frequent recombinatorial events that accompany phage multiplication.

Let us suppose that recombination takes place within a short region of the chromosome corresponding to the effective pairing, or switch, region, and that a few acridine molecules are intercalated at random in one or both of the paired chromosomes. Since the length along the chromosome occupied by an acridine is the same as the length required by a base pair (3.4 Å), wherever there is an intercalation in one of the chromosomes without intercalation at exactly the same place in the other, the pairing will be shifted exactly one step out of register at one side

of the site of intercalation. If the chromosomes are paired in perfect homology below the site of intercalation, the chromosome containing the acridine will offer the base pair corresponding to the next earliest neighbor to the other for pairing above the site of intercalation. After any interval in which the same number of acridines are intercalated into both chromosomes they will return to perfect homology. Within the interval they can be one, two, or more steps out of register in either direction. If the chromosomes break at the same position, side by side, and reunite with the exchange of partners, it will be seen that the reunion will result in the omission of one or more base pairs in one product and the corresponding duplication of one or more base pairs in the other product of the reunion. This mechanism thus has the property of generating insertion and deletion mutations, as required in the analysis of the interactions of suppressor mutations by Crick and collaborators (1961), and will be dependent on the frequency of crossing-over. Mutants will be expected to be recombinant for closely linked outside markers. The same process, crossing-over between paired chromosomes that are displaced from perfect homology by one, or a few, nucleotide pairs, could also be expected to occur spontaneously with the same results. It has been suggested (Fresco, personal comm., 1960) that the spontaneous process proceeds through the formation of short loops of one or more nucleotides excluded from the double helix, as suggested by the stoichiometry pairing of synthetic polynucleotides (Fresco and Alberts, 1960). The occurrence of recombination errors during meiotic division could account for the increased rate of spontaneous mutation found by Magni and Von Borstel (1962) in ascospores as compared with the mutation rate during vegetative growth of yeast. A formal mechanism for spontaneous mutation by unequal crossing-over has also been advanced independently by Demerec (1962).

Summary.—New physical evidence is presented bearing on the structure of the DNA-acridine complex. The results are fully compatible with the intercalated model, and incompatible with other plausible models. A mechanism based on recombination errors is proposed for the production of insertion and deletion mutations by intercalation of acridines.

I should like to acknowledge the assistance of Mr. James Levy in the preparation of DNA, and the help of Mr. James McIntyre with the flow dichroism measurements.

* Contribution No. 202 from the Department of Biophysics, Florence R. Sabin Laboratories, University of Colorado Medical Center, Denver, Colorado. This work was supported by a Research Grant (GM 08894) from the National Institutes of Health. Acquisition of the Cary spectrophotometer was made possible by a grant from the National Science Foundation.

† Research Career Development Awardee of the U.S. Public Health Service.

Albrecht, A. C., *J. Mol. Spec.*, **6**, 84 (1961).
Brenner, S., L. Barnett, F. H. C. Crick, and A. Orgel, *J. Mol. Biol.*, **3**, 121 (1961).
Cavalieri, L. F., B. H. Rosenberg, and M. Rosoff, *J. Am. Chem. Soc.*, **78**, 5235 (1956).
Crick, F. H. C., L. Barnett, S. Brenner, and R. J. Watts-Tobin, *Nature*, **192**, 1227 (1961).
Demerec, M., these PROCEEDINGS, **48**, 1696 (1962).
Fresco, J. R., and B. M. Alberts, these PROCEEDINGS, **46**, 311 (1960).
Kirby, K. S., *Biochem. J.*, **70**, 260 (1958).
Lerman, L. S., *J. Mol. Biol.*, **3**, 18 (1961).
Lerman, L. S., (1963) in preparation.
Luzzati, V., A. Nicolaieff, and F. Masson, *J. Mol. Biol.*, **3**, 185 (1961a).
Luzzati, V., F. Masson, and L. S. Lerman, *J. Mol. Biol.*, **3**, 634 (1961b).
Magni, G. E., and R. C. Von Borstel, *Genetics*, **47**, 1097 (1962).

Morthland, F. W., P. P. H. DeBruyn, and N. H. Smith, *Exp. Cell Res.*, **7**, 201 (1954).
Orgel, A., and S. Brenner, *J. Mol. Biol.*, **3**, 762 (1961).
Peacocke, A. R., and J. N. H. Skerrett, *Trans. Far. Soc.*, **52**, 261 (1956).
Pringsheim, P., *Fluorescence and Phosphorescence* (New York: Interscience, 1949)
Wilkins, M. H. F., R. G. Gosling, and W. E. Seeds, *Nature*, **167**, 759 (1951).

*CHANGES IN THE DISTRIBUTION OF POLYMERASE ACTIVITY DURING DNA SYNTHESIS IN MOUSE FIBROBLASTS**

BY JOHN W. LITTLEFIELD, ALICE P. MCGOVERN, AND KATHARINE B. MARGESON

THE JOHN COLLINS WARREN LABORATORIES OF THE HUNTINGTON MEMORIAL HOSPITAL OF HARVARD UNIVERSITY AT THE MASSACHUSETTS GENERAL HOSPITAL, BOSTON

Communicated by J. C. Aub, December 6, 1962

The availability of partially synchronized cultures of mammalian cell lines[1, 2] provides a new opportunity to investigate the control of DNA synthesis in the cells of higher organisms, which should supplement the extensive studies with lower forms.[3] In this paper will be described the extent and timing of DNA synthesis in mouse fibroblasts (L cells) partially synchronized with 5-fluorodeoxyuridine[4] as well as changes in the intracellular distribution of DNA polymerase activity which suggest that the particulate polymerase may be of more importance than recognized previously. During the course of this work, we learned that results similar to ours have been obtained by Gold and Helleiner.[5] Recently, Billen has described a polymerase-DNA complex in *E. coli*.[6]

Experimental.—L cells were grown in suspension as described previously.[4] Cell counts were obtained with the Coulter electronic counter model A; after preliminary studies an aperture current setting of 3 and threshold of 20 were used routinely. Such cell counts averaged 6 per cent greater than simultaneous chamber counts.[7]

The rate of incorporation of hypoxanthine-8-C^{14} (California Corporation for Biochemical Research) into DNA was determined by incubation of duplicate 1 ml aliquots of the suspension culture with a saturating concentration of hypoxanthine-8-C^{14} (3.7×10^{-5} *M*; 7.6 μc per μM) for 1 hr at 37°C in a Dubnoff shaker. Then the cells were diluted with 4 ml of cold 0.14 *M* NaCl solution and collected by centrifugation; the acid-soluble material was extracted with cold 5 per cent trichloroacetic acid and the residue digested with *N* NaOH for 16 hr at 37°C to hydrolyze RNA. After cooling, DNA and protein were precipitated with acid, collected by filtration on a cellulose filter (Millipore Filter Corporation; type AA filter with pore size 0.8 μ), washed four times by filtration of 5 ml of cold 5 per cent trichloroacetic acid, and assayed for radioactivity as described previously for thymidine-2-C^{14}.[4] All samples were counted to less than 5 per cent error. Essentially all incorporated radioactivity became acid-soluble if the cells were treated with 5 per cent trichloroacetic acid at 90°C for 20 min.

For the usual assay of DNA polymerase activity, 3×10^6 cells were collected by centrifugation, suspended by agitation in 1 ml of cold buffer containing 0.1 *M* KCl and 0.02 *M* tris(hydroxymethyl)aminomethane (pH 7.4), and transferred to a small cellulose test tube. After centrifugation at 4°C, the cells were suspended in 100 μl of cold 0.02 *M* tris(hydroxymethyl)aminomethane (pH 7.4), disrupted by vibration at 10 kc per sec for 2 min in a Raytheon Model DF 101 sonic oscillator, and separated into a supernatant fraction and a pellet by centrifugation at about $6{,}000 \times g$ for 30 min at 4°C. In this paper, the pellet will be referred to as the particulate fraction, although it is recognized that its components have been altered by sonic oscillation. The particulate fraction was washed once with cold 0.02 *M* tris(hydroxymethyl)aminomethane and suspended in 50 μl of the same buffer. The concentration of protein in each fraction was deter-

mined.[8] The incubation mixture (total volume 25 μl) contained: 10 μl of either fraction (25 to 75 μg of protein), as well as ATP 5×10^{-3} *M*; d-ATP, d-CTP, and TTP, each 1.35×10^{-4} *M*; d-GTP-8-C^{14} (3 μc per μM), 4×10^{-5} *M*; $MgCl_2$, 5×10^{-3} *M*; tris(hydroxymethyl)aminomethane, 2×10^{-2} *M* (pH 7.4); and 200 μg per ml of DNA (Worthington Biochemical Corporation) which had been heated at 100°C for 5 min and rapidly cooled. After incubation for 1 hr at 37°C, 5 ml of cold 5 per cent trichloroacetic acid were added to the incubation mixture, and the resulting precipitate was collected on a cellulose filter, washed with cold acid four times, and assayed for radioactivity as described above. 0.1 μg of C^{14}-DNA could be quantitatively recovered on the filter under these conditions, even in the absence of protein.

Essentially no radioactivity was incorporated if the incubation mixture containing the supernatant fraction was held at 0°C or if DNA or enzyme was omitted. A higher concentration of DNA, ATP, or the deoxyriboside triphosphates did not increase the incorporation, nor was it increased by the addition of albumin, KCl, mercaptoethanol, or ethylene-diamine tetraacetate to the cells before disruption or to the incubation mixture. The rate of incorporation was constant for at least 60 min. Over the range of protein concentration used, incorporation was proportional to protein concentration. Polymerase activity did not decline if cells were kept in culture medium at 4°C for 24 hr prior to disruption; the activity of cell-free extracts stored at 0 or −20°C declined after 24 hr. The polymerase activities in Figure 3 and Table 1 represent the average of determinations on fractions from duplicate aliquots of cells.

d-GTP-8-C^{14} was synthesized enzymatically from d-GMP-8-C^{14} (Schwarz BioResearch, Inc.)[9] and separated from the other components of the reaction mixture by paper electrophoresis at pH 3.0.

Results.—Extent and timing of DNA synthesis: The increases in the number of cells and in the amount of DNA per ml during partially synchronized growth of L cells in suspension culture are shown in Figure 1. In three such experiments, approximately 15 per cent of the inoculated cells divided during the first 15 or 16 hr after addition of 5-fluorodeoxyuridine, and the remaining 85 per cent divided after release with thymidine at 15 or 16 hr, mainly between 24 and 32 hr. Other experiments have indicated that delay beyond 16 hr before adding thymidine leads to decreased cell viability, as reported previously for HeLa cells[2, 10] and that concentrations of 5-fluorodeoxyuridine or thymidine other than those used in the experiment shown in Figure 1 or the inclusion of deoxycytidine (2×10^{-5} *M*)[11] did not improve the degree of synchrony.

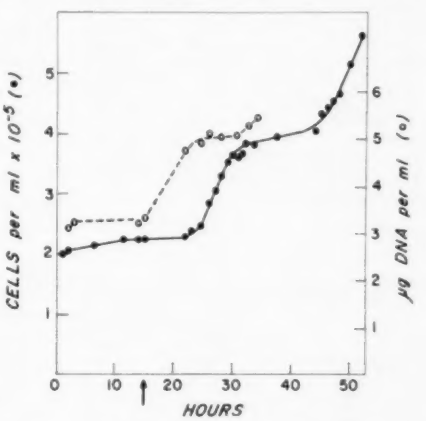

FIG. 1.—Increase in the number of cells and amount of DNA per ml in a partially synchronized culture. To begin the experiment, a logarithmically growing culture was diluted from 7.3×10^5 to 2×10^6 cells per ml with fresh medium at 37°C containing 10^{-6} *M* 5-fluorodeoxyuridine. 0.01 volume of 4.1×10^{-3} *M* thymidine was added at 15 hr (arrow). DNA was assayed fluorometrically on quadruplicate aliquots as previously.[4]

In three experiments exemplified by that shown in Figure 1, the content of DNA per cell averaged 15.4 $\mu\mu$g at the time of addition of 5-fluorodeoxyuridine, 14.8 $\mu\mu$g when thymidine was added, and 20.5 $\mu\mu$g just before cell division. If the amount of DNA present during this division (e.g., at 27 hr in Fig. 1) was regarded as the basal amount for the number of cells present after division (e.g., at 37.5 hr in Fig. 1), the basal amount of DNA per cell

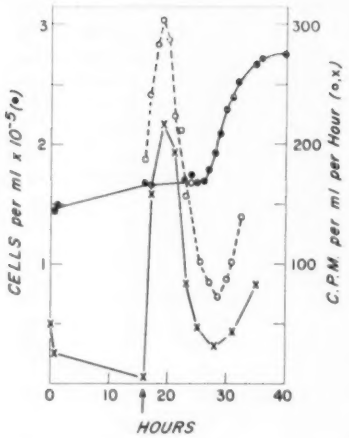

FIG. 2.—Rates of DNA synthesis per ml per hr in a partially synchronized culture. To begin the experiment, a logarithmically growing culture was diluted from 3.8×10^5 to 1.45×10^5 cells per ml with fresh medium at 37°C containing 10^{-6} *M* 5-fluorodeoxyuridine. 0.01 volume of 4.1×10^{-3} *M* thymidine was added at 16 hr (arrow). At the times indicated (×), duplicate 1 ml aliquots were incubated separately for 1 hr with hypoxanthine-8-C^{14} and the radioactivity incorporated into alkali-resistant acid-insoluble material determined (see *Experimental*). Also shown are the rates of DNA synthesis in another culture (○) in which the aliquots (already containing 4.1×10^{-5} *M* thymidine) were incubated with 0.1 volume of 4.1×10^{-4} *M* thymidine-2-C^{14} (6.4 μc per μM) as previously.[4] In this case, the rate at 16 hr represents the first hour after release, rather than before, as with hypoxanthine-8-C^{14}.

averaged 12.9 $\mu\mu$g. Therefore, the logarithmically growing and nonsynchronized cells to which 5-fluorodeoxyuridine was added contained *on the average* 1.2 times the basal amount.[12] Those cells which divided before thymidine release presumably had completed most or all of their DNA synthesis before 5-fluorodeoxyuridine was added.

In Figure 2 are shown for such a culture the rates of DNA synthesis per hr, determined by incubation of aliquots with hypoxanthine-8-C^{14} and subsequent analysis of radioactivity incorporated into alkali-resistant, acid-insoluble material (see *Experimental*). Also shown in Figure 2 are the rates of incorporation into DNA of thymidine-2-C^{14} in a similar culture; in this case, the rate at 16 hr represents the rate for the first hour after release, rather than before, as with hypoxanthine-8-C^{14}. Similar findings have been reported recently by Paul and Hagiwara.[13]

An increasing rate of DNA synthesis over the three hr subsequent to thymidine release, such as that shown in Figure 2, has been studied in HeLa cells by Mueller and co-workers, who have demonstrated that almost all the cells show this increasing rate of synthesis, that it correlates with synthesis at specific chromosomal sites, and that it can be prevented by puromycin.[14, 15]

Changes in DNA polymerase activity: The DNA polymerase activity of the supernatant and particulate fractions of the cell (6,000 × *g*

TABLE 1
CHANGES IN POLYMERASE ACTIVITY FROM BEFORE TO THREE HOURS AFTER THYMIDINE RELEASE

	Supernatant Fraction — cpm in DNA/μg of protein			Particulate Fraction — cpm in DNA/μg of protein		
Experiment	Before release	After release	Per cent change	Before release	After release	Per cent change
1	1.86	1.19	−36	—	—	—
2	2.34	1.23	−47	—	—	—
3	1.53	1.46	−5	—	—	—
4	1.54	1.18	−23	—	—	—
5	2.12	1.64	−23	0.27	0.32	+19
6	1.80	1.76	−2	0.21	0.25	+19
7	2.04	1.42	−30	0.31	0.44	+42
8	1.46	1.61	+10	0.43	0.44	+2
9	2.31	1.22	−47	0.34	0.34	0
10	2.23	1.37	−39	0.35	0.50	+43
11	1.22	1.37	+12	0.33	0.40	+21
Mean	1.86	1.40	−21	0.32	0.38	+21
$S.E._{mean}$			±6.5			±6.4

for 30 min) was examined in cells collected before, during, and after the period of DNA synthesis. In 11 consecutive similar experiments, the supernatant fraction showed an average drop in polymerase activity of 21 per cent from just before thymidine release to three hr afterwards (Table 1). This drop is significant (Student's t test yields $0.001 < P_{n=10} < 0.01$). During the same interval, the average content of protein per cell rose 14 per cent; therefore, a decreased synthesis of polymerase might be responsible for the drop in specific activity. However, three experiments in which consecutive samples were assayed indicated a prompt return to the original specific activity after completion of DNA synthesis (Fig. 3).

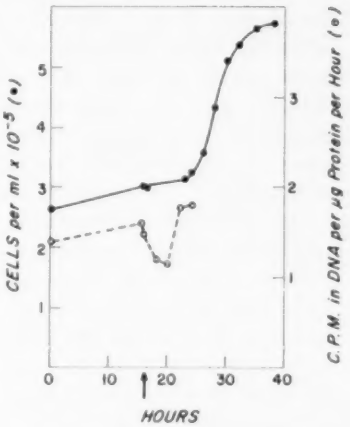

FIG. 3.—Change in DNA polymerase activity in the supernatant fraction of partially synchronized cells. To begin the experiment, a logarithmically growing culture was diluted from 4.5×10^5 to 2.6×10^5 cells per ml with fresh medium at 37°C containing 10^{-6} M 5-fluorodeoxyuridine. 0.01 volume of 4.1×10^{-3} M thymidine was added at 16 hr (arrow). At the times indicated, duplicate aliquots of cells were removed and kept at 4°C for about 24 hr. Then the cells were disrupted and centrifuged, and polymerase activity in the supernatant fractions was determined and averaged (see *Experimental*).

As shown for other cells by previous workers,[16, 17] the particulate fraction was less active than the supernatant fraction (Table 1). Before release, the particulate fraction contained an average of 11 per cent of the cell polymerase activity, as well as 42 per cent of the protein and about 60 per cent of the DNA. Nonetheless, in seven experiments an average increase of 21 per cent in the polymerase activity of the particulate fraction occurred from just before to three hr after release (Table 1). This rise is almost as significant as the decrease in supernatant activity above (Student's t test yields $0.01 < P_{n=6} < 0.02$). In these experiments, the average absolute increase in particulate activity was 9 per cent of the decrease in supernatant activity.

It seemed possible that the rise in particulate polymerase activity was due to residual intact cells or nuclei, which would have increased in activity as shown in Figure 2. Microscopic examination indicated that after disruption an average of 0.05 per cent of the cells remained intact. The nuclei of about 0.2 per cent more of the original cells were recognizable, although distorted. If whole cells and nuclei incorporated d-GTP-8-C^{14} as well as hypoxanthine-8-C^{14}, residual contamination of this magnitude could have accounted for about 5 per cent of the average particulate activity observed. In fact, when tested in the polymerase assay, whole cells incorporated d-GTP-8-C^{14} at about 25 per cent of the rate of incorporation of hypoxanthine. Furthermore, added DNA was not required for incorporation by whole cells, as it was for incorporation by the supernatant or particulate fractions.

Discussion.—In contrast to the intranuclear location of DNA, the studies of Bollum and Potter[16] and Smellie and co-workers[17, 18] have shown that most of the DNA polymerase activity of various mammalian cells is in the soluble fraction of the cell. The present experiments, with those of Gold and Helleiner,[5] indicate

that during DNA synthesis in L cells which are partially synchronized a decrease occurs in the polymerase activity of the supernatant fraction, while an increase usually occurs in particulate activity. These changes might be unrelated; the latter might represent the facilitation, for some reason, of polymerase enzyme already present prior to DNA synthesis in organized subnuclear particles. A more plausible interpretation is that supernatant polymerase enzyme becomes particulate at the time of DNA synthesis and that very likely it is the latter form which is active in the cell. Admittedly, the increase in particulate activity accounted for only 9 per cent of the decrease in supernatant activity. However, studies with certain other systems indicate that an enzyme when particulate may appear less active than when it is soluble.[19-22] Indeed, if the above reasoning is correct, the fact that the average per cent decrease in supernatant activity and increase in particulate activity were the same suggests that the amount of polymerase enzyme protein in these fractions may be similar. If so, the evidence that 11 per cent of the cell polymerase activity was particulate and that the increase in particulate activity accounted for only 9 per cent of the decrease in supernatant activity suggests that, in terms of the usual assay conditions, the enzyme was about 10 per cent as active when particulate as when it was in the supernatant fraction.

Summary.—When suspension cultures of mouse fibroblasts were partially synchronized with 5-fluorodeoxyuridine, DNA synthesis was most active three hr after release of the 5-fluorodeoxyuridine block with thymidine. DNA polymerase activity in the supernatant fraction of the cell decreased 21 per cent from just before thymidine release to three hr after release. During the same period, polymerase activity in the particulate fraction increased 21 per cent, although the absolute amount of increase accounted for only 9 per cent of the decrease in supernatant activity. These results suggest that at the time of DNA synthesis supernatant polymerase became particulate and less active in terms of the usual assay conditions.

The authors are grateful to Paul C. Zamecnik for his interest and encouragement and to Nancy L. R. Bucher and Jesse F. Scott for helpful discussions and critical review of the manuscript.

* This work was supported by U. S. Public Health Service Grant No. C-4670(C2). This is publication No. 1099 of the Cancer Commission of Harvard University.

[1] Newton, A. A., and P. Wildy, *Exper. Cell Research*, **16**, 624 (1959).

[2] Rueckert, R. R., and G. C. Mueller, *Cancer Research*, **20**, 1584 (1960).

[3] Prescott, D. M., in *International Review of Cytology*, ed. G. H. Bourne and J. F. Danielli (New York: Academic Press, 1961), vol. 11, p. 255.

[4] Littlefield, J. W., *Exper. Cell Research*, **26**, 318 (1962).

[5] Gold, M., and C. W. Helleiner, personal communication; Gold, M., Ph.D. thesis, University of Toronto, in preparation.

[6] Billen, D., *Biochem. Biophys. Research Comm.*, **7**, 179 (1962).

[7] Harris, M., *Cancer Research*, **19**, 1020 (1959).

[8] Lowry, O. H., N. J. Rosebrough, A. L. Farr, and R. J. Randall, *J. Biol. Chem.*, **193**, 265 (1951).

[9] Bollum, F. J., *J. Am. Chem. Soc.*, **80**, 1766 (1958).

[10] Eidinoff, M. L., and M. A. Rich, *Cancer Research*, **19**, 521 (1959).

[11] Morris, N. R., and G. A. Fischer, *Biochim. Biophys. Acta*, **42**, 183 (1960).

[12] Stanners, C. P., and J. E. Till, *Biochim. Biophys. Acta*, **37**, 406 (1960).

[13] Paul, J., and A. Hagiwara, *Biochim. Biophys. Acta*, **61**, 243 (1962).

[14] Mueller, G. C., K. Kajiwara, E. Stubblefield, and R. R. Rueckert, *Cancer Research*, **22**, 1084 (1962).

[15] Stubblefield, E., and G. C. Mueller, *Cancer Research*, **22**, 1091 (1962).

[16] Bollum, F. J., and V. R. Potter, *J. Biol. Chem.*, **233,** 478 (1958).
[17] Smellie, R. M. S., H. M. Keir, and J. N. Davidson, *Biochim. Biophys. Acta*, **35,** 389 (1959).
[18] Smellie, R. M. S., and R. Eason, *Biochem. J.*, **80,** 39P (1961).
[19] Beaufay, H., and C. de Duve, *Biochem. J.*, **73,** 604 (1959).
[20] Elson, D., *Biochim. Biophys. Acta*, **27,** 216 (1958).
[21] Isselbacher, K. J., M. F. Chrabas, and R. C. Quinn, *J. Biol. Chem.*, **237,** 3033 (1962).
[22] Ziegler, D. M., and A. W. Linnane, *Biochim. Biophys. Acta*, **30,** 53 (1958).

THYRO-ACTIVITY IN IODO-DERIVATIVES OF PHYTOHORMONAL 5-HYDROXYBENZOFURANS

BY S. M. SIEGEL, C. A. GIZA, GWENDOLYN DAVIS, R. L. HINMAN

UNION CARBIDE RESEARCH INSTITUTE, TARRYTOWN, NEW YORK

Communicated by Johannes Holtfreter, November 13, 1962

The thyronines, especially thyroxine and 3,3′,5-triiodothyronine, have been shown to act as antioxidants in test oxidation systems *in vitro*.[1] Among the factors of quantitative significance in determining the level of antioxidant activity, the presence of a phenyl ether skeleton (or phenoxy group) was foremost and the extent of iodination second.[1, 2]

The previously unnoticed antioxidant activity of thyroxine is consistent with its ability to protect the succinoxidase system against oxygen poisoning[3] and, even more directly, with its ability to maintain a high sulfhydryl/disulfide ratio in the mammalian liver.[4]

Antioxidant activity had also been recognized in the indole hormones and a common basis for this property postulated in both plant and animal substances.[5]

Efforts were subsequently undertaken to devise a single structure which would embody the requirements for phytohormonal and thyro-hormonal activities. The structure conceived was that of a benzofuran, specifically derivatives of 2-methyl-3-carbethoxy-5-hydroxybenzofuran (Fig. 1). This structure may be regarded as (*a*) an indole analog, (*b*) a phenoxy acid, (*c*) a hydroxyphenyl ether. If X_1 and/or X_2 are iodine, the thyroxine-like character is obvious.

When the benzofurans were tested against seeds of turnip, alfalfa, and rye, they were indeed found to be highly active as stimulants of germination and seedling growth at concentrations of 10^{-6} to 10^{-4} *M*.[6] The mono-iodinated benzofurans retained phytohormonal properties, but the 4,6-diiodo derivative was completely inactive. Other studies which will be detailed separately have disclosed stimulatory action in a range of processes from leaf expansion to rooting in cuttings.

We have now verified the hypothesis that the iodination of either or both positions *ortho* to the phenolic group confers thyro-activity by demonstrating the hastening of amphibian metamorphosis by these compounds.

Experimentation and Results.—One-year-old tadpoles of the bullfrog, *Rana catesbiana*, were used in the assay for thyro-activity.[7] They were maintained in shallow aerated tapwater (pH ca. 6) in polyethylene pans at 22–23°C in ordinary laboratory light and were fed once weekly a mixture of spinach, lettuce, and boiled eggyolk.

Duplicate vessels of about 20 animals each (in 5 liters of water) were used for

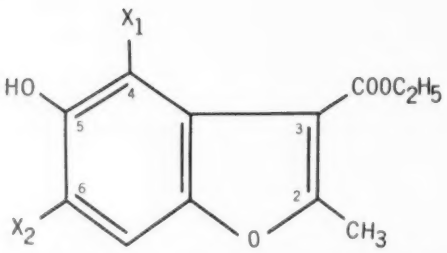

FIG. 1.—The structure of substituted 2-methyl-3-carbethoxy-5-hydroxy-benzofurans. X_1 and/or X_2 indicate positions of iodination.

controls and treatments. Both tail resorption and hind limb appearance were used as indices of hormonal action. At the start of the assays, the animals averaged 45 ± 5 mm (basis of > 200 measurements) in tail length; no limbs or limb buds were macroscopically evident.

As a reference standard, L-thyroxine was used at 10^{-6} *M*. The test compounds were the 4-iodo-, 6-iodo-, and 4,6-diiodo-derivatives of 2-methyl-3-carbethoxy-5-hydroxybenzofuran. They were used at 10^{-6} *M* and 5×10^{-6} *M*. Only data for the 10^{-6} *M* concentration are given (Table 1), as the higher concentration had no effect or was slightly inhibitory relative to the lower one.

TABLE 1

EFFECT OF THYROXINE AND ANALOGS ON METAMORPHOSIS OF *Rana catesbiana*

Treatment	Days from Start 4	8	17	24	$\frac{\Delta \text{ Treated}-\Delta \text{ control}}{\Delta \text{ Thyroxine}-\Delta \text{ control}}$ (as % at 24 days)
(*a*) Change in tail length (Δmm)					
None (control)	0	0	0	+1	—
Thyroxine, 10^{-6} *M*	−2	−4	−6	−28	100
2-methyl-3-carbethoxy-5-hydroxybenzofurans					
4,6-diiodo-, 10^{-6} *M*	0	0	−9	−10	38
4-iodo-, 10^{-6} *M*	−1	−2	−3	−4	17
6-iodo-, 10^{-6} *M*	0	−4	−4	−11	41
(*b*) Change in hind limbs (as per cent of population)					
None (control)	+20	+20	+21	+30	—
Thyroxine, 10^{-6} *M*	+32	+70	+90	+90	100
2-methyl-3-carbethoxy-5-hydroxybenzofurans					
4,6-diiodo-, 10^{-6} *M*	0	0	+40	+40	16
4-iodo-, 10^{-6} *M*	+30	+50	+50	+63	55
6-iodo-, 10^{-6} *M*	+33	+45	+50	+50	33

It is evident from the data that the iodobenzofurans are effective, and possess an appreciable fraction of L-thyroxine activity.

The results warrant the following conclusions:

(*a*) One *ortho*-substitution is sufficient for activity, but the two *ortho* positions are no more equivalent biologically than they are chemically.

(*b*) The presence of substantial activity in molecules which do not possess the general stereochemical properties of L-thyroxine (or L-tri-iodothyronine) calls for a serious re-examination of stereospecificity in the thyroid hormones.

[1] Siegel, S., and P. Frost, these PROCEEDINGS, **45**, 1379 (1959).

[2] Siegel, S., and P. Frost, *J. Am. Chem. Soc.*, **82**, 2773 (1960).

[3] Kriphe, B., and A. Bever, *Arch. Biochem. Biophys.*, **60**, 320 (1956).

[4] Goldstein, B., and E. Gotovtseva, *Biokhimiya*, **22**, 994 (1958).

[5] Siegel, S., and F. Porto, in *Plant Growth Regulation*, ed. R. M. Klein (Ames, Iowa: Iowa State University Press, 1961).

[6] Giza, C. A., and S. Siegel, *Physiologia Plant.*, in press (1962).

[7] Rawson, R., J. Rall, and M. Sonenberg, in *The Hormones*, ed. G. Pincus and K. Thimann (New York: Academic Press, Inc., 1955), vol. 3.

*CARBOXYPEPTIDASE A: APPROACHES TO THE CHEMICAL NATURE OF THE ACTIVE CENTER AND THE MECHANISMS OF ACTION**

By Bert L. Vallee, James F. Riordan†, and Joseph E. Coleman†

BIOPHYSICS RESEARCH LABORATORY, DIVISION OF MEDICAL BIOLOGY, DEPARTMENT OF MEDICINE, HARVARD MEDICAL SCHOOL AND THE PETER BENT BRIGHAM HOSPITAL, BOSTON

Communicated by Eric G. Ball, November 7, 1962

The characteristics of metalloenzymes offer unusual opportunities in the elucidation of their active, enzymatic centers. Carboxypeptidase[1] has proved to be a particularly suitable and experimentally accessible enzyme for such studies, since conclusions concerning the active center[2] need not be based on experiments which destroy activity.[3] This paper briefly summarizes the implications of recent experiments which have been reported and others to be reported elsewhere.[4–9]

Experimental.—The preparations of the native zinc enzyme and the metal-free apoenzyme, the methods for peptidase and esterase assay, the preparation of metallocarboxypeptidases, the determinations of protein concentration, sulfhydryl titrations, gel filtrations and equilibrium dialyses have all been described previously.[5, 6, 10–13] *Dinitrophenylations* of the metalloenzyme and apoenzyme were carried out according to the method of Sanger[14] or Fraenkel-Conrat.[15] The DNP-amino acid derivatives were isolated by two-dimensional paper chromatography. *Phenylisothiocyanate* was employed for Fraenkel-Conrat's modification[15] of the Edman degradation.[16] The phenylthiohydantoins were isolated by paper chromatography and identified by their characteristic Rf's as determined by ultraviolet absorption and starch-iodine. *Acylations* were performed by adding 15- to 60-fold excess of the various anhydrides mentioned in the text to 10^{-4} *M* enzyme in 0.02 *M* sodium Veronal-2 *M* NaCl, pH 7.5 buffer at 0° for a reaction time of thirty min. The pH of the reaction was maintained at 7.5 by the addition of 1 *M* NaOH by means of a pH Stat. Excess anhydride was removed by dialysis against the same buffer at 0° for 48 hr. *Iodinations* were performed with a 35-fold molar excess of I_2 in 0.5 *M* KI at 25° for ten min. *Photooxidations* were carried out in the presence of methylene blue according to the method of Weil and Buchert.[17] All chemicals used in these experiments were reagent grade and used without further purification except for acetic anhydride which was redistilled.

Results and Discussion.—The metal binding site of apocarboxypeptidase: Ag^+, p-mercuribenzoate, or ferricyanide titrate only one —SH group in the apocarboxypeptidase and none in the metallocarboxypeptidase[12] (Table 1). A peptide containing the single cysteine residue of carboxypeptidase to which zinc is bound has recently been isolated.[18]

The sequence and magnitude of the stability constants of different metallocarboxypeptidases, their comparison to those of simple ligands and complexometric titrations indicated early that the metal atom is also bound to nitrogen.[11, 12] The experiments suggesting that the α-amino group of the N-terminal asparagine ($AspNH_2$) (Table 1) may be the second donor group for zinc binding are quite analogous to those employed for the —SH group. On exposure to fluorodinitrobenzene or phenylisothiocyanate, the apoenzyme[13] readily forms DNP-aspartic acid (DNP-Asp) or PTH-asparagine (PTN-$AspNH_2$), respectively, while the yields from the metalloenzyme are significantly less. Zinc appears to be displaced from the enzyme in proportion to the reaction of these reagents with the N-terminal asparagine. The sum of the number of gram atoms of zinc bound per mole of enzyme and the moles of product is unity[7, 19] (Table 1).

Chemical modifications: The search for those groups of carboxypeptidase which might function in specificity, catalysis, and binding of the substrate is a logical ex-

TABLE 1

COMPLEMENTARITY OF —SH AND α-NH_2 GROUPS WITH ZINC CONTENT OF [(CPD) Zn][a]

Sample	Zn^{++}[b] (gm-atom/mole)	−SH[c] (moles/mole)	Σ (Zn^{++} + −SH)
[(CPD) Zn][d]	1.00	0	1.00
(CPD) + 0.5 gm-atom Zn^{++}	0.57	0.42	0.99
(CPD) + 0.25 gm-atom Zn^{++}	0.27	0.63	0.90
(CPD)	0	0.91	0.91
		DNP-Asp (moles/mole)	Σ (Zn^{++} + DNP-Asp)
[(CPD) Zn][e]	1.0		1.00
[(CPD) Zn][f]	0.77	0.25	1.02
(CPD) + 0.5 gm-atom Zn^{++}	0.47	0.52	0.99
[(CPD) Zn][g]	0.23	0.70	0.93
		PTH-AspNH_2 (moles/mole)	Σ (Zn^{++} + PTH-AspNH_2)
[(CPD) Zn] + PTC[h] 2 min	0.72	0.28	1.00
[(CPD) Zn] + PTC 15 min	0.44	0.47	0.91
[(CPD) Zn] + PTC 30 min	0.38	0.69	1.07

[a] Apocarboxypeptidase is designated (CPD); zinc carboxypeptidase is [(CPD) Zn] in accord with previous usage (Vallee, B. L., *Advances in Protein Chem.*, **10**, 317 (1955)).
[b] Determined by chemical analysis.[10]
[c] −SH groups titrated with Ag^+.[12]
[d] Native and fully reconstituted zinc carboxypeptidase.
[e] Native zinc carboxypeptidase, not treated with 1-fluoro-2,4-dinitrobenzene (FDNB).
[f] Native zinc carboxypeptidase, FDNB, 2 hr, 25°, pH 7.0.[13]
[g] Native zinc carboxypeptidase, FDNB, pH 9.0, conditions according to Sanger.[14]
[h] Native zinc carboxypeptidase, phenylisothiocyanate (PTC) 22°. Whatman No. 1 paper strip, conditions according to Fraenkel-Conrat.[15] The N-terminal sequence is Asp-NH_2, Tyr, Ala.[7, 16]

tension of these studies. Alterations in the general three-dimensional structure of enzymes are not likely to account for the mode of action of procedures which result in marked *increases* in activity. Though conformational changes at the active site may have occurred, the enhancement of activity provides evidence that the essential chemical and structural features of the active center have been preserved.

Replacement of Zn^{++} by Cd^{++} and Hg^{++} at the Active Site of Carboxypeptidase.—Effects on peptidase and esterase activities: Cadmium and mercury carboxypeptidases are more active as esterases than native zinc carboxypeptidase, but they exhibit no peptidase activity (Table 2). One activity has been abolished while the other is even enhanced as a *consequence of the replacement of only one atom*,

TABLE 2

SIMULTANEOUS ALTERATIONS IN ENZYMATIC ACTIVITY AND SPECIFICITY OF CARBOXYPEPTIDASE INDUCED BY METAL IONS, ANHYDRIDES, IODINATION, AND IRRADIATION

Enzyme*	Activity: Esterase (%)	Activity: Peptidase (%)
[(CPD) Zn]	100	100
[(CPD) Hg]	116	0
[(CPD) Cd]	152	0
Iodinated [(CPD) Zn]	500	0
Acetyl [(CPD) Zn]	610	0
Succinyl [(CPD) Zn]	150	154
Acetyl-Succinyl [(CPD) Zn]	780	0
Acetyl [(CPD) Zn] + NH_2OH	138	85
i-Butyryl [(CPD) Zn]	134	83
n-Valeryl [(CPD) Zn]	162	80
n-Butyryl [(CPD) Zn]	191	64
Propionyl [(CPD) Zn]	342	49
Photooxidized [(CPD) Zn]	198	36

* Metallocarboxypeptidases were prepared as previously described.[11] Acylations were performed as described under *Experimental*. Iodinations were performed with a 35-fold molar excess of I_2 in 0.5 *M* KI for 10 min at 25°. Photooxidations were carried out at 25° for 90 min using a 500-watt photoflood lamp positioned 6″ from the sample as previously described.[17] Esterase and peptidase activities were measured as previously described.[11]

zinc, by another, cadmium or mercury; in effect, a curtailment of the dual specificity of the enzyme. Changes in the over-all three-dimensional protein structure would not constitute a likely explanation. Optical rotatory dispersion measurements support this prediction. Other organic chemical modifications of this enzyme enhance this view.

Acylation with Monocarboxylic Acid Anhydrides, Iodination, and Photooxidation.—Effects on peptidase and esterase activities: Under appropriate conditions, acylation with monocarboxylic acid anhydrides, iodination, and photooxidation of carboxypeptidase all markedly increase esterase and decrease peptidase activity (Table 2). Acetylation increases esterase activity to about 610 per cent of the native enzyme and peptidase activity is abolished completely; β-phenylpropionate, a competitive inhibitor of the enzyme, selectively prevents both of these changes[8] (Fig. 1). Acetylation overcomes the inhibition of ester hydrolysis at higher substrate concentrations.[9] When acetylcarboxypeptidase is treated with hydroxylamine, both peptidase and esterase activities are restored almost to their original rates (Table 2). Acylations with *i*-butyric, *n*-butyric, *n*-valeric, and propionic anhydrides also increase esterase and decrease peptidase activity. Though qualitatively the same, these changes are quantitatively smaller, as might be expected in view of the known reactivities of these anhydrides. In each case the increase in esterase activity is commensurate with the decrease in peptidase activity. At present, the evidence suggests that acylation of ϵ-amino groups does not account for these reversible alterations of activity.[9] Histidyl or tyrosyl residues or even the single atypical sulfur-containing residue of carboxypeptidase[18] could react with all of these reagents. But alkylation of this atypical sulfur group does not affect activity nor does β-phenylpropionate prevent this alkylation.[18] Esterase activity is markedly enhanced and peptidase activity is diminished or abolished either by acylation or replacement of zinc by cadmium or mercury.[11] Chemical interactions of all of these reagents with a specific group in the active center would be the simplest postulate for the alterations in rate and catalytic specificities of the modified enzyme.

Succinylation: The catalytic properties of succinylcarboxypeptidase differ significantly from those of the other acylenzymes studied so far. Succinylation increases *both* esterase and peptidase activities by 50 per cent, but β-phenylpropionate does *not* prevent these changes. Acetylated succinylcarboxypeptidase is completely inactive toward peptides. However, its esterase activity is 780 per cent of the native enzyme and incorporates the increases due to both modifications. Succinic anhydride apparently does not react with the group affected by the other reagents listed in Table 2, nor does it prevent their reaction. Thus, the effects of successive modifications on the enzymatic properties of carboxypeptidase seem to offer an approach to the identification of its catalytically functional groups.

Succinic anhydride reacts with ϵ-amino groups of the protein as indicated by a decrease in its ninhydrin color, though it is not clear at present whether these are the only groups affected and accounting for the functional changes. There will likely be changes in charge or charge distribution in the vicinity of the active center as well as on the surface of the whole molecule to which these changes in function might be attributable. This hypothesis is being explored in relation to the electrostatic, hydrodynamic, and structural properties of the molecule.

The effect of pH on peptidase and esterase activities of carboxypeptidase: In

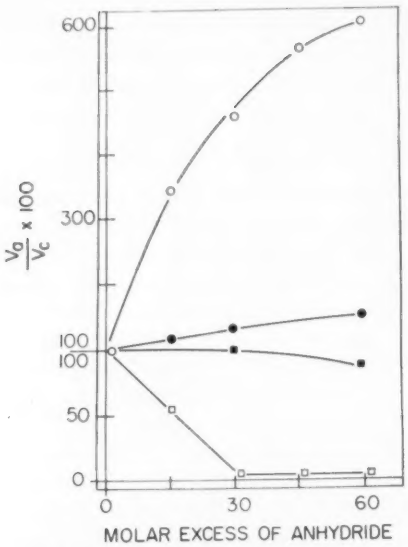

FIG. 1.—Enzymatic activity of acetyl [(CPD)Zn]. Native carboxypeptidase, $10^{-4}M$, was exposed to the indicated molar excess of acetic anhydride (cf. *Experimental*). Esterase activity of enzyme acetylated in the presence (●) or absence (○) of β-phenyl propionate and peptidase activity of enzyme acetylated in the presence (■) or absence (□) of β-phenyl propionate were measured as previously described.[11]

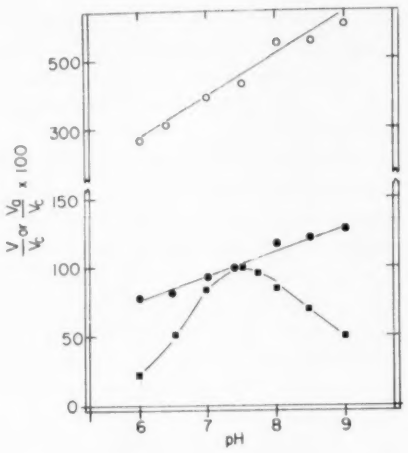

FIG. 2.—pH dependence of enzymatic activity of [(CPD) Zn] and acetyl [(CPD) Zn]: peptidase activity of [(CPD) Zn] (■); esterase activity of [(CPD) Zn] (●); esterase activity of acetyl [(CPD)Zn] (○). The activities of the native and the acetylated enzymes were plotted in one graph but with different ordinate scales as indicated by the break in the axis. Esterase activity of the native enzyme at pH 7.5[11] is set equal to 100 per cent. Hydrolysis of either substrate in the absence of added enzyme could not be detected during the time required for assay. Acetylcarboxypeptidase has no appreciable peptidase activity throughout the pH range studied. This negative data has been omitted from the figure.

agreement with earlier results,[20] the pH-rate profile of peptide hydrolysis exhibits an inflection between pH 6 and 7 which could not be assigned unequivocally to the ionization of only one specific residue.[20] The profile shows a maximum at about pH 7.5 and falls off at higher pH values (Fig. 2). In conjunction with the data on chemical modification presented above and based on the ionization of histidine model compounds, the point of inflection at about pH 6.7 in this pH-rate profile strongly implies that a histidine residue participates in the catalytic mechanism of peptide hydrolysis (*vide infra*). This view is supported by the consequents of acetylation of the enzyme at discrete values of pH between 6 and 7.5: the catalytic rates of the resultant enzymes, when plotted as an activity profile, bear close resemblance to the pH-rate profile for peptidase activity. Since the N-terminal α-amino group is involved in binding zinc, it may be eliminated from consideration. However, the involvement of another group, such as a tyrosyl residue, in the catalytic mechanism remains a possibility which cannot be resolved on the basis of the data presently available. Gel filtration experiments with dipeptide substrates to determine apoenzyme-substrate complex formation as a function of pH[5] demonstrate that substrate binding is constant between pH 6 and 7.5 but decreases progressively thereafter. Apparently, the acidic ionization does not affect binding of dipeptides to the apoenzyme. The effect of pH on esterase activity

has not been reported heretofore. The pH-rate profiles of ester hydrolysis both by the native and the acetylated enzyme differ qualitatively from the peptidase pH-rate profile of the native enzyme (Fig. 2). (Acetylated carboxypeptidase does not exhibit peptidase activity throughout the pH range studied.) Rates of ester hydrolysis have been studied between pH 6 and 9 and increase linearly with pH over this range; both the absolute rate (*vide supra*) and the rate of increase of esterase activity with pH for acetylcarboxypeptidase are greater than those of the native enzyme. The inflection between pH 6 and 7, so prominent in the pH-rate profile of peptidase activity, is not in evidence, pointing to the state of ionization of this group as a significant variable in the mechanisms of catalysis of esters and peptides by this enzyme.

Metallocarboxypeptidase and apocarboxypeptidase substrate complexes: By kinetic means, Bergmann, Neurath, and Smith, have previously delineated the specificity of carboxypeptidase on the basis of those structural and conformational features of synthetic peptides which are critical for *hydrolysis*.[20-22] By means of a gel filtration procedure, it has now been possible to discern at equilibrium those characteristics of substrates which are required for the formation either of the apoenzyme or metalloenzyme complexes or both, confirming and extending these earlier studies.[5,6] Three groups of the peptide, indicated in brackets, are minimally required to form a complex with apocarboxypeptidase: the —NH— function of the C—terminal residue, the —NH— function of the adjacent amino acid residue, and the R group on the α-carbon of the C-terminal residue which may be either an aromatic or branched aliphatic side chain, iodine, or bromine[20]: H—[NH]—CH_2—CO—[NH]—CH[R]—COO^-. When either one of the two —NH— functions is lacking, the apoenzyme complex no longer forms, though the metalloenzyme complex does, and hydrolysis still takes place. Removal of the R group destroys both the activity and formation of either complex.[6]

Mechanisms of action of carboxypeptidase in the hydrolysis of peptides and esters: The data suggest that carboxypeptidase avails itself of distinctly different mechanisms for the hydrolysis of peptides and of esters.

Peptidase: The tentative scheme shown in Figure 3 is not to be regarded as either microscopic or definitive.[23] The R group of the peptide may be thought to fix the substrate to the enzyme, perhaps through hydrophobic bonding and assisted by the two —NH— functions, perhaps through hydrogen bonding to the protein. The C—terminal carboxyl group is thought to be bound to a cationic group of the protein required for proper orientation of the substrate. Since both hydrolysis and binding to the metalloenzyme can take place in its absence, the —NH— function of the penultimate residue can be neglected from a mechanistic point of view.

In Figure 3, a nucleophilic group, *B*, is postulated to initiate peptide hydrolysis by donating a pair of electrons to the carbonyl carbon to form an acylenzyme intermediate. The electron withdrawing effect of a metal atom on the oxygen of the carbonyl would facilitate the attack. A second, acidic group in the active center, AH, might participate in catalysis by donating its proton to the peptide nitrogen of the C—terminal residue in the transition state. This interaction of the peptide nitrogen in conjunction with its coordination to the metal ion would assist the reactivity of the carbonyl, since, simultaneously, the electrons will be withdrawn

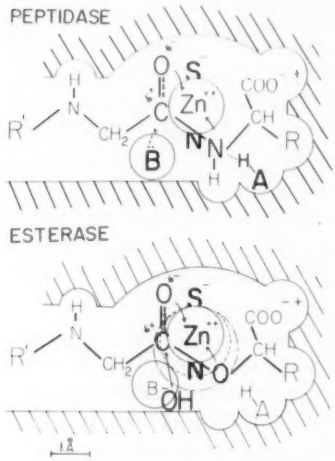

FIG. 3.—*Mechanism of Peptidase Hydrolysis:* Alternative possibilities could include a water molecule between B and the carbonyl carbon (see Rabin[25]). The ionic radius[24] of Zn^{++} is indicated. *Mechanism of Ester Hydrolysis:* The ionic radii[24] of Cd^{++} and Hg^{++} are additionally indicated. "B" is replaced by OH^- (see text).

from the C-N bond. This group is postulated primarily for this reason though there is no experimental evidence for its existence.

Esterase: Carboxypeptidase acts both as a peptidase and an esterase, and a mechanism for peptide hydrolysis by this enzyme must also be compatible with the data obtained when it acts as an esterase. The *chemical* specificity underlying the action common to the agents employed to modify the protein and listed in Table 2 is not obvious. Yet, excepting succinic anhydride, the *biological* consequence of their interaction with carboxypeptidase is qualitatively identical to acetylation in that they increase esterase and decrease peptidase activity, though to varying degrees. Reaction of all these agents with a single amino acid residue would be the simplest chemical event that could account for such similar functional consequences; this assumption underlies the present discussion, much as it is understood that it is an oversimplification.

The distribution of electrons in certain canonical forms of the peptide bond reduces its susceptibility to hydrolysis.[25] Replacement of the peptide by an ester bond would, therefore, greatly facilitate hydrolysis. The properties of acylated, iodinated, and photooxidized carboxypeptidase are consistent with the assumption that all these procedures modify a group, perhaps that designated *B* in Figure 3, which is required for the hydrolysis of the peptide bond but actually inhibits the hydrolysis of the ester. There is no evidence for the ionization of the group which is critical to peptide hydrolysis (Fig. 2). In fact, the pH-rate profile of esterase activity suggests that catalysis can be mediated by OH^- ions. This view gains considerable support from the study of model systems. Kroll[26] found that the metal catalyzed hydrolysis of esters is hydroxyl ion-dependent in much the manner that is described here for the enzymatic hydrolysis of hippuryl-β-phenyllactic acid. Peptides have not been found to be hydrolyzed in model systems under comparable conditions.

As a consequence of the nucleophilic attack, group B is thought to form an acylenzyme intermediate which is indispensable to the hydrolysis of peptides but not to that of esters, since OH^- ions are postulated to substitute for this group. One might speculate that acetic and other monocarboxylic acid anhydrides as well as iodination and photooxidation bring about their functional effects by blocking Group *B*. In this scheme, the resultant decrease in peptidase and increase in esterase activities is attributed to the elimination of group *B* by the various modifications. Once group *B* is destroyed, OH^- ions alone could be the sole attacking agent; the removal of the products of ester hydrolysis would be greatly accelerated (Fig. 3). If additional amino acid residues should be found

experimentally to participate in catalysis, this mechanistic scheme would have to be refined. Further, the effect of these modifications of the enzyme on the binding of substrate remain to be explored as possible causes of altered catalytic rates.

Mechanism of altered enzymatic specificity and rate incident to replacement of zinc by cadmium and mercury: The sequence and magnitude of the stability constants of the complexes of Hg^{++}, Cd^{++}, Cu^{++}, Zn^{++}, Co^{++}, Ni^{++}, and Mn^{++} with carboxypeptidase correlate closely with those of their complexes with nitrogen-sulfur ligands.[11] Among these metals, mercury, cadmium, and zinc much prefer sulfur to other ligands. Mercury and cadmium carboxypeptidases in contrast to zinc carboxypeptidase are only esterases[11] (*vide supra*). In the absence of information concerning the nature of specific, chemically identifiable complexes, the ionic radii of the elements may serve as an approximation to their potential mode of interaction. The Pauling[24] radii of Hg^{++}, Cd^{++}, and Zn^{++} are 1.10 Å, 0.97 Å, and 0.74 Å respectively, while the Goldschmidt[27] radii are 0.93 Å, 0.92 Å and 0.69 Å respectively, those of Cd^{++} and Hg^{++} being larger than those of Zn^{++} by more than 0.2 Å in both scales. The coordination spheres of mercury and cadmium shown schematically in Figure 3 could allow interaction of these ions with other vicinal groups, not accessible to zinc, nickel, cobalt, or manganese under comparable circumstances. Suitable spatial arrangements would bring group *B* into the coordination sphere of the metal; its interaction with mercury and cadmium would then block the formation of the acylenzyme and bring about the observed synchronous increase in esterase and decrease in peptidase activities, which also occurs when the enzyme is modified with other "selective" reagents (Table 2).

This working hypothesis, which invokes the operation of a minimal number of functional groups, provides a means to delineate and characterize the active, enzymatic center of carboxypeptidase. While integrating current knowledge, this model may serve as a basis for further experimental extensions leading to a fuller understanding of the active center of the enzyme. The resolution and integration of these chemical details should provide the knowledge required to discern its catalytic mechanisms more definitively.

Summary.—Acylation with monocarboxylic acid anhydrides, iodination or photooxidation of carboxypeptidase, or the replacement of the zinc of carboxypeptidase by cadmium or mercury all increase esterase and decrease peptidase activities of this enzyme. The pH-rate profiles of peptidase and esterase activities differ significantly. These data, in conjunction with studies identifying the groups of the substrate essential for the formation of enzyme complexes, lead to suggestions concerning the distinctive mechanisms of peptidase and esterase action respectively.

* This work was supported by the Howard Hughes Medical Institute and by a grant-in-aid from the National Institutes of Health, Department of Health, Education and Welfare.

† Fellows of the National Foundation and the NIH, Department of Health, Education and Welfare.

[1] Carboxypeptidase will refer to carboxypeptidase A.

[2] The designation "active site" will refer specifically to the nitrogen-metal-sulfur bond, essential for hydrolysis. "Active center" will refer to all those features of primary, secondary, and tertiary structure of the enzyme—*including* the "active site"—which are required for substrate binding, specificity, or hydrolysis of the substrate.

[3] Vallee, B. L., *Federation Proceedings*, **20**, Suppl. 10, 71 (1961).

[4] Felber, J.-P., T. L. Coombs, and B. L. Vallee, *Biochemistry*, **1**, 231 (1962).

[5] Coleman, J. E., and B. L. Vallee, *J. Biol. Chem.*, **237**, 3430 (1962).
[6] Coleman, J. E., and B. L. Vallee, *Biochemistry*, **1**, 1083 (1962).
[7] Coombs, T. L., and Y. Omote, *Federation Proceedings*, **21**, 234 (1962).
[8] Riordan, J. F., and B. L. Vallee, *Abstracts of the 142nd Meeting of the American Chemical Society*, Atlantic City, September, 1962.
[9] Riordan, J. F., and B. L. Vallee, (in preparation).
[10] Coleman, J. E., and B. L. Vallee, *J. Biol. Chem.*, **235**, 390 (1960).
[11] Coleman, J. E., and B. L. Vallee, *J. Biol. Chem.*, **236**, 2244 (1961).
[12] Vallee, B. L., T. L. Coombs, and F. L. Hoch, *J. Biol. Chem.*, **235**, PC 45 (1960).
[13] Prepared either according to the method of Anson, M. L., *J. Gen. Physiol.*, **20**, 663, 777 (1937) or of Allan, B. J., P. J. Keller, and H. Neurath, in preparation.
[14] Sanger, F., *Biochem. J.*, **45**, 563 (1949).
[15] Fraenkel-Conrat, H., J. I. Harris, and A. L. Levy, *Methods of Biochem. Anal.* **2**, 390 (1955).
[16] Edman, P., *Acta Chem. Scand.*, **4**, 277, 283 (1950).
[17] Weil, L., and A. R. Buchert, *Arch. Biochem. Biophys.*, **34**, 1 (1951).
[18] Walsh, K., S. Kumar, J. Bargetzi, and H. Neurath, *these* PROCEEDINGS, **48**, 1443 (1962).
[19] Omote, Y., T. L. Coombs, and B. L. Vallee (in preparation).
[20] Neurath, H., and G. W. Schwert, *Chem. Revs.*, **46**, 69 (1950).
[21] Bergmann, M., *Harvey Lectures*, **31**, 37 (1935–36).
[22] Smith, E. L., *Advances in Enzymology*, **12**, 191 (1951).
[23] R. J. P. Williams, Wadham College, Oxford, has communicated to us, prior to publication, an alternate mechanism wherein the metal-binding sulfur acts as the nucleophile forming an S-acyl intermediate.
[24] Pauling, L., *Nature of the Chemical Bond* (Cornell U. Press, 1960), p. 281.
[25] Rabin, B. R., *Biochem. Soc. Symp.* (Cambridge, England), **15**, 21 (1958).
[26] Kroll, H., *J. Am. Chem. Soc.*, **74**, 2036 (1952).
[27] Cotton, F. A., and G. Wilkinson, *Advanced Inorganic Chemistry* (New York: Interscience, 1962), p. 43.

---

*SYNTHETIC POLYNUCLEOTIDES AND THE AMINO ACID CODE, VIII**

BY ALBERT J. WAHBA,† ROBERT S. GARDNER, CARLOS BASILIO,‡ ROBERT S. MILLER, JOSEPH F. SPEYER, AND PETER LENGYEL

DEPARTMENT OF BIOCHEMISTRY, NEW YORK UNIVERSITY SCHOOL OF MEDICINE

Communicated by Severo Ochoa, December 3, 1962

In the preceding paper[1] code triplets containing no uracil were assigned to several amino acids as a result of studies with poly A, poly AC, and poly AG. Results with poly ACG, to be reported in this paper, have led to the assignment of 1A1C1G triplets to the amino acids alanine, aspartic acid, and serine. Moreover, poly C has now been found to stimulate the incorporation of proline into acid-insoluble products by the *E. coli* system, leading presumably to the formation of polyproline. Thus, CCC is a code letter for proline. Previous negative results[2] can be explained by (*a*) low affinity of poly C for the ribosomes, and (*b*) partial solubility of polyproline in 5 per cent trichloroacetic acid. In the present experiments poly C was used at a concentration of 200 μg/0.25 ml of reaction mixture and 20 per cent (final concentration) trichloroacetic acid was employed as the precipitating agent. C-rich polymers could therefore be used in the search for additional code letters. Experiments with poly CI, where inosinic acid takes the place of guanylic acid,[3]

have yielded three new 2C1G code letters for the amino acids alanine, arginine, and threonine, and one 1C2G letter for glycine.

Results of experiments with polynucleotides containing analogs of the naturally occurring bases will also be reported in this paper.

Preparations and Methods.—As in the previous paper,[1] the nucleoside 5′-diphosphates used in the preparation of the various polynucleotides were purified by ion-exchange chromatography. Poly ACG (6:1:1), poly ACG (4:1:1), poly C, and poly CI (5:1) were prepared with *Azotobacter* polynucleotide phosphorylase as previously described.[4] The sedimentation coefficients of poly ACG (4:1:1) and poly ACG (6:1:1) were 1.6 and 1.7 *S*, respectively. We are indebted to Dr. J. Y. Chen for these determinations. Base analyses of the copolymers used in this work have not yet been performed.

Polynucleotides containing analogs of the naturally occurring bases were prepared with *Azotobacter* polynucleotide phosphorylase from the corresponding nucleoside 5′-diphosphates. 5-fluorouridine 5′-diphosphate was, as previously stated,[4] a gift of Dr. Charles Heidelberger. Synthetic N(3)-methyluridine 5′-diphosphate was kindly supplied by Dr. D. Shugar, Polish Academy of Sciences, Warsaw. Xanthosine 5′-diphosphate was prepared by deamination of commercial guanosine 5′-diphosphate with nitrous acid.

In all experiments with poly C and poly CI (5:1), 200 μg of the former and 100 μg of the latter polymer were used per 0.25 ml of reaction mixture. After incubation, 1.0 mg of carrier polyproline in 0.5 ml of water was added to each sample. This was followed by the addition of 5 ml of 20 per cent trichloroacetic acid. The samples were centrifuged and the precipitates resuspended in 10 ml of 20 per cent trichloroacetic acid, kept at 95° for 15 min and then cooled to room temperature. The precipitates were plated on Whatman No. 1 filter paper disks, washed with absolute acetone, dried, and their radioactivity was measured in a windowless gas-flow counter. The incubations with poly ACG (30 μg/0.25 ml of reaction mixture) were as described in the preceding paper[1] with use of trichloroacetic-tungstic acid as the precipitating reagent.

Results.—Effect of poly C on proline incorporation: Following the finding that poly A stimulated the incorporation of lysine,[1] it appeared desirable to reinvestigate the problem of whether or not poly C stimulated the incorporation of proline. It may be remembered that poly C had been reported to be active[5] for proline incorporation although later this activity appeared to be explainable by the presence of some uridylic acid residues in the poly C preparations used.[6] In our experience[2, 4] stimulation of proline incorporation by poly C was very small while copolymers containing both U and C were much more effective. Reinvestigation of the problem was made even more desirable by indications that poly C, in contrast to poly U, had low affinity for the ribosomes. Thus, while poly U effectively competed with poly UC and markedly decreased stimulation of serine incorporation by the latter polymer, poly C decreased this incorporation to a very slight extent. Poly C also decreased very slightly, if at all, the poly U-promoted incorporation of phenylalanine. In these experiments all polymers were used at a concentration of 160 μg/ml.

In view of the above, it was possible that, in previous experiments, poly C might have been essentially inactive not because of intrinsic meaninglessness of CCC triplets, but because of the low affinity of the polymer for the ribosomes. This view was substantiated by the experiment of Table 1 showing a marked polymer concentration dependence for proline incorporation in the presence of poly C. At high concentrations (800 μg/ml) the incorporation of proline was effectively promoted by this polymer. In this experiment 20 per cent trichloroacetic acid was used as the precipitating agent as it was found that only about half of the proline counts were recovered in acid-insoluble products when 5 per cent trichloroacetic

TABLE 1

PROLINE INCORPORATION IN *E. coli* SYSTEM AS A FUNCTION OF THE CONCENTRATION OF POLY C

Poly C (μg/ml)	Proline incorporation*
0	0.01
100	0.03
200	0.14
400	0.37
800	0.51

* mμmoles/mg ribosomal protein. Incubation, 60 min at 37°.

acid was used as it had been in previous work. Moreover, as already mentioned, cold polyproline was added as a carrier for precipitation. These results show that previous negative results with poly C were due mainly to low affinity for the ribosomes and, to a lesser degree, to partial solubility of polyproline in 5 per cent trichloroacetic acid. A CCC code letter can therefore be definitely assigned to proline.

Additional code triplet assignments: Table 2 lists the effects of poly ACG (4:1:1), poly ACG (6:1:1), poly C, and poly CI (5:1) on the incorporation of each of 20 amino acids. The trichloroacetic-tungstic procedure[1] was used for the experiments of columns 2, 3, and 4, and the 20 per cent trichloroacetic acid procedure, described in this paper, for those of columns 5, 6, and 7.

The basis of the code triplet assignments, listed in Table 3, in the case of the ACG copolymers is as explained previously[1] for A-rich copolymers. In the case of poly CI (5:1) the stimulation of the incorporation of a given amino acid by this polymer

TABLE 2

AMINO ACID INCORPORATION IN *E. coli* SYSTEM WITH VARIOUS POLYNUCLEOTIDES*

	Polynucleotide†					
Amino acid‡	None	ACG (4:1:1) 120 μg/ml	ACG (6:1:1) 120 μg/ml	None	C 800 μg/ml	CI (5:1) 400 μg/ml
Alanine (7.5)	60	[181]	[126]	24	32	[132]
Arginine (5.0)	40	590	390	15	12	[100]
Asparagine (1.32)	26	380	415	38	30	22
Aspartic acid (5.0)	19	[97]	[78]	18	12	12
Cysteine (7.0)	47	63	50	37	41	37
Glutamic acid (5.0)	27	458	500	14	12	11
Glutamine (2.0)	42	662	678	20	9	9
Glycine (7.8)	52	121	82	13	15	[36]
Histidine (4.0)	59	320	379	23	13	13
Isoleucine (5.5)	33	21	19	12	12	12
Leucine (6.0)	24	16	16	15	9	8
Lysine (1.0)	40	2100	2960	14	14	14
Methionine (4.75)	160	101	97	34	29	25
Phenylalanine (6.8)	23	24	24	15	13	16
Proline (10.0)	8	190	90	5	[725]	[447]
Serine (4.0)	34	[190]	[137]	22	22	22
Threonine (5.0)	42	536	610	20	24	[93]
Tryptophan (3.74)	109	108	...	76	76	79
Tyrosine (6.5)	21	10	10	7	6	7
Valine (5.0)	14	13	12	19	14	11

* μμmoles/mg ribosomal protein. Different precipitation procedures (see *Methods*) were used in the experiments of columns 2, 3, and 4, and columns 5, 6, and 7 of the table. Values for new code triplet assignments are enclosed in rectangles; all other polynucleotide-stimulated amino acid incorporations are underlined.

† Base ratios given are the ratios of ribonucleoside diphosphates used in the preparation of the polymers.

‡ Values in parentheses give specific radioactivities in μc/μmole.

TABLE 3

ADDITIONAL CODE TRIPLET ASSIGNMENTS*

	Polynucleotide: ACG (4:1:1) Found	ACG (4:1:1) Calculated	ACG (6:1:1) Found	ACG (6:1:1) Calculated	CI (5:1) Found	CI (5:1) Calculated	Code triplets†
Alanine	5.9	6.3 + 1.6 = 7.9	2.3	2.8 + 0.5 = 3.3	22.5	20.0	*1A1C1G, 2C1G*
Arginine	26.7	25.0 + 1.6 = 26.6	12.0	16.7 + 0.5 = 17.2	19.2	20.0	2A1G, *2C1G*
Asparagine	17.2	25.0	13.5	16.7	0	...	2A1G
Aspartic acid	3.8	6.3	2.0	2.8	0	...	*1A1C1G*
Glutamic acid	21.0	25.0	16.2	16.7	0	...	2A1G
Glutamine	30.0	25.0 + 6.3 = 31.3	21.8	16.7 + 2.8 = 19.5	0	...	2A1C, 1A2G
Glycine	3.4	6.3 + 1.6 = 7.9	1.0	2.8 + 0.5 = 3.3	5.2	4.0	1A2G, *1C2G*
Histidine	12.7	6.3	11.0	2.8	0	...	1A2C
Lysine‡	100.0	...	100.0	...	0	...	AAA
Proline‡	8.8	6.3 + 1.6 = 7.9	2.8	2.8 + 0.5 = 3.3	100	...	1A2C, *CCC*
Serine	7.6	6.3	3.5	2.8	0	...	*1A1C1G*
Threonine	24.0	25.0 + 1.6 = 26.6	19.5	16.7 + 0.5 = 17.2	16.5	20.0	2A1C, *2C1G*

* The polynucleotide-stimulated incorporation of each amino acid is given as percentage of lysine incorporation by ACG copolymers and of proline incorporation by CI copolymer (Found columns). This is compared with the percentage frequency of certain triplets to frequency of AAA triplets in the ACG copolymers and to frequency of CCC triplets in the CI copolymer (Calculated columns). Agreement or proximity of the two values is the basis for the code triplet assignments in the last column of the table.

† New code triplets are in italics.

‡ Incorporation taken as 100%.

relative to that of proline (taken as 100 per cent) was matched to the calculated per cent frequency of a given triplet relative to that of the CCC triplet in this polynucleotide. All of the matched values, on which the assignment of new additional code triplets (in italics in the table) to alanine (1A1C1G, 2C1G), arginine (2C1G), aspartic acid (1A1C1G), glycine (1C2G), serine (1A1C1G), and threonine (2C1G) is based, agree fairly closely. In the experiments with poly CI, I is considered to be equivalent to G since, in previous experiments,[3] poly UI has been shown to be equivalent to poly UG. Hence, the assignment of C and G-containing code letters based on experiments with poly CI is justified.

Experiments with polynucleotides containing analogs of naturally occurring bases: At the concentrations tried, poly N-methyluridylic acid (poly MeU) and polyfluorouridylic acid (poly FU) did not significantly stimulate incorporation of phenylalanine by the *E. coli* system (Table 4). The insignificant activity of the latter polymer has been previously noted.[4] As also shown in Table 4, the UMeU (9:1) copolymer had one-tenth the activity of poly U, but UFU copolymers were quite active. There is no obvious reason why poly FU (a polymer of 5-fluorouridylic acid) should be inactive unless this is due to a lack of affinity for the ribosomes. On the other hand, in poly MeU (a polymer of N(3)methyluridylic acid) a hydrogen bonding site, the number 3 ring nitrogen, is blocked by a methyl group, and this polymer does not form a twin-stranded complex with poly A.[7] This would interfere with attachment of the AAA adaptor[8] triplet in phenylalanine transfer RNA to the polynucleotide template.

From the results with poly UMeU and poly UFU (Table 4) it would appear that 5-fluorouracil which can pair with adenine through hydrogen bonding, is as effec-

TABLE 4

PHENYLALANINE INCORPORATION IN *E. coli* SYSTEM WITH POLYNUCLEOTIDES CONTAINING XANTHYLIC ACID AND BASE ANALOGS OF URIDYLIC ACID

Polynucleotide (160 μg/ml)	Phenylalanine incorporation*
None	0.1
Poly U	4.9
Poly N-methyl U (MeU)	0
Poly UMeU (9.1)†	0.5
Poly fluoro U (FU)	0.05
Poly UFU (5:1)‡	4.1
Poly UFU (6:4)†	2.2§
Polyuridylic-xanthylic acid (UX) (9:1)†	0.6

* mμmoles/mg ribosomal protein. Incubation, 60 min at 37°. Other conditions as previously described.[4]
† Actual base ratio of polynucleotide.
‡ Ratio of nucleoside diphosphates used in preparation of polymer.
§ In another experiment the value was 4.5. While poly U saturated the system at a concentration of 80 μg/ml, poly UFU (6:4) did not reach saturation at 400 μg/ml.

tive in coding as uracil when the FU residues are copolymerized with U residues, whereas N(3)methyluracil which, through lack of a hydrogen bonding site cannot pair with adenine, is not effective. The activity of the UFU copolymer and the inactivity of the FU homopolymer pose an interesting problem which cannot be explained without further experimental work. The different behavior might be related to ribosomal binding in the former case and lack of binding in the latter.

Comparison of the effects of poly UMeU (9:1) and poly UX (9:1) indicates that both the N-methyluracil and the xanthine residues are inactive in coding. Incorporation of phenylalanine into products insoluble in 5 per cent trichloroacetic acid was reduced in either case to about 10 per cent of the phenylalanine value with poly U (Table 4). These copolymers, because of the short uninterrupted U sequences (average, 10 residues) between meaningless N-MeU or X residues, might give rise to very short, mostly acid-soluble polyphenylalanine chains. The inactivity of xanthine in coding has been previously pointed out.[3]

It may be added that the UX (9:1) copolymer did not promote the incorporation of leucine, serine, tyrosine, or valine, suggesting that X cannot replace A, C, or G. The same was true of poly UFU (6:4). However, due to the limited sensitivity of our assay system, a very small incorporation of these amino acids would have escaped detection.

Discussion and Conclusions.—The results of previous work[1, 9] and the work reported in this paper bring to 41, out of 64 triplets in RNA, the number of triplets in the amino acid code, and the list is probably still incomplete. It may be mentioned that recent experiments with poly UCG (6:1:1) failed again to substantiate the prediction[10] that 1U1C1G is a code triplet for glutamine while, on the other hand, incorporation of this amino acid was promoted by poly AC and poly AG.[1] Hence, 1U1C1G has been excluded from the list as a glutamine triplet. Also, previous results suggesting 1U2C as a code triplet for threonine could not be confirmed, and this has been removed from the list as a threonine triplet.

A summary of the code triplet assignments to date is shown in Table 5. The U-containing triplets have been arranged in the sequences proposed by Jukes.[11] When possible, the sequence of non-U triplets was fitted to that of U-triplets as if triplets for a given amino acid were derived from each other through a single base replacement, e.g., GAG and GCG for an assumed GUG sequence of the U-containing glycine triplet. When this was not possible, non-U sequences for an amino acid

TABLE 5

AMINO ACID CODE TRIPLETS

Amino acid	U-triplets*	Non-U triplets	Shared doublets
Ala	CUG	CAG, CCG	C●G
Arg	GUC	GAA, GCC	G●C
AspN	UAA, CUA	CAA	●AA, C●A
Asp	GUA	GCA	G●A
Cys	GUU	...	...
Glu	AUG	AAG	A●G
GluN	...	AGG, AAC	...
Gly	GUG	GAG, GCG	G●G
His	AUC	ACC	A●C
Ile	UUA, AAU†	...	...
Leu	UAU, UUC, UGU	...	U●U
Lys	AUA	AAA	A●A
Met	UGA	...	...
Phe	UUU	...	...
Pro	CUC	CCC, CAC	C●C
Ser	CUU	ACG	...
Thr	UCA	ACA, CGC	●CA
Try	UGG	...	...
Tyr	AUU	...	...
Val	UUG	...	...

* Sequences from T. H. Jukes.[11]
† Not in Jukes' list.

were written to avoid duplication with sequences of the same base composition for another amino acid. All sequences are of course arbitrary, except for GUU and AUU for cysteine and tyrosine[12] since, with the possibility of extensive degeneracy of the code, sequence assignments based on amino acid replacement data cannot be made with any degree of certainty. It may be noted that in many cases (Table 5, column 4) a doublet is shared, with the same relative position of its bases, by two or three triplets of the same amino acid. It remains to be seen whether, in these cases, one or several transfer RNAs are involved in the read-out process. Weissblum *et al.*[13] have reported on two leucine trans-RNAs corresponding to the 2U1G and 2U1C code letters for this amino acid.

* Aided by grants from the National Institute of Arthritis and Metabolic Diseases (Grant A-1845) of the U.S. Public Health Service and from the Jane Coffin Childs Fund for Medical Research. The abbreviations used in this paper are the same as in previous papers of this series.

† Fellow of the Jane Coffin Childs Fund for Medical Research.

‡ International Postdoctoral Fellow of the National Institutes of Health, U.S. Public Health Service. Permanent address: Instituto de Química Fisiológica y Patológica, Universidad de Chile, Santiago, Chile.

[1] Gardner, R. S., A. J. Wahba, C. Basilio, R. S. Miller, P. Lengyel, and J. F. Speyer, these PROCEEDINGS, **48,** 2087 (1962).

[2] Speyer, J. F., P. Lengyel, C. Basilio, and S. Ochoa, these PROCEEDINGS, **48,** 63 (1962).

[3] Basilio, C., A. J. Wahba, P. Lengyel, J. F. Speyer, and S. Ochoa, these PROCEEDINGS, **48,** 613 (1962).

[4] Lengyel, P., J. F. Speyer, and S. Ochoa, these PROCEEDINGS, **47,** 1936 (1961).

[5] Nirenberg, M. W., and J. H. Matthaei, these PROCEEDINGS, **47,** 1588 (1961).

[6] Matthaei, J. H., O. W. Jones, R. G. Martin, and M. W. Nirenberg, these PROCEEDINGS, **48,** 666 (1962).

[7] Szer, W., and D. Shugar, *Acta Biochim. Polon.*, **8,** 235 (1961).

[8] Chapeville, F., F. Lipmann, G. von Ehrenstein, B. Weissblum, W. J. Ray, and S. Benzer, these PROCEEDINGS, **48,** 1086 (1962).

[9] Speyer, J. F., P. Lengyel, C. Basilio, and S. Ochoa, these PROCEEDINGS, **48,** 441 (1962).

[10] Lengyel, P., J. F. Speyer, C. Basilio, and S. Ochoa, these PROCEEDINGS, **48,** 282 (1962).

[11] Jukes, T. H., these PROCEEDINGS, **48**, 1809 (1962).

[12] Wahba, A. J., C. Basilio, J. F. Speyer, P. Lengyel, R. S. Miller, and S. Ochoa, these PROCEEDINGS, **48**, 1683 (1962).

[13] Weissblum, B., S. Benzer, and R. W. Holley, these PROCEEDINGS, **48**, 1449 (1962).

A MULTIPLE RIBOSOMAL STRUCTURE IN PROTEIN SYNTHESIS

BY JONATHAN R. WARNER,* PAUL M. KNOPF,† AND ALEXANDER RICH

DEPARTMENT OF BIOLOGY, MASSACHUSETTS INSTITUTE OF TECHNOLOGY

Communicated by John T. Edsall, November 3, 1962

It has been well established that the ribosomal particles are the site of protein synthesis, yet we have very little insight into the mechanism.[1] A great deal of attention has been directed toward the question of how the ribosomes contain the information necessary to effect the alignment of amino acids in a specific sequence. This problem has been resolved recently with the discovery of a rapidly metabolizing fraction of RNA, called messenger RNA, which has the ability to attach itself to the ribosomal particle and there to determine the sequence of amino acids.[2, 3] This view has been considerably reinforced by *in vitro* experiments in which naturally occurring RNA, as well as synthetic polyribonucleotides, have been shown to provide the information necessary to determine the sequence of amino acids in a polypeptide chain.[4, 5] Thus, the ribosome has a passive role in transmitting information; it can apparently polymerize a variety of proteins, depending upon the particular messenger RNA which is attached to it.

However, this state of affairs has puzzled many investigators for some time. The purely geometric aspects of the messenger RNA-ribosomal interaction leave several unresolved questions. For example, the polypeptide chains in the hemoglobin molecule each contain roughly 150 amino acids and, using a triplet code,[6] this implies a messenger of 450 nucleotides or a molecule 1,500 Å long if there is one nucleotide every 3.4 Å. How can this long polymer molecule transfer all of its sequence information to the ribosomal site at which the polypeptide chain is believed to grow? This becomes an even greater puzzle if one considers that much longer messenger RNA molecules have been found.[5] Indeed, the length is so great that it would almost be physically impossible for one ribosome 230 Å in diameter to interact with the entire messenger chain. However, Risebrough *et al.*[7] have shown that "heavy ribosomes" are seen in a sucrose gradient when labeled T2 messenger RNA is attached to *E. coli* ribosomes. More recently, several investigators[8–10] have reported that polyuridylic acid induces the formation of a rapidly sedimenting ribosomal peak when it is added *in vitro* to a cell-free bacterial extract. We have therefore been prompted to look for the possible existence of a larger multiple ribosomal structure *in vivo* which might provide insight into the detailed mechanism of protein synthesis.

In these experiments, we have used reticulocyte ribosomes because it is possible to break open the reticulocyte cell wall gently with a minimum of mechanical manipulation. This approach has been successful, and we have been able to demonstrate the existence of a multiple ribosomal structure held together by RNA. In

the reticulocyte, the predominant species contains five ribosomes. Furthermore, our experiments indicate that protein synthesis in the reticulocyte occurs only on this structure and not on a single ribosomal unit.

Materials and Methods.—Blood containing 80–90 per cent reticulocytes was collected by heart puncture from rabbits made anemic with phenylhydrazine as described by Borsook.[11] The cells were washed in a low magnesium saline (0.14 *M* NaCl, 0.005 *M* KCl, 0.0015 *M* $MgCl_2$) and then incubated at 37° in the presence of 0.2 mg/ml glucose, 0.12 mg/ml $NaHCO_3$, and 0.08 mg/ml Fe $(NH_4)_2(SO_4)_2$. After 15-min incubation, C^{14}-amino acids were added from an algal hydrolysate to a final concentration of 4 μc/ml. In one experiment, H^3 leucine was used. The reaction was stopped after 45 sec by the addition of cold saline. After centrifuging, the cells were gently lysed with two volumes of 0.0015 *M* $MgCl_2$ and then diluted with 3–5 volumes of standard buffer (0.01 *M* Tris, pH 7.4; 0.01 *M* KCl; and 0.0015 *M* $MgCl_2$). Cell walls and unbroken cells were removed by centrifugation at 10,000 × *g* for 15 min and the supernatant carefully decanted.

Linear sucrose gradients were made in Spinco SW 25 tubes using either 15 and 30 per cent w/w sucrose or 5 and 20 per cent w/w sucrose solutions containing the standard buffer. 1 ml of the lysate was layered on the sucrose gradient and centrifuged at 25,000 rpm (55,000 × *g*), for a 2-hr period at 5°C. At the end of the centrifugation, the bottom of the tube was punctured and the solution withdrawn by use of a finger pump and collected in 35–55 fractions. The optical density of the fractions was read at 260 mμ. After the addition of carrier serum albumin (0.1 mg/ml), the fractions were precipitated in trichloroacetic acid (5 per cent final concentration) and collected on Millipore filters. C^{14} radioactivity was counted in a Nuclear-Chicago low-background gas flow counter and tritium in a Packard Tricarb Scintillation Counter. C^{14} algal hydrolysate (1.6 mc/mg) and H_3 leucine (3.6 curies/millimole) were obtained from the New England Nuclear Corporation. Ribonuclease (RNAase, 3 × crystallized) and deoxyribonuclease (DNAase, 1 × crystallized) were obtained from Worthington Biochemical Company.

Results.—When the cell contents were isolated by gentle osmotic lysis, a characteristic sucrose density gradient pattern was produced, as in Figure 1(*a*). In addition to the large amount of hemoglobin that remained at the top of the tube, there are two optical density peaks, one sharp and the other heavier and broader. However, it is the heavy peak which contains all of the radioactivity that has sedimented appreciably from the meniscus. Occasional preparations which were handled less carefully produced sucrose gradients that showed some irregularities of the type illustrated in Figure 1(*b*). These will be discussed below. Similar results were

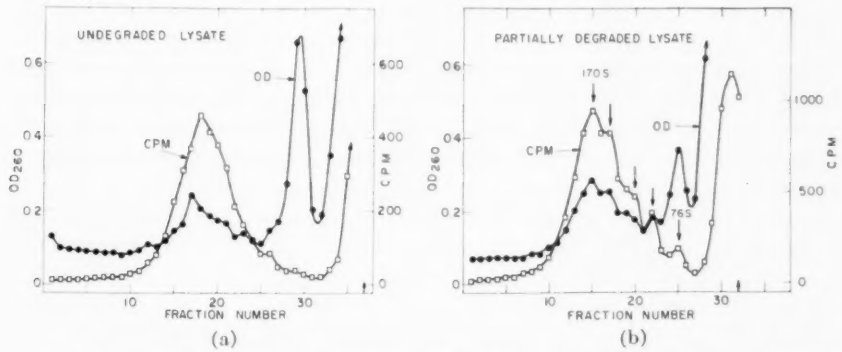

FIG. 1.—Sucrose gradients of lysed reticulocytes after a short incubation with C^{14} amino acids. 1 ml of lysate was layered on 25 ml of a 15–30 per cent sucrose gradient and then centrifuged (55,000 × *g*, 2 hr, 25° C). The short vertical arrow on the base line indicates the last fraction collected. The vertical arrows in the figure indicate peaks. (*a*) Undegraded lysate. (*b*) Partially degraded lysate.

obtained from experiments with a longer incubation period extending up to 20 min. Although there is some variation from one experiment to another, the light peak includes about 70 per cent of the area under the optical density curve, and yet it is totally inactive in the incorporation of amino acids. Since the light peak is so sharp, we conclude that the breadth of the heavy peak represents some heterogeneity, rather than spreading due to diffusion. The sedimentation constants of these peaks were determined in a Spinco Model E analytical ultracentrifuge with UV absorption optics. They were 76S for the small peak and 170S for the heavier peak. The light peak therefore corresponds to 78S ribosomes which have been isolated from reticulocytes by more vigorous methods.[1]

Ribosomes have been found attached to membranes[1] which sediment more rapidly than single ribosomes. Even though there is no endoplasmic reticulum in reticulocytes, experiments were carried out in which the lysate was incubated for 15 min with 0.5 per cent sodium deoxycholate, or 0.5 *M* NaCl. These have been shown to remove ribosomes from membranes,[1] but this treatment did not alter the 170S peak. In addition, no membranes were observed in the electron micrographs.

In order to make sure that we were examining the bulk of the nascent protein, the location of all radioactivity precipitable with trichloroacetic acid was determined (Table 1). After this short incubation time (45 sec), the ribosomes and soluble hemoglobin are about equally labeled and less than 7 per cent of the radioactivity sediments with the cell-wall fraction. Because there are often radioactive materials at the bottom of the tube after sucrose gradient centrifugation of the clarified lysate, a short centrifugation was carried out at low speed. However, no new peaks of optical density or radioactivity appeared, even though anything sedimenting as rapidly as 4,000S would have been seen. Thus, we can conclude that more than 85 per cent of the hemoglobin is being formed in the 170S peak, and this peak is therefore the site of protein synthesis *in vivo*.

From these initial experiments, we began to suspect that the 170S peak was a multiple ribosomal structure, perhaps held together by RNA. Since it is known that very small amounts of ribonuclease have a profound effect on protein synthesis *in vitro*,[12] it seemed likely that the enzyme might similarly affect the sites of synthesis *in vivo*. Therefore, an aliquot of clarified lysate was incubated at 4° for 1 hr with 0.25 μg/ml of ribonuclease and then layered on the gradient. A similar incubation and centrifugation was carried out with deoxyribonuclease at a concentration of 10 μg/ml. These results are shown in Figure 2. The deoxyribonuclease had no effect, while the ribonuclease almost completely destroyed the 170S peak, converting it to the more familiar single ribosomes. The nascent protein, however,

TABLE 1

Cell fraction	CPM	Per cent total count
Cell walls and unlysed cells	3,980	6.6
Ribosomes	28,200	47
Soluble fraction (hemoglobin)	28,000	46.4

0.75 ml of cells were incubated with C^{14} algal hydrolysate for 45 sec, then chilled, washed, and lysed as described in *Methods*. Cell walls were centrifuged at 10,000 × *g* for 15 min and the supernatant carefully decanted. The cell-wall pellet was resuspended in 4.5 ml buffer and again centrifuged for 15 min at 10,000 × *g*, and the supernatant was added to the first supernatant. Ribosomes were collected from the supernatant by centrifuging at 35,000 rpm for 60 min in a Spinco SW 39 rotor and the supernatant (soluble fraction) decanted. Protein from each fraction was purified by a modification of the procedure of Siekevitz[20] and plated on Millipore filters, and the radioactivity was counted. All counts were corrected for self-absorption.

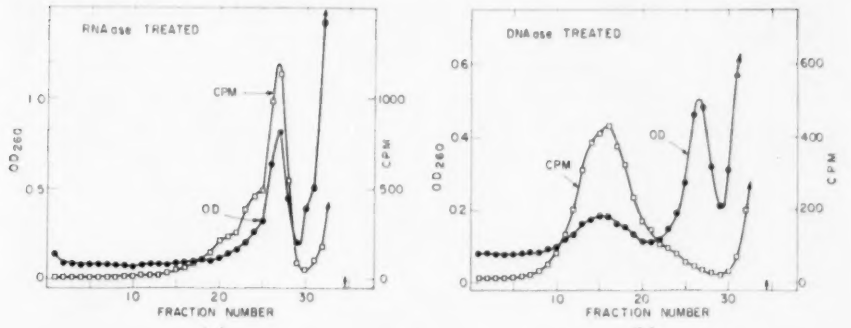

FIG. 2.—Sucrose gradients of reticulocyte lysate as in Figure 1 but incubated at 4°C for 1 hr with (*a*) 0.25 μg/ml RNAase—the 170*S* peak has disappeared and the radioactivity is now in the 76*S* peak, (*b*) 10 μg/ml DNAase—the 76*S* and 170*S* peaks are unchanged from Figure 1.

remained firmly attached to the single ribosomes. Higher concentrations of ribonuclease destroyed even the leading edge of the 78S peak. These experiments suggested that the heavy peak consisted of a multiple ribosome structure held together by RNA. We have called this a "polyribosome" or, a "polysome."

In general, ribosomes are very sensitive to the ionic environment and, in particular, to the concentration of Mg^{++} ions. In order to test the polysome structure for such sensitivity, a clarified lysate was dialyzed for 6 hr against three changes of a thousand-fold volume of 0.01 *M* Tris, pH 7.4, 0.01 *M* KCl, $5 \times 10^{-5} M$ $MgCl_2$. It was then layered on a 15–30 per cent sucrose gradient containing this low Mg^{++} buffer and centrifuged for 2 hr. This treatment had no effect on the centrifugal pattern and the results were the same as in Figure 1(*a*). However, when the lysate was made 0.01 *M* in ethylenediamine tetraacetate, both the polysome peak and the ribosome peak broke down to smaller units of 50S and 30S and most of the nascent protein was stripped off. Thus, in its reaction to changes in Mg^{++} concentration, the polysome resembles the "active" 70S ribosomes from *E. coli*.[4, 12]

In order to compare our results with earlier ribosome data, some experiments were done to test other techniques for preparing ribosomes. After either freeze-thawing or alumina grinding, the usual methods for preparing bacterial ribosomes, most of the optical density and nascent protein appeared in the 76S peak with no evidence of the polysomal structure. Therefore, the polysome is relatively fragile. Some indication of this fragility is suggested in Figure 1(*b*), where some fine structure begins to appear in the region between the 76S and the 170S peak. This is seen more clearly when the normal procedure is used for isolating reticulocyte ribosomes. To purify them, the ribosomes are usually centrifuged, the supernatant decanted, and the ribosomal pellet suspended free of hemoglobin. To study the effects of such treatment on the polysome structure, ribosomes from clarified lysate were pelleted and resuspended three times. The result is shown in Figure 3. Five peaks are clearly evident, both of radioactivity and of optical density. Once again, the heaviest peak has migrated about two and a half times as far as the lightest peak. Two considerations argue against this result being an artifact due to nonspecific aggregation during pellet formation. In the first place, the specific activity of the four heaviest peaks is nearly constant, while that of the lightest peak is much lower.

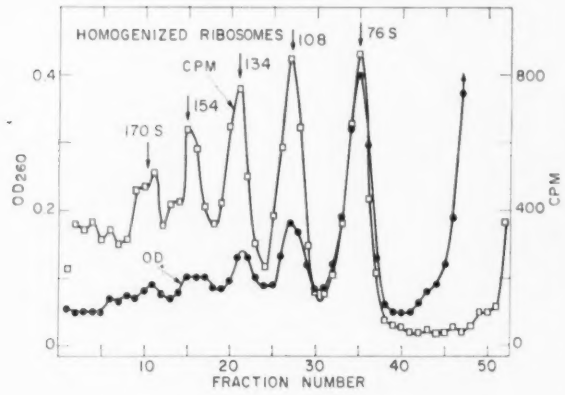

FIG. 3.—Sucrose gradient of lysed reticulocytes after incubation with H^3 leucine. After lysis and low-speed centrifugation, the ribosomes were pelleted three times at 28,000 rpm and resuspended with a homogenizer, as described in *Methods*. A 5–20 per cent sucrose gradient was used. The numbers next to the arrows represent the sedimentation constants associated with each peak.

This is what would be expected if the polysomes were being degraded by steps to monomers. In addition, we have already seen indications of these intermediate peaks in preparations that were never centrifuged into a pellet (Figure 1 (*b*)). By calibrating the sucrose gradient with the 76S and 170S peaks, we could assign S values to the intermediate peaks (108S, 134S, 154S). It is of interest that three earlier papers have presented evidence for these additional peaks without realizing their origin.[13–15]

The regularity of the increments in sedimentation constant clearly suggested that we were observing a sequence of quantized steps in the disintegration of a multiple ribosomal structure, starting from the 170S peak and terminating in the 76S ribosome. The simplest hypothesis is that each new peak is created by the elimination of one ribosomal unit from the polysomal structure. By simple enumeration, we anticipated that the 170S peak should be a pentamer, and this was readily confirmed by studies in the electron microscope. Electron micrographs of shadowed preparations are shown in Figure 4(*a–c*). Figure 4(*a*) shows a typical field of 76S ribosomes, which have a diameter of approximately 230 A. Figure 4(*b*) shows a field taken from the trimer peak (134S), and it can be seen that most of the ribosomes are present as triads. Figure 4(*c*) shows a typical polysomal field from the 170S peak. Here, most of the clusters contain five ribosomal units, although occasional tetramers or hexamers are seen. A common configuration seen in the air-dried preparations is a tightly clumped group. In the air-dried preparation, the center-to-center distance between the ribosomal subunits is usually 300 to 350 Å, although frequently it is somewhat longer. In some cases, it is possible to see a thin fiber of diameter 10–20 Å connecting two adjacent ribosomes. Staining with uranyl acetate resulted in positive staining; occasionally, a thin thread of high electron density could be seen running between two ribosomal units in the polysome structure. The separation between the ribosomes was usually more clearly resolved in the preparations that were stained with uranyl acetate or phosphotungstic acid. A full description of these results will be published elsewhere.[16]

Discussion.—The evidence presented above clearly points to the polysomal structure as the site of protein synthesis. Earlier experiments in which the ribosomal monomers were isolated by more vigorous procedures, including the formation of

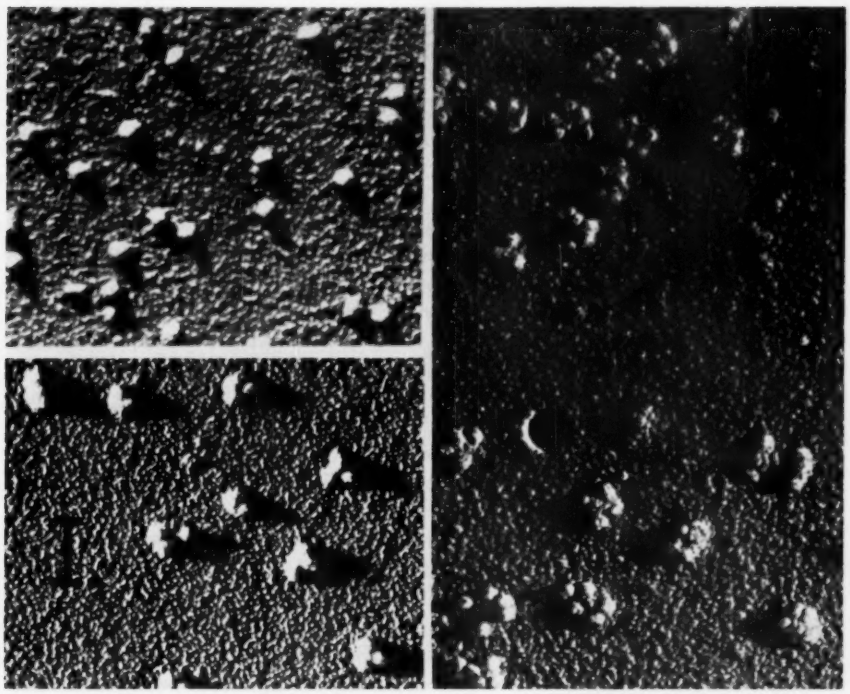

FIG. 4.—Electron micrographs of reticulocyte ribosomes. The ribosomes were deposited on the grid as a droplet from the sucrose gradient, rinsed with buffer, and air-dried. The Pt shadowing was at a 5:1 angle. The vertical mark indicates 0.1μ. (*a*) Upper left—droplet from the 76*S* peak. (*b*) Lower left–droplet from the 134*S* peak showing triplets of ribosomes. (*c*) Right—droplet from the 170*S* peak showing several ribosome pentamers. (Photographs courtesy of C. E. Hall.)

hard pellets and their resuspension, resulted in degradation which suggested that the nascent protein was associated with the 76S particle.[13] Directly this leads us to ask whether such polysomal structures exist in other cells as well. We are inclined to believe that this is the case, even though complete evidence is not available as yet. Palade observed long strings of ribosomes in thin slices made from a ribosomal pellet of guinea pig pancreas.[17] In addition, Risebrough *et al.*[7] have studied the interaction of T_2 virus messenger RNA and *E. coli* ribosomes. Their sucrose density gradient patterns show evidence for the existence of ribosomal dimers, trimers, and even small amounts of tetramers. It is quite likely that the adoption of more gentle preparative procedures will reveal even larger units in bacteria. Langridge and Holmes[18] have shown that ribosomes can apparently form linear aggregates in concentrated gels. It remains to be seen if this is related in some way to polysome formation.

Four lines of evidence suggest that the ribosomal units are held together by RNA, possibly a single strand. Mild treatment with ribonuclease results in dissociation to the ribosomal units; the mechanical fragility of the polysome suggests that the structural link is not large; the 10–20 Å threads seen in the electron micrographs are consistent with a single RNA strand; finally, these threads stain posi-

tively with uranyl acetate, which is known to react with nucleic acids. Somewhat less direct evidence suggests that the ribosomes are held together by messenger RNA. As mentioned above, the attachment of labeled T_2 messenger RNA to *E. coli* ribosomes leads to the formation of ribosomal aggregates with high *S* values.[7] Ribonuclease also breaks up that polysomal structure. In addition, the attachment of synthetic messenger RNA, polyuridylic acid, results in the formation of aggregates with large *S* values.[8-10] The simplest interpretation for all of these experiments is that the long thread of messenger RNA is attached to several ribosomes, five being the predominant number for hemoglobin synthesis. By comparing the center-to-center distance between ribosomes with their diameter, we note that there is a 50–100 Å spacing between ribosomes. Five ribosomal diameters plus these spacings have an overall length near the 1,500 Å which is the anticipated length for a messenger RNA strand coding for approximately 150 amino acids. However, further work will be needed to define the exact length of the hemoglobin polysome.

The width of the 170S peak suggests that it may include other species than the pentamer. A qualitative survey of electron micrographs confirms this, since tetramers as well as hexamers are seen. Air drying is known to produce an artificial clumping; accordingly, we cannot say much about the polysome configuration. We believe it to be a linear structure with considerable flexibility because the ribosomes are separated by short stretches of flexible RNA. However, we cannot exclude a circular arrangement.

Let us assume for the moment that a strip of messenger RNA has five ribosomal units attached to it. It has been shown by Dintzis[19] that the polypeptide chain grows sequentially from the amino to the carboxyl end. Since the ribosomes are slightly separated, it is most reasonable to assume that the growing polypeptide chain remains attached to an individual ribosome rather than skipping from one ribosome to the next. Since the ribosome must use the sequence information in the messenger RNA to govern the assembly of amino acids, it follows that the messenger RNA strand must move in some fashion relative to the ribosome. The possibility of such a ribosomal movement was first raised by Gilbert[8] in connection with his experiments on polyphenylalanine synthesis in an *E. coli* cell-free extract. A tentative view which we can adopt is that ribosomal particles begin protein synthesis by attaching to one end of a messenger RNA strand and then move along it as the polypeptide chain lengthens. If the messenger strip is very long, a correspondingly greater number of ribosomes will be attached at any one time. When the ribosomes reach the end of the strand, they release the polypeptide chain as well as the RNA. Thus, the released ribosome would contribute to the pool of inactive 76S monomers which we observe.

Of course, such a model raises questions. For example, what makes the ribosome flow over the messenger RNA strand? Is it possible that there is an energy-consuming mechanism, perhaps distantly related to that which occurs in muscle contraction? However, in addition to raising questions, such a model gives rise to some suggestions. For example, this represents a very efficient use of messenger, since several ribosomes are operating on it at the same time. It is possible that the hemoglobin messenger RNA may be stabilized by its five ribosomes. A new ribosome may attach just as another ribosome falls off at the other end with its completed chain. If these two events do not occur simultaneously, a certain

number of tetramers or hexamers will form; this might account for the broad spread observed in the 170S peak. In addition, the mechanism described above raises the possibility that related groups of proteins are all manufactured at the same time. Thus, one genetic locus in the β-galactosidase system controls the production of a series of enzymes. If one long piece of messenger RNA was produced containing the information for all of these enzymes, ribosomes flowing over this strip might then produce the entire group of enzymes, one after another. Much of this is speculation at the present time, since it is based on the assumption that a messenger RNA strand passes through the five ribosomes. In any case, the demonstration that protein synthesis occurs in a polysomal structure will undoubtedly enhance our understanding of the function of the ribosome.

Summary.—It has been demonstrated that protein synthesis in the reticulocyte takes place in a multiple ribosomal structure containing five ribosomes. These ribosomes appear to be held together by an RNA strand, probably messenger RNA. The mechanism of protein synthesis is discussed in light of these observations.

We would like to thank C. E. Hall and Marsha Glynn for their assistance in obtaining electron micrographs. We acknowledge the capable technical assistance of Melissa Quinn. This research was supported by research grants from the National Institutes of Health and the National Science Foundation.

* Predoctoral Fellow of the National Science Foundation.

† Present address: MRC Laboratory of Molecular Biology, Cambridge, England.

[1] A review of ribosomal properties is published by Ts'o, P. O. P., *Ann. Rev. Plant Physiol.* **13,** 45 (1962).

[2] Gros, F., H. Hiatt, W. Gilbert, C. G. Kurland, R. W. Risebrough, and J. D. Watson, *Nature,* **190,** 581 (1961).

[3] Brenner, S., F. Jacob, and M. Meselson, *Nature,* **190,** 576 (1961).

[4] Nirenberg, M. W., and J. H. Matthaei, these PROCEEDINGS, **47,** 1588 (1961).

[5] Tsugita, A., H. Fraenkel-Conrat, M. W. Nirenberg, and J. H. Matthaei, these PROCEEDINGS, **47,** 846 (1962).

[6] Crick, F. H. C., L. Barnett, S. Brenner, and R. J. Watts-Tobin, *Nature,* **192,** 1227 (1961).

[7] Risebrough, R. W., A. Tissières, and J. D. Watson, these PROCEEDINGS, **48,** 430 (1962).

[8] Gilbert, W., personal communication.

[9] Spyrides, G., and F. Lipmann, these PROCEEDINGS, **48,** 1977 (1962).

[10] Barondes, S. H., and M. W. Nirenberg, *Science,* **138,** 813 (1962).

[11] Borsook, H. C., L. Deasy, A. J. Haagen-Smit, G. Keighley, and P. H. Lowy, *J. Biol. Chem.,* **196,** 669 (1952).

[12] Tissières, A., D. Schlessinger, and F. Gros, these PROCEEDINGS, **46,** 1450 (1960).

[13] Wallace, J. M., R. F. Squires, and P. O. P. Ts'o, *Biochim. et Biophys. Acta,* **47,** 130 (1960).

[14] Arnstein, H. R. V., *Biochem. J.,* **81,** 24 P.

[15] Lamfrom, H., and E. R. Glowacki, *J. Mol. Biol.,* **5,** 97 (1962).

[16] Warner, J. R., A. Rich, and C. E. Hall, *Science* (in press).

[17] Palade, G. E., in *Microsomal Particles and Protein Synthesis* (New York: Pergamon Press, 1958), p. 36.

[18] Langridge, R., and K. C. Holmes, *J. Mol. Biol.* (in press).

[19] Dintzis, H. M., these PROCEEDINGS, **47,** 247 (1961).

[20] Siekevitz, P., *J. Biol. Chem.,* **195,** 549 (1952).

*ASPECTS OF CONTROL OF PROTEIN SYNTHESIS IN NORMAL AND REGENERATING RAT LIVER, I. A CYTOPLASMIC RNA-CONTAINING FRACTION THAT STIMULATES AMINO ACID INCORPORATION**

By Mahlon B. Hoagland and Brigitte A. Askonas†

DEPARTMENT OF BACTERIOLOGY AND IMMUNOLOGY, HARVARD MEDICAL SCHOOL, BOSTON

Communicated by Herman M. Kalckar, November 15, 1962

The discovery of messenger RNA and the concept of control of protein synthesis by repression have laid the groundwork for understanding the chemistry of information transfer and its control in bacteria.[1, 2] The present work was initiated to determine whether such mechanisms operated in higher organisms and whether they could be studied in cell-free preparations.

We chose to examine certain properties of the cell-free protein-synthesizing system of rat liver as an approach to these problems. The ability of the liver to regenerate in response to partial hepatectomy supplies a valuable comparative system: the heightened protein synthetic activity of the regenerating liver may be compared with that characteristic of the normal adult state with respect to the occurrence of messenger RNA and possible cytoplasmic and nuclear control mechanisms.

The present paper is a more definitive account of work previously reported.[3] A number of reports have since appeared of the occurrence in animal cells of a nuclear RNA fraction having turnover and sedimentation properties similar to those of bacterial messenger RNA (see *Discussion*). The studies recounted here indicate that liver cytoplasm contains a fraction having certain properties in common with messenger RNA including the ability to stimulate the *in vitro* amino acid incorporation system. The paper to follow presents evidence that microsomes from normal liver are intrinsically less responsive to the messenger-like fraction (and to other manipulations of their *in vitro* environment) than are those from regenerating liver. This difference in microsomal responsiveness appears to be due to the presence in the normal system of a dissociable inhibitor which renders microsomes from either normal or regenerating liver less active *in vitro*.

Materials and Methods.—Female Sprague-Dawley rats (Charles River Breeding Company), weighing 250–300 gm, were used for the experiments. Partial hepatectomies, removing approximately 65 per cent of the liver, were performed according to the technique of Higgins and Anderson.[4] The animals were killed by decapitation 20 to 24 hr later, and the livers were excised and immediately chilled. Normal rats of the same stock and weight were used in comparative studies. All animals were deprived of food for 20 to 24 hr before killing.

Preparation of cytoplasmic fractions: The livers were homogenized in two volumes of a medium containing: tris (hydroxymethyl) amino methane (Tris) buffer (pH 7.3) 0.1 M· $MgCl_2$ 0.005 M; sucrose 0.15 M; KCl 0.0025 M; and 3-mercaptoethanol 0.005 M. Microsomes (M) were prepared from a 15,000 gm supernatant fraction by centrifugation at 100,000 g for 1 hr. The microsomal supernatant fraction was then further centrifuged at 105,000 g in the Spinco No. 40 rotor for 12–13 hr. The resulting pellet, after suspension in medium, is referred to as the X fraction. The supernatant solution from this centrifugation was used to prepare a pH 5 fraction by diluting it with an equal volume of water, adding 1 N acetic acid to pH 5.2, collecting the resultant precipitate, suspending it in distilled water, and, after recentrifugation, dissolving it in medium. This fraction is referred to as the pH 5(−X) fraction; it differs from the usual pH 5 fraction in that it lacks X. All operations were performed in the cold. All three fractions were stored at −70°C, the M and X fractions as pellets and the pH 5(−X) redissolved in medium. Under these con-

ditions, they retained their activity for at least 2–3 weeks. All quantities of fractions are expressed as gram equivalents (gm eq): i.e., the wet weight of liver from which the particular fraction was derived. In our hands, fractions from equal weights of normal and regenerating liver were equal in RNA content (within 15 per cent). With all fractions, the subscripts N and R, following their abbreviated designation, refer to the source—normal or regenerating liver. The standard assay system used throughout these experiments contained half the concentration of the medium components given above except for KCl, whose final concentration was 0.07 *M*. The following added components were present in a total volume of 1.0 ml: 0.15 gm eq *M*; 0.2 gm eq pH 5(−X); 10 μmoles of phosphoenolpyruvate; 0.5 μmoles of GTP; 0.5 μmoles of ATP; 50 μgrams of pyruvate kinase; and 0.025 μmoles of C^{14}-leucine containing from 8 to 10×10^4 cpm. The excess gm eq of pH 5(−X) fraction was found to be adequate to insure that this fraction was not limiting. Incubations were carried out for 30 min at 37°C, and the reaction was stopped by addition of 5 ml of 4 per cent trichloracetic acid. Proteins were washed with hot trichloracetic acid and lipid solvents,[5] plated on aluminum planchets from ether, dried, and counted in a Nuclear Micromil window gas flow counter. In experiments where *in vivo* P^{32} labeling of the RNA of the above fractions was determined, the P^{32} (200 μc) was injected intraperitoneally at various times before killing. The RNA from the fractions obtained was extracted and counted essentially as described by Hecht *et al.*[6]

Fractionating and extraction techniques: A DEAE-Sephadex column was used to remove soluble RNA from the X fraction. DEAE-Sephadex (grade A-25, coarse) from Pharmacia, Sweden, was washed briefly with 0.1 *N* HCl and distilled water, treated for 10 min with 0.5 *N* NaOH, and then washed to neutrality with water containing several drops of dilute HCl. The Sephadex was equilibrated with 0.05 *M* Tris buffer, pH 6.9, and columns were prepared by permitting the Sephadex to settle by gravity. The buffer used for the final column contained 0.05 *M* Tris pH 6.9, 0.001 *M* $MgCl_2$, and 0.001 *M* 3-mercaptoethanol, and columns were washed with cold buffer under slight air pressure before use. Concentrated X fraction (from 3 to 4 gm of liver, suspended in 0.5 ml of the above buffer) was loaded onto a column (1 × 8 cm), permitted to sink in, and washed through with the above cold buffer. A large part of the protein and the stimulatory activity were not adsorbed onto the column—and were eluted with the buffer front which was easily recognized by its yellowish color. About 90 per cent of the material passing through the column could be collected in a volume of 2 ml (as verified by absorption density of the collected fractions at 260 and 280 mμ). Although the column was run at room temperature, the X material was kept as cold as possible by the use of ice-cold buffers and cold collecting tubes.

RNA was extracted from X fraction by the following modification of the phenol method. The X pellet from 4 gm of liver was dissolved in 1 ml of medium and extracted with an equal volume of redistilled phenol previously saturated with the medium. The emulsion was stirred for 10 min at 15°C, and all subsequent handling was done at +3°C. The emulsion was centrifuged for 10 min at 5,000 *g*, the aqueous layer removed, and extracted five times with several volumes of ether. Ether was removed from the solution by bubbling nitrogen through it for 10 min. The absorption density (per ml) of the resulting RNA solution was about 14–20 at 260 mμ, with a 260/280 ratio of 2. This procedure recovers about 80 per cent of the RNA present in the X pellet. Crystalline ribonuclease, deoxyribonuclease (highest grade), and trypsin were Worthington Chemical Company products. Adenosine and guanosine triphosphates were obtained from Sigma Chemical Company, phosphoenolpyruvate and pyruvate kinase from California Biochemical Corporation, and L-leucine-1-C^{11} (~25 mc/m mole) from New England Nuclear Corporation. RNA was determined spectrophotometrically after partial alkaline hydrolysis, using an extinction coefficient at 260 mμ of 31.8 cm^2/mg (cf. ref. 6). Sucrose gradients were prepared and used according to the method of Britten and Roberts.[7]

Results.—It has previously been noted[8, 9] that the soluble components of the *in vitro* incorporation system from regenerating liver are more active than those from normal liver. It has been suggested that the difference is due in part to levels of activating enzymes.[9] In our hands, however, pH 5(−X) fractions which contain most of the soluble RNA and activating enzymes exhibited essentially the same activity whether prepared from normal or regenerating livers. The activity was measured both by over-all incorporation of amino acids into microsomal protein and

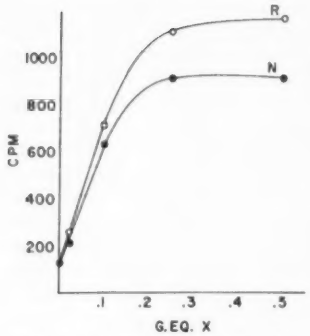

FIG. 1.—Effect of X fractions from normal (N) and regenerating (*R*) liver on microsomal protein synthesis. Assay conditions were as described in the text, using 0.2 gm eq pH $5(-X)_{R,N}$ and 0.15 gm eq M_R. Radioactivity in counts per min represents the C^{14}-leucine incorporated into the total protein of the system after correction for self-absorption of samples.

by adenosine triphosphate-dependent attachment of amino acids to soluble RNA. Hence, in the following experiments we have simply pooled the pH $5(-X)$ fractions from normal and from regenerating livers (designated pH $5(-X)_{R,N}$).

The present paper deals with the properties of the X fraction. The X pellet is a brownish-red, hard-packed, translucent sediment which contains both RNA and protein. In a typical preparation the RNA content of various fractions (in mg per gm eq of liver) was: 15,000 *g* supernatant, 2.24; microsomes, 2.09; X, 0.16; and pH $5(-X)$, 0.09. The quantity of RNA in equivalent normal and regenerating fractions is approximately equal (± 15 per cent).

Figure 1 shows the effect of adding increasing amounts of X_N and X_R to the assay system. Maximal stimulation was generally achieved when X was present in a 1.5- to 2-fold tissue equivalent excess. We have consistently found that X_R has more activity (20 to 30 per cent in this figure) than X_N, on the basis of either tissue equivalence of RNA content. It should also be noted that the curves attain and maintain different maxima, a finding inconsistent with the postulate that there is simply a different quantity of stimulatory component(s) in X fractions from the two sources. It suggests that X_N may contain in addition a factor limiting its stimulatory capacity. The nature of this inhibitory activity is the subject of a paper to follow.

In the absence of microsomes, the X fractions have no intrinsic incorporating ability when supplemented with pH $5(-X)$ and cofactors. X activity is, as mentioned previously,[3] precipitable at pH 5. Owing to the prolonged centrifugation required to clear the supernatant of X, amino acid-activating enzymes and soluble RNA are present in this fraction (as measured by adenosine triphosphate-dependent amino acid labeling of RNA). It is for this reason that X is assayed in the presence of nonlimiting levels of pH $5(-X)$ fraction. Under the conditions described in the *Methods* section, DEAE Sephadex adsorbs about 85 per cent of the RNA in the X fraction. However, the material passing through the column at neutrality gives the same degree of stimulation of microsomes (per gm eq) as the original X fraction. The presence of pH $5(-X)$ fraction is required for this stimulation, indicating that the bulk of the soluble RNA has been removed by the column. The use of buffered concentrated KCl (0.5–0.8 *M*) elutes a large part of the RNA from the column.[10] No stimulatory activity could be demonstrated when this RNA (following dialysis) was added to the assay system consisting of microsomes and pH $5(-X)$. Finally, it was ascertained that following passage through the column the residual RNA is unable to bind amino acids in the presence of ATP, though added transfer RNA was rapidly labeled by the preparation. It would thus appear that transfer RNA is retained by the column, while amino acid-activating enzymes and the material responsible for X activity pass through.

RNA extracted directly from X by the phenol method has stimulatory activity (Fig. 2, curve labeled X). Attempts to extract active RNA from the DEAE Sephadex column effluent of X were unsuccessful, but the amount of RNA was very small. These RNA derivatives of X, however, never give the degree of stimulation of the system obtained with the native X or the column effluent of X.

Figure 2 also shows the stimulatory effects of RNA preparations from other sources: bacterial (B), tumor (T), and liver nuclear (N). The results show that heterologous RNA also is able to affect the assay system, although bacterial RNA appears to be less effective than RNA from animal sources. Soluble RNA was essentially inactive in the system, and in concentrations above 100 μg/ml it was inhibitory. Whole ribosomal RNA gave the same degree of stimulation as X-RNA if supplied in high enough concentration (150 μg/ml).

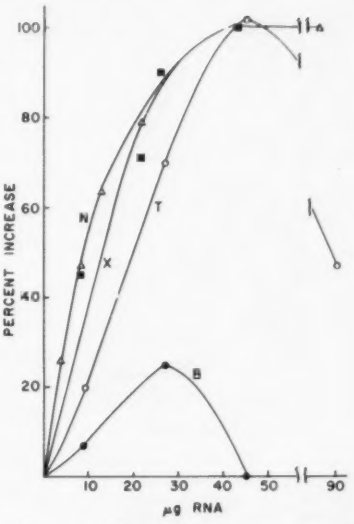

FIG. 2.—Stimulation of amino acid incorporation into protein by phenol-extracted RNA from X and from other tissue fractions. RNA samples were assayed using 0.15 gm eq M_R and 0.2 gm eq pH $5(-X)_{R.N}$ as described in the text. The data are plotted as per cent increase in radioactivity (C^{14}-leucine incorporated into total protein in the system).

RNA was extracted as described in the text from: ■ X fraction from regenerating liver; △ the 1,000 *g* sediment of liver homogenate (containing mainly nuclei and whole cells); ○ a homogenate of mouse plasma cell tumor RPC-5 obtained from M. Potter, National Cancer Institute, Bethesda; and ● bacteria (*E. coli*).

The stimulatory effect of the RNA extracted from X is labile to low concentrations of ribonuclease, as shown in Figure 3. It is of considerable interest that native X, or the column effluent of X, is remarkably insensitive to ribonuclease. Thus, treatment of the native X suspension with as much as 40 μg of ribonuclease per ml (for 5 min at 37°C) has no observable effect on the stimulatory activity of the RNA subsequently extracted from it by the phenol method. This is in marked contrast to the extremely high sensitivity of the microsomes to RNase, which will be discussed in a subsequent publication. DNase has essentially no effect on the activity of the complete system at levels of 0.5 μg/ml, and small variable effects (± 5–20 per cent) at levels of 5.0 μg/ml (30 min at 37°C). (There is no detectable DNA in the fractions used in these experiments.) Trypsin (for 30 min at 37°C) has no effect on the complete system at 0.5 μg/ml, but at 5.0 μg/ml it causes 64 per cent inhibition. This latter effect, taken together with the failure of the active material to be adsorbed by the column, its resistance in the native state to ribonuclease, and the failure of the RNA to account for all the X activity, suggests that the RNA is not free but complexed and that there may be an additional protein component important for its biological action.

We next undertook to determine whether the RNA of the X fraction became labeled more rapidly *in vivo* than other cytoplasmic RNA fractions. At intervals preceding the killing of animals whose livers were regenerating, they were exposed

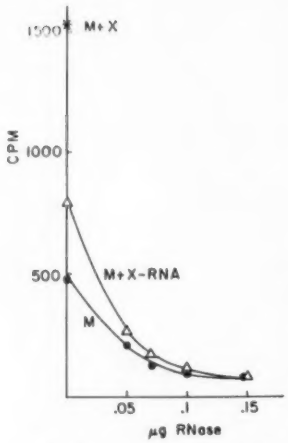

FIG. 3.—Ribonuclease sensitivity of X-RNA stimulation of amino acid incorporation into protein. Varying amounts of ribonuclease (RNase) alone (●) and with 40 μg of RNA extracted by phenol from X (△) were preincubated for 8 min at 37°C. The usual assay system was then added; radioactivity as cpm represents the C^{14}-leucine incorporated into protein. The point marked "*M* + *X*" is the stimulatory effect of the native X fraction from which the RNA was derived.

to P^{32} (see *Materials and Methods*) and the rate of uptake of P^{32} into the three RNA-containing fractions was measured. Figure 4 depicts the results of such an experiment. In spite of the crude nature of the X fraction it does appear to incorporate P^{32} into its RNA at a more rapid rate than does the soluble RNA of the pH 5(−X) fraction or the ribosomal RNA.

If the microsomes from such P^{32}-labeled livers are suspended in a small volume of water, incubated at 37° for 5 min, and resedimented for an hr at 100,000 *g*, the resulting supernatant contains RNA that is also labeled more highly than microsomal or soluble RNA (Fig. 4, curve labeled M_s). RNA derived from this (M_s) fraction by the phenol method has stimulatory activity comparable to X-RNA in the M, pH 5(−X) assay system. Equal amounts of this active material are obtained from normal and regenerating liver microsomes.

X fractions from such P^{32}-labeled animals have been passed through DEAE-Sephadex columns to reduce their soluble RNA content and then centrifuged through sucrose gradients in attempts to locate a P^{32}-labeled peak coinciding with the peak of biological activity. As previously reported,[3] sucrose gradients of X do show peaks of stimulatory activity in regions corresponding roughly to S values below 20. Figure 5 shows the outcome of two such experiments. It is clear that there is considerable stimulatory activity over the upper third of the gradient under the conditions employed and that its distribution does not conform to the distribution of the bulk of the 260 mμ absorption (a part of which, according to 280/260 ratios, is due to protein). The distribution of P^{32}, furthermore, follows the 260 mμ absorption, indicating that in spite of the removal of most of the transfer RNA by the column, some RNA (perhaps protein bound) remains and contributes largely to the P^{32} peak. However, there is a shoulder of P^{32}-labeled material that appears to coincide with the major areas of stimulatory activity. Attempts to increase the amount of this peak relative to the larger peak by shorter periods of exposure to P^{32} have thus far been unsuccessful. The activity would appear, then, to be associated with material larger than soluble RNA, but generally of lower sedimentation coefficient than messenger RNA in bacteria.

Gradients performed on phenol-extracted X-RNA gave broad bands of activity extending from the 15S region to material smaller than 4S. The 260 mμ-absorbing material in such gradients in the 4S region could not be labeled with amino acids. Hence, the active material in this fraction does not appear to include transfer RNA.

Discussion.—The X fraction appears to contain important components of the amino acid incorporation system of rat liver. It stimulates incorporation *in vitro*, part of its activity being in a fraction with higher sedimentation rate than transfer

RNA. Phenol extraction yields an RNA moiety that is labeled more rapidly *in vivo* than transfer or ribosomal RNA and that retains some of the *in vitro* stimulatory activity of the native X fraction. A fraction having similar properties may be obtained by water extraction of microsomes.

Though the active material in X resembles bacterial messenger RNA in several respects, it is insensitive to ribonuclease in the native state, and it does not behave like free RNA or DEAE-Sephadex columns. The failure of the RNA alone to give as high a stimulation as native X suggests either that more than one factor accounts for the X effect or that the RNA is damaged in the process of isolation. The native fraction may contain transfer enzymes such as those described by Nathans and Lipmann[11] and Grossi and Moldave.[12]

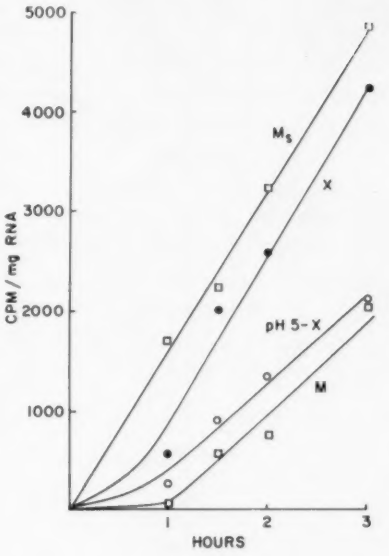

FIG. 4.—Rate of incorporation of P^{32} into liver cytoplasmic RNA fractions *in vivo*. Rats were killed 24 hr after partial hepatectomy. A pair of animals was used for each time point, being exposed to 200 μc of P^{32} for the time indicated before killing. Cytoplasmic fractions, i.e., microsomes, 13 hr X pellet, and pH 5(−X), were prepared. A portion of the microsomes (corresponding to about 2 gm of liver) was washed in the buffered medium and then treated with 5 ml. of water for 5 min at 37°C. The microsomes were then reisolated by spinning for 2 hr at 100,000 *g*. RNA was salt-extracted (as described in the *Methods* section) from the microsomal water extract (M_s), the stripped microsomes (M), X pellet, and pH 5(−X).

As mentioned earlier, numerous recent studies suggest that there is a nuclear RNA fraction in animal cells having turnover and sedimentation properties similar to those of bacterial messenger RNA. Thus, Cheng has found such a fraction in human amniotic cells;[13] Sibatani *et al.*, in thymus nuclei;[14] Hiatt, in rat liver nuclei;[15] Marks *et al.*, in white blood cells;[16] and Scherrer and Darnell, in HeLa cells.[17] These fractions have not been found to have biological activity. Amos and Kearns have reported that whole bacterial RNA stimulates the production of protein, immunologically identified as bacterial, by chick fibroblasts in tissue culture.[18] Niu *et al.*[19] have observed the synthesis of liver enzymes by ascites tumor cells exposed to whole liver RNA. It has also been reported that RNA polymerase activity increases in the rat liver following the induction of regeneration.[20] We have found that the high-turnover nuclear RNA fractions obtained by Hiatt (and supplied to us by him) are inactive in our system. (This might be due to the use of sodium dodecyl sulfate in their isolation.) As noted in Figure 2, a phenol-extracted RNA from crude liver nuclei gives as good stimulation as X-RNA and is, in fact, obtained in larger amounts from nuclei than from cytoplasm.

The paucity of evidence for a rapidly labeled *cytoplasmic* RNA fraction (excepting the data shown in Fig. 4) may be explained by assuming that in animal cells there is a small cytoplasmic pool that is replenished with a lag. It may be that in cells of higher organisms, with a nuclear membrane, messenger RNA accumulates in the

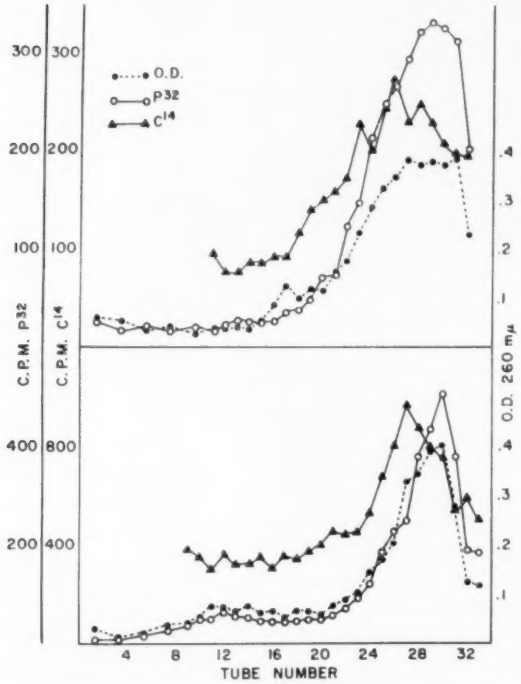

FIG. 5.—Distribution of P^{32} and stimulatory activity of X on sucrose gradients. X was prepared from regenerating livers from rats injected 1.5 hr previously with 200 μc P^{32} intraperitoneally. X was treated with DEAE Sephadex as described in the *Methods* section and 1.2 ml, equivalent to 3 gm of liver, was layered onto a sucrose gradient. A linear gradient of 5 to 20% sucrose, containing the buffered medium, was used. The gradient tube was centrifuged for 5 hr at 25,000 rpm in the swinging bucket rotor Spinco type SW-25. 33 fractions of 0.71 ml each were collected, tube #1 representing the bottom of the gradient. 0.2 ml of each was used for determining absorption at 260 mμ (●) and cpm due to P^{32} (○). 0.3 ml of each gradient fraction was assayed for stimulatory effect on protein synthesis using regenerating microsomes (0.15 gm eq) and pH 5(−X) (0.2 gm eq). ▲ shows incorporation of C^{14}-leucine into protein. Two separate experiments are shown.

nucleus and is supplied to the cytoplasm only after a delay. Our results further suggest the possibility that outside the nucleus the messenger may be bound to protein. It is of interest that an RNA with turnover and specific stimulatory activity very similar to X may be extracted from the microsomes.

Since the RNA in X is only about 5 per cent of the total cytoplasmic RNA and the active material of X is present in at most 15 per cent of its RNA, there is probably very little of this material normally present in the cytoplasm.

It would appear that the X fraction accounts in part for the enhanced activity of soluble fractions from regenerating, as compared with normal, liver.

Summary.—Evidence is presented for the occurrence in rat liver cytoplasm of an RNA-containing fraction having certain properties in common with bacterial messenger RNA. The material stimulates amino acid incorporation in microsomes, is labeled more rapidly *in vivo* with P^{32} than are other cytoplasmic RNA fractions, and sediments in a sucrose gradient more rapidly than soluble RNA and

more slowly than ribosomes. Preparations of this material from regenerating liver are more active than those from normal liver. Phenol-extracted RNA from the preparation is also active in the *in vitro* system. It is emphasized, however, that the material appears to differ from bacterial messenger RNA in certain other properties. Notable among these is the insensitivity of the RNA, in the native state, to ribonuclease.

Note added in proof: After this paper was completed, two further reports appeared on biologically active RNA fractions from liver: E. S. Maxwell, these PROCEEDINGS, **48**, 1639 (1962), and Barondes, S. H., C. W. Dingman, and M. B. Sporn, *Nature*, **196**, 145 (1962).

We wish to express our sincere thanks to Lorraine Cassidy for her excellent technical assistance. Thanks are also due N. L. R. Bucher for familiarizing us with regenerating liver lore.

* Supported by a grant to one of us (M. B. H.) from the U.S. Public Health Service.

† On leave of absence from the National Institute for Medical Research, Mill Hill, London.

[1] Volkin, E., and L. Astrachian, *Virology*, **2**, 149 (1956).

[2] *Cellular Regulatory Mechanisms*, Cold Spring Harbor Symposia, vol. 26 (1961).

[3] Hoagland, M., *ibid.*, p. 153.

[4] Higgins, G. M., and R. M. Anderson, *A. M. A. Arch. Pathol.*, **12**, 186 (1931).

[5] Siekevitz, P., *J. Biol. Chem.*, **195**, 549 (1952).

[6] Hecht, L. I., P. C. Zamecnik, M. L. Stephenson, and J. F. Scott, *J. Biol. Chem.*, **233**, 954 (1958).

[7] Britten, R. J., and R. B. Roberts, *Science*, **131**, 32 (1960).

[8] Hultin, T., and A. Von der Decken, *Exptl. Cell Research*, **15**, 581 (1958).

[9] Rendi, R., *Biochim. Biophys. Acta*, **31**, 266 (1959).

[10] Stephenson, M. L., and P. C. Zamecnik, these PROCEEDINGS, **47**, 1627 (1961).

[11] Nathans, D., and F. Lipmann, these PROCEEDINGS, **47**, 497 (1961).

[12] Grossi, L. G., and K. Moldave, *J. Biol. Chem.*, **235**, 2370 (1960).

[13] Cheng, P.-Y., *Biochim. Biophys. Acta*, **53**, 232 (1961).

[14] Sibatani, A., S. deKloet, V. Allfrey, and A. Mirsky, these PROCEEDINGS, **48**, 471 (1962).

[15] Hiatt, H. H., *J. Mol. Biol.*, **5**, 217 (1962).

[16] Marks, P. A., C. Willson, J. Kruh, and F. Gros, *Biochem. Biophys. Res. Comm.*, **8**, 9 (1962).

[17] Scherrer, K., and J. E. Darnell, *ibid.*, **7**, 486.

[18] Amos, H., and K. E. Kearns, *Nature*, **195**, 806 (1962).

[19] Niu, M. C., L. C. Cordova, L. C. Niu, C. L. Radbill, these PROCEEDINGS, **48**, 1964 (1962).

[20] Busch, S., P. Chamber, P. Mandel, and J. Weill, *Biochem. Biophys. Res. Comm.*, **7**, 255 (1962).

INFORMATION TO CONTRIBUTORS

THE PROCEEDINGS OF THE NATIONAL ACADEMY OF SCIENCES publishes promptly brief first announcements of the results of original research by members of the Academy or others. Articles are limited to 8 printed pages and no author may have more than 8 pages altogether in any one issue. Wherever practicable, results should be made clear without elaborate technical details; figures, tables, and formulae should be kept as simple as possible.

MANUSCRIPTS should be in the form of current numbers of the PROCEEDINGS, typewritten in duplicate with double spacing, the author retaining one copy, and addressed to THE PROCEEDINGS OF THE NATIONAL ACADEMY OF SCIENCES, 2101 Constitution Avenue, Washington 25, D. C. They will be accepted only from the members of the Academy who will assume responsibility for their propriety and scientific standards and for any printing costs in excess of those allowed them by the Academy.

GALLEY PROOF will be sent; as authors' corrections are charged to them, typewritten manuscripts should be letter-perfect. Original art work or figures will be returned if requested when the manuscript is submitted. Because of the time limitations, page proofs will not be sent. Reprints should be ordered when proof is returned on the reprint form enclosed therewith; they will be furnished at cost.

CONTENTS

Page

CHEMISTRY.—CRYSTAL STRUCTURE OF POTASSIUM OZONIDE 1
By Leonid V. Azároff and Irene Corvin

CHEMISTRY.—THE DETERMINATION OF THE ELECTROPHORETIC CONTRIBUTION TO CONDUCTANCE FROM THE CONCENTRATION DEPENDENCE OF TRANSFERENCE NUMBERS . . . . . *By Robert L. Kay and James L. Dye* 5

CHEMISTRY.—THE BUOYANT BEHAVIOR OF VIRAL AND BACTERIAL DNA IN ALKALINE CsCl . . . *By Jerome Vinograd, Janet Morris, Norman Davidson, and William F. Dove, Jr.* 12

MATHEMATICS.—GENERALIZED RIEMANNIAN GEOMETRY, II . . . . *By Luther P. Eisenhart* 18

MATHEMATICS.—RELATIVE HOMOLOGICAL ALGEBRA MADE ABSOLUTE . . *By Peter Freyd* 19

MATHEMATICS.—THE SAMPLING DISTRIBUTION OF PRIMES . . . . . *By D. D. Kosambi* 20

MICROBIOLOGY.—DEPRESSION OF HOST-CONTROLLED RNA SYNTHESIS IN HUMAN CELLS DURING POLIOVIRUS INFECTION . . . . . *By John J. Holland* 23

MICROBIOLOGY.—TRANSFORMATION INDUCED BY SIMIAN VIRUS 40 IN NEWBORN SYRIAN HAMSTER RENAL CELL CULTURES . . . . . *By Harvey M. Shein, John F. Enders, Jeana D. Levinthal, and Anne E. Burket* 28

PHYSICS.—ON A PLANE ISING LATTICE WITH FIRST AND SECOND INTERACTIONS . . . . . *By A. Pais* 34

PHYSICS.—NOTE ON THE SQUARE-INTEGRABILITY OF THE KERNEL OF THE LINEARIZED BOLTZMANN INTEGRAL EQUATION FOR RIGID SPHERE MOLECULES . . *By C. L. Pekeris* 38

PHYSIOLOGY.—ON THE EFFECT OF SODIUM-FREE SOLUTIONS UPON ISOLATED, SINGLE FROG NERVE FIBERS . . . . . *By V. Honrubia and R. Lorente de Nó* 40

ZOÖLOGY.—ACTION SPECTRUM FOR PALING (DECREASE IN REFRACTIVE INDEX) OF ULTRAVIOLET-IRRADIATED CHROMOSOME SEGMENTS . . . . . *By Raymond E. Zirkle and Robert B. Uretz* 45

GENETICS.—GENE EXPRESSION IN DIFFERENTIATED CELLS . . . . . *By E. H. Davidson, V. G. Allfrey, and A. E. Mirsky* 53

GENETICS.—EFFECTS OF MECHANICAL SHEAR ON GENETIC ACTIVITY OF *Bacillus subtilis* DNA . . . . . *By Eugene W. Nester, A. T. Ganesan, and Joshua Lederberg* 61

BIOCHEMISTRY.—PHYSICAL PROPERTIES OF MESSENGER RNA OF BACTERIOPHAGE T4 . . . . . *By Ekkehard K. F. Bautz* 68

BIOCHEMISTRY.—INSULIN—A PROBABLE GROSS MOLECULAR STRUCTURE . . . . . *By J. Ralph Einstein, A. Stewart McGavin, and Barbara W. Low* 74

BIOCHEMISTRY.—STUDIES ON POLYNUCLEOTIDE-STIMULATED AMINO ACYL TRANSFER FROM SOLUBLE-RNA TO RAT LIVER RIBOSOMES . . . . . *By June M. Fessenden, Judith Cairncross, and Kivie Moldave* 82

BIOCHEMISTRY.—RIBONUCLEIC ACID POLYMERASE OF *Azotobacter vinelandii*, I. PRIMING BY POLYRIBONUCLEOTIDES . . . . . *By Joseph S. Krakow and Severo Ochoa* 88

BIOCHEMISTRY.—THE STRUCTURE OF THE DNA-ACRIDINE COMPLEX . . *By L. S. Lerman* 94

BIOCHEMISTRY.—CHANGES IN THE DISTRIBUTION OF POLYMERASE ACTIVITY DURING DNA SYNTHESIS IN MOUSE FIBROBLASTS . . . . . *By John W. Littlefield, Alice P. McGovern, and Katharine B. Margeson* 102

BIOCHEMISTRY.—THYRO-ACTIVITY IN IODO-DERIVATIVES OF PHYTOHORMONAL 5-HYDROXYBENZOFURANS . . . *By S. M. Siegel, C. A. Giza, Gwendolyn Davis, and R. L. Hinman* 107

BIOCHEMISTRY.—CARBOXYPEPTIDASE A: APPROACHES TO THE CHEMICAL NATURE OF THE ACTIVE CENTER AND THE MECHANISMS OF ACTION . . . . . *By Bert L. Vallee, James R. Riordan, and Joseph E. Coleman* 109

BIOCHEMISTRY.—SYNTHETIC POLYNUCLEOTIDES AND THE AMINO ACID CODE, VIII . . . . . *By Albert J. Wahba, Robert S. Gardner, Carlos Basilio, Robert S. Miller, Joseph F. Speyer, and Peter Lengyel* 116

BIOCHEMISTRY.—A MULTIPLE RIBOSOMAL STRUCTURE IN PROTEIN SYNTHESIS . . . . . *By Jonathan R. Warner, Paul M. Knopf, and Alexander Rich* 122

BIOCHEMISTRY.—ASPECTS OF CONTROL OF PROTEIN SYNTHESIS IN NORMAL AND REGENERATING RAT LIVER, I. A CYTOPLASMIC RNA-CONTAINING FRACTION THAT STIMULATES AMINO ACID INCORPORATION . . . . *By Mahlon B. Hoagland and Brigitte A. Askonas* 130